

# **Investigation of factors affecting the aerosol transmission of *Mycobacterium tuberculosis***

**Mutlaq Alshammri**

Thesis submitted to The University of Leicester for the  
Degree of Doctor of Philosophy

May 2020

Department of Infection, Immunity and Inflammation  
College of Medicine, Biological Sciences and  
Psychology  
University of Leicester

University Road, Leicester, LE1 7RH

# Abstract

**Background:** *Mycobacterium tuberculosis* (Mtb) is transmitted via aerosol droplets generated by infected persons. Transmission of Mtb is thought to be a selective process and that cell surface hydrophobicity (CSH) influences this selectivity. On expulsion into the environment, bacilli will be exposed to rapidly changing physical conditions (temperature, water activity, osmolarity and oxygen tension) as the droplet evaporates to a stable droplet nucleus. Adaptation of the bacilli to the changing environment will be a feature supporting their fitness for survival in the aerosol phase and will impact the phenotype of subsequent *infection*. In this project, the role of CSH on mycobacterial aerosolisation and techniques to measure CSH were investigated. Additionally, survival and changes in transcriptional profile of *M. tuberculosis* H37Rv and *M. bovis* BCG in aerosols over a period of 2 hours have been explored.

**Methods:** Lawn growth of either Mtb H37Rv or *M. bovis* BCG were scrapped and suspended in distilled water (DW) medium. Bacterial suspensions were nebulised using either Collison 3-Jet or ultrasonic Omron nebuliser for 5 min into a rotating drum. Aerosols samples were collected in DW or Guanidinium thiocyanate (GTC) at different time points over 2 hours for survival and transcriptional profile experiments, respectively. Survival of cells in aerosols was determined by colony-forming units (CFU), most probable number (MPN) and qPCR. For transcriptional changes, samples were subject to RNA-sequencing analysis by Illumina NextSeq-500. Differentially expressed genes were detected at q-value < 0.01.

**Results:** Mtb H37Rv and *M. bovis* BCG consistently showed > 50 % survival in aerosol for up to 2 hours. Differentially expressed genes of Mtb H37Rv were detected at different stages during aerosolisation and due to the nebulisation process. However, no obvious transcriptional pattern of Mtb cells under the tested conditions was obtained. Genes of Mtb universal stress regulon (DosR) were up-regulated at pre-nebulisation samples compared to the post nebulisation and aerosol samples.

**Discussion:** Investigation into the survival of Mtb and *M .bovis* BCG under different environmental conditions could provide better insight into the survival of these cells in aerosols. DosR regulon was induced prior nebulisation process indicating early stress conditions for Mtb cells during inoculum preparation.

# Acknowledgment

I am extremely grateful for the support I have received from my parents past years and always. First and foremost, I would like to acknowledge my supervisor Professor Mike Barer for his immeasurable great effort, encouragement and support. Thank you for your patient guidance, sincere advice and the very useful critiques throughout the years of study. This PhD was funded by the Saudi Ministry of Health, to whom I am very grateful.

Many thanks are owed to Dr Natalie Garton for her help and knowledge throughout my PhD. To Dr Helen O`Hare for her suggestions and comments. To Dr Natalie Lazar-Adler and Malgorzata Wegrzyn for their assistance in Cat3 lab work. I am also grateful to Dr Richard Haigh for his help in the RNA-sequencing work.

Many thanks for the people who helped in the work at PHE, Porton Down, Allan Bennett, Simon Clark and Thomas Pottage. Special thanks to Dr. Katy-Anne Thompson for her contribution and organisation of the experiments at PHE, Porton Down. Big thanks for Professor Peter Andrew and Professor Martha Clokie who assisted on my progress review panel, for providing me with useful feedbacks which have been valuable to my project.

I would like to thank members of labs 136 for support, ideas and friendship, and to the department support staff.

The biggest thanks go to my family who supported and motivated me during my studies.

# List of Abbreviations

Ac1/Ac2PIM2	Acyl/diacyl phosphatidylinositol dimannosides
ACDP	Advisory Committee on Dangerous Pathogens
ADC	Albumin-dextrose-catalase
AG	Arabinogalactan
AGI	All-glass impingers
ALF	Airway lining fluid
BCG	Bacillus Calmette-Guérin
bp	Base pair
BFFB	Bronchiolar fluid film burst
CL	Containment level
COSHH	Control of substances hazardous of to health regulations
CR	Complement receptors
CSH	Cell surface hydrophobicity
DAT	Diacyltrehaloses
D-CFU	Colony-forming units, drop plate
ddDNA	Dideoxynulceotides
DDT	Dithiothreitol
DE	Differentially expressed
DNA	Deoxyribonucleic acid
DosR	Dormancy survival regulator
DW	Distilled water
GPLs	Glycopeptidolipids
GTC	Guanidinium thiocyanate
HEPA	High Efficiency Particulate Air
HIC	Hydrophobic-interaction chromatography
HIV	Human immunodeficiency virus
II	inhibition index
INF	Interferon

KDa	Kilo Daltons
LAM	Lipoarabinomannan
LM	Lipomannan
LOSs	Lipooligosaccharides
LPSs	Lipopolysaccharides
LTBI	Latent tuberculosis <i>infection</i>
mAGP	Mycolyl-arabinogalactan-peptidoglycan
MAs	Mycolic acids
MATH	Microbial adhesion to hydrocarbons
Mb	Million base
Med	Median
MIM	Mycobacterial inner membrane
MOM	Mycobacterial outer membrane
MPN	Most probable number
Ms	Semi-folded methoxymycolate
Mtb	<i>Mycobacterium tuberculosis</i>
MTBC	<i>Mycobacterium tuberculosis</i> complex
NTM	Non-Tuberculosis mycobacteria
OD	Optical density
PAT	Pentaacyl trehalose
PBS	Phosphate-buffered Saline
P-CFU	Colony-forming unit, Pour plate
PCR	Polymerase chain reaction
PDIM	phthiocerol dimycocerosates
PG	Peptidoglycan
PHE	Public Health England
PI	phosphatidylinositol
PMA	Propidium monoazide
PUM	Phosphate-urea-magnesium
Q	Quantile
RH	Relative humidity

RI	Resuscitation index
RT	Room temperature
RIN	RNA integrity number
RNA	Ribonucleic acid
RNIs	Reactive nitrogen intermediates
ROIs	Reactive oxygen intermediates
RPKM	Reads per Kilobase per Million mapped reads
RT	Room temperature
RT-qPCR	Reverse-transcriptase quantitative PCR
SAT	Salt aggregation test
SBS	Sequencing by synthesis
S-CFU	Colony-forming unit, Spread plate
SGL	Sulfoglycolipid
SN	Supernatant
SP	Surfactant protein
TB	Tuberculosis
TC	Total count
TF	Transcription factor
TMM	Trimmed Mean of M values
TPM	Transcript per Million
UQ	Upper quartile
WGS	Whole genome sequencing

# List of Figures

Figure 1.1. Photomicrograph of <i>M. tuberculosis</i> .	6
Figure 1.2. The cell envelope of <i>M. tuberculosis</i> .	14
Figure 2.1. Diagrammatic representation of the assembly of the chamber block.	44
Figure 3.1. Schematic of the basic MATH procedure used in this study	52
Figure 3.2. Fluorescent hydrophobic microspheres attached to <i>M. bovis</i> BCG cells.	58
Figure 3.3. Overview of the organization of equipment used for aerosolisation experiment inside class II safety cabinet.	59
Figure 3.4. Schematic diagram of the aerosolisation system.	59
Figure 3.5. Collison nebuliser.	60
Figure 3.6. A3 complete Omron nebuliser.	61
Figure 3.7. Ultrasonic NE-780 Omron nebuliser.	62
Figure 3.8. Overview of steps in MATH technique.	64
Figure 3.9. Influence of vortex duration and hexadecane-aqueous phase volume ratio on the CSH measurements of <i>M. smegmatis</i> and <i>M. bovis</i> BCG.	66
Figure 3.10. Effect of growth cycle on CSH.	68
Figure 3.11. Colony morphology of <i>M. abscessus</i> smooth and rough phenotypes.	69
Figure 3.12. CSH of <i>M. abscessus</i> smooth and rough phenotypes was assessed Using MATH and Congo Red binding assays.	69
Figure 3.13. CSH measurement using fluorescent microsphere beads method.	70
Figure 3.14. Heterogeneity of <i>M. bovis</i> BCG using Congo Red and microsphere beads assays.	71
Figure 3.15. Influence of 4 % formaldehyde fixation on CSH measurements of <i>M. bovis</i> BCG.	72
Figure 3.16. CSH measurements of Mtb strains.	73
Figure 3.17. Decreased in hydrophobicity post nebulisation.	74
Figure 4.1. Modifications were applied when Omron nebuliser was used in the experiment to maintain similar internal air flow to Collison nebuliser.	89



Figure 4.2. The Goldberg drum system. ....	90
Figure 4.3. Schematic diagram of the Goldberg drum system. ....	90
Figure 4.4. Formula of the calculation of the dilution factor. ....	91
Figure 4.5. Example of the final analysis after correction to the dilution factor. ....	91
Figure 4.6. Survival pattern of <i>M. bovis</i> BCG and Mtb H37Rv with the theoretical dilution. ....	98
Figure 4.7. Survival pattern of <i>M. bovis</i> BCG and Mtb H37Rv as a percentage of the theoretical dilution. ....	99
Figure 4.8. Comparison between S-CFU and P-CFU methods to detect <i>M. bovis</i> cells in aerosols. ....	100
Figure 4.9. CFU counts of the aerosol samples before and after the freeze-thaw cycle. ....	103
Figure 4.10. Comparison between P-CFU and MPN techniques to study survival of Mtb H37Rv in aerosols. ....	104
Figure 4.11. Comparison between aerosolised Mtb H37Rv cells treated and not treated with PMA.. ....	105
Figure 4.12. The decline pattern of the aerosolised Mtb H37Rv intact cells over a period of two hrs. ....	106
Figure 4.13. Comparison between the P-CFU counts of the suspensions inside the reservoir pre- and post-nebulisation. ....	107
Figure 4.14. Comparison between PMA resistant cells' proportion in the suspension inside the reservoir pre- and post-nebulisation. ....	108
Figure 5.1. A typical RNA-sequencing experiment.. ....	119
Figure 5.2. Structure of sequence library molecules for different platforms.. ....	122
Figure 5.3. Illumina sequencing. ....	123
Figure 5.4. An example of intensity values for the first 10 cycles of a read.....	124
Figure 5.5. The parallel set diagram showing DE genes detected at between pre-neb and post-neb samples.....	141
Figure 5.6. The parallel set diagram showing DE genes detected at between T0 and post-neb samples.....	142
Figure 5.7. The parallel set diagram showing DE genes detected at between T30 and T0 samples. ....	143

Figure 5.8. The parallel set diagram showing DE genes detected at between T120 and T30 samples. ....	144
Figure 5.9. The parallel set diagram showing DE genes detected at between T120 and T0 samples. ....	145

# List of tables

Table 1.1. The primary hosts of currently defined MTBC members. ....	4
Table 1.2. Methods commonly employed to assess microbial CSH measurements. ....	18
Table 1.3. Factors that affect survival and infectivity of airborne microorganisms. ....	24
Table 1.4. Description of some of the aerosol generation mechanisms used in Aerobiology experiments. ....	27
Table 1.5. Description of some of the sampler mechanisms used in Aerobiology. ....	29
Table 1.6. Description of advantages and disadvantages of some commonly used techniques in gene expression studies. ....	35
Table 2.1. Bacterial strains. ....	39
Table 2.2. Filters sets which were used for epifluorescence microscopy. ....	45
Table 2.3. Display of significance used in this thesis. ....	46
Table 3.1. PUM buffers. ....	53
Table 3.2. pH buffers. ....	54
Table 3.3. Ionic strength buffers. ....	54
Table 3.4. Parameters related to the MATH procedure. ....	55
Table 3.5. Other parameters were modified to investigate the influence of these parameters on CSH measurement using MATH technique. ....	55
Table 3.6. Summary of the results of the impact of different parameters on the measurement of CSH using MATH technique. ....	65
Table 4.1. Culture supernatant assessment assay of <i>M. bovis</i> BCG using Collison and Omron nebulisers. ....	102
Table 4.2. Absolute numbers of <i>Mtb</i> H37Rv cells detected by P-CFU, MPN and PMA- qPCR. ....	106
Table 5.1. Compositions of GTC solutions. ....	129
Table 5.2. Reads information taken after RNA-sequencing for <i>Mtb</i> H37Rv. ....	137
Table 5.3. Overview of the Alignments % of <i>Mtb</i> H37Rv and <i>M. bovis</i> BCG. ....	138

Table 5.4. Proportion of rRNA to total RNA.....	139
Table 5.5. Genes with no expression detected. ....	139
Table 5.6. Number of DE genes between the different conditions.....	140
Table 5.7. . List of the top 5 significantly DE genes in comparison between post-nebulisation and post-nebulisation samples.....	141
Table 5.8. List of the top 5 significantly DE genes in comparison between T0 and post-nebulisation samples. ....	142
Table 5.9. List of the top 5 significantly DE genes in comparison between T30 and T0 samples. ....	143
Table 5.10. List of the top 5 significantly DE genes in comparison between T120 and T30 samples. ....	144
Table 5.11. List of the top 5 significantly DE genes in comparison between T120 and T0 samples. ....	145
Table 5.12. TF associated with DE genes at five different stages.....	146
Table 5.13. Expression of genes regulated by DosR regulon at different stages .....	148

# Table of contents

Abstract.....	i
Acknowledgment.....	iii
List of Abbreviations .....	iv
List of Figures .....	vii
List of tables .....	x
Table of contents .....	xii
1. Introduction .....	1
1.1. General introduction .....	2
1.2. The genus <i>Mycobacterium</i> .....	3
1.2.1. <i>Mycobacterium tuberculosis</i> complex (MTBC) .....	3
1.2.2. Non-Tuberculosis mycobacteria (NTMs) .....	7
1.3. Tuberculosis .....	9
1.3.1. Tuberculosis in history .....	9
1.3.2. Pathogenesis of tuberculosis .....	10
1.3.3. Latent tuberculosis .....	11
1.4. Cell surface characteristics .....	11
1.4.1. Mycobacterial Cell envelope .....	12
1.4.2. Bacterial cell surface hydrophobicity (CSH).....	15
1.4.3. Mycobacterial cell surface hydrophobicity .....	15
1.4.4. Hydrophobicity and aerosol transmission .....	16
1.4.5. Measurement of cell surface hydrophobicity .....	17
1.5. Transmission of tuberculosis .....	20
1.5.1. Bioaerosol Formation in the Lungs.....	20
1.5.2. Airborne Mtb transmission.....	21
1.5.3. Measuring transmission in populations .....	22
1.5.4. Survival in aerosols .....	24
1.6. Aerobiology.....	26
1.6.1. Aerosol generation .....	26
1.6.2. Aerosol sampling techniques.....	28
1.6.3. Post-sampling process .....	29
1.6.4. Experimental considerations .....	30
1.7. Studying bacterial transcriptome .....	31
1.7.1. Techniques to measure gene expression .....	32
1.8. Aim and objectives.....	37

2.	Materials and Methods .....	38
2.1.	Mycobacterial strains.....	39
2.2.	Materials, culture media and reagents .....	39
2.2.1.	Growth media .....	40
2.2.2.	Reagents .....	40
2.3.	General methods .....	42
2.3.1.	Measurement of optical density.....	42
2.3.2.	Enumeration of colony-forming units, drop plate method (D-CFU) .....	42
2.3.3.	Preparation of stock cultures for long-term storage.....	42
2.3.4.	Disperse of aggregates.....	43
2.3.5.	Cultivation of containment level 2 (CL2) mycobacterial organisms.....	43
2.3.6.	Cultivation of CL3 mycobacterial strains .....	43
2.3.7.	Inactivation of CL3 mycobacterial strains.....	44
2.4.	Fluorescence microscopy.....	44
2.4.1.	Immobilising of mycobacterial cells onto slides for microscopy.....	44
2.4.2.	Recording fluorescence images .....	45
2.4.3.	Image analysis.....	45
2.5.	Statistical analyses and graphical representation of significance .....	46
3.	Hydrophobicity studies .....	47
3.1.	Introduction .....	48
3.2.	Methods.....	52
3.2.1.	Bacterial suspension preparation .....	52
3.2.2.	CSH measurement using MATH technique .....	52
3.2.3.	Variations in the MATH method investigated .....	53
3.2.4.	Investigating the Influence of bacterial growth phase on CSH .....	55
3.2.5.	Effect of fixation on CSH measurements.....	56
3.2.6.	CSH measurements of Mtb strains .....	56
3.2.7.	Other techniques to measure CSH .....	56
3.2.8.	Aerosolisation system.....	58
3.2.9.	Nebulisers used.....	60
3.2.10.	Investigating the influence of CSH on the propensity of cells for aerosolisation.....	63
3.3.	Results.....	64
3.3.1.	Influence of operational factors on CSH results with the MATH method....	64
3.3.2.	CSH increased at stationary phase compared to exponential phase.....	68
3.3.3.	Additional techniques to measure CSH .....	69

3.3.4. CSH measurement was not affected by fixation .....	72
3.3.5. Different Mtb strains showed different CSH values .....	73
3.3.6. CSH decreased significantly post nebulisation .....	74
3.4. Discussion .....	75
3.4.1 Influence of operational parameters on CSH measurement.....	75
3.4.2 The growth cycle influenced the CSH of <i>M. bovis</i> BCG .....	79
3.4.3. Evaluation of additional techniques to measure CSH .....	80
3.4.4. CSH of different Mtb strains .....	82
3.4.5. Reduced CSH significantly post nebulisation.....	82
3.5. Conclusions .....	84
4. Aerosol Survival Studies.....	85
4.1. Introduction .....	86
4.2. Methods.....	88
4.2.1. Bacterial strains and growth conditions .....	88
4.2.2. Aerosol generation .....	88
4.2.3. Aerosol sampler .....	89
4.2.4. Test procedure.....	89
4.2.5. Calculation of the dilution factor in the survival studies.....	91
4.2.6. Processing samples at PHE, Porton Down .....	92
4.2.7. Processing samples at Leicester University .....	92
4.2.8. Enumeration of colony-forming units (CFU).....	92
4.2.10. Propidium monoazide (PMA test) .....	94
4.2.11. DNA extraction.....	95
4.2.12. In-house qPCR IS6110 TaqMan assay .....	95
4.2.13. Calculation of the genome/ml from the real time assay.....	96
4.3. Results.....	97
4.3.1 Survival patterns of <i>M. bovis</i> BCG and Mtb H37Rv in aerosols.....	97
4.3.2 Comparison of methods used to assess bacillary survival .....	100
4.3.3 Effect of nebulisation on Mtb H37Rv cells .....	107
4.4. Discussion .....	109
4.4.1 Survival patterns of <i>M. bovis</i> BCG and Mtb H37Rv in aerosols.....	109
4.4.2 Comparison of methods used to assess bacillary survival .....	110
4.4.3 Effect of nebulisation on Mtb H37Rv cells .....	114
4.5. Conclusions .....	116
5. Transcriptional changes in <i>M. tuberculosis</i> H37Rv on aerosol In vitro Studied by RNA-Sequencing .....	117

5.1 Introduction .....	118
5.1.1 RNA Library preparation .....	120
5.1.2 Preparation of cDNA library .....	121
5.1.3 Sequence library preparation .....	121
5.1.4 Base calling and quality score .....	123
5.1.5 Alignment and annotation of transcripts .....	125
5.1.6 Normalisation methods .....	126
5.1.7 Detection of differentially expressed (DE) genes .....	128
5.1.8 Aims and objectives .....	128
5.2 Methods .....	129
5.2.1 5M Guanidinium thiocyanate (GTC) solution .....	129
5.2.2 Growth condition and test procedure .....	130
5.2.3 DNase I solution (digestion buffer) .....	130
5.2.4 RNA extraction .....	130
5.2.5 Turbo Dnase treatment .....	131
5.2.6 On-column DNase digestion .....	132
5.2.7 Measuring RNA integrity number (RIN) .....	132
5.2.8 NextSeq-500 Illumina workflow .....	133
5.2.9 Trimming low-quality reads .....	134
5.2.10 Alignment and normalisation of reads .....	135
5.2.11 Differential expression of genes .....	135
5.3 Results .....	137
5.3.1 Sequencing results .....	137
5.3.2 Alignment of reads .....	138
5.3.3 Proportion of ribosomal RNA .....	139
5.3.5. Genes with no detected expression .....	139
5.3.4 Differentially expressed (DE) genes .....	140
5.3.5 Transcriptional pattern of DosR regulon .....	147
5.4 Discussion .....	149
5.4.1 Sequencing results .....	149
5.4.2 Quality control of extracted RNA .....	150
5.4.3 Alignment of reads .....	150
5.4.4 Genes with no detected expression .....	151
5.4.5 Differentially expressed genes .....	151
5.5 Conclusions .....	155



6.1 General Discussion .....	156
6.2 Conclusions and Future work .....	160
References .....	162

# **Chapter One**

## **1. Introduction**

## 1.1. General introduction

Tuberculosis (TB) is one of the oldest recognised diseases in the world (Hett and Rubin, 2008). In humans, it is mainly caused by the bacterium *Mycobacterium tuberculosis* (Mtb) (Banuls *et al.*, 2015). TB is spread between individuals via airborne droplets containing bacilli generated by persons with a pulmonary Mtb infection (Dutt, 2011). These aerosols can be generated by multiple activities including coughing, sneezing, singing or even speaking (Leung, 1999).

It has been recognised that there is a relation between the cell envelope lipid composition and cell surface hydrophobicity (CSH) of mycobacteria (Pedley *et al.*, 2004). This hydrophobicity is proposed to influence the mycobacteria propensities for aerosol transmission (Minnikin *et al.*, 2015). A relationship between the cell surface hydrophobicity and aerosol transmission in non-tuberculosis mycobacteria has previously been proposed and investigated (Falkinham, 2003).

During aerosol transmission, Mtb cells encounter different stresses, including desiccation and changes in light exposure and oxygen and carbon dioxide concentrations (Table 1.2) (Cox, 1989, Bartek *et al.*, 2014; Haddrell and Thomas, 2017). Many of these environmental factors might affect the survival of Mtb within aerosols (Srikanth *et al.*, 2008) while the size and density of the droplets expelled will be affected by other environmental factors such as the relative humidity (RH) and temperature (Srikanth *et al.*, 2008).

A microarray study of the Mtb transcriptome in clinical samples of sputum revealed a pattern similar to non-replicating persistence described in *in vitro* (Garton *et al.*, 2008). A recent transcriptome study showed that the bacterial transcriptome in the aerosol differs from the contemporaneous transcriptome in clinical samples of sputum (Nardell *et al.*, 2016). However, transcriptional signatures of the Mtb during survival in aerosols are yet to be explored.

In this study the influence of CSH on the propensity of cells for aerosolisation, the survival of Mtb in aerosols and transcriptional signatures of Mtb in aerosols were all investigated.

## **1.2. The genus *Mycobacterium***

### **1.2.1. *Mycobacterium tuberculosis* complex (MTBC)**

*Mycobacterium* is a genus within the family *Mycobacteriaceae*, order Actinomycetales, class Actinomycetes (Shinnick and Good, 1994). Bacilli appear microscopically as straight or slightly curved rods, 1 to 10 µm in length and 0.3 to 0.6 µm in width. They grow at temperatures ranging between 30 and 45 °C. They are non-motile, non-spore forming, weakly Gram-positive, acid-fast bacilli (Ryan and Ray, 2004). Their acid-fast feature was determined when they showed resistance to decolourisation by mineral acids (e.g. acid alcohol) after staining with cationic dyes, such as carbol-fuchsin (Allen *et al.*, 1992). This characteristic is associated with the high lipid content in the cell envelope, where mycolic acids (MAs) and waxes are the major components (Watanabe *et al.*, 2011).

Many mycobacteria are slow growers, taking between 2 and 8 weeks to grow on solid media; the doubling time of Mtb, for example, is typically about 17 to 18 hrs (Ratledge and Stanford, 1982). Other mycobacteria are fast growers, taking 24-48 hrs for colonies to appear on solid media; for instance, *Mycobacterium smegmatis* has a doubling time of about 2-3 hrs (Stephan *et al.*, 2005).

There are three broad categories of mycobacteria: *Mycobacterium tuberculosis* complex species (MTBC), non-tuberculosis mycobacterial species (NTM) and *Mycobacterium leprae*, the causative agent of leprosy (Young *et al.*, 1985, Ryan and Ray, 2004). Human tuberculosis is predominantly (though not exclusively) a pulmonary disease caused by members of the MTBC. This group contains eight members, where three are human-specific, namely *M. tuberculosis*, *Mycobacterium canetti* and *Mycobacterium africanum*. The five remaining members mainly cause tuberculosis in animals but also have the potential to infect humans; this is further highlighted in Table 1.1 (van

Soolingen *et al.*, 1999, Niemann *et al.*, 2004, Ryan and Ray, 2004). *M. bovis*, the causative agent of bovine tuberculosis, is the most prominent of the non-human-specific members. Bovine tuberculosis results in a large economic burden within the UK livestock industry. In the last decade, around £500 million has been paid in compensation across England (Defra, 2014). *M. bovis* can infect humans, causing zoonotic tuberculosis. Prior to the establishment of milk pasteurisation and strict cattle culling programmes between 1935 and 1950, it was estimated that about 2500 people were dying annually from zoonotic TB in Great Britain (De la Rua-Domenech, 2006).

Member	Primary Host
<i>Mycobacterium tuberculosis</i>	Human (Gagneux, 2013)
<i>Mycobacterium africanum</i>	Human (De Jong <i>et al.</i> , 2010)
<i>Mycobacterium bovis</i>	Cattle (Garnier <i>et al.</i> , 2003)
<i>Mycobacterium canetti</i>	Human (Gutierrez <i>et al.</i> , 2005)
<i>Mycobacterium caprae</i>	Deer (Niemann <i>et al.</i> , 2002)
<i>Mycobacterium mungi</i>	Mongoose (Alexander <i>et al.</i> , 2010)
<i>Mycobacterium pinnipedi</i>	Pinnipeds (seals and sea lions) (Cousins <i>et al.</i> , 2003)
<i>Mycobacterium microti</i>	Voies (Frota <i>et al.</i> , 2004)

**Table 1.1. The primary hosts of currently defined MTBC members.**

NTM include over 150 mycobacterial species. They are present in environmental reservoirs such as soil, ground water, drinking water and even pasteurised milk (Spahr and Schaefroth, 2001). They are generally non-pathogenic for humans. However, certain species including *Mycobacterium abscessus* and *Mycobacterium kansasii* can be opportunistic pathogens (Nguyen, 1997). *M. abscessus* has been associated with individuals diagnosed with cystic fibrosis (Cullen *et al.*, 2000). In addition to pulmonary disease, NTM can also cause skin, lymphatic, soft tissue and disseminated infections (Uslan *et al.*, 2006).

### **1.2.1.1. *Mycobacterium tuberculosis***

Clinically, Mtb is the major concern amongst the *Mycobacteriaceae*. Genome sequencing of the type strain, H37Rv (Laboratory strain), revealed a genome size of ~4.4 mega bases (Mb) encoding roughly 4000 genes (Cole *et al.*, 1998). Mtb is an obligate pathogen that depends on transmission between hosts for survival outside laboratories. The principle host is *Homo sapiens*, although Mtb can also infect animals (Sakamoto, 2012) such as cattle (Ocepek *et al.*, 2005), cats and dogs that come in contact with infected individuals (Hackendahl *et al.*, 2004).

In pulmonary TB, the bacillus is found in the upper lobes of the lung where the level of oxygen is high. Although, tubercle bacilli have also been grown under hypoxic conditions *in vitro* (Ford *et al.*, 2011). The doubling time of Mtb under optimum conditions is around 18 hrs when it grows *ex vivo*, while the doubling time in humans or non-human primates is unknown (Delogu *et al.*, 2013, Gutierrez-Vazquez, 1956). Taking this into account, alongside the slow generation time, the ability of Mtb to persist in the host may be linked to the need for the long treatment required. Mtb being a successful pathogen in multiple host microenvironments is in part due to its ability to reprogram its metabolism according to the available carbon source. Thus sugars, fatty acids (Munoz-Elias and McKinney, 2006), cholesterol (Pandey and Sasseti, 2008) and glycerol (Daniel *et al.*, 2011) are carbon sources that Mtb can metabolise.

Mtb cannot be stained using the conventional Gram staining method as the cell envelope is impervious to basic dyes. Dyes have to be assisted with phenol or heat during the staining procedure. Once stained, bacilli resist decolourisation with acidified organic solvents gaining the description acid-fast (Lawn and Zumla, 2012). The Ziehl-Neelsen stain was first described by these authors contemporaneously with Robert Koch's identification of Mtb 130 years ago and remains a standard method for analysing sputum to this day (Figure 1.1) (Pandey *et al.*, 2008).

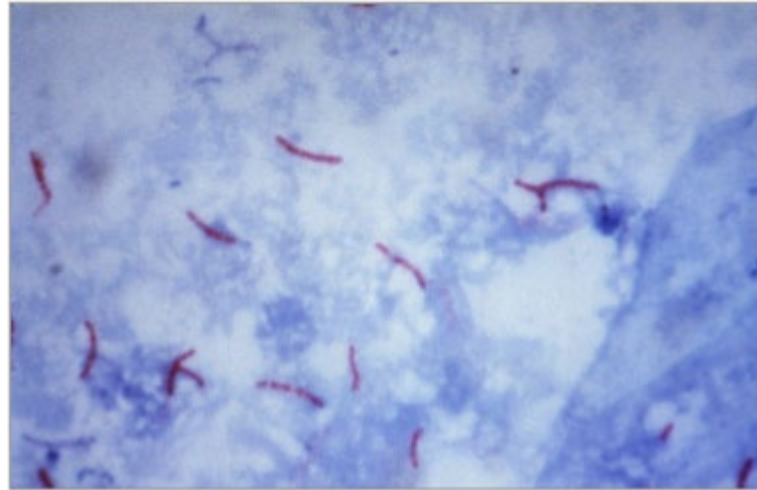


**Figure 1.1. Photomicrograph of *M. tuberculosis*.** Photomicrograph shows acid-fast *M. tuberculosis* bacilli visualised using Ziehl-Neelsen staining; carbol fuchsin stain is retained by the lipids of the mycobacterial cell envelope during acid-alcohol de-staining (acid-fast). Image taken under 1000x magnification (Kent, 1985).

#### **1.2.1.2. *Mycobacterium bovis* BCG**

*M. bovis*, also a member of the MTBC, is responsible for TB in cattle (Michel *et al.*, 2010) and has been reported on all continents except Antarctica (Smith *et al.*, 2006). It accounts for a small proportion of human TB compared to Mtb. Clinically, there is little difference between human TB caused by *M. bovis* or Mtb. *M. bovis* was responsible for around 6 % of all human tuberculosis deaths in Europe before the introduction of milk pasteurisation (Lawn and Zumla, 2012).

Bacille Calmette-Guérin (BCG) is a live attenuated form of the virulent *M. bovis* developed by extensive passage *in vitro* in the early part of the 20<sup>th</sup> century. This vaccine strain has been administered to over three billion individuals (Hilda *et al.*, 2012). It was established in 1921 and its efficacy varies; in some cases no protection could be demonstrated (Huebner, 1996). Due to its lowered virulence, *M. bovis* BCG has been used as a surrogate for Mtb in a variety of experimental settings and in many biomedical studies, including the present study. *M. bovis* shares 99.95 % sequence identity with Mtb while Mtb and BCG share more than 99.90 % genome sequence identity (Carroll *et al.*, 2009).

Although, *M. bovis* BCG mimics Mtb in which it survives phagocytosis by macrophages and elicits protective immunity in animals, it has some disadvantages as a model of Mtb. These disadvantages were acquired during the attenuation process when the regions RD1 and RD3 of the genome were lost. The loss of these regions has impacts on *M. bovis* BCG virulence (Mahiras et al, 1996).

## **1.2.2. Non-Tuberculosis mycobacteria (NTMs)**

### **1.2.2.1. *Mycobacterium smegmatis***

*M. smegmatis* is a widely used non-pathogenic rapid growing model organism for Mtb. It is useful for establishing methods without high level containment and for exploring a variety of adaptive mechanisms that have been utilised by Mtb in different microenvironments (Snapper *et al.*, 1990). *M. smegmatis* is also valuable, owing to its ability to be transformed by a plasmid (genetically manipulated easily). Additionally, *M. smegmatis* can be grown in defined and nutrient-limited media containing simple carbon and nitrogen sources together with salts and trace elements (Altaf *et al.*, 2010, Greening *et al.*, 2014).

The genome size of *M. smegmatis* comprises ~7 Mb compared to ~4.4 Mb for Mtb (Cook *et al.*, 2009). Both organisms can adapt to microaerobiosis by switching from active growth to a dormant state (Lim and Dick, 2001). *M. smegmatis* has been used to study several processes related to Mtb pathogenicity, such as the cell envelope proteome (He and De Buck, 2010), spontaneous mutation (Kucukyildirim *et al.*, 2016) and responses to nitrogen and carbon starvation (Williams *et al.*, 2013).

The non-pathogenic nature of *M. smegmatis* and its short doubling time (2-3 hrs) make it easy to work with as a surrogate for Mtb. *M. smegmatis* shares a highly similar cell wall structure to Mtb. Although both species generate some lipids that are different, however, the major cell wall components including peptidoglycan (PG), arabinogalactan (AG), and mycolic acids are fairly well conserved between both species (Rana, 2014).



Moreover, large number of *M. smegmatis* genes were characterised by genetic manipulation, some of which are homologues to Mtb (Bahatt and Jacobs, 2009, Rana et al., 2012 Chen et al., 2012).

Yet, there are limitations of using *M. smegmatis* as a model for Mtb. Around 30 % of Mtb proteins do not possess orthologues in *M. smegmatis*. Hence, it is not an appropriate model for Mtb in screening for an effective anti-tuberculosis drug and potential drug targets (Altaf *et al.*, 2010). In addition, *M. smegmatis* has been disregarded for the study of virulence and pathogenicity because it survives poorly in macrophages (Jordao *et al.*, 2008), exhibits no detectable pathogenicity in mice (Bange *et al.*, 1999), and has none of the pathogenic properties described for Mtb (Reyrat and Kahn, 2001).

#### **1.2.2.2. *Mycobacterium abscessus***

*M. abscessus* belongs to the NTM group and can be found in soil and water (Brown-Elliott *et al.*, 2002). It is an opportunistic pathogen causing pulmonary diseases in susceptible individuals, particularly those with cystic fibrosis (Floto *et al.*, 2016). It also causes skin and soft tissue, central nervous and bacteraemic infections (Lee *et al.*, 2015). *M. abscessus* is fast-growing with the ability to grow in most synthetic or complex laboratory liquid and solid media; it forms visible colonies in 3 to 5 days depending on the solid medium (Cortes *et al.*, 2010). In addition to its pathogenicity, *M. abscessus* is multi-drug resistant and resists most disinfectants and biocides, a feature that makes it adapted to hospital acquired infection (Brown-Elliott *et al.*, 2002). *M. abscessus* has a genome of ~5 Mb encoding roughly 5000 genes (Ripoll *et al.*, 2009).

There are two phenotypes of *M. abscessus* - a smooth, non-cording (irregular clumps), biofilm-forming phenotype and a rough, cording (oriented clumps where long axis of each cell is parallel to the long axis of the cord) , non-biofilm-forming phenotype (Howard *et al.*, 2006). According to epidemiological studies, the rough phenotype is associated with the most severe cases of pulmonary infection (Catherinot *et al.*, 2009).

Furthermore, the rough phenotype has been shown to persist for years to decades in infected hosts (Jönsson *et al.*, 2007). The different pathogenicity of the two phenotypes of *M. abscessus* has also been reported with other strains of mycobacteria. For example, the smooth form of *M. canettii* showed lower virulence and less persistence in experimentally infected mice than the rough Mtb (Supply *et al.*, 2013). Glycopeptidolipids (GPLs) are found in the outer membrane of the cell envelope of several mycobacteria including in that of *M. abscessus*. The lack of GPLs in the cell envelope is associated with a rough colony phenotype while presence is associated with smooth (Howard *et al.*, 2006). It has been reported previously that *M. abscessus*' rough phenotype is more hydrophobic than the smooth phenotype; this might increase the propensity of the rough phenotype for aerosolisation (Jankute *et al.*, 2017).

## **1.3. Tuberculosis**

### **1.3.1. Tuberculosis in history**

Tuberculosis (TB) is one of the oldest diseases and can be dated back thousands of years (Sandhu, 2011). Signs of TB have been found in the fossils of an extinct bison in Wyoming, US, 17,000 years ago (Rothschild *et al.*, 2001). TB has also been detected in the spines of Egyptian mummies dating back to 3000-2400 BC (Zink *et al.*, 2004). Genome-based studies have also suggested the presence of TB in America since AD 1200 (Konomi *et al.*, 2002). TB, which was also known as the great white plague or phthisis, can be said to be responsible for the death of billions of people. According to the World Health Organisation 2018 report, TB is responsible for about 1.6 million deaths yearly worldwide. One in every four of the world's population is estimated to be infected with Mtb latently. However, only 5-10 % of infected people will develop active tuberculosis during their lifetime (WHO, 2018).

In 1865, a French specialist named Jean-Antoine Villemin demonstrated that TB was infectious (Gawad and Bonde, 2018). On 24<sup>th</sup> March 1882, the causative agent of TB was described by Robert Koch, a German researcher. The agent was named *Mycobacterium*

*tuberculosis* (Mtb). “TB World Day” was established on that date to commemorate this discovery (Al-Humadi *et al.*, 2017).

### **1.3.2. Pathogenesis of tuberculosis**

When aerosol containing Mtb is inhaled by an individual, the tubercle bacilli are deposited into the lower respiratory tract where an initial interaction occurs between the pathogen and alveolar macrophages. As a consequence of this interaction, most of the bacilli are cleared, while some adapt to survive within the macrophages (Bermudez and Goodman, 1996). Studies of health-care workers and other people with close and repeated contact with TB patients demonstrated a significant proportion of individuals who showed no sign of adaptive immunity to Mtb, possibly indicating early eradication of tubercle bacillus (Zwerling *et al.*, 2012, Verrall *et al.*, 2014).

Several receptors have been implicated in the immune system’s recognition of Mtb. These receptors include C-type lectins such as the mannose receptor (MR,CD206), complement receptors (CR), surfactant protein (SP) receptors, scavenger receptors, and glycosylphosphatidylinositol (GPI) anchored receptors such as CD14 (Kleinnijenhuis *et al.*, 2011). Following macrophage phagocytosis, the bacteria encounter a hostile environment where multiple bactericidal activities of activated macrophages occur. Examples of these activities include reactive oxygen intermediates (ROIs), reactive nitrogen intermediates (RNIs), lysosomal enzymes, acidic pH and toxic peptides (Smith, 2003, Ehrt and Schnappinger, 2009). Inside macrophages, Mtb cells avoid these bactericidal activities via a number of survival mechanisms. These mechanisms include the inhibition of phagosomal maturation, inhibition of apoptosis and inhibition of macrophage responses to interferon- $\gamma$  (INF-  $\gamma$ ) through the 19-KDa protein (Fortune *et al.*, 2004).

Phagocytosis activates a pro-inflammatory response and leads to the accumulation of multiple mononuclear cells which eventually form the hallmark of pulmonary TB, the granuloma (Russell, 2007). The granuloma is then surrounded by layers of macrophages with high-lipid content called foamy macrophages, and other mononuclear cells,

notably lymphocytes (Ulrichs *et al.*, 2005, Russell, 2007). At this stage of *infection*, which can last for decades, the host will not develop disease signs and will prevent further dissemination of the pathogen (Ulrichs *et al.*, 2005). Later, if the immune system becomes disrupted by any condition which affects the function of CD4+ T cells, the granuloma will break and thousands of viable and infectious bacilli will spill out into the airways (Sia *et al.*, 2015). As a result, a productive cough will develop, allowing the infectious bacilli to spread via generated aerosols (Sia *et al.*, 2015).

### **1.3.3. Latent tuberculosis**

Latent tuberculosis *infection* (LTBI) refers to a non-active, asymptomatic, non-infectious TB *infection*. It can be viewed as a state of equilibrium existing between the host and the bacilli. Individuals with LTBI have a 10 % chance of developing active TB during their lifetime (Corbett *et al.*, 2003). The likelihood of progression to active disease from LTBI increases when the infected individual's immune system becomes compromised due to age, malnutrition, illness (particularly HIV *infection*) or immunosuppressive therapy (Flynn and Chan, 2001).

It is estimated that a quarter of the world's population have LTBI, essentially acting as a reservoir, supporting the disease's continuous presence and making eradication a key challenge (Flynn and Chan, 2001, Houben and Dodd, 2016). In this thesis, latency refers to the clinical presentation of the disease, whereas dormancy refers to the condition of the surviving Mtb bacilli in an infected host. Bacterial dormancy is defined as 'a reversible state of low metabolic activity at a level that maintains viability' (Kaprelyants *et al.*, 1993).

## **1.4. Cell surface characteristics**

The bacterial outer surface may include a combination of polysaccharides (capsular and glycocalyx), lipopolysaccharides (LPS), lipoproteins, lipids, lipoteichoic acids, teichuronic acids, as well as covalently and non-covalently bound proteins (Hancock, 1991). Together with ultrastructural features this chemistry underpins the physiochemical properties of bacteria and influences the nature and extent of their interactions with

surrounding surfaces. However, these structures are not constant and vary depending on environmental conditions. Similarly, cells can modify their structure and functions as a survival mechanism under adverse conditions (Hancock, 1991).

Two mechanisms are recognised for microbial surface interactions. Specific interactions require a complementary site on the receiving surface to the adhesive structure on the cell surface, and occur between cell to cell attachments (Fletcher, 1996). Non-specific interactions are facilitated by interaction forces (electrostatic force), surface macromolecules and hydrophobic interactions (Beuth and Uhlenbruck, 1995). These features have particularly been investigated in aquatic bacteria as well as in microbial-hydrocarbon interactions (Mills and Powelson, 1996).

### **1.4.1. Mycobacterial Cell envelope**

One of the unique features of mycobacteria is their thick hydrophobic cell envelope which plays a significant role in virulence and antimicrobial resistance (Brennan and Nikaido, 1995). The extraordinary cell envelope architecture offers mycobacteria a remarkably impermeable and hydrophobic armour. The cell envelope is composed of a polysaccharide-rich capsule, a mycomembrane, an arabinogalactan layer (AG), a peptidoglycan layer (PG) and plasma membrane (Crick *et al.*, 2001, Valera, 21014). This sophisticated architecture becomes a highly difficult barrier for anti-TB agents to cross (Valera, 2014).

Mycolic acids (MAs) are  $\alpha$ -alkyl  $\beta$ -hydroxyl long chain fatty acids which generally consist of two parts: the non-functionalised “mycolic motif” and the “meromycolate chain” (Verschoor *et al.*, 2012). Mycobacteria produce these MA chains ranging from 60 to 90 carbons in length, these being the longest fatty acids recognised (Lopez-Marin, 2012). *Mycobacterium* species depend fully on these MAs for their growth and survival both *in vitro* and *in vivo* (Portevin *et al.*, 2004). There are three classes of MAs,  $\alpha$ -mycolates, methoxy-mycolates and keto-mycolates, all of which contain cyclopropane rings in their carbon chains.  $\alpha$ -mycolates tend to only form an extended ‘U’ shape, while keto mycolates tend to form a ‘W’ shape and methoxy-mycolates a ‘W’ shape and an

intermediate semi-folded 'sZ' shape (Minnikin *et al.*, 2015). The majority of mycolic acids are covalently attached via ester linkages to arabinogalactan, which is in turn covalently attached to peptidoglycan, forming the mycolyl-arabinogalactan-peptidoglycan (mAGP) complex (McNeil *et al.*, 1990, McNeil *et al.*, 1991). This structure forms the core of the mycobacterial cell envelope (Brennan, 2003).

MAs are responsible for many mycobacterial species' unique characteristics, including resistance to chemical injury and dehydration, low access to hydrophilic chemotherapies and virulence (Dubnau *et al.*, 2000, Glickman *et al.*, 2000, Glickman and Jacobs, 2001). They also give the mycobacterial species their acid-fastness characteristic (Bhatt *et al.*, 2007). Moreover, MAs play a significant role in mycobacterial biofilm formation, which may help Mtb to persist within the host (Ojha *et al.*, 2008). The presence of MAs in high amounts in the mycobacterial cell envelope renders its extreme hydrophobicity (Marrakchi *et al.*, 2014), which will be discussed in detail in Section 1.4.3. Additionally, enzymes that are involved in mycolate biosynthesis are good candidates for anti-mycobacterial therapies (Bhatt *et al.*, 2007).

The permeability of the mycobacterial cell envelope is lower by approximately one order of magnitude when compared to *Pseudomonas aeruginosa*, an organism recognised for its low cell envelope permeability (Jarlier and Nikaido, 1990). The low permeability of the Mtb cell envelope makes it sensitive only to aminoglycosides (e.g. streptomycin), and rifamycins (e.g. rifampicin) among antibiotics, and to fluoroquinolones among general chemotherapeutic agents (Brennan and Nikaido, 1995). Furthermore, mycobacteria are relatively resistant to alkali, drying, and many chemical disinfectants and this may underpin their transmission in multiple environments (Brennan and Nikaido, 1995).

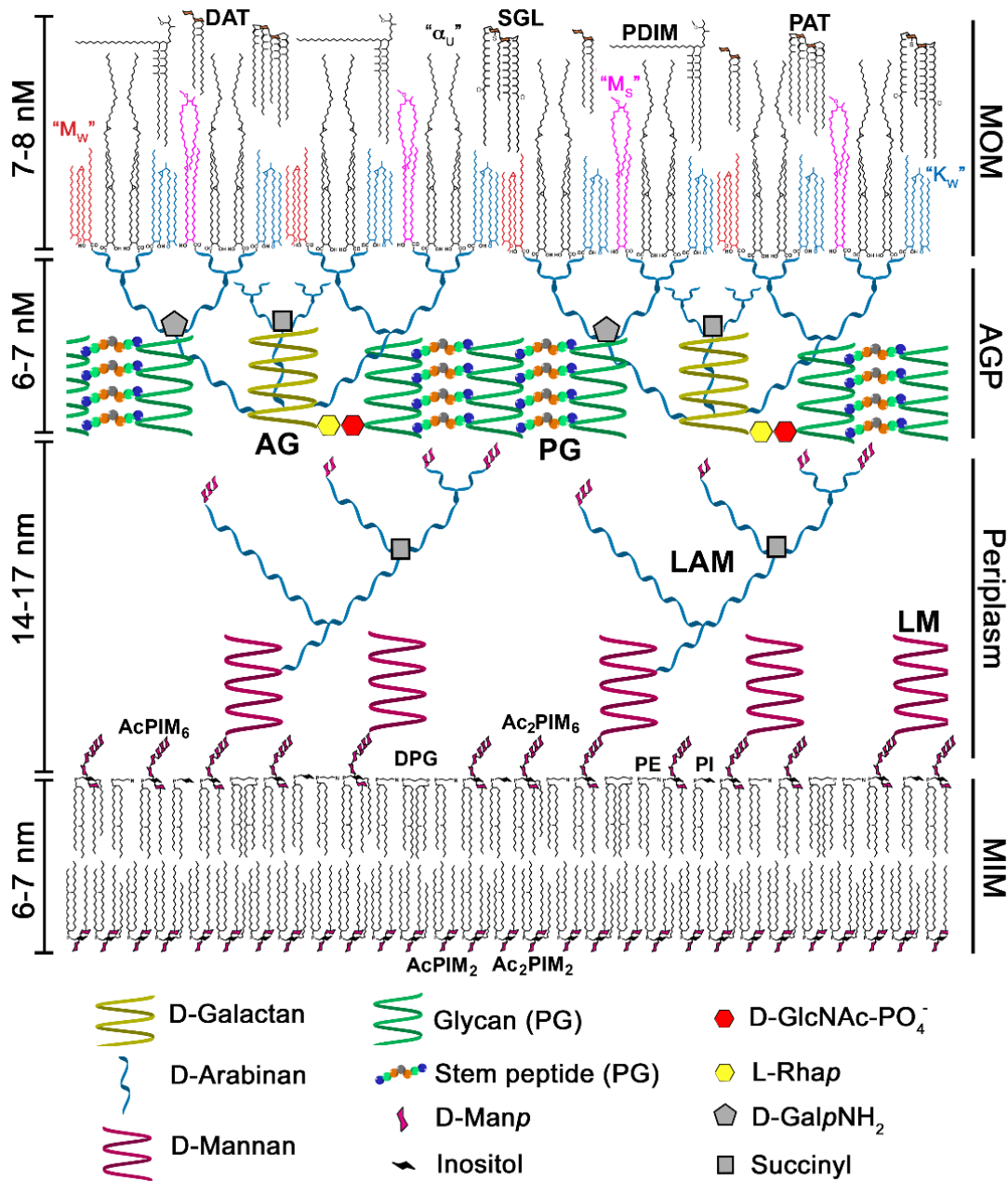


**Figure 1.2. The cell envelope of *M. tuberculosis*.** Schematic of the *M. tuberculosis* cell envelope. adapted from (Minnikin *et al.*, 2015). Dimensions correlate to cryo-electron microscopy and cell envelope proteins are not shown. Depicts the mycobacterial inner membrane (MIM), arabinogalactan peptidoglycan (AGP), the mycobacterial outer membrane (MOM). The capsule is not shown. DAT, diacyltrehaloses; SGL, Sulfoglycolipid; PDIM, phthiocerol dimycocerosates; PAT, Pentaacyl trehalose;  $\alpha_U$ , fully extended  $\alpha$ -mycolate;  $K_w$  and  $M_w$ , folded keto and methoxy-mycolate respectively;  $M_s$ , semi-folded methoxymycolate; AG, arabinogalactan; PG, peptidoglycan; LAM, lipoarabinomannan; LM, lipomannan; Ac<sub>1</sub>/Ac<sub>2</sub>PIM<sub>6</sub>, acyl/diacyl phosphatidylinositol hexamannosides respectively; DPG, diphosphatidylglycerol; PE, phatidylethanolamine; PI, phosphatidylinositol; Ac<sub>1</sub>/Ac<sub>2</sub>PIM<sub>2</sub> acyl/diacyl phosphatidylinositol dimannosides respectively.

### **1.4.2. Bacterial cell surface hydrophobicity (CSH)**

CSH reflects the ratio between hydrophobic and hydrophilic constituents of the cell envelope (Geertsema-Doornbusch *et al.*, 1993); it contributes to partitioning at liquid/liquid and liquid/air interfaces as well as attachment to surfaces. Hydrophobic cells adhere to hydrophobic surfaces and hydrophilic cells adhere to hydrophilic surfaces (Kochkodan *et al.*, 2008). In a microbial population, some cells are more hydrophobic than others, therefore, only a proportion of the population adheres to hydrophobic surfaces. Furthermore, microorganisms can respond to environmental conditions (temperature, composition of nutrients, growth phase, etc.) by altering their CSH properties (Bujdáková *et al.*, 2013).

Hydrophobic bacteria are relevant to a variety of situations such as medical practice, where hydrophobic organisms may adhere to plastic used in medical devices (Esteban *et al.*, 2014). They have also been shown to adhere to host tissues (Hazen *et al.*, 1991). The importance of hydrophobic organisms can also be found in the petroleum industry, where quick and inexpensive methods are required to remove insoluble hydrocarbons. The ability of hydrophobic cells to adhere to hydrocarbon-water interfaces may play a significant part in developing such methods (Goswami and Singh, 1991). In the food industry, hydrophobic pathogens have been reported to attach to materials used in installations such as rubber and stainless steel (Sinde and Carballo, 2000). Furthermore, bacteria with higher CSH have more propensity to attach to food components such as lipids and proteins, causing food contamination and subsequently resulting in the wastage of millions of dollars annually (Brooks and Flint, 2008).

### **1.4.3. Mycobacterial cell surface hydrophobicity**

A comparison study between Mtb and its relatives *M. kansasii* and *M. canettii* revealed a significant difference in their CSH (Jankute *et al.*, 2017). A proposed route for the development of CSH from the hydrophilic *M. kansasii* to the modern hydrophobic Mtb was introduced by Jankute and associates (Jankute *et al.*, 2017). These authors proposed a series of genetic alterations affecting the cell envelope of *M. kansasii* (or its



ancestor) leading to an intermediate smooth phenotype, *M. canettii*. Subsequently, loss of hydrophilic components led to the hydrophobic rough phenotype members of the modern MTB complex (Jankute *et al.*, 2017).

Mtb has longer  $\alpha$ -mycolic acids than both *M. kansasii* or *M. canettii*, contributing to increased CSH (Minnikin *et al.*, 2015). In *M. kansasii*, the presence of the hydrophilic lipooligosaccharides (LOSs), relatively polar phenolic glycolipids (PGLs) and phthiocerol/phthiodiolone dimycocerosate waxes (PDIMs) accounts for its hydrophilic cell surface. These lipids are found in the intermediate species *M. canettii* with slight modifications. Additionally, *M. canettii* has two extra classes of lipids known as pentaacyl trehalose glycolipids and diacyl trehalose glycolipids (PATs and DATs) (Minnikin *et al.*, 2015, Jankute *et al.*, 2017). The key differences between the hydrophobic modern Mtb and the hydrophilic ancestors are that the LOSs and PGLs classes of lipids are deleted from Mtb. In addition to this, three apolar lipids, PDIMs, PATs and DATs, a new class of hydrophobic lipids named sulfoglycolipids (SGLs), are present in the outer membrane of Mtb. This combination appears to account for the high CSH of Mtb and related members of the MTB complex (Soto *et al.*, 2000, Minnikin *et al.*, 2015).

#### **1.4.4. Hydrophobicity and aerosol transmission**

A link between CSH and the aerosol transmission of environmental mycobacteria has been previously indicated by Parker and colleagues (Parker *et al.*, 1983). In their study, *Mycobacterium avium-intracellulare* cells were found to be in greater number than *Mycobacterium scrofulaceum* in aerosols ejected from natural seawater and in laboratory experiments. They observed microscopically that *M. intracellulare* formed aggregates while *M. scrofulaceum* did not. This aggregation was attributed to the hydrophobic nature of *M. intracellulare* (Parker *et al.*, 1983). In 1975, Gruft and colleagues found that *M. intracellulare* infections are more frequent among humans than *Mycobacterium scrofulaceum* infections and that the ocean waters were the source of such infections (GRUFT *et al.*, 1975). Taking these findings into account, a link between CSH, aerosolisation and transmission can be postulated (Wendt *et al.*, 1980).

*M. canettii*, a member of the MTB complex, has been shown to be restricted to the Horn of Africa and is less extensively transmitted than the modern Mtb (Koeck *et al.*, 2011). A comparison between Mtb and possible evolutionary ancestors, *M. kansasii* and *M. canettii* using Congo red and partitioning to hexadecane has shown that Mtb is more hydrophobic (Jankute *et al.*, 2017). According to these authors, the enhanced CSH of Mtb is due to changes in the lipid composition of its cell envelope and as a subsequent result, its successful aerosol-transmission (Jankute *et al.*, 2017).

Another example of the potential link between CSH, propensity for aerosolisation and transmission is the smooth colony morphotype of *M. abscessus*. The cell envelope type of this pathogen contains hydrophilic GPLs whilst the rough colony form of *M. abscessus* lacks GPLs (Jankute *et al.*, 2017). The rough colony *M. abscessus* exhibited higher CSH than the smooth morphotype when Congo red and partitioning to hexadecane assays were applied (Viljoen *et al.*, 2018). Moreover, it has been found that isolates causing chronic airway colonisation/*infection* are usually of the rough morphotype, while wound isolates mainly exhibit smooth colony morphology (Jönsson *et al.*, 2007).

#### **1.4.5. Measurement of cell surface hydrophobicity**

In 1924, Mudd and Mudd demonstrated, for the first time, the ability of bacteria to partition at oil-water interfaces (Mudd and Mudd, 1924). These pioneering observations led to many subsequent studies of microbial CSH and the development of methods to measure it (Doyle and Rosenberg, 1990). There are general considerations that must be taken into account when measuring CSH, regardless of the method used. Firstly, hydrophobic interactions can promote adhesion to surfaces and interfaces. Thus, it is common for some microorganisms to adhere to the walls of vessels or glass used in experiments (Hori *et al.*, 2008). Secondly, since most CSH measurement methods use aqueous buffers, attention must be paid to the properties of the buffer such as salt concentrations and pH, which can have a marked effect on the measurement outcomes (Doyle and Rosenberg, 1990). Thirdly, the growth conditions have a significant impact on the surface properties of a wide range of microorganisms. Thus, differences in culturing conditions must be considered (Wrangstadh *et al.*, 1986). Moreover, in some

cases, clinical isolates lose their hydrophobic properties due to sequential sub-culturing (Westergren and Olsson, 1983). Fourthly, hydrophobic microorganisms sometimes have a tendency to form aggregates leading to underestimation of the real state of adherence to hydrocarbon (Voloshin and Kaperlyants, 2004). Finally, the adhesion of microorganisms is sometimes dependent on cell density (Van Pelt *et al.*, 1985). Table 1.2 displays the advantages and disadvantages of the most commonly used methods to measure CSH.

**Table 1.2. Methods commonly employed to assess microbial CSH measurements.**

Method	Features	Advantages	Disadvantages
Microbial adhesion to hydrocarbons (MATH)  (Doyle and Rosenberg, 1990, Vanhaecke and Pijck, 1988)	Microorganisms adhere to hydrocarbon-aqueous phase interfaces; removal of cells from the aqueous phase can be measured via spectrophotometry.	Easy to conduct Low cost of materials. Basic equipment (Vortex, spectrophotometer). Quick in both operation and data analysis. Adherence of cells can be observed microscopically. Measurement of overall hydrophobicity of microbial suspension.	Semi-quantitative method to measure overall CSH. No standardised procedure, making the comparison of results difficult across studies. Aggregation of bacteria makes optical density readings unreliable. Some hydrocarbons can cause cell lysis. The possibility of cooperative interaction among the adhering cells themselves that cause indirect adhesion to hydrocarbon.
Contact angle measurements (CAM)  (Reid and Tester, 1992, Busscher, 1990, Doyle and Rosenberg, 1990)	When water droplets are placed on dried lawns of microorganisms, the droplets form contact angles. The larger the angle created by the droplet, the lower the hydrophobicity value.	Accurate and reproducible results. Dose not affected by continued sub-culturing of the bacteria.	Slow procedure. Excessive drying process of the filter could lead to erroneous data. Requires special equipment (real-time image analyser) and technical expertise. It is sometimes observer-dependent.

Hydrophobic-interaction chromatography (HIC)  (Doyle and Rosenberg, 1990)	Octyl-Sepharose columns serve to trap hydrophobic microorganisms, whereas non-hydrophobic variants or strains do not adhere.	Useful in separating hydrophobic from hydrophilic organisms.	This does not work well when bacteria are capable of binding to agarose. Not useful when cells tend to aggregate.
Salt aggregation test (SAT)  (Lindahl <i>et al.</i> , 1981, Doyle and Rosenberg, 1990)	When mixed with ammonium sulfate, hydrophobic microorganisms tend to aggregate; rates of aggregation can be monitored via turbidity readings.	Easy to conduct. Requires no specialised equipment. Stain can be added to improve visualisation of the aggregation.	Hydrophobic bacteria tend to aggregate without the addition of ammonium sulfate. Only provides qualitative estimates for SCH. Electrostatic interactions have a significant influence on the results. Cell density is an important factor.
Adhesion of hydrophobic microspheres  (Zita and Hermansson, 1997, Heard <i>et al.</i> , 2009)	Some hydrophobic microorganisms bind to polystyrene microspheres; this binding can be determined by light microscopy.	Measures CSH at the single-cell level. Can determine the hydrophobic site of the cell surface.	Time consuming technique. Size of microsphere can affect the adherence. Aggregation with the microsphere is problematic.
Relative Congo red assay  (Jankute <i>et al.</i> , 2017, Yakupova <i>et al.</i> , 2019)	It is an amphiphilic dye that can stain hydrophobic area of the bacterial cell envelope	Cost-effective assay Can be used to CSH at the single-cell level. Can measure CSH of bacterial biomass	It is toxic and possibly carcinogenic dye. Time consuming technique.

While there are a variety of methods that can be used to measure CSH, the work in this study was conducted using the MATH as a main method. There are two reasons why MATH was chosen. Firstly, it is a simple (easy to conduct) technique and requires only a vortex and a spectrophotometer. Secondly, the high number of samples requires a fast technique in both operation and data analysis. The Microsphere beads and relative Congo red assays were also investigated here as they can measure CSH on a single cell level and have the potential to be used with aerosol samples where low numbers of cells are present.

## **1.5. Transmission of tuberculosis**

The predominant route for the transmission of Mtb is through inhalation of aerosols containing the tubercle bacillus by susceptible hosts (Wampande et al., 2015). The fundamentals of airborne transmission have been described by Wells, Riley and later, Loudon (Rieder, 1999). Interruption of any process related to the aerosol transfer of Mtb increases our understanding of the pathogen and could further contribute to reducing the rates of its transmission (Yates *et al.*, 2016).

### **1.5.1. Bioaerosol Formation in the Lungs**

Two mechanisms have been proposed for the production of aerosols in the lungs, both of which take place in different regions of the lung. The first is after the turbulence which occurs in the respiratory tract during inhalation and expiration (Fiegel *et al.*, 2006). The second is due to the reopening of closed peripheral airways during breathing (Johnson and Morawska, 2009). However, other mechanisms could also be responsible for aerosol formation in the respiratory tract; this could occur anywhere between the alveoli and the mouth (Patterson and Wood, 2019).

In more detail, the turbulence theory (during multiple daily habits i.e coughing, sneezing, and breathing) suggests that during inspiration and expiration, the air flows over the airway lining fluid (ALF), causing destabilisation of the ALF surface due to sheer force. This phenomenon leads to a wave-like disturbance resulting in the formation of aerosols, which may contain lung fluid components and trapped pathogens (Fiegel *et al.*, 2006). Studies involving mucus-like film showed that there are several factors influencing the formation of aerosols inside the respiratory tract. These factors include surface tension, air speed, film thickness and the physical properties (viscosity and elasticity) of the surface and bulk of the mucus layer (Basser *et al.*, 1989, Moriarty and Grotberg, 1999, Fiegel *et al.*, 2006). The influence of alteration of the physiological properties of the lung lining fluid by administration of isotonic saline on the formation of aerosols has been investigated previously. In 2004, Edward and colleagues have conducted an experiment where exhaled bioaerosol particles from 11 healthy

volunteers were measured before and after receiving isotonic saline by inhalation. The authors have found that 50 % of the subjects produced an average of > 500 particles per litre over 6-hrs (high producers). When these subjects received approximately 1 g isotonic saline by inhalation, the amount of expired aerosols was reduced by 72 % (Edwards *et al.*, 2004).

The reopening of closed peripheral airways theory was proposed after discovering that the concentration of exhaled aerosols decreased after a breath is held. In 2009, Johnson *et al.* proposed a model known as bronchiolar fluid film burst (BFFB). This model is based on exhaled droplets forming in the lower bronchioles during inhalation of normal breathing. In brief, during exhalation, the bronchiolar wall is contracted, and a fluid layer forms over the interior surface of these contracted bronchioles, preventing it from collapsing. This fluid layer can completely block the airway. During *inhalation*, the closed bronchioles will expand and reduce the fluid blockage, leading to the formation of the aerosols (Johnson and Morawska, 2009).

### **1.5.2. Airborne Mtb transmission**

As mentioned above, tubercle bacilli are aerosolised by individuals with pulmonary disease during multiple daily activities such as coughing, sneezing, speaking and singing or even during normal breathing (Loudon and Roberts, 1968, Wurie *et al.*, 2016). Due to the rapid evaporation which occurs post-aerosolisation, the droplets become low in mass and hence remain suspended in the air until they are either inhaled or ventilated out of the room (Wells, 1934). In cough sampling experiments, tuberculosis patients were coughing as frequently as was comfortable for them for 5 min in a cough aerosol sampling system. The experiments suggested that most aerosolised Mtb is in small droplets, even without evaporation, to remain suspended in the air (Fennelly *et al.*, 2012). These experiments, as well as studies from guinea pig facilities and molecular epidemiological observations, suggested that people infected with tuberculosis are not all equally infectious (Sultan *et al.*, 1960, Fennelly *et al.*, 2012, Jones-López *et al.*, 2013, Walker *et al.*, 2013, Ypma *et al.*, 2013). Moreover, the transmission of Mtb to guinea

pigs was reduced by 56 % when the patients wore surgical masks (Dharmadhikari *et al.*, 2012).

Conventional assessment of patient infectiousness depends on the positivity of sputum smears and sputum culture conversion (Conditions and NICE, 2011). While for most patients, the smear and sputum cultures appear negative after two weeks of treatment, for other patients, more than a month is required (Fitzwater *et al.*, 2010). The risk of patients spreading *infection* was diminished significantly after 2-4 weeks of treatment, regardless of the status of the smear or sputum culture (Gunnels *et al.*, 1974). The frequency of coughing diminished with treatment and subsequently, the generation of Mtb aerosols through coughing also diminished (Loudon and Spohn, 1969). However, the assumptions about infectiousness on the basis of culture conversion times might overestimate risk. Conversely, organisms that grow in culture might not survive when exposed to several stressors in the hostile immune system present in the alveoli (Yates *et al.*, 2016).

### **1.5.3. Measuring transmission in populations**

The prevalence and annual incidence of active TB is less than 2 %, even in the highest burden countries (Yates *et al.*, 2016). The challenges associated with obtaining proper measurements of Mtb transmission in populations arise from the infrequent outcomes, incomplete surveillance, and poor diagnostic tests for infection. Examples of these tests include the microscopic test for the presence of the tubercle bacilli in samples. This test is insensitive and many positive cases are missed among many negatives (Keflie and Ameni, 2014). Another poor diagnostic test is the chest radiographs. Even though this test is sensitive, it is not specific for active tuberculosis (Dye *et al.*, 2008). Conclusions about transmission therefore depend on the chosen measurements, assumptions and a combinations thereof. Since transmission, development from *infection* to an active disease with symptoms, and duration of the disease all have an impact on prevalence, it is difficult to draw proper conclusions about the prevalence of transmission (Cobelens *et al.*, 2014).

Molecular epidemiological approaches such as strain typing (spoligotyping) and whole genome sequencing (WGS) can provide evidence for or against linkages between two or more cases of active TB, which can lead to gaining an important insight into Mtb transmission (Borgdorff and Van Soolingen, 2013). Since these techniques require a bacterial isolate in most cases, they only capture *infections* that have developed into active TB (Du Plessis *et al.*, 2001).

The detection of aerosolised Mtb directly by sampling air within a chosen environment is of great interest. This allows for the quantification of Mtb exposure in putative sites of transmission (Wood *et al.*, 2016). In 1999, Mastorides and colleagues have introduced for the first time the use of a combination of filtration and PCR technique to detect aerosolised Mtb. In their study, the air samples were collected from suspected TB patient rooms over a period of 6 hrs filtration time (Mastorides *et al.*, 1999). In later studies, the combination of filtration and PCR to detect Mtb in aerosols was used in health care settings (Wan *et al.*, 2004, Matuka *et al.*, 2015). In 2016, a small personal clean room in which airborne Mtb could be isolated in a clinical setting called the respiratory aerosol sampling chamber (RASC) was designed (Wood *et al.*, 2016). The RASC enables the quantitation and characterisation of aerosol particles produced by the seated patient during normal breathing, coughing and talking. Inside this device, the sampling filters, Biosamplers and impactors can be placed to collect aerosol samples for different investigations including the morphological and molecular characteristics of Mtb in aerosols (Wood *et al.*, 2016).

Although PCR detection of Mtb DNA does not mean that the organism is viable, it does demonstrate that people with pulmonary TB have aerosolised Mtb in the environment that was sampled. In theory, this finding should be a reasonable measure for the risk of transmission (Yates *et al.*, 2016).



### 1.5.4. Survival in aerosols

When microorganisms, including Mtb, are aerosolised into the environment, they experience different conditions than those in bulk liquid. One obvious condition is the concentration of solute in the droplet, which reaches supersaturation due to a decreased water level inside the droplet (Clegg *et al.*, 2001). The equilibrium level with atmospheric RH can be reached with the addition or removal of water. This phenomenon depends on the relative abundance of each chemical species in the solute, where each component will contribute to the uptake or loss of water (Clegg *et al.*, 2003). It has been shown that the survival of *Bacillus subtilis* and *Pseudomonas fluorescens* was significantly affected by the solute concentrations (Johnson, 1999). Infected individuals will produce droplets with different mucus and solutes than healthy individuals. Similarly, microorganisms in *in vitro* studies are grown using different mediums (liquid broth, solid agar and nutrient composition), and these factors affect the concentration and types of nutrients present in the spray suspension, and subsequently influence the survival of the pathogen in aerosols (Brown, 1953, Handley and Webster, 1995, Hersen *et al.*, 2008).

**Table 1.3. Factors that affect survival and infectivity of airborne microorganisms. (Haddrell and Thomas, 2017).**

Factor	Description
Relative humidity	Levels studied generally range from 20 to 90 %
Temperature	Levels studied range from subzero to 50 °C
Solar radiation	Variability in spectra examined but inclusive of UV-A and UV-B wavelengths
Oxygen	Generation of reactive oxygen species during aerosol survival
Ozone	Reactive with pollutant gases and pinenes
Pollutant gases	CO, SO <sub>2</sub> , NO <sub>2</sub> , ethane and cyclohexene
Growth phase	Exponential or stationary
Particle size	Microbial aggregates have greater survival than single microorganisms
Aerosol age	Infectivity decreased prior to culturability with extended time in aerosol

Another stressor that affects the survival of cells in aerosols is the presence of atmospheric oxidants (e.g., reactive oxygen and nitrogen species, ozone) which can act directly on an organism or indirectly with constituents in the droplet (Estillore *et al.*, 2016). The presence of reactive oxygen species may result in oxidative damage to critical enzymes (Webb, 1969), phospholipids and nucleic acids. As a result, metabolic imbalance, membrane destabilization and reduction of repair activity can occur at the molecular and physiological levels of bacterial cells (Cox, 1987). Bioaerosols exposed to atmospheric ozone concentrations and variations in RH showed alteration in fluorescence spectra related to oxidation and in the hydrolysis of tryptophan (Santarpia *et al.*, 2012).

The influence of temperature and RH on the survival of microorganisms in aerosols has been studied on many occasions. It has been reported that Gram-negative bacteria survive better at low temperatures and low RH, while Gram-positive bacteria survive better at low temperatures and high RH (Cox, 1989, Grayston *et al.*, 1989). The influence of these factors on the survival of pathogens in aerosols is strain-dependent, as some microorganisms survive well regardless of these factors. For example, *Staphylococcus epidermidis* has shown similar patterns of survival in aerosols at RH ranging from 20 % to 90 % (Thompson *et al.*, 2011).

While there are many studies about the survival of microorganisms in aerosols, Mycobacteria studies are limited. In 2007, Gannon and colleagues have studied the survival of *M. bovis* in aerosols. They have claimed that a half-life time of *M. bovis* in aerosols was around 90 min (Gannon *et al.*, 2007). In 2016, Fletcher and co-workers have demonstrated that clinical samples of *M. abscessus* were able to survive for 80.6 sec and travel 4 m within the aerosols using a 110-mm diameter air-tight pipe (Fletcher *et al.*, 2016). To our knowledge, there are only two reports about the survival of Mtb in aerosols. First study was conducted in 1969 by Loudon and colleagues who demonstrated a half-life of Mtb in aerosols to be around 6 hrs (Loudon *et al.*, 1969). The second study was assessed by Lever and associates who claimed a half-time of Mtb in aerosols is less than 30 min (Lever *et al.*, 2000). These discrepancies in these results

were because of the different settings used in the two studies and will be discussed in details in Chapter 4.

In 2011, Clark and colleagues have studied the influence of different factors on the viability of Mtb during aerosolisation experiments; these were duration of aerosolisation, effect of the concentration of Mtb in the nebuliser, and the effect of freeze / thaw cycles of the challenge suspension (Clark et al., 2011). According to the results from Clark's study, aerosolisation of freshly grown Mtb suspension did not affect the viability of the bacilli over time. In contrast, frozen/thawed suspension of Mtb showed reduction in viability (in the nebuliser) of approximately 1 log<sub>10</sub> CFU / ml within the first 10 min post-nebulisation. The factor that did not affect Mtb viability in aerosolisation was the concentration of the bacterial suspension inside the nebuliser. The reduction of viability in the nebuliser fluid using frozen/thawed suspension needs to be considered when conducting aerosolisation experiments (Clark et al., 2011).

## **1.6. Aerobiology**

Aerobiology-related research was established many decades ago. Examples of research in this area include studying the survival rate of microorganisms in aerosols, investigations into inhaled infectious dose, efficiency of decontamination strategies and evaluation of bioaerosol sampling technologies. The general schematic of an aerobiology experiment is aerosol generation, collecting aerosol samples then post-sampling processing. Importantly, cells can be damaged during any of the stages mentioned (Hambleton, 1971, Terzieva *et al.*, 1996, Haddrell and Thomas, 2017).

### **1.6.1. Aerosol generation**

Table 1.4 outlines some major aerosol generators used in aerobiological studies and their operating mechanisms. The reflux aerosol generators in conjunction with impingement is widely used in aerobiological studies for sampling aerosols. Although this system can be safely used in biocontainment laboratories, it has been reported that reflux nebulisers damage cells to a greater extent than nonrefluxing nebulisers

(Reponen *et al.*, 1997, Zhen *et al.*, 2014). The damage caused by refluxing nebulisers can be linked to membrane damage (Thomas *et al.*, 2011), release of ions into the medium (e.g.,  $\text{PO}_4^{2-}$ ) (Anderson and Dark, 1967), cell fragmentation (Zhen *et al.*, 2014) and reduction in ATP activity (Han *et al.*, 2015); since the bacteria remain in the nebuliser during aerosolisation, they pass through the device nozzles repeatedly (Turgeon *et al.*, 2014). In contrast to refluxing nebulisers, the nonrefluxing nebulisers are less damaging to the cells, as the microorganisms only pass through the nozzle once (Zhen *et al.*, 2014).

**Table 1.4. Description of some of the aerosol generation mechanisms used in Aerobiology experiments. (Haddrell and Thomas, 2017).**

Aerosol generation mechanism	Apparatus example(s)	Description
Reflux nebulisation 1-,3- and 6-Jet version usually used	Collison nebuliser, Wells atomizer, aerosol gun	Bacteria are passed through the nebuliser nozzles repeatedly with wall impaction and liquid recirculation occurring every 6 s in the 3-Jet. The rate of aerosol generation and recirculation increased with increase of the number of jets.
Nonreflux nebulisation	Single-pass nebuliser	Bacteria are passed through the nebuliser nozzles once without wall impaction or recirculation occurring.
Aerosol bubbling	Sparging liquid nebuliser	The liquid is dripped onto a membrane then broken into droplets by airflow through the membrane. Next, the droplets break down into small aerosols due to the increased pressure gradient inside and outside the device.
Centrifugal atomisation	Spinning top aerosol generator	The liquid is moved to a rotating disc toward the edges by centrifugal forces. This process produces ligands that break into aerosols.
Flow focusing	flow-focusing aerosol generator, C-Flow nebuliser	Liquid flows through an orifice forming jets that break up into aerosols by aerodynamic suction of an accelerated air stream.

### 1.6.2. Aerosol sampling techniques

Sampling methods for airborne microorganisms include impingement, impaction, filtration, cyclonic separation, and electrostatic precipitation. As explained in table 4, each sampling method has pros and cons, and all have the potential to cause damage to cells (Kesavan and Sagripanti, 2015). It has been claimed that using impingement (AGI-30) to collect *P. fluorescens* aerosols for 15-60 min led to structural damage, with recovery achieved in nonselective media (Terzieva *et al.*, 1996). It is worth noting that the majority of studies which looked to determine the infectious dose and aerosol survival used sampling times ranging from 1 to 10 min to minimize the impact of microbial damage (Dabisch *et al.*, 2012). Several comparative studies assessing the efficiency of different sampling mechanisms demonstrated that the sampler efficiency is highly influenced by the strain being sampled. For example, *Bacillus* spp. endospores tend to be less affected by aerosol sampling methods (Dabisch *et al.*, 2012). The difference between sampler efficiencies can be due to the variations in sampling velocities; for impingement, the velocity reaches 260 m/s, 10-fold greater than other samplers (Table 1.5) (Mainelis, 1999).

**Table 1.5. Description of some of the sampler mechanisms used in Aerobiology. (Haddrell and Thomas, 2017).**

Aerosol sampling	Apparatus example (s)	Description
Impingement	All-glass impingers (AGI-4, AGI-30, AGI model 7541 AGI), SKC biosampler.	In AGI, particles are drawn through a small orifice that increases their velocity, thereby causing them to impinge on the bottom surface of the container. The velocity reaches 265 m/s (greater than other samplers). The SKC biosampler possesses three angled nozzles, creating gentle swirling motions of bioaerosol during collection.
Impaction	<b>Cascade impactors:</b> Andersen, Mercer, Ultimate, MAS-100, Burkard.	These operate on the principle of inertial impaction. Each stage of the impactor comprises a series of nozzles and has a different cutoff size. The organisms impact differently on each stage according to their size.
Filtration and impaction	Gelatin filter, nitrocellulose, polycarbonate	This has greater physical sampling efficiencies than other samplers. However, the biological sampling efficiency can be influenced by the elution of material from the filter surface (e.g., vortexing, shaking, solution volume and type).
Cyclonic separation	NIOSH cyclonic biosampler	A rotated cylindrical container draws airflow, causing larger particles to deposit and collect on the walls by centrifugal force.
Electrostatic precipitation	Ionizers (AS150, model 3100) aerosol sampler	Airborne particles are electrically charged and subjected to an electric field, causing gentle deposition velocity onto the collection substrate. Spores have greater bioefficiency than Gram-negative bacteria. Velocities reach 0.01-1 m/s.

### 1.6.3. Post-sampling process

The post-sampling process, including storage, is a stage during which damage to the cells can occur because an extra stress is added to the organisms during impaction onto agar (Stewart *et al.*, 1995), spread plating (Thomas *et al.*, 2012) and culture medium (Terzieva *et al.*, 1996). Alternative methods to quantify cells in aerosols involve the use

of microscopy or flow cytometry in conjunction with various dyes (Rule *et al.*, 2007). Also, quantitative PCR can indicate the physiological activity of the collected microorganisms (Allegra *et al.*, 2016). Storage temperature, sampling solution and storage period can lead to a misrepresentation of the actual state of the sampled organisms by either promoting replication or death (Li and Lin, 2001). It is best to process bioaerosol samples immediately after collection to minimize the stress of storage, however, this is highly dependent on the microorganism. A comparison study between *Bacillus* spp. endospores and *E. coli* revealed that *E. coli* is more affected by storage temperature (4 and 25 °C). However, both strains showed an increase in CFU counts after extended periods of storage at 25 °C compared to initial counts after sampling. This indicates a significant disaggregation and/or replication in the collection medium during storage periods. It should be noted that in this study, the authors used sterile deionized water with 0.01 % Tween 80 as a storage medium (Li and Lin, 2001).

#### 1.6.4. Experimental considerations

In aerobiology experiments, where studying the survival of organisms in aerosols is the aim, it is vital to minimise the stresses that occur during aerosol generation and sampling to avoid inaccurate representation (Zhen *et al.*, 2014). Using a single-pass nebuliser can reduce the probability of microorganisms being damaged (Haddrell and Thomas, 2017). Depending on the biosampler used, there are several ways to maximise recovery of microbes. Moreover, the reduced viability associated with prolonged sampling times can be minimised by shortening collection times (Juozaitis *et al.*, 1994). The cell membrane of Gram-negative bacteria is a major site for damage during aerosolisation and sampling; this was previously demonstrated by increased sensitivity to hydrolytic enzymes (Hambleton, 1971). Sampling into liquid can be optimised to reduce the associated osmotic shock and enhance the repair and recovery of aerosolised cells. For example, the addition of compatible solutes such as trehalose, raffinose, polyhydric alcohols and betaine can promote better survival rates of aerosolised cells, despite the stresses resulting from aerosol generation, transport, and sampling (Cox, 1969). The collection efficiency of the six-stage Andersen sampler and viability loss reduction was significantly enhanced with vegetative *Bacillus subtilis* and

*E. coli* by applying a thin film of mineral oil on plates (Xu *et al.*, 2013). In filtration methods, the bioefficiency depends on filtration time and the post-processing procedure (Li and Lin, 2001). A major drawback of the filtration method is that the continued drawing of air through the filter leads to the desiccation of collected microorganisms in a time-dependent manner. However, using gelatine membranes and placing them into warm media to recover collected microorganisms has been demonstrated to improve bioefficiency (Dabisch *et al.*, 2012, Zhen *et al.*, 2014).

Within these considerations, minimising the stress that occurs during aerosolisation was achieved in the study here by reducing the nebulisation time to 5 min. Although single-pass nebuliser was recommended to be used in aerosolisation experiments, the main nebuliser used in the work here was the ultrasonic Omron nebuliser. The 3-Jet Collison nebuliser was used here to make an appropriate comparison to the two previous *Mtb* studies by Loudon and Lever. Omron nebuliser was used mainly here as it can deliver higher number of cells during the 5 min period of nebulisation and showed similar level of cells damaging during nebulisation.

## **1.7. Studying bacterial transcriptome**

In 1958, Francis Crick introduced the central dogma of molecular biology that outlines the flow of information from DNA to RNA via transcription and then to protein via translation (Crick, 1970). This genetic information can change depending on surrounding environmental factors characterising the phenotype of an organism. The transcription of a subset of genes into complementary RNA molecules determines the identity of a cell and regulates the biological activities within it (Kukurba and Montgomery, 2015). Collectively defined as the transcriptome, it is a transcript profile which provides valuable information regarding almost the entire transcripts produced by an organism under specific conditions. This information includes transcript content, determination of transcriptional start sites, mRNA abundance and antisense RNAs (Filiatrault, 2011). Investigations into bacterial gene expression profiles can be used to show how bacteria function under different conditions, including in response to stressors, and can identify genes that are critical for specific conditions (Brown, 2016).



Several technologies for analysing transcriptomes have been developed over the last decades.

### **1.7.1. Techniques to measure gene expression**

#### **1.7.1.1. Northern blot**

The northern blot was developed in 1977 by Alwine and colleagues to detect RNA or isolated mRNA in a sample for studying gene expression (Alwine *et al.*, 1977). In this method, cellular RNAs are separated depending on their size using gel electrophoresis. Next, the separated RNA species are then transferred to a solid support (e.g., microcellulose or nylon), where the presence and abundance of an RNA species of interest is inferred by the hybridisation of a complementary radioactively labelled nucleic acid probe (Morozova *et al.*, 2009). The northern blot is a low-throughput technique that requires the use of radioactivity and large amounts of input RNA. This technique's complex requirements and detection ability that is limited to a few known transcripts at a time are drawbacks that can be avoided with other sequencing techniques (Morozova *et al.*, 2009).

#### **1.7.1.2. Real time Reverse transcription-PCR**

Also known as RT-qPCR, it provides unmatched sensitivity and speed for determining levels of specific transcripts (Wong and Medrano, 2005). In this method, RNA is isolated and reverse-transcribed using primers to form cDNA. Then, an amplification of the segment of the cDNA of interest is done using gene-specific PCR primers. The reaction is followed in real time by detecting fluorescence intensity characterised by a value called the threshold cycle ( $C_t$ ), the time at which fluorescence intensity is greater than the background fluorescence. The lower the  $C_t$  value, the greater the initial copy numbers of the target gene (Wagner, 2013). Advantages of the RT-qPCR method include increased experimental throughput and reduced quantity of input RNA required; however, it is limited to being able to order only hundreds of known transcripts at a time and does not cover large-scale transcriptomes (VanGuilder *et al.*, 2008).

### **1.7.1.3. Sanger sequencing**

In contrast to RT-qPCR, the Sanger sequencing technique uses one primer instead of two. The amplification process copies one strand but not the reverse strand. Each amplification cycle produces one copy in the same direction of the primer and cannot be used as a template for following cycles. The original template DNA in the sample is the source of all amplifications in the reaction. Therefore, sufficient copies of the original template DNA must be included in order for the sequencing amplification to be visualised by the automated sequencing equipment (Heather and Chain, 2016).

A new component called dideoxynucleotides (ddNTPs) has been introduced in Sanger sequencing. These ddNTPs are bases that function as terminators of the amplification process. They include a fluorescent tag for automated sequencing equipment and sit on the DNA template randomly during amplification and terminate the extension. The deoxynucleotides (dNTPs) sit on the remaining templates and continue extending. At the end of the amplification process, a ladder of PCR products is generated which increases by a single base. Each terminating base is tagged with fluorescent dye with different colours representing the A, G, C, and T bases in DNA (Heather and Chain, 2016).

### **1.7.1.4. DNA microarray**

DNA microarray is a high-throughput technology that allows the rapid identification of the expression levels of thousands of genes in a tissue or organism in a single experiment. In this technology, an orderly arrangement of thousands of identified sequenced genes is printed on an impermeable solid support, glass or silicon chip slides. Each glass or chip slide contains thousands of spots which in turn contain single-stranded DNA molecules called probes, representing a single gene and collectively the entire genome of an organism. The probes' targets can either be RNA molecules or single-stranded DNA molecules complementary to the RNAs being measured (cDNAs). The targets are prepared from mRNA from the cellular phenotypes of interest and each target is labelled with a fluorescent dye. When the sample is passed over the slide, each probe binds to its complementary sequence (hybridisation process). Once this process

has occurred, the slides are washed, not only to remove any labelled cDNA that did not hybridise on the array, but also to increase the stringency of the experiment and reduce cross-hybridisation. Finally, the expression level of each target can be measured according to the intensity of the emitted light coming from each probe on the slide (Hegde *et al.*, 2000, Allison *et al.*, 2006).

### **1.7.1.5. RNA-sequencing**

Also known as short-read sequencing, RNA-sequencing is a high-throughput sequencing technology that provides a digital measure for the abundance of transcripts present at a specific time within a sample. The overview principle of RNA-sequencing is that a population of extracted RNA is converted to a library of cDNA, which is then ligated to sequencing adaptors and subjected to a sequencing process (Wang *et al.*, 2009). In an RNA-sequencing experiment, the total RNA extracted from a biological sample and mRNA is enriched using oligo-dT attached magnetic beads. RNA is then fragmented and primed for cDNA synthesis. The first-strand cDNA is synthesised via reverse transcription using random primers. The second-strand cDNA is generated by separating the RNA template from the first strand via AMPure XP beads and synthesising a complementary strand to make double-stranded cDNA. Overhangs are created due to the DNA fragmentation and therefore, a polishing process using 3' to 5' exonuclease activity occurs, resulting in the production of blunt-ended DNA fragments. The 5' overhangs are filled in via polymerase activity. The 3' ends of fragments tend to ligate to each other and to prevent that, a single adenine nucleotide is added. Additionally, a complementary thymine is added to create an overhang for adapter ligation. Indexing adapters are then ligated to the double-stranded cDNA ends in preparation for hybridisation. DNA fragments containing adapters on both ends are selectively amplified via PCR. Next, DNA library templates must be quantified and quality control analysis should be performed. To prepare the DNA templates for cluster generation, indexed DNA libraries are normalised and pooled (if applicable) (Copeland, 2018). RNA-sequencing technology is explored in more detail in chapter 5.

**Table 1.6. Description of advantages and disadvantages of some commonly used techniques in gene expression studies.**

Technology	Advantage	Disadvantage
Northern blot  (Alwine <i>et al.</i> , 1977, Streit <i>et al.</i> , 2009, Unamba <i>et al.</i> , 2015).	High specificity. Detection of RNA size. Observation of alternate splice products. Partial homology probes can be used. The membranes can be stored and re-probed for years after blotting. Able to detect small changes in gene expression. Quantity and quality of RNA can be easily verified after electrophoresis and before further processing is done.	Low sensitivity. Only one or a small number of genes can be visualised. Detection with multiple probes is difficult. Risk of mRNA degradation during electrophoresis. Involves the use of harmful chemicals such as formaldehyde, radioactive material, ethidium bromide and UV light.
Real time RT-PCR  (Gachon <i>et al.</i> , 2004, VanGuilder <i>et al.</i> , 2008, Smith and Osborn, 2009).	Cost-effective. High sensitivity. Quick to provide reliable data. Considered as the gold standard validation method for results from other technologies such as microarray. Useful in monitoring biomarkers. Requires small amount of RNA.	High costs of machine and reagents. Prior knowledge about the sequence data of the specific target gene of interest is required. Cannot detect alternative splicing or partial transcript degradation.
Sanger sequencing  (Arsenic <i>et al.</i> , 2015, Jamuar and Tan, 2015, Heather and Chain, 2016).	Useful in detecting DNA mutations. High sensitivity and specificity. Typical error probability is 0.0001.	Expensive. Unable to perform parallel investigation of multiple targets. Labour-intensive process. Only single nucleotide polymorphisms (SNPs) and small-scale insertions and deletions can be identified.
Microarray  (Pozhitkov <i>et al.</i> , 2007, Morozova <i>et al.</i> , 2009).	Relatively inexpensive. Glass cDNA microarrays also have increased detection sensitivity due to longer target sequences (2 kbp). High specificity and reproducibility. Can detect noncoding RNAs, SNPs and alternative splicing events.	Requires prior knowledge of the genome to design the sequence probes. Cross-hybridisation causes lower signal-to-noise ratio. Small dynamic range of detection. Complex normalisation methods are required. Unable to detect novel transcripts. Requires high quantities of input RNA.

<p>RNA-sequencing</p> <p>(Wang <i>et al.</i>, 2009, Morozova <i>et al.</i>, 2009, Haas <i>et al.</i>, 2012)</p>	<p>High level of accuracy and reproducibility in detecting gene expression levels. Requires low amount of input RNA. Does not require prior knowledge of the reference genome and reference transcriptome. High resolution to the single nucleotide. Low background noise. Can identify short or poorly expressed transcripts. Can detect novel transcripts. Can identify the origin of transcription. This permits the precise mapping of sRNAs that contain highly repetitive regions. Requires less input RNA. Useful for non-model organisms with genomic sequences that are yet to be determined. It has no upper limit of detection and thus has a large dynamic range of expression levels over which transcripts can be detected.</p>	<p>Expensive. Biological replicates are required to evaluate reproducibility of the conditions being assessed. Bias can occur during library construction. Due to the large amount of data generated by RNA-sequencing, a software with high capacity is required for storage, retrieval and processing. It is time consuming and requires bioinformatics expertise.</p>
-----------------------------------------------------------------------------------------------------------------	-----------------------------------------------------------------------------------------------------------------------------------------------------------------------------------------------------------------------------------------------------------------------------------------------------------------------------------------------------------------------------------------------------------------------------------------------------------------------------------------------------------------------------------------------------------------------------------------------------------------------------------------------------------------------------------------------------------------------------------------------	--------------------------------------------------------------------------------------------------------------------------------------------------------------------------------------------------------------------------------------------------------------------------------------------------------------------------------------------------------------------------

While there are a variety of techniques to be used in transcriptomic studies, the RNA-sequencing technique was used in this study. The advantages of this technique over the other available techniques are outlined in Table 1.6. justify the choice of this technique for this project.

## 1.8. Aim and objectives

The overall aim of this study was to achieve further understanding of the physiological state of Mtb relevant to aerosol transmission. The hypothesis and objectives were:

### Hypotheses:

1. Aerosol transmission of Mtb is influenced by bacterial cell surface hydrophobicity (CSH)
  - a. More hydrophobic cells are more easily aerosolised
  - b. More hydrophobic strains show greater tendency for transmission.
2. *In vitro* aerosol studies with Mtb will enable identification of factors critical for transmission and its prevention
  - a. Inconsistencies in available aerosol study results can be resolved by standardising Goldberg drum procedures
3. Mtb cells in sustained aerosols will show transcriptional responses to this environment

### Objectives:

1. To investigate the influence of CSH on propensity of cells for aerosolisation.
2. To determine the survival pattern of *M. tuberculosis* H37Rv and *M. bovis* BCG in aerosols.
3. To determine the pattern of H37Rv and *M. bovis* BCG transcriptional changes on aerosolisation and survival stages during transmission.

# **Chapter two**

## **2. Materials and Methods**

## 2.1. Mycobacterial strains

**Table 2.1. Bacterial strains.**

Strain	Description	Source
<i>M. smegmatis</i> MC <sup>2</sup> 155	Rapid-growing non-pathogenic mycobacterium	Laboratory stocks
<i>M. bovis</i> BCG Glaxo	Attenuated category II TB vaccine strain	Laboratory stocks
<i>M. abscessus</i> ATCC19977	Clinical isolate	BCCM/ITM
<i>M. tuberculosis</i> H37Rv	Virulent laboratory strain	Laboratory stocks (W. Jacobs, New York)
<i>M. tuberculosis</i> Beijing 65	Clinical isolate	Laboratory stocks (M. Nicholls, Cape Town)
<i>M. tuberculosis</i> CH	Clinical isolate	Leicester Royal Infirmary
<i>M. tuberculosis</i> Loughborough strain	Clinical isolate	Leicester Royal Infirmary

## 2.2. Materials, culture media, and reagents

All chemicals and materials were obtained from Sigma-Aldrich (Poole, Dorset, UK) or Fisher Scientific (Loughborough, Leicestershire, UK), and bacterial culture media were obtained from Becton Dickinson Biosciences (Oxford, UK), unless otherwise stated. Polypropylene centrifuge tubes (Falcon 15 and 50 ml) were from Greiner Bio-One (Stonehouse, UK), universal tubes, 1.5 ml and 2 ml microfuge tubes were from StarLab (Milton Keynes, UK).

The sterilisation of media and reagents was achieved by autoclaving at 121 °C at 15 psi for 15 min unless otherwise stated.



### 2.2.1. Growth media

#### 7H9 broth

7H9 broth (Middlebrook) was made according to the manufacturer's specification. In 900 ml distilled water (DW), 4.7 g of 7H9 powder and 2.5 g glycerol were dissolved. The prepared solution was then autoclaved and stored at room temperature (RT) away from light until used. Prior to use, the broth was supplemented with 10 % (v/v) Albumin-dextrose-catalase (ADC) and 0.05 % (w/v) Tween 80 (designated as supplemented 7H9).

#### 7H10 agar

7H10 agar (Middlebrook) was made according to the manufacturer's specification. In 360 ml DW, 7.6 g of agar powder and 2.5 g glycerol were dissolved. The prepared media was boiled for 10 min to fully dissolve the powder and then autoclaved for sterilisation. The sterilised media was stored at RT away from light until used. Prior to use, the agar was supplemented with 10 % (v/v) OADC (Oleic Albumin Dextrose Catalase) (designated as 7H10).

### 2.2.2. Reagents

#### Albumin-Dextrose-Catalase (ADC) supplement

The ADC supplement was prepared by dissolving the following components in 100 ml DW.

Bovine Serum Albumin fraction V	7.50 g
D-Glucose	3.00 g
Sodium Chloride	1.28 g
Catalase	6.0 mg

The solution was stirred for 30 min to ensure complete dissolving of the components. The solution then was made up to 150 ml with DW. Finally, the supplement was filter-sterilised (0.2 µm filter, Nalgene, Hereford, UK) and stored at 4 °C.

**Oleic Acid-Albumin-Dextrose-Catalase (OADC) supplement**

The OADC supplement was prepared by dissolving the same components of the ADC above except with the addition of 8.63 ml of Oleic Acid solution (1 % (w/v) in 0.2 M sodium hydroxide). The prepared solution was sonicated (Decon, Ultrasonic Ltd, UK) for 30 min to permit emulsification of the oleic acid. Finally, the supplement was filter-sterilised and stored at 4 °C.

**10 % (w/v) Tween 80**

Tween 80 supplement was prepared by dissolving 15 g of stock solution in 150 ml DW (10 % (w/v) final concentration). The supplement was filter-sterilised and stored at 4 °C.

**Phosphate-buffered Saline (PBS)**

The phosphate buffered saline (PBS) was prepared by dissolving one PBS tablet in 200 ml DW to give a solution with a final concentration of 0.01 M phosphate buffer, 0.002 M potassium chloride and 0.137 M sodium chloride at pH 7.4. The solution was autoclaved for sterilisation.

**10 % (w/v) glycerol solution**

The glycerol solution was prepared by dissolving 10 g of concentrated glycerol in 100 ml PBS. The solution was filter-sterilised and stored at RT.

**4 % (v/v) formaldehyde**

In consideration of safety, the preparation of formaldehyde solution was done in fume hood following the precautions in the COSHH form. The solution was prepared by making a dilution from the stock solution at a concentration of 37 – 40 %. The stock solution was diluted to working solution at a concentration of 4 % by adding 90 ml of DW to 10 ml of the stock solution.

## 2.3. General methods

### 2.3.1. Measurement of optical density

The optical density (OD) of bacterial cultures was measured by transferring 1 ml from the bacterial suspension to 1.5 ml cuvette. Next, the cuvette was sealed with autoclave tape and laboratory sealing film. OD<sub>580</sub> was determined in a Sanyo SP75 UV/Vis spectrophotometer (Watford). Cultures with OD<sub>580</sub> >1 were diluted 10-fold prior measurement. The OD for all cultures was measured against blank of the appropriate medium.

### 2.3.2. Enumeration of colony-forming units, drop plate method (D-CFU)

This was modified from the Miles and Misra (surface viable count) method (Miles *et al.*, 1938). Ten-fold serial dilutions of cell suspension were performed by adding 50 µl of the cell suspension to 450 µl of 7H9-ADC-Tween 80 medium in 1.5 ml microfuge tubes. Three 20 µl drops from each dilution were plated onto 7H10-OADC agar plate. Each agar plate was separated into 4 sectors and each sector was designated to one of the dilutions. Once the drops were dried, the plates were sealed with laboratory sealing film and incubated inverted at 37 °C until isolated colonies became visible.

Final counts of 10-100 colonies (averaged over the three replicate spots) were used for the final calculation of colony forming units (CFUs), using the following equation;

$$\text{D-CFU / ml} = A \times D \times 50$$

A = Average colony count per 20 µl spot  
D = Dilution factor

### 2.3.3. Preparation of stock cultures for long-term storage

Frozen stocks of *M. smegmatis* or *M. bovis* BCG were prepared in 1.5 ml microfuge tubes and stored at -80 °C for future work. The preparation was done by mixing 500 µl exponentially growing the culture (doubling every 3 or 24 hrs, respectively, as assessed

by optical density readings) with an equal volume of 50 % (v/v) filter-sterilised glycerol solution in DW.

#### **2.3.4. Disperse of aggregates**

To break up bacterial clumps, a blunt 25G needle (Henke Sass Wolf, Germany) was used. The cell suspension was passed through the needle 5-7 times.

#### **2.3.5. Cultivation of containment level 2 (CL2) mycobacterial organisms**

A -80 °C frozen stock of *M. smegmatis*, *M. bovis* BCG or *M. abscessus* rough and smooth variants (OD 0.8-1) was used to inoculate 3 universal tubes contain 5 ml 7H9-ADC-Tween-80 broth and incubated at 37 °C with shaking at 200 rpm overnight (*M. smegmatis*), 48 hrs (*M. abscessus*). For *M. bovis*, the incubation was statically for 1 week. Then, the cultures were used to inoculate 3 conical glass flasks, each contains 25 ml 7H9-ADC-Tween 80 broth to OD<sub>580</sub> of 0.05, and incubated as above until grown to stationary phase. *M. smegmatis* was harvested after 24 hrs (OD = 4.5). *M. abscessus* was harvested after 48 hrs (OD = 2.5). *M. bovis* was harvested after 18-20 days (OD = 2.5).

#### **2.3.6. Cultivation of CL3 mycobacterial strains**

Mycobacteria that are classified by the Advisory Committee on Dangerous Pathogens (ACDP) as CL3 hazardous pathogens require biohazard containment at level 3. Therefore, all work with these strains was carried out in Class I or Class II microbiological safety cabinets within the containment laboratory suite, in accordance with the suite code of practice.

Cultivation of Mtb strains was done as described above for CL2 mycobacterial organisms. The initial cultures were incubated statically at 37 °C for 2 weeks. Then subcultured in 3 polycarbonate conical flask (Corning Life Science, Massachusetts, USA) at OD<sub>580</sub> 0.05, and incubated in shaking incubator (100 rpm) at 37 °C until stationary phase (OD = 1.9). Mtb strains were heat-killed before harvesting for hydrophobicity measurements.

### 2.3.7. Inactivation of CL3 mycobacterial strains

As a part of safety regulations at CL3 laboratories, it is obligatory to inactivate CL3 microorganisms before transferring them outside the CL3 laboratory. To do so, and in accordance with the suite code of practice, 10 ml of cells were transferred to 50 ml Falcon tubes and sealed with Micropore tape (Cat: 1530-0, 3M science, UK). The tubes were then fixed on a plastic rack inside the water bath. The validated temperature to kill CL3 microorganisms is 85 °C for 2 hrs.

## 2.4. Fluorescence microscopy

### 2.4.1. Immobilising of mycobacterial cells onto slides for microscopy

Mycobacterial cells were immobilised onto 76 x 26 mm glass slides using chamber block system (Figure 2.1). A 50 µl cell suspension was dispensed into each well of the silicone block followed by centrifugation at 1000 x g for 10 min in an IEC Centra-4X centrifuge (International Equipment Company, Dunstable, Bedfordshire, UK). The supernatant then was removed and the coverslip was air dried in the dark. Smears then were mounted in 10 % (w/v) glycerol in PBS and sealed with transparent nail varnish.

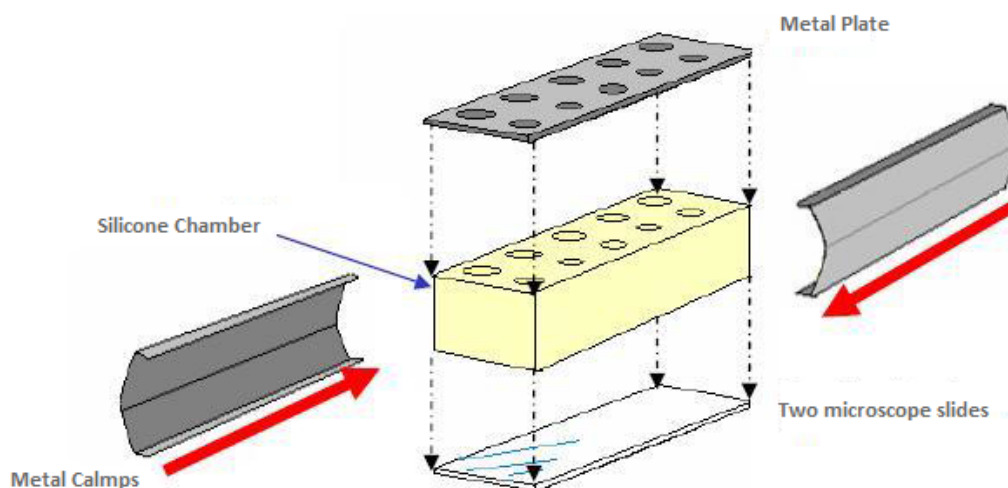


**Figure 2.1. Diagrammatic representation of the assembly of the chamber block.** The chamber block used to prepare bacterial monolayers for microscopy. Image taken from (Sherratt, 2008).

### 2.4.2. Recording fluorescence images

All stained slides were prepared and imaged on the same day using an inverted microscope (Nikon Eclipse Ti) under X100 objective oil immersion. Images were recorded with a 12/10bit, high speed DS-U3 CCD camera Build 831 (Nikon Corporation, Japan) using Nikon NIS Elements Imaging Software. The two sets of filters were used for epifluorescence microscopy are shown in Table 2.2.

**Table 2.2. Filters sets which were used for epifluorescence microscopy.**

Filter Block (Chroma)	excitation	Dichroic mirror	emission
ET-GFP (FITC) (49002)	470 $\pm$ 20nm	500DCLP	525 $\pm$ 25nm
ET-Texas Red/mCherry (49008)	560 $\pm$ 20nm	585LP	630 $\pm$ 37.5nm

### 2.4.3. Image analysis

The image analysis was done using a method developed by Andrew Bell at the University of Leicester (Bell, 2013). The method based on calculating fluorescence intensity data using ImageJ-based software (National Institutes of Health, Bethesda, Maryland). For each phase image, regions of interest were identified by ImageJ through thresholding. The region of interest then was applied to the corresponding fluorescent image and the pixel fluorescent intensity was measured (Bell, 2013). The fluorescence intensity of each cell per unit area was calculated and compared the cell intensity with the cut off value determined automatically by the imageJ software (Bell, 2013). The R Project Software Environment for Statistical Computing (R Development Core Team, GNU General Public License and The University of Auckland, New Zealand) was used to filter out non-cellular fluorescence signals (Bell, 2013).

## 2.5. Statistical analyses and graphical representation of significance

All statistical analyses in this project and significance tests were performed using multiple t-test with the Sidak correction, unless otherwise stated, using Prism 7 (GraphPad Software, Inc.) statistical software. The significance between results is displayed graphically according to Table 2.3.

**Table 2.3. Display of significance used in this thesis.**

Significance	Denoted by
$P \leq 0.05$	*
$P \leq 0.01$	**
$P \leq 0.001$	***
$P \geq 0.05$	NS

# **Chapter three**

## **3. Hydrophobicity studies**



### 3.1. Introduction

Mtb is a highly successful and widely transmitted pathogen causing extensive morbidity and mortality. It is transmitted via airborne droplets expelled by infected individuals. A preliminary study in this lab has indicated that the bacterial composition and Mtb transcriptome of aerosol from TB patients is distinct from that in contemporaneous sputum (Nardell *et al.*, 2016). This led to the hypothesis that aerosolisation from the respiratory tract may be a selective process in which only a sub-population of bacterial cells with specific features is expelled. The features of these successfully aerosolised cells are still to be explored. As noted in chapter 1, Minnikin and colleagues have suggested that cell hydrophobicity may contribute to the selection process (Minnikin *et al.*, 2015, Jankute *et al.*, 2017). Mycobacteria are unique in their high (60 % by dry weight) lipid composition and the presence of hydrophobic long chain fatty acid in their cell envelope that renders them hydrophobic (Chen *et al.*, 2006). To explore this hypothesis further, mycobacterial CSH has been investigated using *M. smegmatis* and *M. bovis* BCG as model organisms.

CSH of microbes can be measured by several techniques (chapter 1 section 1.4.5.). Amongst these techniques, the MATH technique is the most widely used as it is easy-to-conduct, rapid, and requires only basic equipment (vortex mixer and spectrophotometer) (Rosenberg, 1991, Rosenberg, 2006).

Since the MATH assay was first described in 1980, several studies have used modifications and no standard protocol is available. This may have contributed to discrepant results between studies. Aside from the period allowed for phase separation, multiple conditions have been reported to affect the CSH measurement, notably the suspension medium pH and ionic strength (Bunt *et al.*, 1993). Since different organisms respond to these modifications differently (Donlon and Colleran, 1993, Busscher *et al.*, 1995, Saini, 2010), it was important to establish standardised conditions here.

While the MATH technique is a semi-quantitative method applicable to sufficient biomass to be measured by optical density, hydrophobic fluorescent microsphere beads

can be used to measure CSH at the single cell level (Zita and Hermansson, 1997). This approach can be used to study heterogeneity of CSH in a population of bacteria (Zita and Hermansson, 1997). The *in vitro* work described here is intended to inform understanding of the mycobacteria exhaled and coughed up by patients with TB. Parallel studies in this laboratory are concerned with defining the phenotypes of these bacilli in samples of sputum and exhaled material (Garton *et al.*, 2008, Williams *et al.*, 2014, Williams *et al.*, 2018) and the microsphere method has been evaluated here as a candidate method to achieve CSH determinations in such samples.

The Congo Red assay to assess relative CSH was also used here. Congo Red is an amphiphilic dye that associates with lipophilic regions in the cell wall (Cangelosi *et al.*, 1999). It has previously been used to distinguish between virulent and avirulent strains of several bacterial species (McKay *et al.*, 1985, Qadri *et al.*, 1988) and has also been used to assess the presence of hydrophobic cell surface proteins in colonies of enterovirulent *Shigella* spp. and curli-producing *E. coli* (Ambalam *et al.*, 2012). Jankute and co-workers used the Congo Red assay to distinguish the low CSH of smooth colony-forming *M. canettii* and rough colony-forming Mtb H37Rv (Jankute *et al.*, 2017). In the current study, this assay was used to distinguish *M. abscessus* rough and smooth phenotypes and compared to the MATH and microsphere bead assays. The possibility of applying Congo Red determinations at the single cell level was also explored.

Cell wall lipid composition and CSH of mycobacteria are related and it has been proposed that CSH influences mycobacterial cell propensity for aerosolisation (Minnikin *et al.*, 2015). In non-tuberculosis mycobacteria, a relationship between inferred CSH and aerosolisation was previously demonstrated (Falkinham, 2003). Once the tubercle bacilli are aerosolised, they remain suspended in the air. When a new host inhaled these bacilli, and depending on the aerosol particle size, the aerosol will be located at different locations inside the respiratory tract (Teitelbaum *et al.*, 1999).

A noteworthy example of the potential link between CSH, propensity for aerosolisation and transmission is the smooth colony *Mycobacterium canettii*. The cell wall of this pathogen contains the hydrophilic lipooligosaccharides (LOSs) and phenolic glycolipids

(PGLs) and it expresses relatively low CSH (Minnikin *et al.*, 2015). While this pathogen causes TB in East Africa, it has not spread outside this region and therefore appears less transmissible than the modern more hydrophobic and more disseminated strains of Mtb (Koeck *et al.*, 2011).

Bacterial aerosols have been studied extensively in the past and regardless of specific study aims, nebulisers have been used to generate the test aerosols. The most widely used system is the Collison nebuliser (one, three or six jet). In the current work, in addition to the 3-jet Collison nebuliser, the A3 complete Omron and the ultrasonic Omron nebulisers have been used. The rationale behind using multiple nebulisers in this study was first to try to mimic the natural aerosol formation inside the respiratory tract and second to investigate the influence of different mechanisms of aerosolisation on the outcomes. The nebulisation mechanisms of these instruments are discussed in the method section 3.2.9. The impact of these nebulisers on the bacterial cells tested is investigated in chapters 4 and 5.

## Aim and objectives

The main aim here was to investigate mycobacterial CSH and begin to explore the relationship of this parameter to aerosolisation. In this regard, the work has been divided into three stages. First, an investigation of the factors affecting results from the MATH and its subsequent optimisation for the present study along with preliminary studies of alternate methods to determine CSH at the single cell level (to enable recognition of heterogeneity within populations and to establish potential to measure CSH in low abundance clinical samples). Second, the establishment of a system in which aerosolisation could be studied; and third, a comparison of different nebulisers.

The work was conducted predominantly with *M. bovis* BCG as a surrogate model for *Mtb* but initial experiments were done with *M. smegmatis*. *M. abscessus* strains were also investigated because smooth and rough variants provided an opportunity to test aspects of CSH measurement.

The objectives were:

- 1) To investigate the influence of different assay parameters on the measurement of CSH using the MATH method.
- 2) To determine the effect of BCG growth phase on CSH.
- 3) To evaluate potential of the fluorescent bead and Congo Red method to determine CSH at the single cell level.
- 4) To compare CSH of lab and clinical isolates of *Mtb* strains.
- 5) To establish a simple contained system for aerosolisation experiments with different nebulisers.

## 3.2. Methods

### 3.2.1. Bacterial suspension preparation

CL2 (*M. smegmatis*, *M. bovis* and *M. abscessus*) and CL3 (Mtb H37Rv, Mtb Beijing 65, Mtb CH and Mtb Loughborough) organisms were grown to stationary phase as described in sections 2.3.5. and 2.3.6., respectively and harvested on the day of the experiment. All experiments were done one time in three biological and technical replicates (total 9 samples) for each experiment.

### 3.2.2. CSH measurement using the MATH technique

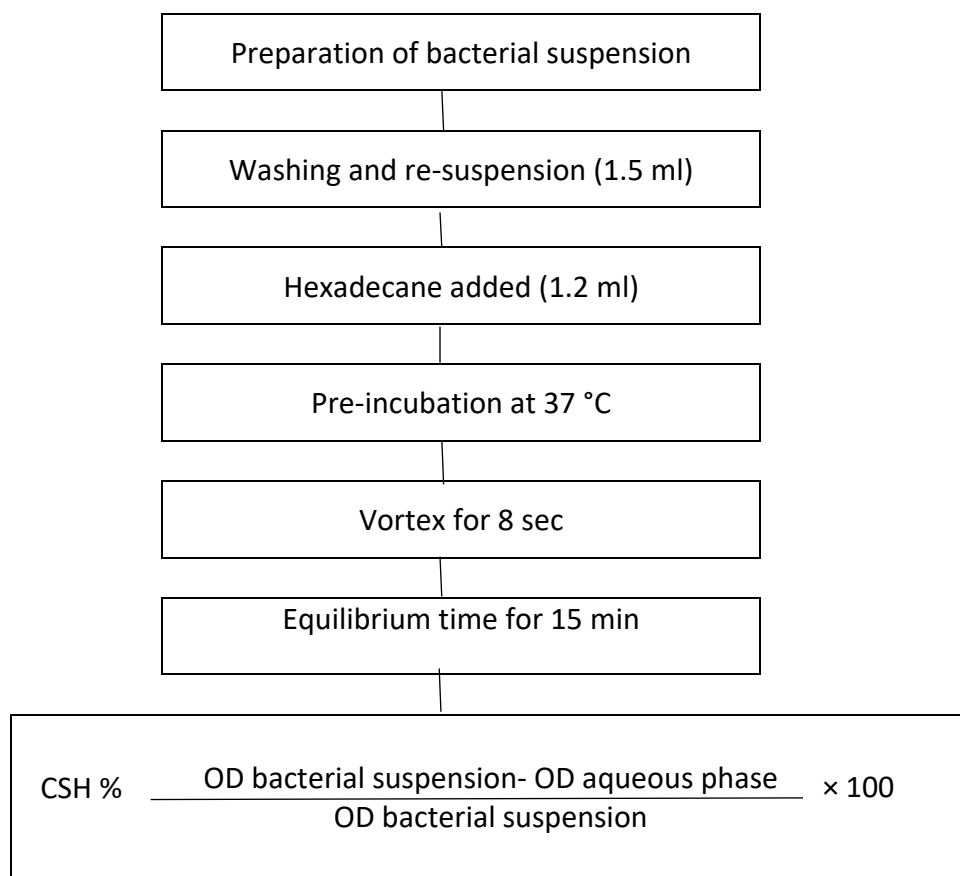


**Figure 3.1. Schematic of the basic the MATH procedure used in this study.** After (Stokes et al., 2004).

Basic method: 10 ml of bacterial suspension was pelleted by centrifugation at 3000 x g for 20 min and resuspended in Phosphate-urea-magnesium (PUM) buffer (see below). The optical density (OD<sub>600nm</sub>) was then adjusted to 0.7 and 1.5 ml transferred to borosilicate glass tubes (11 by 120 mm) and 1.2 ml of hexadecane added. This preparation was incubated at 37 °C for 8 min then vortexed for 8 sec. The tubes were then stood at RT for 15 min to allow the aqueous and organic phases to separate. Finally, the lower aqueous layer was transferred to a plastic spectrophotometer cuvette with a glass Pasteur pipette and OD<sub>600nm</sub> measured. The hydrophobicity measurement was calculated with the formula shown in figure 3.1.

### 3.2.3. Variations in the MATH method investigated

The CSH measurement was assessed following the protocol used by Stokes *et al.*, 2004. This was modified to investigate the influence of buffer composition and protocol steps such as phase separation time, temperature, and vortexing duration. In addition to other parameters such as initial cell concentration, hydrocarbon-aqueous phase volume ratio, and suspended medium were also assessed.

#### 3.2.3.1. Variations in buffer composition

##### Urea concentration

In addition to the PUM buffer as a control, three other PUM buffers with different urea concentration (Table 3.1.) were prepared and used.

Components of Buffer	PUM	PUM (U-)	PUM (3X)	PUM (10X)
Potassium phosphate dibasic trihydrate (K <sub>2</sub> HPO <sub>4</sub> ·3H <sub>2</sub> O)	22.2 g	22.2 g	22.2 g	22.2 g
Potassium Phosphate Monobasic (KH <sub>2</sub> PO <sub>4</sub> )	7.26 g	7.26 g	7.26 g	7.26 g
Urea	1.8 g	-	5.4 g	18 g
Magnesium Sulfate Heptahydrate (MgSO <sub>4</sub> ·7H <sub>2</sub> O)	0.2 g	0.2 g	0.2 g	0.2 g

**Table 3.1. PUM buffers.** The components were dissolved in 1 L DW and autoclaved for sterilisation (Rosenberg *et al.*, 1980).

## pH

Three different buffers with constant ionic strength (similar to the PUM buffer, 150 mM) and different pH were prepared and used (Table 3.2.).

Buffer	Composition	pH
A	Acetic acid + KOH	5.0
B	Potassium phosphate monobasic ( $\text{KH}_2\text{PO}_4$ ) + Sodium phosphate dibasic ( $\text{Na}_2\text{HPO}_4$ )	7.0
C	Sodium tetraborate decahydrate ( $\text{Na}_2\text{B}_4\text{O}_7$ ) + $\text{H}_3\text{BO}_3$	9.0

**Table 3.2. pH buffers.** Compositions of buffers used for the pH experiment. The reference used to prepare these buffers was Data for Biochemical Research. Dawson *et al.*, 1969. The components were prepared and dissolved in 100 ml DW each. The buffers then sterilised by autoclave or filter sterilisation where appropriate (Dawson *et al.*, 1969).

## Ionic strength

Five different phosphate buffers (PBs) with constant pH (similar to the PUM buffer, 7.0) and different ionic strength were prepared and used (Table 3.3.).

Buffer	Composition	Ionic Strength
PUM (0.15M)	PUM buffer (control)	0.15 M
PB (0.01M)	Potassium phosphate monobasic ( $\text{KH}_2\text{PO}_4$ ) + Sodium phosphate dibasic ( $\text{Na}_2\text{HPO}_4$ )	0.01 M
PB (0.1 M)	Sodium phosphate dibasic ( $\text{Na}_2\text{HPO}_4$ ) + Sodium phosphate monobasic ( $\text{NaH}_2\text{PO}_4$ ) + Sodium chloride (NaCl)	0.1 M
PB (0.2M)	Sodium phosphate dibasic ( $\text{Na}_2\text{HPO}_4$ ) + Sodium phosphate monobasic ( $\text{NaH}_2\text{PO}_4$ ) + Sodium chloride (NaCl)	0.2 M
PB (0.5M)	Sodium phosphate dibasic ( $\text{Na}_2\text{HPO}_4$ ) + Acetic acid.H <sub>2</sub> O + Potassium chloride (KCl)	0.5 M
PB (1.0M)	Sodium phosphate dibasic ( $\text{Na}_2\text{HPO}_4$ ) + Acetic acid.H <sub>2</sub> O + Potassium chloride (KCl)	1.0 M

**Table 3.3. Ionic strength buffers.** Compositions of the buffers used for the ionic strength experiment. The reference used to prepare these buffers was Data for Biochemical Research. Dawson *et al.*, 1969. The components were prepared and dissolved in 100 ml DW each. The buffers then sterilised by autoclave or filter sterilisation where appropriate (Dawson *et al.*, 1969).

### 3.2.3.2. Variations in protocol steps

Parameter	Standard	Modifications	
Phase-separation time	15 min	3.5, 7, 30, 60 min	
Temperature	Pre-incubation at 37 °C Vortexing at RT Phase-separation at RT	Pre-incubation at <b>37 °C</b> Vortexing at RT Phase-separation at <b>37 °C</b>	Pre-incubation at <b>RT</b> Vortexing at RT Phase-separation at <b>RT</b>
Vortexing duration	8 sec	NO vortex, 4, 16 sec	

**Table 3.4. Parameters related to the MATH procedure and the modifications applied to each step.** In light of results (table 3.6) a digitally controlled vortexer (Scientific Industries, Digital Vortex Mixer (SI-A236, UK) was used to standardise this step.

### 3.2.3.3. Other variations

Parameter	Original	Modifications
Cell density	OD <sub>600</sub> 0.7	OD <sub>600</sub> 0.2, 0.4, 0.6, 0.7
Hexadecane-aqueous phase volume ratio	0.8 (1.2 ml hexadecane vs 1.5 ml bacterial suspension).	0.2, 0.4, 2.0, 3.0
Suspended medium	PUM	PBS, 7H9 without supplementation, RPMI, DW

**Table 3.5. Other parameters were modified to investigate the influence of these parameters on CSH measurement using the MATH technique.**

### 3.2.4. Investigating the Influence of bacterial growth phase on CSH

*M. bovis* BCG was grown as in section 2.3.6, and CSH measurements was assessed at early exponential (1 week), late exponential (2 weeks), stationary (3 weeks) and late stationary phase (4 weeks).



### 3.2.5. Effect of fixation on CSH measurements

This experiment was done prior to conducting the CSH experiments with some of CL3 Mtb strains. The aim of this experiment was to investigate whether fixing mycobacterial cells will alter CSH measurement. *M. bovis* BCG at stationary phase was used as a surrogate for Mtb.

10 ml of *M. bovis* culture was transferred to 50 ml Falcon tube and pelleted by centrifugation at 3000 x g for 10 min. The supernatant was discarded and 10 ml of 4 % Formaldehyde was added to the tube and incubated at RT overnight. CSH measurement assay using the MATH method and un-treated live *M. bovis* BCG was used as control.

### 3.2.6. CSH measurements of Mtb strains

Beside the laboratory strain, H37Rv, three clinical isolates of Mtb were used in this experiment. The mycobacterial strains were grown as described in section 2.3.8 and heat-killed as described in section 2.3.9. The MATH technique was used to measure CSH measurements of these strains.

### 3.2.7. Additional techniques to measure CSH

#### 3.2.7.1. Relative Congo Red binding assay

Congo Red binding is an established CSH assessment in which test bacterial strains are grown on dye containing medium and show differences in colony colour that reflect CSH level. Red colonies indicate more absorbance of the dye and hence higher CSH. White colonies indicate no absorbance of the dye and hence lower CSH. These differences are quantified by measuring absorbance of dye after extraction from a known biomass of bacterial growth. A particular interest here was the investigation of the possibility that Congo Red binding could be assessed at the single cell level. *M. abscessus* was used so that rough and smooth strains could be compared.

*M. abscessus* rough and smooth strains were kindly provided by Ms Enass Al-Mkhadree of this lab and included the type strain and clinical isolates. These were grown in Middlebrook 7H10-OADC-Tween 80 plate supplemented with Congo Red dye at a final concentration of 100 µl/ml and incubated at 37 °C until colonies became visible. 10-15 colonies were scraped off the plates and added to 3.5 ml SDW and OD<sub>600</sub> adjusted to 0.5. After recording the OD<sub>600</sub> of the suspension, cells were pelleted, resuspended in 200 µl acetone, vortexed and allowed to sit at RT for 2 hrs. Cells were then pelleted by centrifugation at 5,000 x g for 5 min and absorbances measured at 490nm in the supernatants in a microplate reader (model: LE808, BioTek, Dorest, UK,) using acetone as the blank. The final results were calculated by dividing the value at OD<sub>490</sub> by the value of the OD<sub>600</sub> of the original cell suspension (Cangelosi *et al.*, 1999).

Preparation for Congo Red assay to measure CSH on a single level variant was done following an optimised in-house protocol as follow:

Congo Red solution was prepared by dissolving Congo Red powder (Cat: C6767, Sigma-Aldrich, UK) in water at a concentration of 10 mg/ml. 990 µl of *M. bovis* BCG at stationary phase was add to a microfuge tube then 10 µl of the Congo Red solution was add to the tube to make a final concentration of 100 µl/ml. the tube was incubated in the dark at 37 °C for 1 hr. The labelled cells were harvested by centrifugation at 5,000 x g for 5 min and washed with DW twice then re-suspended with DW. Finally, slides were prepared using the chamber block system (section 2.4.1) and at least 100 labelled bacterial cells were imaged by fluorescence microscope. The excitation/emission wavelengths were 590/620 nm) (Clement and Truong, 2014).

### 3.2.7.2. Fluorescent microsphere beads

Fluorescent polystyrene microspheres (diameter 0.2  $\mu\text{m}$ ) with a modified surface that rendered them hydrophobic (sulfate-modified, FluoSpheres, ThermoFisher Scientific cat. no. F-8847) were used in this investigation. The excitation/emission wavelengths were 505/515 nm.

The protocol was that described by Zita *et al.*, 1997. The microspheres were diluted in DW to 10 % (v/v) and sonicated for  $\sim 100$  min to achieve uniform dispersal. Next, 10  $\mu\text{l}$  of the preparation and 10  $\mu\text{l}$  of bacterial suspension were added to 100  $\mu\text{l}$  SDW in a 2 ml microfuge tube and vigorously mixed by vortexing for 2 min. Finally, slides were prepared using the chamber block system (section 2.4.1). At least 100 bacterial cells were examined by a fluorescent microscope for attached microspheres (Zita and Hermansson, 1997) (Figure 3.2.).

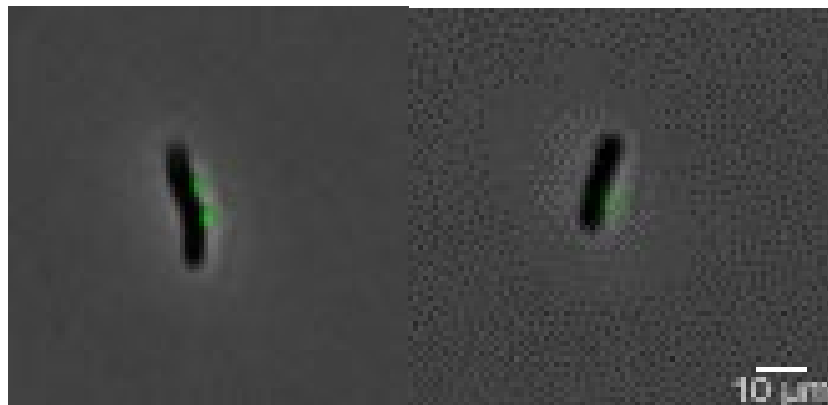


Figure 3.2. Fluorescent hydrophobic microspheres attached to *M. bovis* BCG cells.

### 3.2.8. Aerosolisation system

The components of the system are shown in figure 3.3 and a schematic diagram of the system is illustrated in Figure 3.4. A perspex board was inserted inside an autoclave bag. The board was held by a stand holder on the upper left corner of the autoclave bag. The bag was then cut into the appropriate size and sealed using a plastic heat sealer. A small hole on the lower left corner of the bag was created to hold the HEPA filter (Parker Finite Filter, IND-6G, Max press: 100 PSIG, Max temp: 50 °C, Body material: NYLON) and sealed

with tape. Another hole was created on the upper right corner to connect the nebuliser and sealed with a tape. A second stand holder was used to hold the nebuliser. The nebuliser was connected to the pump via a tube (Figure 3.3).

It should be noted that in different types of experiments conducted in our lab, the perspex board was used to hold strips and filters to investigate the ability of these materials to capture aerosolised cells.



**Figure 3.3.** Overview of the organization of equipment used for aerosolisation experiment inside class II safety cabinet.

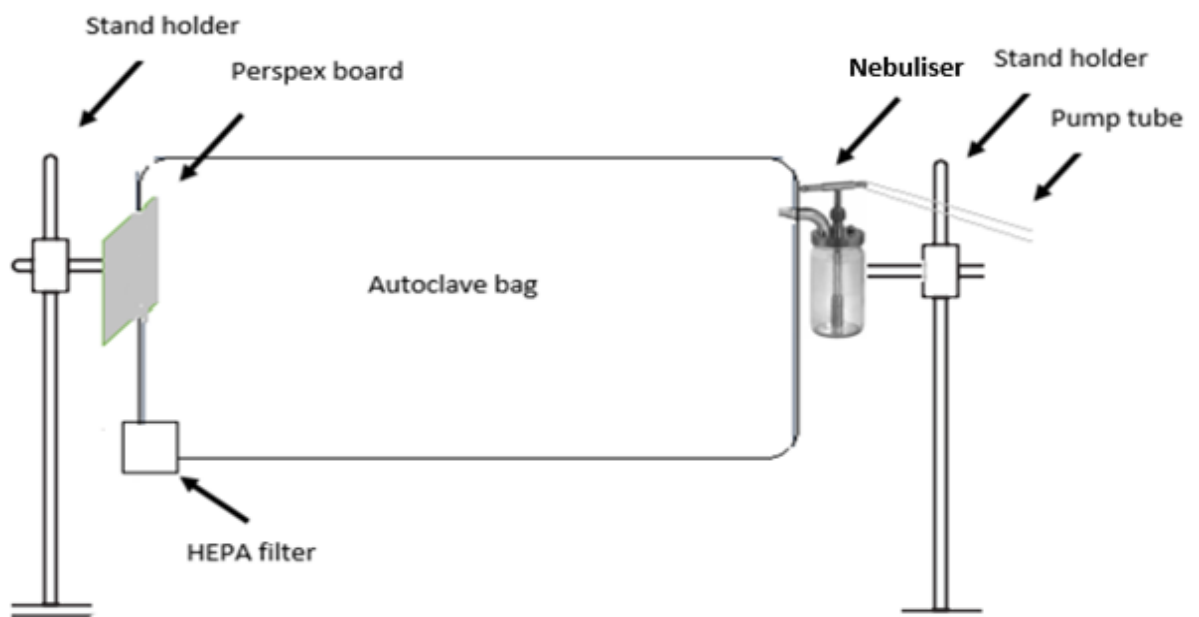


**Figure 3.4.** Schematic diagram of the aerosolisation system.

### 3.2.9. Nebulisers used

#### 3-Jet Collison nebuliser

This device was introduced for the first time by W. E. Collison in 1932 and used in several applications including bioaerosol studies (May, 1973). Compressed air is generated from an external pump (Model 35/20, Bambi-Air, Birmingham, UK) at 26 psi and passed through the gas inlet. When this compressed air reaches the jet orifice, a jet will be formed that expands through the jet expansion channel creating negative pressure. This negative pressure causes suction of the liquid suspension in the reservoir through the siphon tube. The liquid being siphoned forms droplets due to the strong shear of high-speed jet flow. The liquid droplets produced have a very wide size distribution. Large droplets are impacted against the nebuliser wall resulting in the generation of smaller droplets that aerosolised. The average droplet size aerosolised is  $\sim 3 \mu\text{m}$  (Feng, 2018) (Figure 3.5).

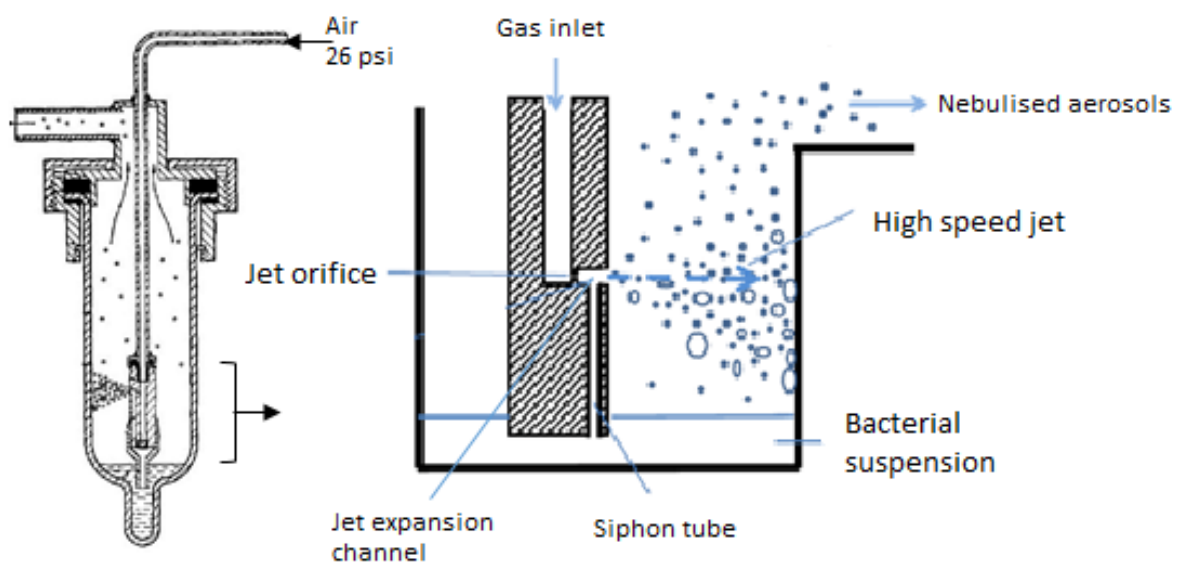


**Figure 3.5. Collison nebuliser.** The liquid in the reservoir withdrawn by the action of compressed air. Droplets are generated then broken into smaller droplets and aerosolised, image taken from (Feng, 2018).

### A3 complete Omron nebuliser

This device (Omron (<https://www.omron-healthcare.com/en>)) includes an internal pump producing compressed air forced through a narrow hole which is mixed with the bacterial suspension inside the reservoir. This mixture is aerosolised when in contact with the baffle (Figure 3.6). The size of the aerosol can be controlled by adjusting the ring on the medication cup. There are 3 positions for the ring to control the aerosol size; position 1  $\approx 10\ \mu\text{m}$ , position 2  $\approx 5\ \mu\text{m}$  and position 3  $\approx 3\ \mu\text{m}$ . Because the aerosol particle size of 3-Jet Collison nebuliser was  $3\ \mu\text{m}$ , it was the choice of position 3 when the A3 Omron nebuliser was used in this study to make an appropriate comparison between the two nebulisers.

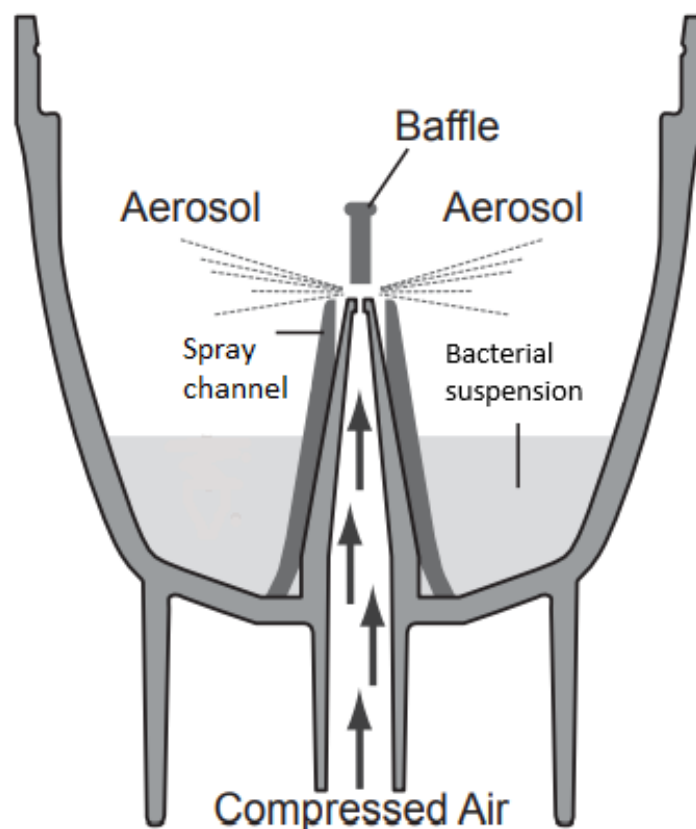


**Figure 3.6. A3 complete Omron nebuliser.** The bacterial suspension is drawn up through a spray channel by compressed air and turned into fine particles and sprayed when in contact with the baffle (Image from Omron instruction manual).

### Ultrasonic NE-U780 Omron nebuliser

This device (<https://www.omron-healthcare.com/en>) has a vibrator/sonicator located under a water bath. The vibrations are transferred through the water to the medication cup (containing the bacterial suspension) producing the bacterial aerosol and a fan drives the aerosols outside the nebuliser (Figure 3.7). The size of the aerosol produced is approximately  $4.6\ \mu\text{m}$  and there is no option to modify it.

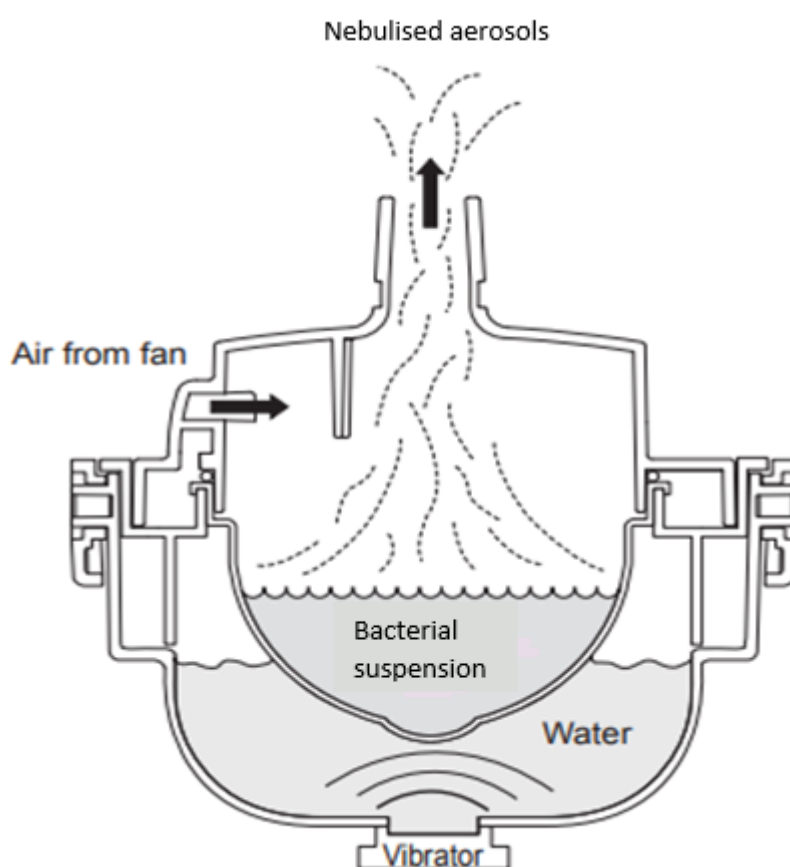


**Figure 3.7. Ultrasonic NE-780 Omron nebuliser.** The bacterial suspension is placed inside the medication cup (Image from Omron instruction manual).

**3.2.10. Investigating the influence of CSH on the propensity of cells for aerosolisation**

*M. bovis* BCG was grown in 7H9-OADC-Tween 80 to stationary phase (21 days old, OD = 2.4-2.6). 15 ml of bacterial suspension was added to the reservoir of the Collison and ultrasonic nebulisers. Due to the maximum capacity of A3 Complete Omron nebuliser, only 13 ml of the bacterial suspension was added to the reservoir. Aerosols were generated over 10 min. After nebulisation the remaining suspension in the reservoir was designated as the post-nebulisation sample, while the original suspension before nebulisation was designated the pre-nebulisation sample. CSH was assessed for both samples using the MATH technique.



### 3.3. Results

At the beginning of this work the basic methods were established using *M. smegmatis* as a convenient surrogate with a doubling time of 2-3 hrs (Stephan *et al.*, 2005). The influence of the parameters on the CSH measurements using *M. smegmatis* was similar to that with *M. bovis*.

#### 3.3.1. Influence of operational factors on CSH results with the MATH method

Stationary cultures of *M. smegmatis* (48 hrs) and *M. bovis* BCG (3 weeks) were prepared as described above (section 2.3.5) and washed once in PUM buffer or the variants indicated then added to the MATH assay. The variations tested are indicated in figure 3.8 and the results displayed in table 3.6. Influence of vortex duration and hexadecane-aqueous phase volume ratio is shown in Figure 3.8.

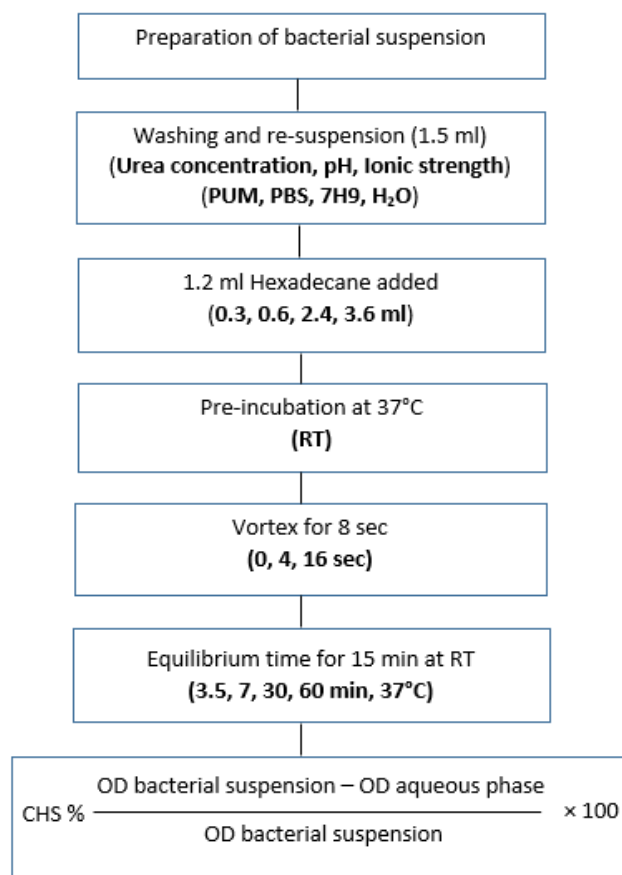


**Figure 3.8. Overview of steps in the MATH technique.** Parameters modified are shown in bold.

**Table 3.6. Summary of the results of the impact of different parameters on the measurement of CSH using the MATH technique.** All experiments done one time in biological and technical replicates.

(A) Factors related to the buffer		<i>M. smegmatis</i>			<i>M. bovis</i> BCG		
Factor investigated	Tested Condition	% CSH + SD	Control (PUM)	Anova	% CSH + SD	Control (PUM)	Anova
Urea concentration	PUM (U-)	44 ± 7.8	51 ± 5.0 (PUM (U1X))	NS	61 ± 3.0	65 ± 1.3 (PUM (U1X))	NS
	PUM (U3X)	52 ± 2.7			73 ± 7.8		
	PUM (U10X)	45 ± 7.9			66 ± 10.8		
pH	5.0	56 ± 1.8	55 ± 1.6 (pH =7)	NS	66 ± 8.2	71 ± 3.0 (pH =7)	NS
	7.0	55 ± 1.5			79 ± 12.6		
	9.0	54 ± 2.7			74 ± 8.1		
Ionic strength	0.01 M	40 ± 5.3	46 ± 8.0 (0.15 M)	NS	77 ± 9.2	66 ± 7.9 (0.15 M)	NS
	0.1 M	43 ± 2.9			70 ± 5.7		
	0.2 M	47 ± 8.5			64 ± 9.1		
	0.5 M	46 ± 6.5			65 ± 6.9		
	1 M	45 ± 2.1			65 ± 2.1		
(B) Factors related to the procedure steps							
Temperature	37 RT	ND	ND	ND	60 ± 7.5 63 ± 5.6	62 ± 6.6	NS
Equilibrium time	3.5 (min)	46 ± 3.9	44 ± 1.5 (15 min)	NS	69 ± 10.8	69 ± 9.3 (15 min)	NS
	7 (min)	46 ± 2.5			70 ± 9.6		
	30 (min)	44 ± 3.9			71 ± 10.6		
	60 (min)	45 ± 1.8			70 ± 9.5		
Vortex duration	0 (sec) *	12 ± 5.8	51 ± 3.4 (8 sec)	<i>p</i> < 0.0001	6.0 ± 2.4	66 ± 3.2 (8 sec)	<i>p</i> < 0.0001
	4 (sec) *	43 ± 5.4			48 ± 3.1		
	16 (sec) *	59 ± 3.7			82 ± 1.1		
(C) Other factors							
Cell concentration	0.2 (OD)	44 ± 2.8	46 ± 5.3 (OD = 0.7)	NS	76 ± 1.0	68 ± 5.3 (OD = 0.7)	NS
	0.4 (OD)	47 ± 4.0			72 ± 3.5		
	0.6 (OD)	41 ± 1.5			73 ± 2.9		
	0.8 (OD)	49 ± 3.0			72 ± 2.0		
Hexadecane volume	0.3 (ml) *	ND	ND	ND	57 ± 9.2	70 ± 1.8 (1.2 ml)	NS
	0.6 (ml)				65 ± 3.4		
	2.4 (ml)				68 ± 1.7		
	3.6 (ml)				75 ± 1.8		
Suspended medium	DW *	ND	ND	ND	51 ± 5.5	69 ± 5.6 (PUM)	NS
	PBS				61 ± 11.6		
	7H9				70 ± 4.0		
	RPMI				68 ± 2.3		
<i>M. smegmatis</i> vs <i>M. bovis</i> BCG controls variations			49 ± 4.2			67 ± 2.8	<i>p</i> < 0.0001

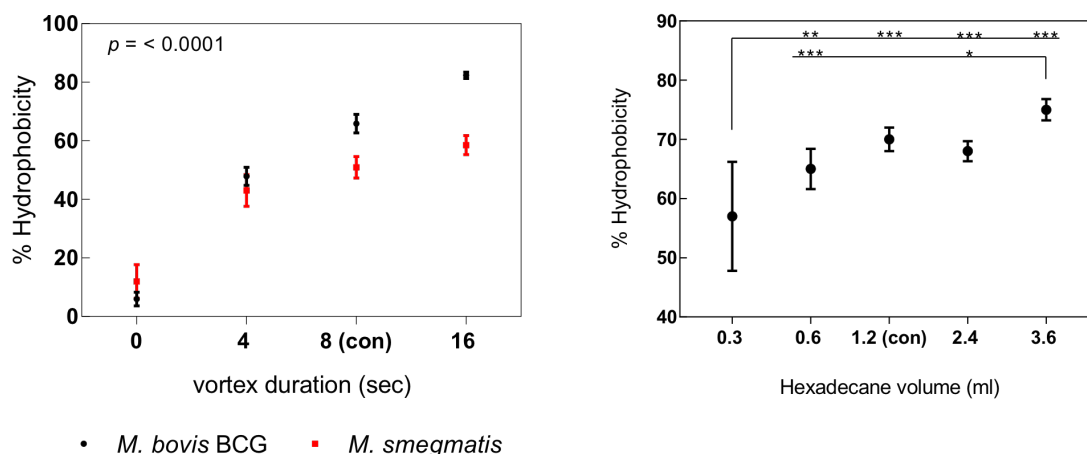


**Figure 3.9. Influence of vortex duration and hexadecane-aqueous phase volume ratio on the CSH measurements of *M. smegmatis* and *M. bovis* BCG..** Statistical analysis was performed using multiple t-test with the Sidak correction. (\* =  $P=0.02$ , \*\* =  $P=0.006$ , \*\*\* =  $P=0.0004$ ).

Urea concentration in the aqueous buffer was tested as urea is a chaotropic agent that interferes with non-covalent interactions. CSH measurements of both strains were not changed significantly by alteration of the urea concentration compared to the control buffer (U1X). However, CSH measurements of *M. bovis* BCG increased significantly when the buffer (U3X) was compared to (PUM-U) (\*  $P$  value = 0.01).

The influence of ionic interactions on CSH measurement was assessed by modifying the pH of the aqueous buffer. There was no significant change with either strain under the conditions used compared to the control. While CSH values of *M. smegmatis* were  $55 \pm 1$  regardless the aqueous buffer pH, the lowest CSH value of *M. bovis* BCG was 66 % at pH 5. This value was significantly different when compared to CSH value of 79 % at pH 7 (\*  $P$  value = 0.02).

Electrostatic interaction effects on CSH measurement were tested by altering the ionic strength of the aqueous buffer. CSH values of *M. smegmatis* showed an ascending trend with increased ionic strength without reaching statistical significance. In contrast, CSH values of *M. bovis* BCG showed a descending trend with increased ionic strength. A

significant difference was observed when the ionic strength of 0.01 M was compared to the other ionic strengths except for that of 0.1 M (\* P value =0.01).

Conducting the MATH technique at 37 °C or RT showed no significant difference in CSH values of *M. bovis* BCG. Furthermore, equilibrium time had no influence on CSH measurement of *M. smegmatis* or *M. bovis* BCG. However, the SD variations were higher (9-11 %) with *M. bovis* compared to (2-4 %) with *M. smegmatis*.

There was a strong positive correlation between CSH values and the duration of vortexing for both strains. There was a steep increase in CSH values of *M. smegmatis* from 12 % with no vortexing to 43, 51, and 59 % with 4, 8, and 16 sec duration of vortexing. This sharp increase was also observed with *M. bovis* BCG, where CSH value increased from 6 % with no vortexing to 48, 66, and 82 % with 4, 8, and 16 sec duration of vortexing (Figure 3.9).

Hexadecane-aqueous phase volume ratio was another parameter that appeared influential. CSH values of *M. bovis* BCG showed a significant ascending pattern with increasing volume of hexadecane. The lowest value of CSH was observed with 0.3 ml hexadecane (57 %) ascending to 75 % with 3.6 ml (Figure 3.9).

The influence of initial cell density was also explored. Although comparison of some values indicated significant differences there was no consistent trend with either *M. smegmatis* or *M. bovis* BCG.

Regarding the suspending medium, DW showed a significant effect with the lowest CSH value found over the whole series of experiments with *M. bovis* BCG at 51 %. None of the other media showed significant effects.

### 3.3.2. CSH increased at stationary phase compared to exponential phase

This experiment was done to investigate the influence of bacterial growth phase on CSH. Cultures were grown for one to four weeks and CSH was assessed.

Figure 3.10 shows that CSH was around 67 % at exponential and late exponential phases. The CSH then increased significantly to 72 % and 75 % when the cells reached stationary and late stationary phases, respectively.

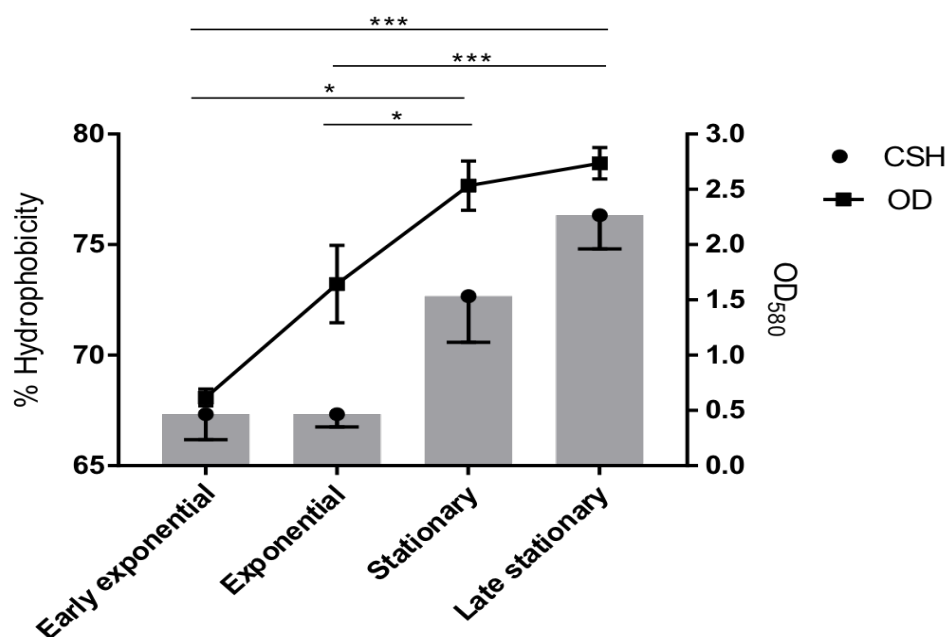


**Figure 3.10. Effect of growth cycle on CSH.** *M. bovis* BCG was grown to different growth phases and the CSH was assessed at each phase. The experiment was done from the same flasks in 1-week time intervals, early exponential (1-week-old culture), exponential (2-week-old culture), early stationary (3-week-old culture) and late stationary (4-week-old culture). The line graph shows the growth curve. The experiment was done one time in biological and technical triplicates and the error bar represents the standard deviation. Statistical analysis was performed using multiple t-test with the Sidak correction. (\* =  $P=0.01$ , \*\*\* =  $P=0.001$ ).

### 3.3.3. Additional techniques to measure CSH

#### Relative Congo Red binding assay

This experiment was done with *M. abscessus* smooth and rough phenotypes. On Congo Red agar plates (section 3.2.7.1), smooth phenotype colonies appear white and moist while rough phenotype colonies appear red and dry (Figure 3.11). A comparison between MATH and relative Congo Red binding assay showed compatible results, where the rough strain was significantly more hydrophobic than smooth strain (Figure 3.12).

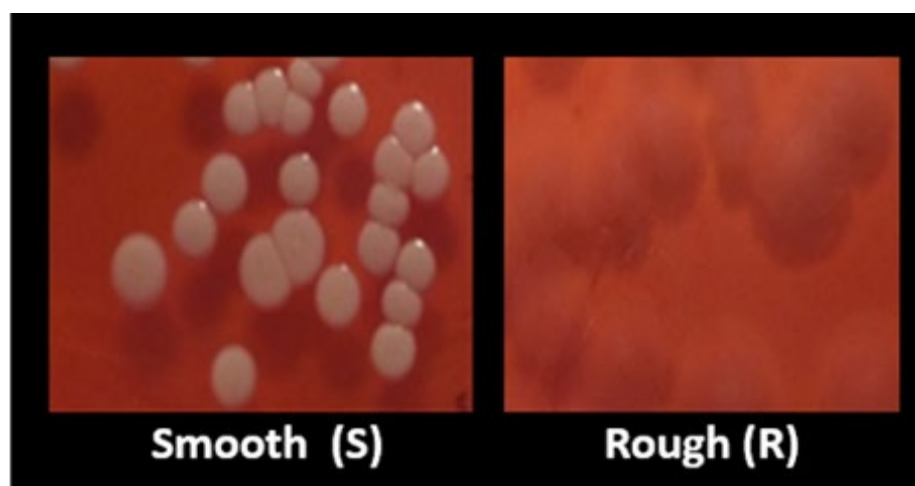


**Figure 3.11. Colony morphology of *M. abscessus* smooth and rough phenotypes.** Smooth phenotype colonies appear white and moist (left side) and rough phenotype colonies appear red and dry (right side). For the rough colonies it was impossible to obtain a higher-quality image because of the red colour of colonies “merged” with the red background.

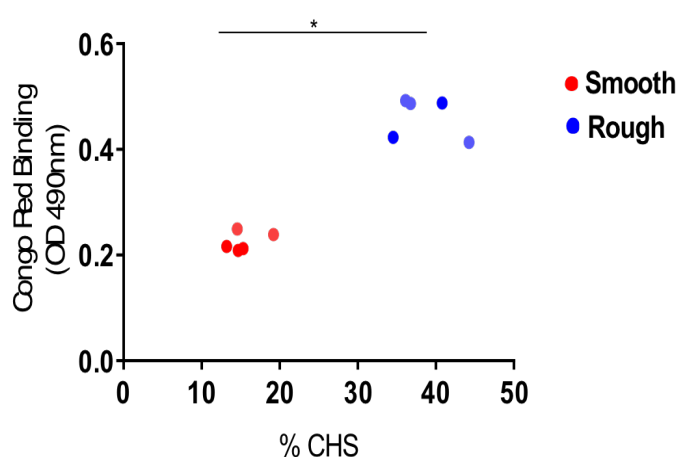


**Figure 3.12. CSH of *M. abscessus* smooth and rough phenotypes was assessed using the MATH and Congo Red binding assays.** Rough phenotype showed higher CSH values compared to smooth phenotype with both MATH and Congo Red assays. The experiment was done one time and the data represents the average of three replicates of each sample. Statistical analysis was performed using multiple t-test with the Sidak correction. (\* =  $P=0.01$ ).

### Fluorescent Microsphere beads

In contrast to MATH and Congo Red assays, fluorescent microsphere beads assay showed no significant difference in CSH between *M. abscessus* rough and smooth phenotypes (Figure 3.13).

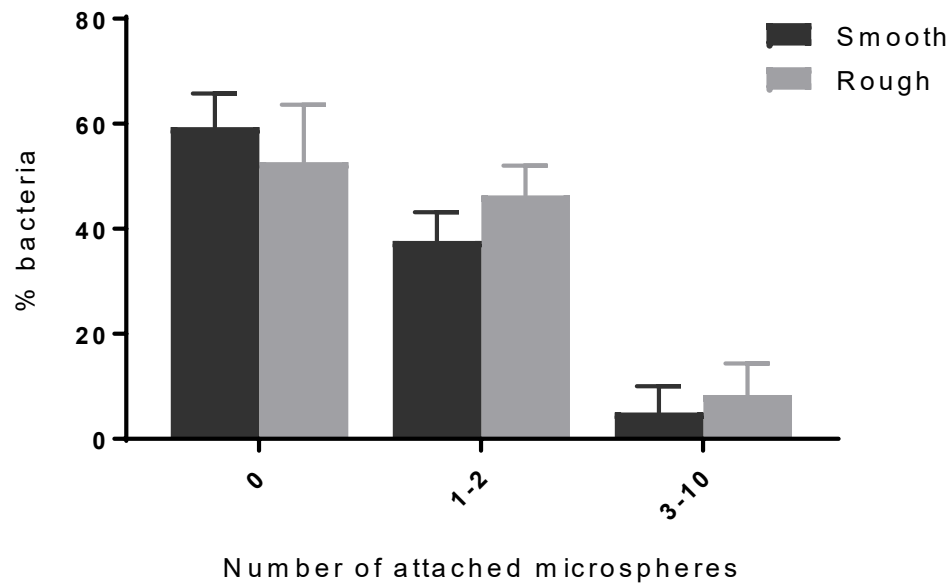


**Figure 3.13. CSH measurement using fluorescent microsphere beads method.** Similar pattern of distribution of cells with attached microsphere was obtained by smooth and rough *M. abscessus* phenotypes. The data represent the average of three replicates of each sample. The error bars show standard deviation. Statistical analysis was performed using multiple t-test with the Sidak correction.

Relative Congo Red and Microsphere beads assays were able to determine CSH of *M. bovis* BCG at the single-cell level. These experiments were done independent of each other. There were clear variations in the ability of cells in a single sample to absorb Congo Red dye (Figure 3.14A). Moreover, half of the cells in the population were without any microsphere attachment while the other half of cells adsorbed different numbers of microspheres (Figure 3.14B).

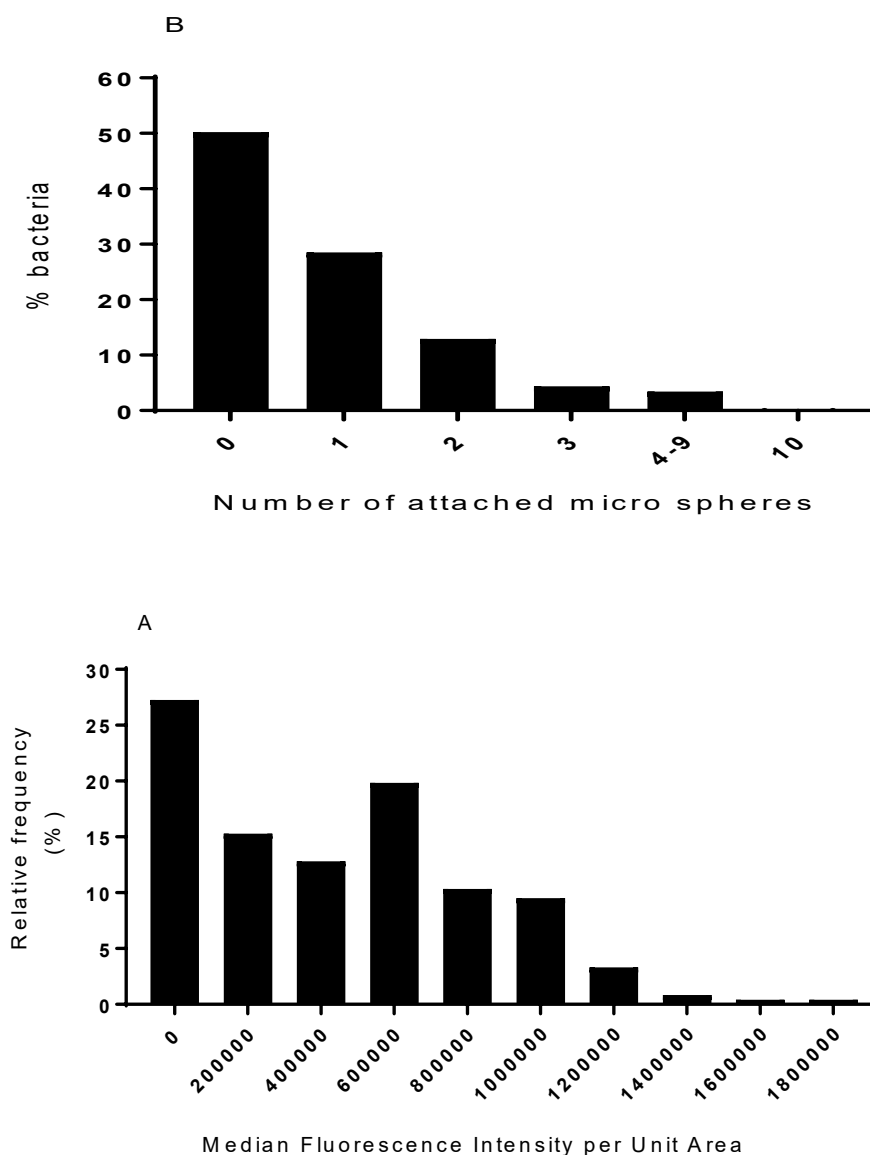


**Figure 3.14. Heterogeneity of *M. bovis* BCG using Congo Red and microsphere beads assays.** A) Histogram showing variations of *M. bovis* BCG cells in uptake Congo Red dye. B) Distribution of *M. bovis* BCG cells with attached microsphere beads. The experiment was done one time and the data represents the average of three replicates.



### 3.3.4. CSH measurement was not affected by fixation

*M. bovis* BCG culture at stationary phase was split into two halves; the first was treated with 4 % formaldehyde overnight and the second was untreated (section 3.2.5). CSH measurements were assessed for both halves using the MATH. Figure 3.15 shows that there was no significant difference between treated and control samples ( $P > 0.05$ ).

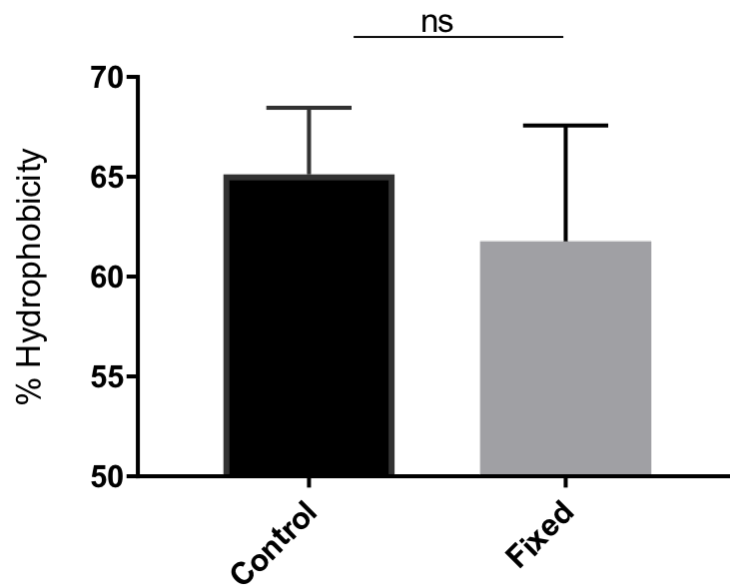


**Figure 3.15. Influence of 4 % formaldehyde fixation on CSH measurements of *M. bovis* BCG.** *M. bovis* BCG from stationary phase was fixed with 4 % formaldehyde overnight and measurement of CSH was assessed with the MATH technique. Error bar represents the standard deviation of three biological replicates. T-test was used for statistical analysis, ns = not significant.

### 3.3.5. Different Mtb strains showed different CSH values

Three clinical isolates of Mtb were grown to stationary phase (section 2.3.6) and heat-killed (section 2.3.7) then added to the MATH assay. Virulent laboratory strain H37Rv was included in this experiment. Figure 3.16 shows that Mtb CH was significantly less hydrophobic compared to Mtb H37Rv (\*\* =  $P=0.004$ ) while both Mtb Beijing and Mtb Loughborough strains were significantly more hydrophobic than Mtb H37Rv (\*\* =  $P=0.004$ , \*\*\* =  $P=0.0001$ ).

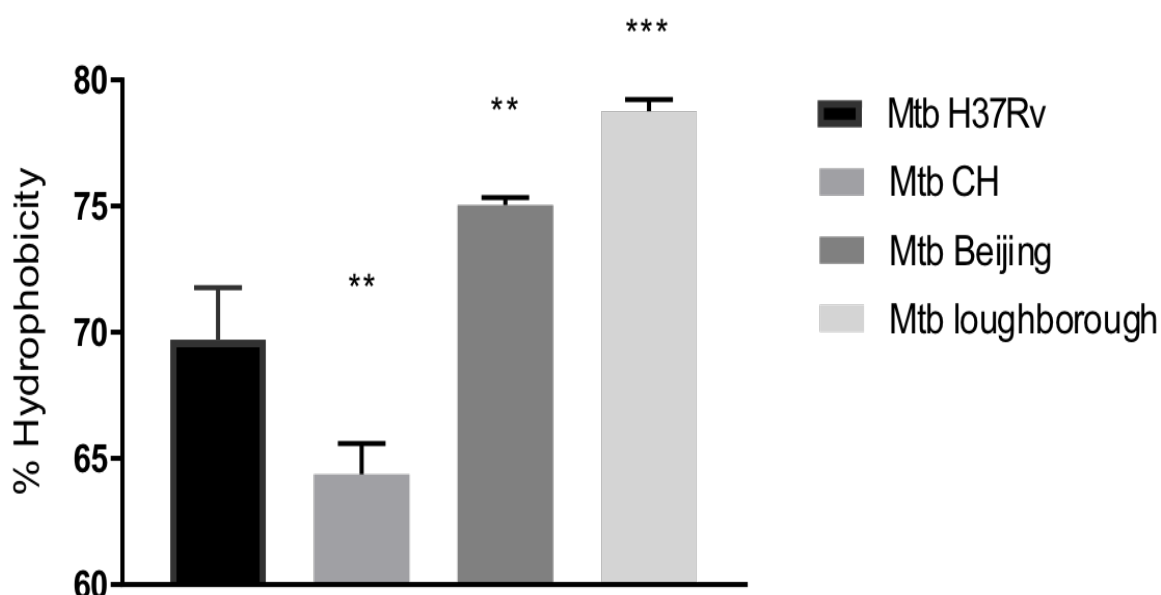


**Figure 3.16. CSH measurements of Mtb strains.** Multiple clinical isolates of Mtb strains were grown to stationary phase and CSH measurements were assessed and compared to laboratory strain H37Rv. The error bars show standard deviation. The experiment was done one time in three biological and three technical replicates. Error bars show standard deviation. Statistical analysis was performed using multiple t-test with the Sidak correction. (\*\* =  $P=0.004$ , \*\*\* =  $P=0.0001$ ).

### 3.3.6. CSH decreased significantly post nebulisation

The initial focus of this study was to test the hypothesis that propensity of cells to be successfully aerosolised is influenced by their CSH. This hypothesis was tested by conducting aerosolisation experiments using three different nebulisers. Stationary phase of *M. bovis* BCG Glaxo strain with a mean initial cfu of  $1.71 \times 10^7$ ,  $8.6 \times 10^6$  and  $1.2 \times 10^7$  / ml for Collison, A3 Complete and Ultrasonic nebulisers, respectively, were used. Figure 3.17 demonstrates a reduction in the CSH post-nebulisation compared to the pre-nebulisation with three nebulisers. It should be noted that three experiments were conducted with each nebuliser on different days with different bacterial suspensions.

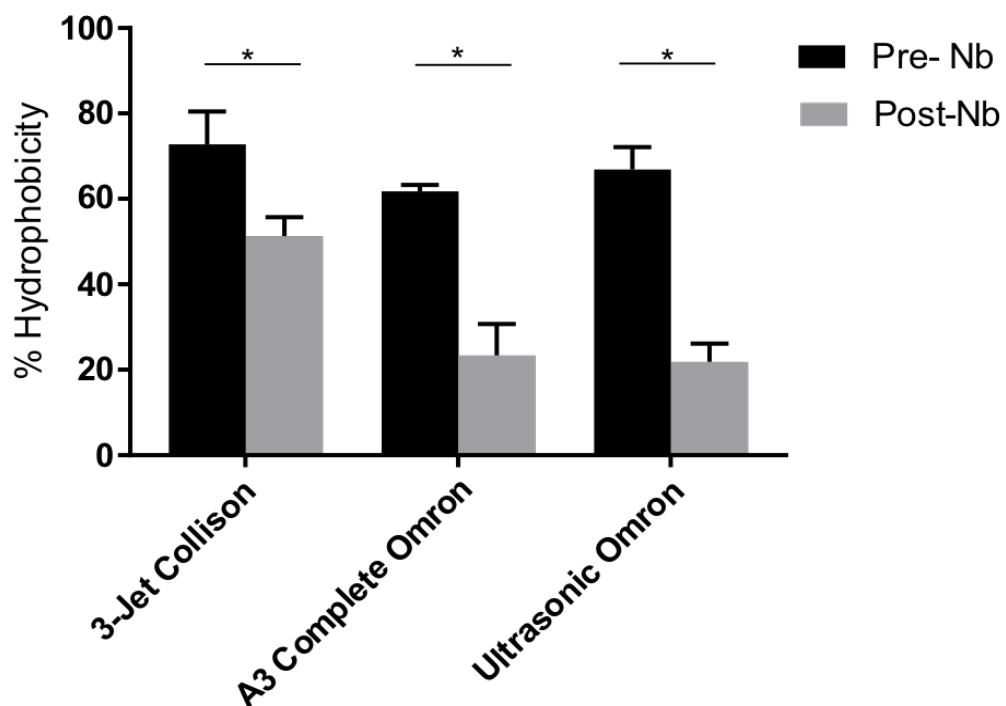


**Figure 3.17. Decreased in hydrophobicity post nebulisation.** *M. bovis* BCG from stationary phase was nebulized using three different nebulisers for 10 min. The hydrophobicity of pre- and post-nebulisation samples was assessed with the MATH technique. The error bars show standard deviation of three biological replicates. Statistical analysis was performed using multiple t-test with the Sidak correction. (\*\* =  $P=0.001$ , \*\*\*\* =  $P < 0.0001$ ).

### 3.4. Discussion

The main aim of the work in this chapter focused on the relationship between CSH and the propensity of cells for aerosolisation. The MATH technique was chosen as it is a relatively simple, rapid, and low-cost method to measure CSH. However, comparison between results from the literature is difficult to achieve as no standardised protocol was followed and several operational parameters have been shown to influence the CSH measurement (Rühs *et al.*, 2014).

In 1980, Rosenberg and colleagues studied the relationship between adhesion to oil droplets and their subsequent degradation by hydrocarbon-degrading bacteria (Rosenberg *et al.*, 1980, Rosenberg, 2006). Their study led to the development of the MATH technique. The original protocol used PUM buffer and this has subsequently been used extensively (Rosenberg, 2006). Alternative buffers have been used and these have been associated with differences in the CSH result (Rosenberg, 2006, Saini, 2010). The work described here represents the most systematic investigation of these and other factors in MATH-generated results.

#### 3.4.1 Influence of operational parameters on CSH measurement

The parameters investigated in the current study can be grouped depending on their relation to the procedure. The first group included parameters related to the aqueous buffer such as Urea concentration, while the second related to procedure steps such as mixing duration and finally parameters such as cell density were explored.

There are two proposed mechanisms by which urea denature proteins when it is present in the aqueous solution. Firstly, an indirect mechanism by altering the water structure via disrupting hydrogen bonding. This mechanism was suggested after experiments that showed increase solubility of hydrocarbons in aqueous urea. Secondly, the direct mechanism which is by interactions with the polar/apolar side chains and the peptide backbone of proteins (Canchi *et al.*, 2010). In this study, urea concentration had limited influence on CSH measurements of *M. bovis* BCG and *M.*

*smegmatis* were not affected significantly by the urea concentration in the aqueous buffer. This finding can be due to the low urea concentrations applied (maximum 10 X) and CSH measurement alteration required a higher concentration.

In 1982, Nesbitt and colleagues have shown that CSH measurement of *Streptococcus sanguis* using the MATH technique was maximum with low pH. They also have demonstrated a positive correlation between CSH measurement and ionic strength of the aqueous buffer (Nesbitt *et al.*, 1982). These findings were confirmed in later studies with *E. coli* (Bunt *et al.*, 1993). This observation was not seen in the current study as altering the pH or the ionic strength of the aqueous buffer did not affect the CSH measurements of *M. bovis* BCG and *M. smegmatis* significantly. It is worth noting that in the previous studies, they have tested pH ranges from 2.2 to 10 with two ionic strengths (0.5 and 1 M). However, in our study, we tested pH at 5, 7, and 9 at constant ionic strength (150 mM similar to the original PUM buffer). Also, when the ionic strength was altered (ranged from 0.01 to 1 M), the pH was constant at 7 (similar to the original PUM buffer). The discrepancy of these results can be explained by the difference in the species used as Mycobacteria species are generally more hydrophobic than Enterobacteriaceae. Also, the difference in the experimental design is a critical factor that can influence the results.

To our knowledge, the only study that investigated the influence of temperature on the CSH measurement using the MATH method was conducted by Nesbitt and co-workers. They have demonstrated that CSH value of *S. sanguis* increased significantly when conducting the MATH method at 37 °C compared with RT (23 °C) (Nesbitt *et al.*, 1982). However, in the study here, the result showed that assessing the CSH measurement using the MATH technique at 37 °C or RT has no significant difference. The difference in these findings can be due to the nature of the strains used in the studies. *M. bovis* in this study is more hydrophobic than *S. sanguis* which Nesbitt and colleagues used in their investigation (Nesbitt *et al.*, 1982).

Another step which has been modified largely in the MATH technique was the time applied to separate the organic and the aqueous phases (15 min in the original

protocol). The choice of the time applied across studies was arbitrary and ranged from 5 min to 60 min (Hsu and Huang, 2002, Duary *et al.*, 2011). In the current study, variations in phase separation period did not significantly affect CSH measurements of *M. bovis* BCG and *M. smegmatis* (ranged from 3.5 min to 60 min). These findings can potentially be attributed to the achievement of an equilibrium hexadecane saturation of aqueous phase at very early stage (3.5 min). These results are of importance for researchers dealing with multiple samples, as insensitivity to phase separation period eases samples process.

Increased CSH values resulting from increased mixing duration have been reported previously in studies with *Acinetobacter venetianus* (Baldi *et al.*, 1999), *Acinetobacter* sp strain (Hori *et al.*, 2008), and *Streptococcus pyogenes* (Lichtenberg *et al.*, 1985). These findings were consistent with the result obtained in the current study, where increased vortexing duration was accompanied with increased CSH measurements of *M. bovis* BCG and *M. smegmatis* (Figure 3.9). Vortexing duration has been associated with hydrocarbon droplet size, where smaller droplet sizes are generated with longer vortexing durations, hence increasing potential attachment area for cells (Rosenberg, 1991). This could potentially explain the ascending CSH trend with vortexing duration.

In the MATH assay, the results might be influenced by the cells concentration in the aqueous suspension. The higher number of cells in the suspension leads to higher cell removal rate upon vortexing with hexadecane (Doyle, 2000). The reason for the higher removal rate of cells upon vortexing could be due to the cooperative interactions among adhering cells where the binding of one cell to hexadecane droplet favours the binding of another cell. In this regard, proportion of cells are not adhere to hexadecane droplets, but appear to bind adjacent to each other (Doyle and Rosenberg, 1990). Several studies have used initial density between OD = 0.2 - 1.0 and this is based on random choice rather than any specific rationale (Van der Mei *et al.*, 1991, Doyle and Rosenberg, 1995). The result obtained here showed that CSH measurements were not affected by the initial density used (ranged from OD = 0.2-0.8). This result was in contrast with a previous study with *Candida albicans*, where the adhesive levels were higher when higher cell concentration was mixed with hexadecane (Rosenberg, 1991).

The effect of hexadecane-aqueous phase volume ratio on CSH measurements has been explored previously. Hori and associates have demonstrated increased CSH values of *Acinetobacter* sp. when hexadecane-aqueous phase volume ratio was increased from 0.01 to 0.4 (Hori *et al.*, 2008). The possibility of cells attaching to each other and not directly to the solvent droplets has been proposed previously (Doyle and Rosenberg, 1990). Two reasons could contribute to the occurrence of this phenomenon, the low hydrocarbon-aqueous phase volume ratio (insufficient interaction surface) and the ability of some strains to form aggregations (Rosenberg, 1984). An increase in hydrocarbon-aqueous phase volume ratio has also been shown to cause a saturation in CSH values in some cases (Rosenberg *et al.*, 1983, Hori *et al.*, 2008). The results obtained here agreed with this possibility as variations of hexadecane-aqueous phase volume ratio showed a significant ascending pattern with increased hexadecane volume (Figure 3.9).

The original suspension medium used with the MATH assay was PUM buffer. The reason behind that is PUM buffer was originally used to grow the petroleum degrading *Acinetobacter calcoaceticus* and no specific reason was given by the authors relating it to CSH measurement (Rosenberg *et al.*, 1980, Rosenberg, 2006). Thus, several studies have replaced it with alternative buffers including PBS (Amaral *et al.*, 2006), KCl (Walker *et al.*, 2005), basal salt (Hori *et al.*, 2008), and phosphate buffer (Lather *et al.*, 2016). It should be noted that PUM buffer is still widely used (Obuekwe *et al.*, 2007, Jankute *et al.*, 2017). Direct comparison between PUM buffer and other buffers have been done in some studies previously. In studies comparing PUM buffer to PBS, PUM buffer showed higher CSH values with *Streptococcus epidermidis*, *Micrococcus variants* and lower values with *Bacillus subtilis* and *Micrococcus roseus* (Kadam *et al.*, 2009). In another study with *Yarrowia lipolytica*, there was no significant difference in CSH values using PUM or PBS buffers. The authors subsequently continued using PUM buffer in their experiments (Amaral *et al.*, 2006). In the current study, there was no significant change in CSH values with the buffers used except for DW. The decrease of CSH values when water was used is in agreement with a study done with *S. sanguis* (Nesbitt *et al.*, 1982).

The variations of total control samples of the whole series of experiments of *M. smegmatis* and *M. bovis* BCG ranged from 44-55 % and 62-71 %, respectively. This observation suggested that reproducibility of the MATH technique was not limited. However, the MATH technique showed good discrimination between the *M. smegmatis* and *M. bovis* BCG with each experiment. Reasons for variation between experiments could include, the possibility of the impact of the washing step where subpopulation can be lost during such step. A second possible reason is that mycobacterial cells tend to aggregate causing sedimentation of the proportion of cells. As forming aggregation is a feature of mycobacteria species, it would be reasonable to consider the second possibility as the main influence factor on the results of this thesis. To investigate this possibility, further microscopic experiments could be done in the aqueous phase. While the glass tubes used here were cleaned and autoclaved prior to conducting the experiment, some studies have demonstrated that cells might adhere to the glassware during mixing (Hori *et al.*, 2008). This could be avoided by wash the tubes with 12 M HCl (Zoueki *et al.*, 2010).

Although, most parameters investigated here have been reported to influence the CSH measurements with the MATH technique, CSH of *M. smegmatis* and *M. bovis* BCG were not affected significantly by most of these parameters. This could be due to the characteristic feature of the mycobacterial cell envelope where long fatty acids are major components.

### **3.4.2 The growth cycle influenced the CSH of *M. bovis* BCG**

Analysis of Mtb transcription in sputum revealed a pattern similar to that observed in non-replicating persistent (NRP) bacilli. In the same study, 182 genes including genes related to the Mtb stress regulon DosR were upregulated in comparison with log-phase aerobic growth. Moreover, 334 genes including aerobic respiration and ribosomal genes were downregulated in comparison with log-phase aerobic growth (Garton *et al.*, 2008). These properties of Mtb populations in sputum are thought to be required for transmission of the disease (Garton *et al.*, 2008). Therefore, *M. bovis* BCG at stationary phase was used in the series of the experiments in this work. *M. bovis* BCG at stationary



phase showed a significant increase in CSH values compared to exponential phase (Figure 3.10). This can be due to the starvation stress that occurred during stationary phase. Increased CSH values at stationary phase was reported previously with *E. coli* (Walker *et al.*, 2005) and *A. calcoaceticus* (NIKOVSKAYA *et al.*, 1989).

### 3.4.3. Evaluation of additional techniques to measure CSH

As a part of this project will deal with aerosol samples in chapter 4 and 5, the quantity of cells in aerosols are expected to be inadequate for MATH technique. Thus, it was critical to evaluate additional methods as an alternative for the MATH to study CSH. These methods include Congo Red stain and microsphere attachment beads. The advantages of these techniques over MATH is their ability to determine CSH at the single-cell level. Therefore, they have the potential to be useful in measuring CSH when a smaller number of cells are present in the sample.

In certain pathogens, including mycobacteria, virulent strains are more hydrophobic than avirulent strains (Qadri *et al.*, 1988). Congo Red binding assay is one of the tests that have been used previously to measure CSH and has been linked to virulence and pathogenicity (Qadri *et al.*, 1988, Cangelosi *et al.*, 1999). Congo Red stain is an amphiphilic dye that associates with lipids and lipoproteins of the mycobacterial cell envelope, providing a measure of overall CSH (Cangelosi *et al.*, 1999). The uptake of Congo Red dye by microorganisms is related to their phenotype. For example, glycopeptidolipids (GPL)- deficient *M. smegmatis* mutant strain absorbed more Congo Red dye than the wild type (Etienne *et al.*, 2005). The Congo Red binding assay to measure CSH was included in the current study.

Another method to measure the CSH was also tested in the current work. This method involves the use of fluorescent polystyrene microspheres with a modified surface that rendered them hydrophobic (Zita and Hermansson, 1997). This method has been used in previous studies to measure CSH directly in wastewater samples prior to cultivation (Hazen and Hazen, 1987, Zita and Hermansson, 1997).

Both techniques showed the ability to detect the heterogeneity in CSH of cells in one population of *M. bovis* BCG (Figure 3.14A &B). This observed heterogeneity could be influenced by the fact that these assays were performed on stationary phase suspensions of *M. bovis* BCG where the cell length could account for this variation in response. However, the variation in the cell length in the populations used was not investigated during these experiments and might be a target in future work.

It has been claimed that *M. abscessus* rough phenotype is more hydrophobic than the smooth phenotype (Minnikin *et al.*, 2015). This fact has been confirmed using the MATH technique. The rough strain showed higher propensity for partitioning into the hexadecane phase than the smooth strain (Viljoen *et al.*, 2018). On one hand, these findings were confirmed in our lab using lab and clinical isolates *M. abscessus*. Moreover, rough strain *M. abscessus* absorbed marginally more Congo Red dye than smooth strain (Figure 3.12). This positive correlation between MATH and Congo Red binding assay confirmed that CSH of the rough and smooth variants is significantly different. It should be noted that, Congo Red assay was performed here only with *M. abscessus* rough and smooth phenotypes to confirm the results of partitioning to hexadecane. Comparison between other strains of mycobacteria including Mtb using Congo red was reported previously (Jankute *et al.*, 2017).

On the other hand, fluorescent microsphere beads assay failed to distinguish between *M. abscessus* variants (Figure 3.13). It is worth noting that counting the number of attached beads was assessed manually and this might raise bias toward the results. An attempt to develop a new analysis tool within the ImageJ software was established to deal with this problem. However, it was not processed further as new objectives of the project were prioritised. Another drawback associated with this method is that it is time consuming which make it less practical with a large sample size.

#### 3.4.4. CSH of different Mtb strains

To minimise the biohazard risks associated with working in CL3 laboratory, it was convenient to inactivate Mtb strains then transfer them to Cat 2 laboratory to run MATH assays. To test the impact of killing mycobacterial strains on CSH measurement, *M. bovis* BCG was fixed with 4 % formaldehyde and CSH was measured before and after fixation. There was no significant difference in CSH before and after fixation (Figure 3.15). This findings was compatible with previous study with Mtb strains were killed by autoclaving (Jankute *et al.*, 2017). This observation is critical for future work as it enables one to overcome some of the technical and regulatory challenges such as safety regulations associated with working with CL3 strains.

An investigation in the different CSH features of three clinical isolates of Mtb strains was assessed and compared to the virulent lab strain H37Rv using the MATH technique. There was a significant difference between the strains. The lower CSH was found with Mtb CH strain (64 %). The CSH was 70, 75, and 79 % with Mtb H37Rv, Mtb *Beijing*, and Mtb *Loughborough* strains, respectively (Figure 3.16). These differences in CSH features might contribute to the degree of transmission of these strains. The highest CSH among the tested strains was with Mtb *Loughborough* strain. This strain is currently under investigation to define its full features compared to Mtb H37Rv and there are still no published reports regarding its transmissibility. The second highest CSH was with Mtb *Beijing* strain. This strain has been reported previously to be more transmissible than other Mtb strains (Yang *et al.*, 2012).

#### 3.4.5. Reduced CSH significantly post-nebulisation

Previous studies in laboratories at the University of Leicester have provided emerging evidence that the bacterial population in aerosols is different from the bacterial population in sputum (Nardell *et al.*, 2016). Identification of these differences and determination of the features that influence the bacterial propensity for aerosolisation is a key challenge. The relation between CSH and propensity of cells for aerosolisation was proposed previously (Jankute *et al.*, 2017). Moreover, Falkinham has demonstrated this relation in non-tuberculosis mycobacteria (Falkinham, 2003). It should be noted

that the experiments here were conducted to investigate the ability of hydrophobic cells to be aerosolised from the reservoir more readily.

The main aim of the work here was to investigate the influence of CSH on the propensity of cells for aerosolisation. To answer this question, three nebulisers with different mechanisms (section 3.2.9) were used to nebulise stationary phase cells of *M. bovis* BCG suspension. The CSH before and after nebulisation was assessed using the MATH technique. The results of all experiments were compatible as they showed a significant decrease in the number of hydrophobic cells in the reservoir post nebulisation (Figure 3.17). These findings can be attribute to the fact that the more hydrophobic cells were preferentially aerosolised compared to those with less hydrophobicity characteristics, supporting the hypothesis of the work in the current study. It should be noted that other factors might contribute to this phenomenon including the impact of the nebulisation process on the cell surface characteristics of cells and the adherence of the hydrophobic cells to the nebuliser vessels. However, these possibilities were not investigated further. Another observation here was that the decrease of the hydrophobic cells was higher with A3 complete and ultrasonic Omron nebulisers compared to the 3-jet Collison nebuliser. This could be explained by the fact that aerosol generation was higher using A3 Complete and Ultrasonic Omron nebulisers compared to the 3-jet Collison (data not shown). Moreover, when A3 complete Omron nebuliser was used, the position 3 where aerosol particle size is approximately 3  $\mu\text{m}$  was applied. A comparison between the other positions with different aerosol particle sizes could be a target in future experiments.

### 3.5. Conclusions

- Vortex duration, hexadecane-aqueous volume ratio and DW as a suspended medium showed significant impacts on CSH measurement using the MATH technique. *M. bovis* BCG showed higher CSH values at the stationary phase compared to exponential phase.
- Rough strain of *M. abscessus* was more hydrophobic than the smooth strain using the MATH and Congo Red binding assays.
- Microsphere beads technique was time consuming and failed to distinguish between hydrophobic and hydrophilic cells.
- CSH of *M. bovis* BCG cells was not affected by 4 % formaldehyde fixation using the MATH technique providing validation evidence to use the MATH with inactivated CL3 strains.
- Different Mtb strains showed different CSH characteristics suggesting the influence of CSH of these strains on their transmissibility.
- Percentage of hydrophobic cells in the reservoir was decreased significantly post aerosolisation providing preliminary indirect evidence relating the role of CSH on propensity of cells for aerosolisation.
- Decrease percentage of hydrophobic cells in the reservoir post nebulisation was constant regardless the mechanism of the nebuliser used, supporting the main hypothesis of this chapter.

# **Chapter four**

## **4. Aerosol Survival Studies**

## 4.1. Introduction

A particular concern here has been to address discrepant results obtained in experiments conducted at two different centres. In 1969, Loudon and associates showed that 50 % of *Mtb* bacilli survived in aerosols after 6 hrs (Loudon *et al.*, 1969). Later, Lever and colleagues showed that *Mtb* exhibited a half-life time of < 30 min within aerosols (Lever *et al.*, 2000). Better understanding in this area is important, as a key goal has been to understand *Mtb* survival mechanisms. This is explored further in the next chapter, by investigating transcriptional signatures of cells in sustained aerosols. Thus, the results of the present chapter enabled the outline experimental plan for the next chapter. The work in this chapter focuses mainly on studying the survival of the H37Rv and *M. bovis* BCG in aerosols using a Goldberg drum in conjunction with a contained Henderson apparatus.

A key feature has been to establish standardised and reproducible conditions to enable systematic downstream investigation of factors that affect survival outcomes. While survival is a standard assessment in this sort of experiment, it is recognised that there are multiple ways of assessing this and that, ultimately, infectivity in a system representing human *infection* is a key measure desired in the long term.

### Goldberg drum

This apparatus (2 feet wide and 6 feet in diameter) was first introduced by Goldberg and colleagues in 1958 (Goldberg *et al.*, 1958). It was originally designed to study the survival of microorganisms within aerosols (size 1-6  $\mu\text{m}$ ) under controlled temperatures and RH. Since its introduction, different rotating drums with different capacities were designed according to the researchers' aim (Verreault *et al.*, 2008, Huang *et al.*, 2019). The drum used in this study was manufactured in 2010, based on the original Goldberg drum by the Microbiological Research Establishment (MRE) at Porton Down (personal communication with Dr. Simon Parks, PHE, Porton Down). It is made of aluminium and can hold up to 70 litres. The aerosols are nebulised by the aerosol generator and introduced into the rotating drum. The drum is rotated at 3.5 rpm (revolutions per min) and has a series of internal baffles. These baffles are designed to prevent the deposition of particles during the rotation of the drum. Moreover, it contains a temperature and

humidity data logger, allowing for the continuous monitoring of environmental conditions (Thompson *et al.*, 2011).

## **Henderson apparatus**

This device is used in conjunction with the Goldberg drum. It has two main functions; controlling the RH inside the drum and delivering the generated aerosols to the drum. It consists of a chamber and a spray tube. An external compressor generates the air, then a pump located inside the chamber creates the air flow around the system. The air flow is controlled by a critical orifice to 55 l/min. The chamber also contains a silica gel tank (dry air) and a water tank (wet air). The generated compressed air is passed through both tanks before it reaches the spray tube. Depending on the desired RH, the volume of air passing through each tank is controlled by directional flow controllers. For health and safety reasons, the system is run under slightly negative pressure, which can be controlled by the piccolo apparatus. A second spray tube is located inside the isolator and the nebuliser connected to it. The purpose of this spray tube is to create a homogenous mixed aerosol after the nebuliser sprays directly into it (Druett, 1969). Other examples of equipment that fulfil a similar purpose include; AeroMP and Aero3G from Biaera Technologies.

## **Aim and objectives**

The overall aim of the work in this chapter was to investigate the survival of Mtb H37Rv and *M. bovis* BCG in aerosols over a period of two hrs.

The objectives were;

- To compare different techniques to assess bacterial 'viable counts' with and without storage at -80 °C. (Storage allowed use of a wider set of viability assessments at the University of Leicester).
- To investigate the effect of the nebulisation process on the cells' integrity.
- To investigate the survival pattern of Mtb H37Rv and *M. bovis* BCG in aerosols using two nebulisers.



## 4.2. Methods

### 4.2.1. Bacterial strains and growth conditions

The growth conditions were based on a previous study conducted by Lever and colleagues to investigate the survival of Mtb in aerosols (Lever *et al.*, 2000). 100 µl of a frozen stock of Mtb H37Rv or *M. bovis* BCG (OD = 0.8-1) was inoculated onto 7H10 supplemented with OADC plates, and spread both horizontally and vertically over the plates using a cotton-tipped swab (Alpha laboratories; Code 42141500) to form a confluent lawn of bacterial growth. Two weeks post-incubation at 37 °C, cells were scraped off plates using a cell scraper (250mm, Fisher Scientific) and resuspended into 25 ml DW. To avoid the presence of clumps in the suspension, 2-3 mm glass beads were added to the suspension and vortexed vigorously, until no obvious clumps were seen. The OD<sub>600</sub> of the suspension was adjusted to 2.2-2.5. Aerosol generation and sampling were performed in containment level 3 flexible film isolator held within a designated Advisory Committee of Dangerous Pathogens (ACDP) containment L3 laboratory for Mtb H37Rv. As *M. bovis* BCG is categorised as an ACDP L2 pathogen, the processing of samples was performed in a designated flexible film isolator held within an ACDP containment L2 laboratory.

### 4.2.2. Aerosol generation

Aerosols were generated via the Henderson apparatus with bacterial suspensions in an Omron ultra-sonic or a three-jet Collison nebuliser, with 15- or 10-ml suspensions, respectively. As the nebulisers have different internal flow rates to transfer the aerosols outside the nebulisers, it was necessary to add a modification to the system to achieve an equal internal flow rate. To achieve this, the Omron nebuliser was connected to an empty Collison nebuliser via a T-shaped tubing system and the Omron internal fan was blocked (Figure 4.1). The nebulisers were operated at 26–28 psi. The aerosols were delivered to the rotating Goldberg drum (Goldberg *et al.* 1958), and maintained at a mean RT of 22 ± 2 °C and a mean RH of 85 ± 10 %. The high RH was used previously to study the survival of Mtb in aerosols (Lever *et al.*, 2000). The choice of this high RH was to make an appropriate comparison to Lever's study.



**Figure 4.1.** Modifications were applied when an Omron nebuliser was used in the experiment to maintain similar internal air flow to the Collison nebuliser.

### 4.2.3. Aerosol sampler

All-glass impingers (AGI-30), as described by Wolf *et al.*, were used to collect all aerosol samples (Wolf *et al.*, 1959). These samplers have a constant flow rate of 11.5 l/min.

### 4.2.4. Test procedure

The Goldberg drum was connected to the Henderson apparatus. Air running through the drum was allowed to equilibrate to the desired RH for 30 min before the start of each experiment. Negative aerosol samples were taken from the drum before starting the nebulisation to ensure there was no cross contamination between experiments. The aerosols were sprayed into the Goldberg drum for 5 min. Samples of aerosolised bacteria were collected into AGIs containing 10 ml DW at  $t = 0, 15, 30, 60, 90,$  and  $120$  min. The aerosol samples were collected for 1 min. The air extracted from the drum during each sampling time was replaced by new air from the Henderson apparatus (preconditioned at the appropriate RH). Subsequently, the aerosols were diluted within the drum each time a sample was extracted. After sampling, glycerol was added to each sample at a final concentration of 20 %. Two samples were collected from the reservoir of the nebuliser, both before and after the nebulisation process, to enable the effect of the nebulisation process on the spray suspension to be assessed. These were also

treated with glycerol to a final concentration of 20 %. These two samples were considered as pre-nebulisation and post-nebulisation samples. The Goldberg drum system is shown in Figure 4.2 and the schematic diagram of the system is shown in Figure 4.3.

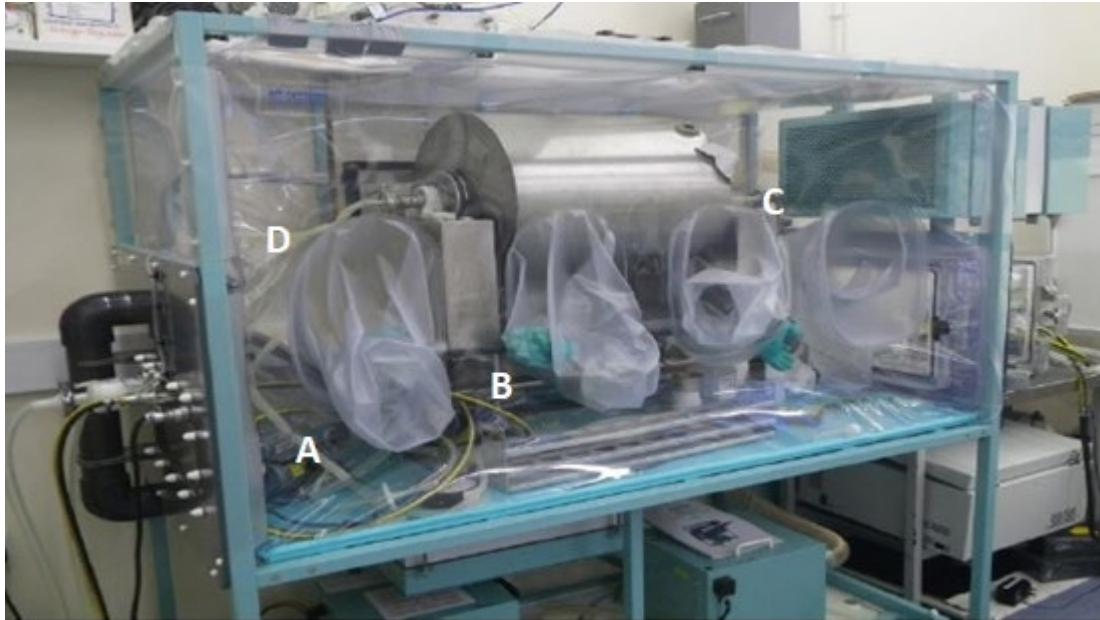


**Figure 4.2. The Goldberg drum system.** The nebuliser is placed at the drum's left side (A) and connected to the spray tube (B). Organisms are sprayed into the drum at the far end (C) and maintained in an aerosol by means of rotation (3.5 rpm) and a series of internal baffles. Samples are extracted from the drum via the sampling device located at the near end (D).

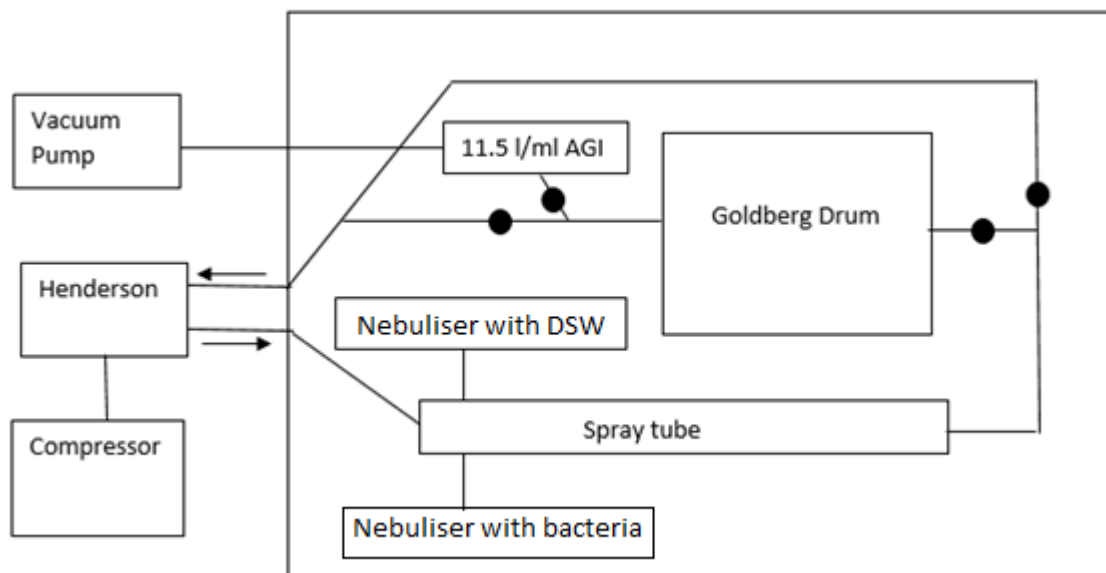


**Figure 4.3. Schematic diagram of the Goldberg drum system.** Inside the isolator, there is a spray tube connected to two nebulisers, one containing the bacteria and the other one containing DW to mix the generated aerosols inside the spray tube. The spray tube is connected to the Goldberg drum via tubing. The Goldberg drum is connected to an AGI sampler. Clamps (●) are opened and closed during sampling.

### 4.2.5. Calculation of the dilution factor in the survival studies

As mentioned above the aerosol samples were collected for 1 min at each time point. This is equal to 11.5 L. Removal of this air was replaced with fresh air with the same amount (11.5 L). This decrease in the actual concentration in the drum was corrected in the final analysis using the formula shown in Figure 4.4. Example of the calculation with an experiment is shown in Figure 4.5.

	11.5L/min sampler would remove $(11.5 / 70) \times 100 = 16\%$ of drum volume						0.164286
10 <sup>6</sup> /ml in 70L							
time (min)	0.00	15	30	60	90	120	
	S1	S2	S3	S4	S5	S6	
max cfu in 70L in drum	7.00E+07						Theoretical decline
16% removed	1.12E+07						T15 8.40E+01
remaining in drum		5.88E+07					T30 7.06E+01
16% removed		9.41E+06	4.94E+07				T60 5.93E+01
			7.90E+06				T90 4.98E+01
				4.15E+07			T120 4.18E+01
				6.64E+06			
					3.49E+07		
					5.58E+06		
						2.93E+07	
						4.68E+06	

**Figure 4.4. Formula of the calculation of the dilution factor.** 11.5 L was removed each time point of sampling and replaced with fresh air. 70 L is the holding capacity of the drum. 6 aerosol samples were collected in each experiment at time points, 0, 15, 30, 60, 90 and 120 min.

Absolute cfu count												
Experiment replicates												
Timepoint	1st	2nd	3rd	% survival at base line								
0	11900	451	17100	100	100	100						
T15	9300	237	18200	78.1513	52.5499	106.433						
T30	7900	322	8300	66.3866	71.3969	48.538						
T60	5700	236	8500	47.8992	52.3282	49.7076						
T90	7000	38	6500	58.8235	8.42572	38.0117						
T120	3400	30	4600	28.5714	6.65188	26.9006						
Dilution factor												
100				100	100	100	survival as % dilution factor			av	std dev	
8.40E+01				78.1513	52.5499	106.43	93.0372	62.5594	126.706	0	100	0
7.06E+01				66.3866	71.3969	48.538	94.0853	101.186	68.7897	T15	94.1008	32.0864
5.93E+01				47.8992	52.3282	49.708	80.8146	88.2872	83.8658	T30	88.0203	17.0285
4.98E+01				58.8235	8.42572	38.012	118.15	16.9235	76.3484	T60	84.3225	3.75714
4.18E+01				28.5714	6.65188	26.901	68.3181	15.9055	64.3229	T90	70.474	50.8683
										T120	49.5155	29.1755

**Figure 4.5. Example of the final analysis after correction to the dilution factor.** Percentage of survival at baseline was calculated by dividing the absolute number at each time point by the absolute number at T0 × 100 (Ex; 9300 / 11900 × 100). Survival as percentage dilution factor was calculated by dividing the % survival at baseline by the dilution factor × 100 (Ex; 78.1513 / 84 × 100). Average and standard deviation of three replicates were calculated and used to generate the graph of the result.

#### **4.2.6. Processing samples at PHE, Porton Down**

Each experiment produced six aerosol samples and two reservoir samples (pre- and post-nebulisation). A ten-fold serial dilution was performed on each sample, and the CFU was calculated for each dilution using spread and pour plate methods (section 4.2.7). The media used was 7H10 Middlebrook agar supplemented with OADC. When possible, the MPN assay was performed on each sample (section 4.2.8). Finally, the remainder of the primary sample was split and stored (in duplicate) at -80 °C until they were shipped to Leicester University for further investigations.

#### **4.2.7. Processing samples at Leicester University**

The neat samples were freeze-thawed and then ten-fold serially diluted, as was performed at PHE, Porton Down. Then, the CFU was assessed for each dilution using the pour plate method. Additionally, the MPN assay was performed.

#### **4.2.8. Enumeration of colony-forming units (CFU)**

##### **Spread plate method (S-CFU)**

Ten-fold serial dilutions of aerosol samples were performed by adding 1 ml of the neat aerosol sample to 9 ml of DW in 30 ml universal tube. CFU assay was applied to each dilution sample on a single 7H10-OADC agar plate. 100 µl of the dilution sample was inoculated onto the agar plate and spread both horizontally and vertically over the plate, using a cotton-tipped swab. Next, the plates were sealed with laboratory sealing film, double-bagged, and incubated inverted at 37 °C until isolated colonies become visible. The final count of 10-300 colonies in a single plate was used for the final calculation of colony forming units (CFUs), using the following equation;

$$S\text{-CFU/ml} = C \times D \times 10$$

C= Count per plate

D= Dilution factor

### Pour plate method (P-CFU)

This method was explored for its convenient (fewer dilutions are required and no spreading is needed) and for its provision of an initial microaerobic environment for growth, as this is known to favour resuscitation of injured bacteria (Berney *et al.*, 2006). The agar was melted and separated into 9 ml aliquots (50 ml falcon tubes) and stored in a water bath at 50 °C. Prior to use, 1 ml of OADC supplement was added to the tube, and 1 ml of the sample dilution was also added to the tube. Next, the tubes were mixed gently, and the agar was poured into labelled petri dishes and left to solidify. Once the agar solidified, the plates were incubated as indicated above. Calculation of the CFU was done with the following equation;

$$\text{P-CFU/ml} = C \times D$$

C= Count per plate

D= Dilution factor

### 4.2.9. Enumeration of most probable number (MPN)

MPN assay counts were carried out in 48-well micro-titre plates (Greiner Bio-One, Frickenhausen, Germany), and each plate was separated into two sections. Each section contained 4 replicates for each sample. 450 µl was added from the 7H9-ADC-Tween 80 into each well. Thereafter, 50 µl of the neat aerosol sample was added to the 10<sup>-1</sup> dilution of 7H9-ADC-Tween 80. Then, 50 µl was taken from each 10<sup>-1</sup> dilution, mixed thoroughly by pipetting, and added to the next dilution. The pipetting tips were discarded, and new tips were used each time. The serial dilution was repeated with the rest of the wells. Each sample had at least 6 series of dilutions (10<sup>-1</sup> to 10<sup>-6</sup>).

Next, all 48-well plates lids were sealed to the base with electrical tape, placed in double zip-lock bags to avoid drying, and incubated at 37 °C statically for 6 weeks. The first check was performed after 5 days to exclude mould-contaminated samples. Once ready, The MPN counts were performed by using a program which can be found at:

<https://www.wiwiss.fu->

[berlin.de/fachbereich/vwl/iso/ehemalige/professoren/wilrich/MPN\\_ver6.xls](https://www.wiwiss.fu-berlin.de/fachbereich/vwl/iso/ehemalige/professoren/wilrich/MPN_ver6.xls) (Jarvis *et al.*, 2010)

A freeze-dried pellet stored at  $-20^{\circ}\text{C}$  (kindly supplied by Professor Galina Mukamolova) from 32 ml of Mtb H37Rv culture supernatant (SN), prepared as described by Mukamolova *et al.* (2010), was used for the Rpf-dependency assays. Prior to use, H37Rv SN was dissolved in 16 ml of DW and 16 ml of 7H9-ADC-Tween 80, and then kept on ice for 30-60 min before use (Mukamolova *et al.*, 2010).

For the Rpf-dependency assays, a 48-well plate was divided into two sections. The first section contained 7H9-ADC-Tween 80 as a control. The second section contained 7H9-ADC-Tween 80 + SN (50 %, v/v). The procedure and the counts were done as per section 4.2.9.

#### **4.2.10. Propidium monoazide (PMA test)**

PMA dye was purchased from Biotium, UK. Following the manufacturer's procedure, 500  $\mu\text{l}$  of the aerosol sample was transferred to an Eppendorf tube, then the PMA stain was added at a final concentration of 50  $\mu\text{M}$ . The tubes were then incubated for 5 min in the dark at RT and were flicked occasionally to mix. The samples were exposed to light to cross-link the PMA to the DNA; this was done for 15 min. Finally, the cells were pelleted by centrifugation at 5,000  $\times g$  for 10 min and the genomic DNA was extracted for qPCR analysis.

PMA is a high-affinity, photoreactive DNA-binding agent; it can access cells with compromised membranes. When exposed to bright visible light, its photoreactive azido group is converted to a highly reactive nitrene radical that can form covalent cross-links with DNA. These cross-links prevent the subsequent qPCR amplification of the target DNA of non-viable cells. In contrast, cells with intact membranes are resistant to PMA. Thus, only DNA from intact (i.e., viable) cells can be amplified when bacteria are treated with PMA prior to DNA extraction (Nocker and Camper, 2009).

#### 4.2.11. DNA extraction

Isolation of DNA from mycobacterial species is complicated by the presence of mycolic acids, which contribute to the creation of thick and waxy cell walls, which are difficult to lyse compared to Gram-negative and Gram-positive bacteria. Commercial DNA extraction kits are designed to lyse Gram-positive and Gram-negative bacteria, and thus are relatively inefficient when applied to a mycobacteria (Käser et al., 2009). The protocol used in this thesis was in-house optimised in our laboratory and has been found to yield satisfactory DNA amounts for qPCR assays (Abdulwhhab, 2019).

The pellets were suspended with 100 µl of Tris-EDTA buffer (20 mmol Tris/ 2mmol EDTA, pH : 8) and 100 µl of Chelex suspension (50 % w/v Chelex-100, 1 % w/v Nonidet P-40, 1 % w/v Tween 20). 0.25 gram of lysing matrix B (MP-Biomedicals, UK) was added to the suspension. Cells were then disrupted in a FastPrep bead beater with a speed setting of 6.5 m/s for 45 sec (FastPrep™-24, MP Biomedicals, UK) and incubated in an ice box for 2 min. This step was repeated 4 times. Finally, the samples were centrifuged at 15,000 x g for 10 min and the supernatant (genomic DNA) was transferred to a new Eppendorf tube.

#### 4.2.12. In-house qPCR IS6110 TaqMan assay

The primary protocol was established by Akkerman *et al.* (2013) to be run on the Light Cycler 480 Instrument II (Roche) and optimized as below for the Rotor-Gene 6000 real-time DNA analysis system on the Corbett PCR machine (Akkerman *et al.*, 2013).

25 µL PCR mixture contained 12.5 µL of TaqMan universal PCR master mix +AmpErase UNG (Applied Biosystems, UK), 1 µL of 10 µM *IS6110*-forward (5'-AGCGTAGGCGTCGGTGAC-3'), 1 µL of 10 µM of *IS6110* reverse (5'-GGGTAGCAGACCTCACCTATGTGT-3'), 0.5 µL of 10 µM TaqMan *IS6110* probe (5' 6-FAM TCGCCTACGTGGCCTTT-3' MGBNFQ), 10 µL of DNA template and 2.5 µL molecular-grade



water. Cycling conditions were 1 holding cycle at 50 °C for 2 min, 1 holding cycle at 95 °C for 10 min, 45 cycles at 95 °C for 15 sec and 60 °C for 6 sec with acquisition on the FAM/Green channel (470nm), and 1 holding cycle at 40 °C for 20 sec. DNase-RNase free water was used as a negative control of amplification.

All primers were obtained from Integrated DNA Technologies, UK, and the probes were obtained from Life Technologies Ltd. Invitrogen, UK.

#### **4.2.13. Calculation of the genome/ml from the real time assay**

The genome/ml calculations were done using the following equation:

$$\text{Genome/ml} = \text{Average copies}/\mu\text{l} \times 200 \mu\text{l} \times 2 / 16$$

(200  $\mu\text{l}$  is the volume of eluted DNA, 2 is the dilution factor [DNA was extracted from 500  $\mu\text{l}$  sample], 16 is the number of copies of S6110 per cell).

### 4.3. Results

As will be shown in later sections, the pour plate method (P-CFU) was found to provide the most amenable means of assessing survival in aerosol. Results from this approach will be shown first, then the alternate methods of viability assessment will be reviewed.

#### 4.3.1 Survival patterns of *M. bovis* BCG and Mtb H37Rv in aerosols

The recovery of Mtb H37Rv and *M. bovis* BCG, expressed as a percentage of P-CFU at baseline, is presented in Figure 4.6, using the Collison and Omron nebulisers. The theoretical dilution effect due to the material withdrawn in sample is calculated and shown on the same graph. The recovery of both strains declined faster than the theoretical dilution line, regardless of the aerosol generator used. The error bars of these strains overlapped, indicating that the difference between them is statistically insignificant.

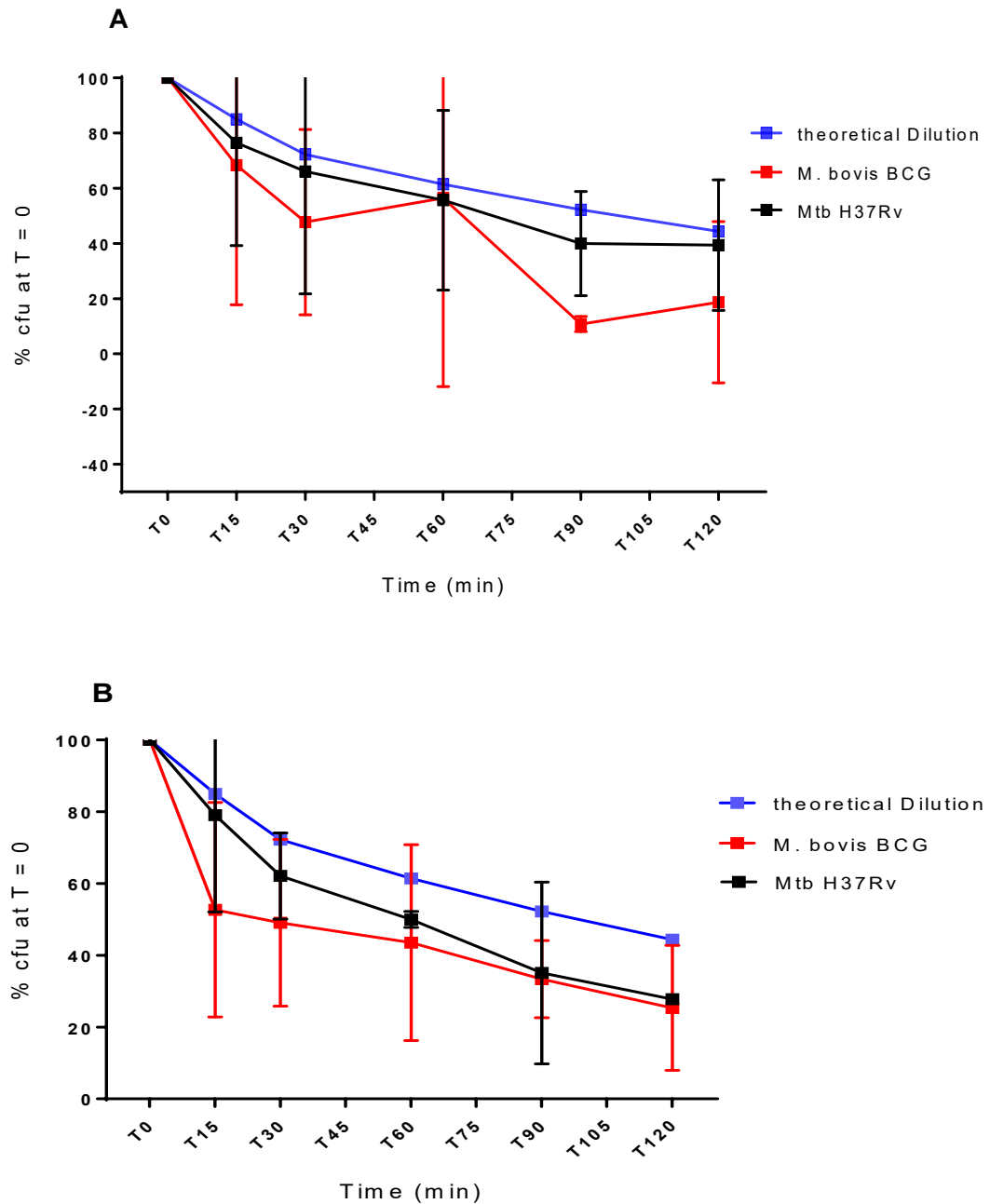


**Figure 4.6. Survival pattern of *M. bovis* BCG and Mtb H37Rv with the theoretical dilution.** Bacterial suspensions were prepared and nebulised for 5 min, and aerosol samples were collected over a period of two hrs. P-CFU count for each sample was performed and the theoretical dilution was calculated. (A) 3-Jet Collison nebuliser (B) Omron nebuliser. Error bars represent the SD of three independent experiments.

The survival ratio of *M. bovis* BCG and Mtb H37Rv was calculated and is shown in Figure 4.7. It is defined as the percentage recovery of the strain, divided by the percentage recovery of the theoretical decline  $\times 100$ . With both nebulisers, the strains show a survival rate above 50 % in aerosols over a period of 2 hrs. The error bars of these strains overlapped, indicating that the difference between them is statistically insignificant.

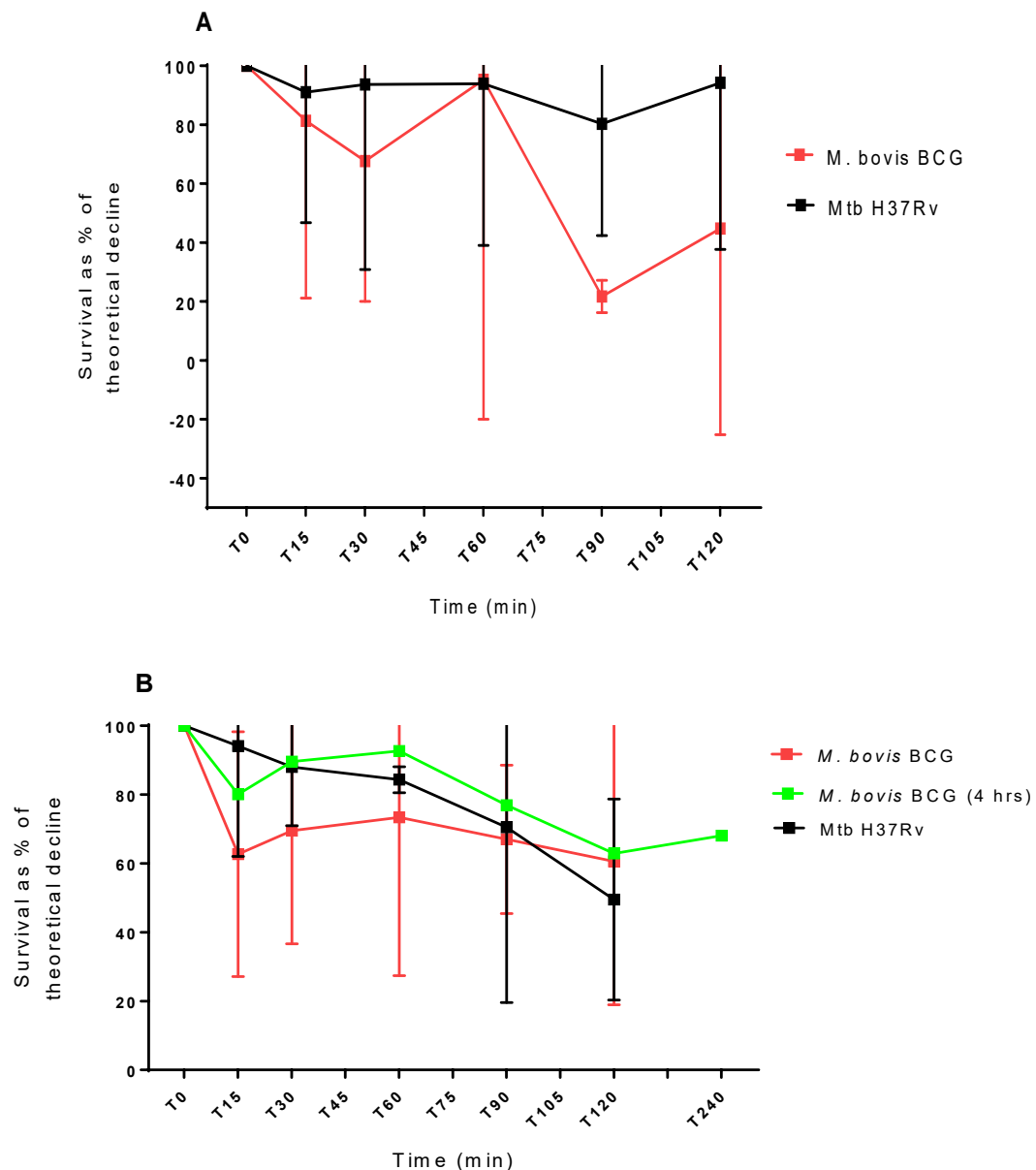


**Figure 4.7. Survival pattern of *M. bovis* BCG and Mtb H37Rv as a percentage of the theoretical dilution.** Bacterial suspensions were prepared and nebulised for 5 min, and aerosol samples were collected over a period of two hrs. P-CFU count for each sample was performed and expressed as a percentage of the theoretical dilution. (A) 3-Jet Collison nebuliser (B) Omron nebuliser. Error bars represent the SD of three independent experiments. A single experiment was assessed with *M. bovis* BCG for 4 hrs showed in red line.

From the previous experiments, it can be seen that using either a 3-Jet Collision or Omron nebuliser has no significant different effect on the survival pattern of *M. bovis* BCG and Mtb H37Rv. Additionally, both nebulisers' impact on the cells' viability within the reservoir was similar. However, the Omron nebuliser aerosolised more cells than the Collision nebuliser in most instances (Average P-CFU at baseline is 1553 and 5044 for Collision and Omron, respectively). Therefore, subsequent experiments in the project were performed with the Omron nebuliser.

### 4.3.2 Comparison of methods used to assess bacillary survival

#### 4.3.2.1 The P-CFU method gave higher counts than the S-CFU method.

Aerosols samples collected in *M. bovis* BCG survival experiments were plated on 7H10-OADC by both the P-CFU and S-CFU methods. Figure 4.8 demonstrates around a half log reduction in CFU count of *M. bovis* BCG cells in aerosols when S-CFU method was applied, compared to P-CFU method at all-time points.

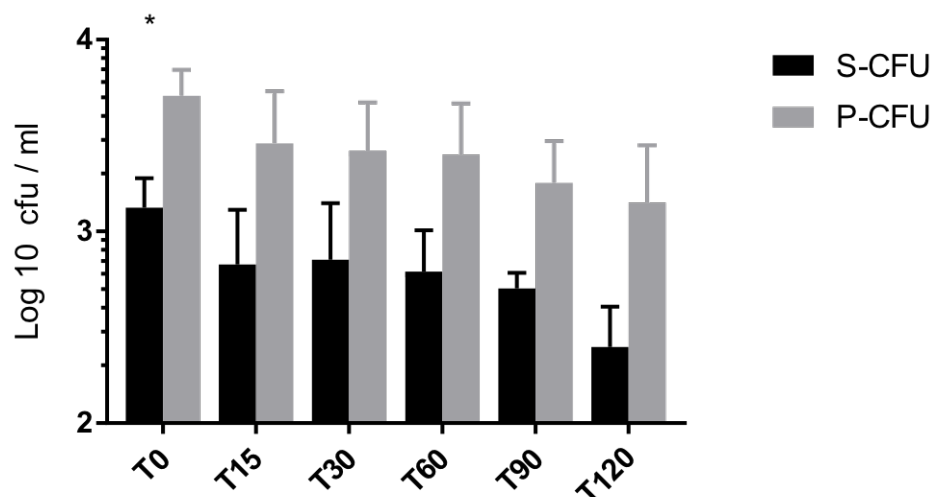


**Figure 4.8. Comparison between S-CFU and P-CFU methods to detect *M. bovis* cells in aerosols.** *M. bovis* BCG suspension was aerosolised for 5 min, and aerosol samples were collected at different time points. CFU count was conducted using S-CFU and P-CFU methods. Error bars represent the SD of three independent experiments. Statistical analysis was performed using multiple t-test with the Sidak correction. (\* = P=0.01).

#### 4.3.2.2 Culture supernatant supplementation had no significant effect on BCG recovery

This experiment was conducted at an early stage of the series of survival experiments, where *M. bovis* BCG was used as a surrogate for Mtb. As there was no statistically significant difference in the results of *M. bovis* BCG, no further experiments were done with Mtb.

To investigate whether stress can produce Rpf-dependent populations in aerosols, MPN assay with and without TB supernatant was applied to aerosol samples using a 48-well plate (section 4.2.9). This experiment was performed with *M. bovis* BCG aerosol samples after storage of samples from Collison and Omron nebulisations at -80 °C (see next section).

Table 4.1 shows the samples that were investigated. The resuscitation index (RI) was calculated by subtracting the log<sub>10</sub> MPN+SN by the log<sub>10</sub> P-CFU values. The 2<sup>nd</sup> RI was calculated by subtracting the log<sub>10</sub> MPN+SN by the log<sub>10</sub> MPN-SN. A significant RI should be equal to or more than 1.

Table 4.1 shows that, for the samples used, the RI value did not exceed 1, indicating that the difference is not significant.

**Table 4.1. Culture supernatant assessment assay of *M. bovis* BCG using Collison and Omron nebulisers.**

<b>Collison (Log10)</b>					
<b>Sample</b>	<b>P-CFU</b>	<b>MPN</b>	<b>MPN +SN</b>	<b>RI (MPN SN-CFU)</b>	<b>RI (MPN SN-MPN)</b>
<b>Pre-Nb</b>	<b>7.2</b>	<b>7.4</b>	<b>7.8</b>	<b>0.6</b>	<b>0.4</b>
<b>T60</b>	<b>2.6</b>	<b>2.7</b>	<b>2.6</b>	<b>0</b>	<b>-0.1</b>
<b>T120</b>	<b>1.9</b>	<b>2.1</b>	<b>1.6</b>	<b>-0.3</b>	<b>-0.5</b>
<b>Omron (Log10)</b>					
<b>Sample</b>	<b>P-CFU</b>	<b>MPN</b>	<b>MPN +SN</b>	<b>RI (MPN SN-CFU)</b>	<b>RI (MPN SN-MPN)</b>
<b>Pre-Nb</b>	<b>8.2</b>	<b>8.0</b>	<b>7.5</b>	<b>-0.7</b>	<b>-0.5</b>
<b>T60</b>	<b>3.3</b>	<b>3.4</b>	<b>3.6</b>	<b>0.3</b>	<b>0.2</b>
<b>T120</b>	<b>3.0</b>	<b>3.3</b>	<b>3.1</b>	<b>0.1</b>	<b>-0.2</b>

P-CFU = colony forming unit (Pour plate method)

MPN = most probable number

MPN + SN = most probable number + supernatant

RI = resuscitation index

### 4.3.2.3 H37Rv P-CFU counts from aerosol were not significantly affected by freezing

In order to explore options for processing samples at different sites, aerosol samples taken in multiple experiments were frozen at -80 °C following the addition of 20 % glycerol, then shipped to the University of Leicester for further investigation. The effect of the freeze-thaw cycle was investigated by re-plating the samples using P-CFU technique (as had been done at the PHE, Porton Down). There was no statistically significant difference in the P-CFU count before and after the freeze-thaw cycle (Figure 4.9). Assays reported below were performed at the University of Leicester.

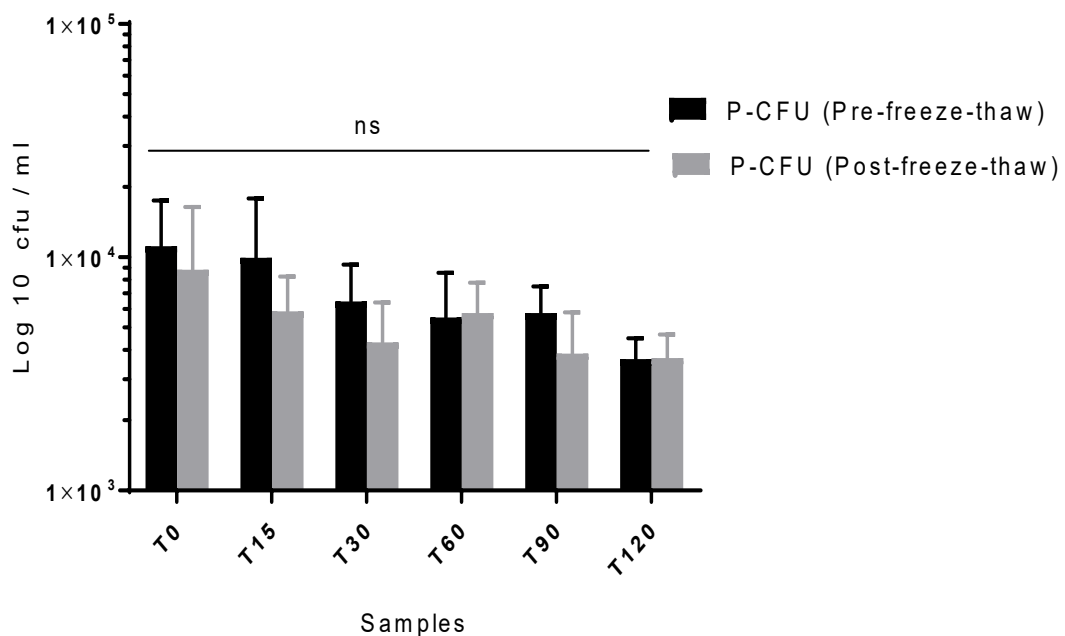


**Figure 4.9. CFU counts of the aerosol samples before and after the freeze-thaw cycle.** Mtb H37Rv aerosol samples were frozen at -80 °C and transferred to University of Leicester. CFU assay was performed using P-CFU technique. Error bars represent the SD of three independent experiments. Statistical analysis was performed using multiple t-test with the Sidak correction, ns = non-significant.



#### 4.3.2.4 MPN showed stable pattern compared to P-CFU

Figure 4.10 shows the comparison between MPN and P-CFU techniques in detecting *Mtb* cells in aerosols. Both techniques showed survival of at least 50 % of *Mtb* cells in aerosols. The detection of *Mtb* in aerosols using the MPN technique results in a stable pattern, compared to that obtained with the P-CFU count technique.

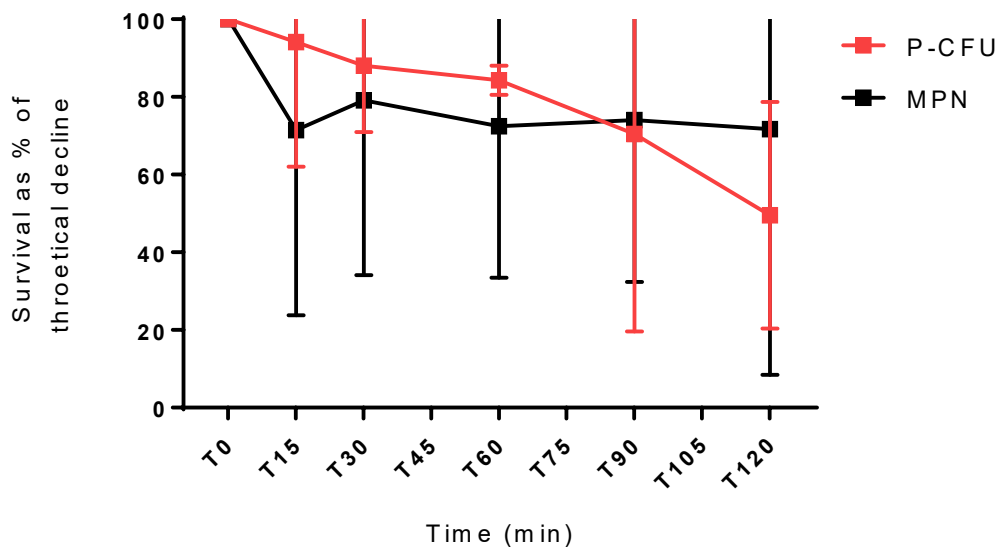


**Figure 4.10. Comparison between P-CFU and MPN techniques to study survival of *Mtb* H37Rv in aerosols.** Aerosol samples were freeze-thawed and P-CFU and MPN assays were performed. Error bars represent the SD of three independent experiments.

### 4.3.2.5 PMA exclusion

An aliquot of 1 ml of Mtb H37Rv aerosol samples (generated from Ultrasonic Omron nebuliser) was split into two halves. The first half was treated with the PMA stain, while the other half was not. DNA was extracted from the samples, and a qPCR assay was performed. Figure 4.11 shows that there was approximately one log reduction in the numbers of intact cells in aerosols compared to the total of aerosolised cells. A reduction in the percentage of intact aerosolised cells was observed in all the aerosol samples.

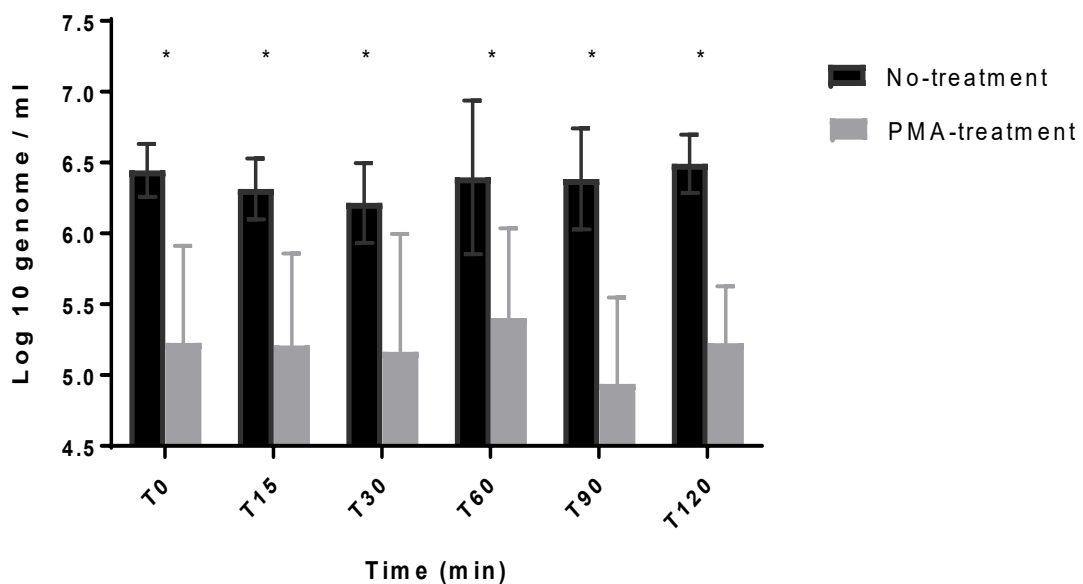


**Figure 4.11. Comparison between aerosolised Mtb H37Rv cells treated and not treated with PMA.** DNA was extracted from samples and a qPCR assay was performed. Error bars represent the SD of three independent experiments. Statistical analysis was performed using multiple t-test with the Sidak correction. (\* = P=0.01).

The detection of intact cells in aerosols, presented as a percentage of the theoretical dilution, is shown in Figure 4.12. The proportion of intact cells was stable over a period of two hrs. The absolute numbers of Mtb H37Rv cells detected by P-CFU, MPN and PMA-qPCR are shown in Table 4.2.

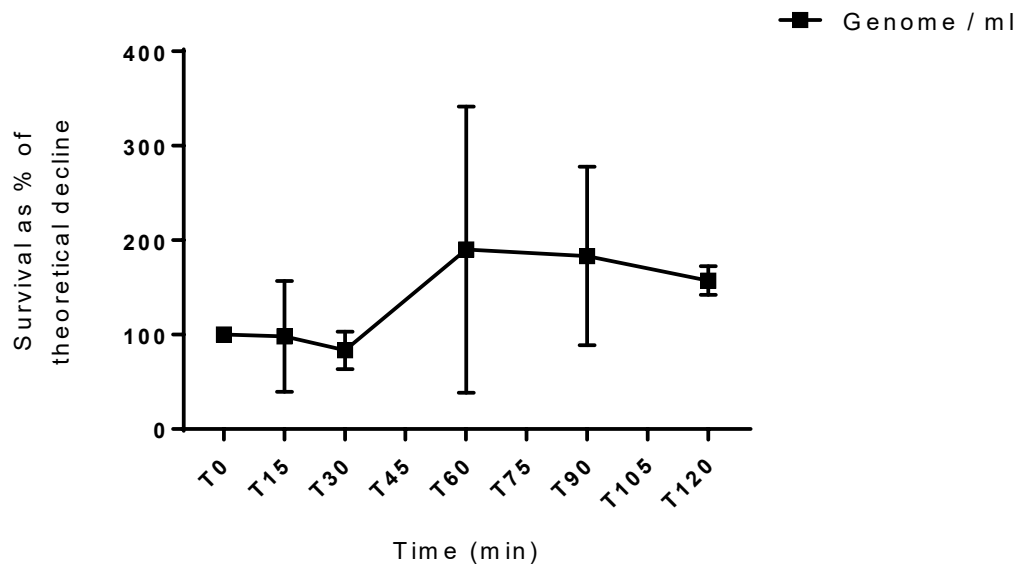


**Figure 4.12.** The decline pattern of the aerosolised Mtb H37Rv intact cells over a period of two hrs. Aerosol samples were freeze-thawed then treated with PMA stain, and a qPCR assay was performed. Error bars represent the SD of three independent experiments.

**Table 4.2.** Absolute numbers of Mtb H37Rv cells detected by P-CFU, MPN and PMA-qPCR.

Ultrasonic Omron Nebuliser (absolute no.)			
Sample	P-CFU /ml	MPN /ml	Genome /ml (PMA-qPCR)
T0	8.85E+03	1.25E+04	3.67E+05
T15	5.87E+03	6.33E+03	2.65E+05
T30	4.31E+03	7.13E+03	3.97E+05
T60	5.77E+03	6.80E+03	5.21E+05
T90	3.86E+03	4.67E+03	1.52E+05
T120	3.70E+03	4.17E+03	2.11E+05

### 4.3.3 Effect of nebulisation on Mtb H37Rv cells

A significant concern in these experiments has been the potential of the nebulisation process to damage the aerosolised bacilli. This potential problem was assessed by P-CFU counting and by PMA dye exclusion.

#### 4.3.3.1. P-CFU counts

Lawn growth on the 7H10-OADC plate was used to prepare bacterial suspensions in DW and nebulised for 5 min (to minimise the effect of the nebulisation process on cell integrity). P-CFU counts of the suspensions in the reservoir were taken before and after nebulisation. Figure 4.13 shows that the P-CFU count increased post-nebulisation with both nebulisers. The difference in P-CFU counts between pre and post nebulisation was significant with the Omron nebuliser.

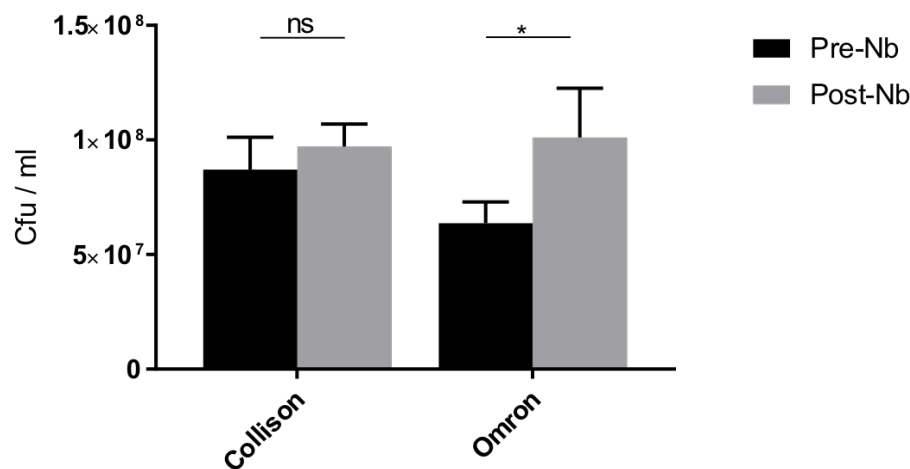


**Figure 4.13. Comparison between the P-CFU counts of the suspensions inside the reservoir pre- and post-nebulisation.** Mtb H37Rv suspensions were prepared and nebulised for 5 min. Samples from pre- and post-nebulisation were collected, and the P-CFU was calculated using the pour plate technique. Error bars represent the SD of three independent experiments. Statistical analysis was performed using multiple t-test with the Sidak correction. (ns = non-significant, \* = P=0.01).

#### 4.3.2.2. PMA exclusion

Pre- and post-nebulisation of samples after the freeze/thaw cycle were treated with PMA (section 4.2.10), and qPCR was done for both samples. The proportion of intact cells of the total cells inside the reservoir was calculated. The result indicated a significant decrease in the proportion of intact cells inside the reservoir in the post-nebulisation samples when compared to pre-nebulisation samples with both the Collison and Omron nebulisers (Figure 4.14A). There was no significant difference in the % of cell damage by Collison or Ultrasonic Omron nebulisers (Figure 4.14B).

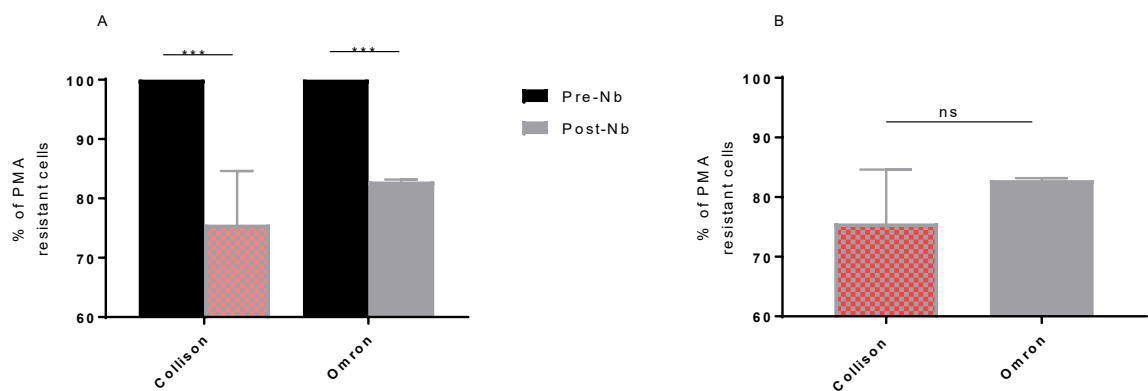


**Figure 4.14. Comparison between PMA resistant cells' proportion in the suspension inside the reservoir pre- and post-nebulisation.** Mtb H37Rv suspensions were prepared and nebulised for 5 min. Samples from pre- and post-nebulisation were collected and stained with PMA, DNA was extracted, then the qPCR assay was assessed. A) Shows % of damaged cells against normalised control (pre-nebulisation). B) Shows comparison between % of damaged cells post-nebulisation by Collison and Omron nebulisers. Error bars represent the SD of three independent experiments. Statistical analysis was performed using multiple t-test with the Sidak correction. (\*\*\*) =  $P=0.0001$ , ns = non-significant).

## 4.4. Discussion

Mtb transmission involves three stages: aerosolisation from the host, survival while airborne, and inhalation by a new host. The second stage is the focus of the work in this chapter. As noted in Section 4.1, the two studies on the viability of Mtb in air demonstrated discrepant results. To address the discrepancy of these two findings, the survival pattern of *M. bovis* BCG and Mtb H37Rv in aerosols was investigated.

### 4.4.1 Survival patterns of *M. bovis* BCG and Mtb H37Rv in aerosols

This investigation was conducted using the Goldberg drum system with two nebulisers, the conventional 3-Jet Collison nebuliser and the ultrasonic Omron nebuliser. The results obtained by P-CFU analysis showed that Mtb and *M. bovis* have survival half-lives in excess of 2 hrs regardless of the sample generator (Figures 4.6 & 4.7). This contrasts with the study of Lever and colleagues, who demonstrated that only 10 % of the initial cells made colonies (S-CFU) after 30 min (Lever *et al.*, 2000). The experimental designs shared some similarities and differences. For example, the preparation of the inoculum was done by harvesting a growth solid medium. However, there was a difference in the period of plate incubation before the harvesting (21 days in Levers' study, and 14 days in this study). Another difference is the starting inoculum was  $10^{10}$  and  $10^8$  viable cells  $\text{ml}^{-1}$  in Lever's and here, respectively. In both studies, the AGI-30 sampler was used, containing 10 ml DW and 6 aerosol samples were collected. However, the time points of collecting the aerosol samples were different. In Levers' study, they collected aerosol samples at 5, 10, 20, 30, 40 and 60 min post-nebulisation, while this study aerosol samples were collected at 0, 15, 30, 60, 90 and 120 min post-nebulisation. The RH in Lever *et al.*'s study was around 75 %, while it was 85 % in the current study. One possible reason for the difference may have been that, in the Lever study, the plates were incubated for only 10 days before counting, while 28 days was allowed here. The longer period here was chosen for convenience as colonies were very small and difficult to count after 3 weeks. Another possibility for the difference in results

could be the suspending medium; as in Levers' study, saline and artificial saliva were used, whereas DW was used here.

Interestingly, the earlier study by Loudon and colleagues demonstrated an Mtb half-life of ~6 hrs. In their study, liquid culture was used for the preparation of the inoculum, and they also used lower RH (45-50 %).

It should be noted that aerosol particle sizes during experiments were not investigated here and the difference in particle sizes could have contributed to the large variability between experiments.

A key feature here has been careful standardisation of the procedure with use of defined preparative procedures, sampling, and survival assessment. This will provide the basis for systematic assessment of experimental parameters, particularly those relevant to the natural transmission process.

#### **4.4.2 Comparison of methods used to assess bacillary survival**

##### **4.4.2.1 P-CFU method gave higher counts than S-CFU method**

As was mentioned in section 1.6, in conducting aerobiology experiments, bacterial cells are challenged with several stressors, starting from preparation of the inoculum through the nebulisation and sampling process, to plating and storage of the samples (Haddrell and Thomas, 2017). As a result, a proportion of cells are potentially becoming injured, leading to slow or lost culturability (Wu, 2008). Enhanced growth of Mtb under a microaerophilic atmosphere compared to normal oxygen tension has been reported previously (Ghodbane *et al.*, 2014). Thus, in the current study, the P-CFU method, where an initial microaerophilic atmosphere is achieved, was compared to the conventional method used in survival studies, S-CFU. According to the result (Figure 4.8), even though both techniques shared similar patterns of reduction, a higher CFU number of *M. bovis* BCG was observed within P-CFU with all the aerosol samples. Therefore, the P-CFU method was assigned as the reference method for the experiments.

#### **4.4.2.2 Culture supernatant supplementation had no significant effect on BCG recovery**

In the current work, *M. bovis* BCG cells in aerosols were assessed for the presence of Rpf- dependent populations. Three samples were chosen for this experiment, Pre-nebulisation sample, an aerosol sample taken at 60 min, and an aerosol sample taken at 120 min, due to a limited supply of H37Rv culture supernatant at the time of the experiment. The pre-nebulisation sample was chosen as a baseline. Early aerosol samples were not included, as they might reflect the aerosolisation process rather than the survival of cells in aerosols.

As shown by the RI in Table 4.1., there was no significant difference between the P-CFU and the MPN+SN results. Moreover, there was no significant difference in MPN results when SN was added (RI < 1 log<sub>10</sub> difference). These findings suggest that Rpf-dependent cells were not present in or generated, by the aerosol samples. The presence of Rpf-dependent cells has been reported in sputum and biofilm in previous studies with *Mtb* H37Rv (Mukamolova *et al.*, 2010, Binjomah, 2014). This experiment was performed with *M. bovis* BCG, and further studies with *Mtb* H37Rv would be required to make an appropriate comparison of these studies.

#### **4.4.2.3 H37Rv P-CFU counts were not significantly affected by freezing**

In order to validate deferred sample processing at the University of Leicester, it was necessary to evaluate the effects of freezing the samples on survival assessments. Results from direct and deferred plating after freezing in 20 % glycerol were compared.

The choice of glycerol as a cryopreservation solution was because it showed satisfactory storage and preservation of *Mtb* populations in decontaminated sputum (treated with 4 % (wt/vol) NaOH, 14 % (wt/vol) KH<sub>2</sub>PO<sub>4</sub> and 10 % glycerol) (Turapov *et al.*, 2016). The freezing and storage of *in vitro* *Mtb* cultures and sputum-based samples did not influence the viability of the mycobacterial cells in several studies (Kim and Kubica,



1972, Shu *et al.*, 2012, Turapov *et al.*, 2016). However, the effect of freezing on Mtb cells in aerosols has not previously been explored. According to the result of this study, the aerosol samples were not significantly affected by the freeze-thaw cycle step (Figure 4.9). As the subsequent investigations were done after exposing the samples to freeze-thaw cycle, this finding provided support and validation to the outcomes of these investigations. This is a critical finding, and provides solid evidence for the validation of future collaborative studies with different institutions where the availability of facilities to run Mtb aerosolisation experiments can be an obstacle. For example, different investigations of Mtb aerosol samples were assessed at University of Leicester while the actual aerosolisation experiments were done at PHE, Porton Down.

#### **4.4.2.4 MPN and P-CFU counts gave similar patterns**

The majority of survival studies on microorganisms in aerosols have used the conventional method of CFU counts to detect cells in aerosols. However, plate counts can be subject to underestimation of the bacterial populations in air samples. This can be due to the fact that although cells exposed to aerosolisation can be viable, they lose the ability to form colonies (Heidelberg *et al.*, 1997). To avoid this underestimation, some survival studies have used microscopy as an alternative to CFU counts (Carrera *et al.*, 2005, Thomas *et al.*, 2011). To the best of our knowledge, no previous study has demonstrated the survival of cells in aerosols in a liquid culture. In the current study, P-CFU and MPN assays were used to investigate the survival of Mtb in aerosols. Additionally, in the next section, the PMA-qPCR assay was performed to investigate the proportion of intact cells.

It can be seen that similar survival patterns of Mtb in aerosols were uncovered by the MPN technique and P-CFU (Figure 4.10). This result provides extra evidence regarding the survival of Mtb cells in aerosols. When the absolute number detected by P-CFU was compared to the MPN (Table 4.2), no significant difference was found. This suggests that neither the aerosolisation process nor the aerosol phase induced the production of liquid culture-dependent populations within the aerosols.

#### 4.4.2.5 Propidium monoazide (PMA) viability assessments

Molecular-based (DNA) analysis has been used previously to detect Mtb-carrying aerosols in the room air of respiratory-isolated TB patients (Mastorides et al., 1999). However, this molecular-based technique does not distinguish between cells with intact membranes from cells with compromised (or damaged) membranes (Kim et al., 2014). In this regard, researchers have used DNA-binding dyes to differentiate between intact and non-intact cells. The most common membrane-impairment dye is propidium iodide (PI), which has been used for microscopic live-dead discrimination and increasingly in flow cytometry (Nocker et al., 2006). Other DNA-binding methods include the use of DNA-binding dyes in combination with real-time PCR. Ethidium monoazide (EMA) and Propidium monoazide (PMA) are examples of these dyes. In a previous study using several bacterial species including *M. avium*, EMA and PMA were equally efficient in removing DNA from dead cells; however, EMA partly reduced the DNA yield from live cells when compared to untreated or PMA-treated cells (Nocker et al., 2006). In addition, PMA has been reported to be a useful approach for differentiating dead from live bacilli in AFB smear-positive sputum samples (de Assunção et al., 2014, Kim et al., 2014).

The proportion of intact cells was investigated in the current study using the PMA-qPCR assay. Figure 4.11 shows that there was approximately 1 log<sub>10</sub> difference in the proportion of intact cells compared to the total aerosolised cells in all the aerosol samples. When the PMA stain was applied to the suspension pre-nebulisation, around 35 % of cells were intact. This may be due to the aggregation of cells generated during the preparation of the inoculum. The presence of these clumps might have led to the aerosolisation of free DNA from damaged cells in greater proportion when compared to intact cells. Moreover, the intact cells in the aerosols were exposed to additional stress during the sampling process, which used the AGI 30 impinger, leading to a decrease in the number of intact cells. A comparison study with *S. aureus* between this sampler and the Biosampler (SKC) demonstrated that the AGI 30 achieves a lower preservation of bioaerosol viability than the SKC sampler (Tseng et al., 2014). However, the work here was done with Mtb, and this difference in species might not reflect an appropriate

comparison between the two samplers. Further investigations using Mtb could be a target in future work to evaluate the impact of these samplers.

The detection of Mtb in aerosols by PMA-qPCR was higher by over one order of magnitude compared to the P-CFU and MPN (Table 4.2). Yet, the rate of decline was not significantly different over the period of two hrs (Figure 4.12). This observation further confirms the survival results obtained in the current study.

### 4.4.3 Effect of nebulisation on Mtb H37Rv cells

#### 4.4.3.1 P-CFU counts

The 3-jet Collison nebuliser has been used in several survival studies of microorganisms, including the above two studies. The effect of this pneumatic nebuliser on cells during nebulisation has been investigated on many occasions. In 2011, Thomas and colleagues reported a decline in the P-CFU count of *E. coli* in the 3-jet Collison reservoir post-nebulisation by 65 % compared to pre-nebulisation. This observation was not seen with *P. aeruginosa* when it was aerosolised using the same nebuliser (Clifton *et al.*, 2010, Thomas *et al.*, 2011). With regards to Mtb, Clark and associates demonstrated a one log<sub>10</sub> decrease in the P-CFU in the reservoir of the Collison nebuliser during the initial 10 min of aerosolisation (Clark *et al.*, 2011). This was not the case in the current study (Figure 4.13), where P-CFU count was higher by 7-18 % and 29-40 % in the reservoir post-nebulisation with Collison and Ultrasonic nebulisers, respectively. This difference can be due to the inoculum preparation used in Clark *et al.*'s study, as they used liquid suspension, while lawn growth suspensions were used in this study. There are two possible reasons for the increase seen in our study. First, the aerosolisation process may have led to breaking of the clumps in the original suspension, resulting in the production of small single cells. Second, the aerosolisation process produced heat, which resulted in the evaporation of the water and increased the concentration of cells in the reservoir. Similar observations were seen in a previous study with *B. subtilis* (Stone and Johnson, 2002).

#### 4.4.3.2 PMA exclusion

When the PMA stain binds to DNA, UV exposure leads to formation of covalent links so that amplification of the bound molecules is prevented. This approach can be used to differentiate between intact and non-intact cells within one suspension by a qPCR assay. There was a significant decrease in the percentage of intact cells post-nebulisation when using both nebulisers (Figure 4.14A). On one hand, this decrease could confirm the two possible reasons mentioned above, as clumping can be a barrier against the stain. When clumps were broken up by the aerosolisation process and while evaporation occurred, there were more single cells accessible to the PMA stain. On the other hand, it might also point to the damage of the cells during aerosolisation. However, the decline in the percentage of intact cells was limited to 20-25 % with both nebulisers (Figure 4.14B). It should be noted that the aerosol samples used here were exposed to a freeze/thaw cycle before treatment. The influence of freeze/thaw cycles on the permeability of PMA and the results was not investigated here. However, the assumption that both samples (treated and non-treated) were exposed to the same freeze/thaw cycle could account to the validity of the results obtained here.

Finally, all the comparison investigations in this chapter were done using a 3-Jet Collison nebuliser and an Ultrasonic Omron nebuliser. The different of aerosol particle sizes generated from these nebulisers was not investigated here. While the 3-Jet Collison nebuliser generates aerosol particle size around 3  $\mu\text{M}$  (Lever et al., 2000), the Ultrasonic Omron nebuliser generates aerosol particle size around 4.6  $\mu\text{M}$  (manufacture manual instruction). The nebulisation volume setting of Omron was set to maximum, however, the internal fan was blocked to achieve equal internal flow rate with the Collison nebuliser (Section 4.2.2). The difference in aerosol particle sizes generated from these nebulisers did not affect the general pattern of the results in this chapter, as both nebulisers showed insignificant differences in the results. However, the Omron nebuliser generated higher number of aerosols particles with less variability compared to the Collison nebuliser. This observation can be taken into consideration in future aeroaolisation studies and general Mtb aerosol research.

## 4.5. Conclusions

- Mtb H37Rv and *M. bovis* BCG show a survival in aerosols of at least two hrs post-nebulisation.
- P-CFU counts of *M. bovis* BCG in aerosol samples were consistently greater than S-CFU.
- Rpf-dependent cells of *M. bovis* BCG were not induced by the aerosolisation process using the Collison or Omron nebulisers.
- Mtb H37Rv cells in aerosols were not significantly affected by the freeze-thaw cycle.
- P-CFU and MPN techniques used to detect Mtb H37Rv in aerosols resulted in the detection of similar survival patterns.
- The difference in damaged Mycobacterial cells was insignificantly higher with the Collison nebuliser compared to the Ultrasonic Omron nebuliser.
- The PMA-qPCR assay detected Mtb H37Rv cells in aerosols by over one order of magnitude when compared to P-CFU and MPN.

## Chapter five

# 5. Transcriptional changes in *M. tuberculosis* H37Rv on aerosol In vitro Studied by RNA- Sequencing

## 5.1 Introduction

One way to understand an organism's adaptation to its surrounding environment is to study its transcriptome profile under different conditions. The transcriptome provides valuable information, including transcript content, determination of transcriptional start sites, mRNA abundance and antisense RNAs (Filiatrault, 2011). It is challenging to achieve a comprehensive analysis of global gene expression in prokaryotes due to the abundance of rRNA and tRNA, and the insurvival of transcripts (Filiatrault, 2011). A significant challenge when studying bacterial transcriptomics is the fact that mRNAs represent only around 5 % of the total cellular RNA. To overcome this difficulty, rRNA can be removed from isolated RNA samples to enrich mRNA content. The rapid advancements in high-throughput sequencing technology have provided valuable tools for the study of microbial transcriptomes, even in the presence of such difficulties (He *et al.*, 2010).

The ideal method of transcriptome analysis depends on its ability to provide detailed information about all RNA species, regardless of their abundance and size. Such a technique can be achieved by applying an RNA-sequencing which is not limited to the gene expression level but can also be a useful tool for characterising the whole transcriptome of an organism. The advantages and disadvantages of this, and other technologies, were discussed earlier (in section 1.7.1). In this chapter, RNA-sequencing was used to study the transcriptional signatures of *M. bovis* BCG and Mtb during aerosolisation and survival within aerosols. More details about RNA-sequencing technology are discussed below.

In a single RNA-sequencing experiment, two major processes occur; data generation (Figure 5.1 A) and data analysis (Figure 5.1 B).

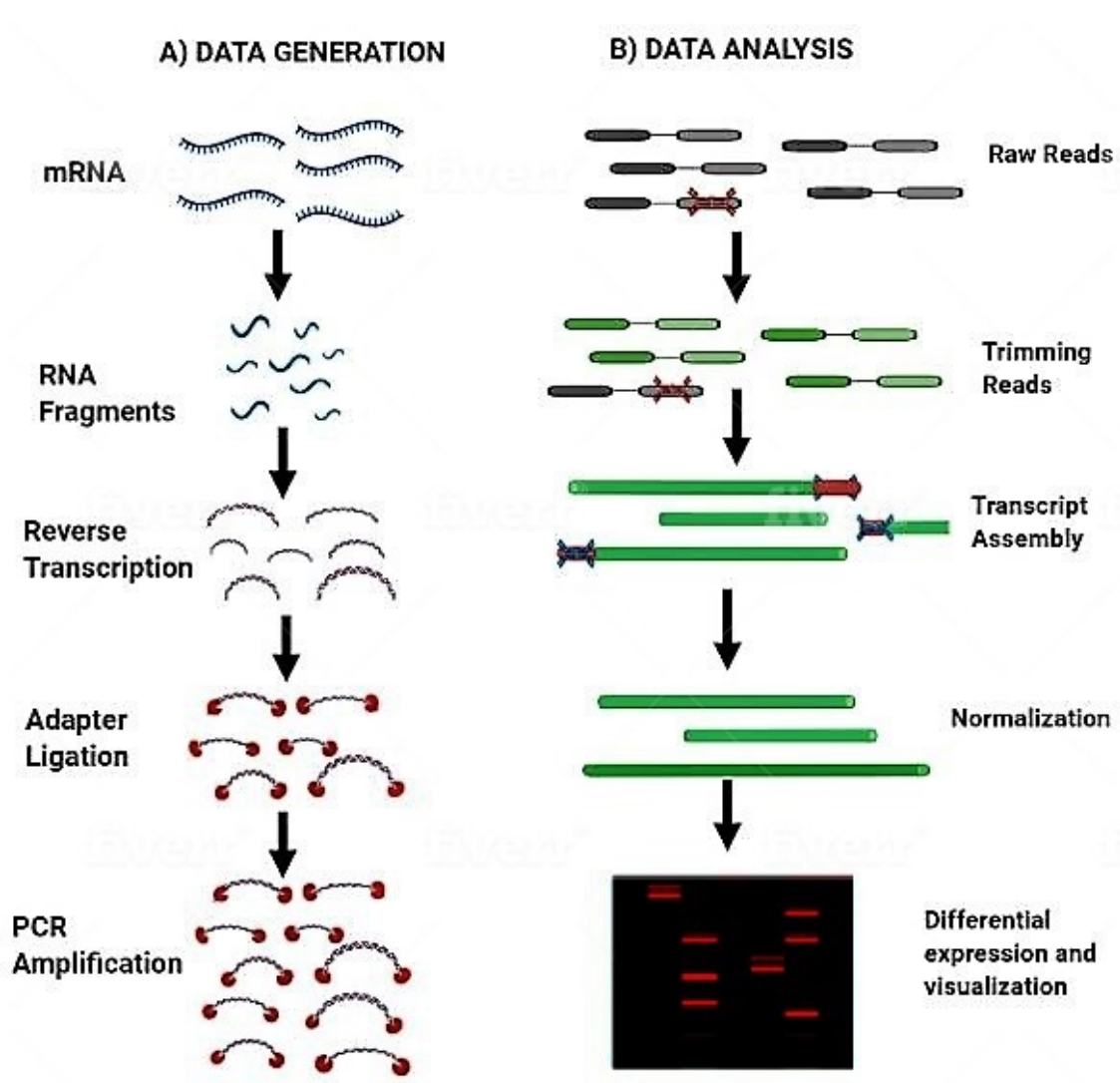


**Figure 5.1. A typical RNA-sequencing experiment.** A) Data generation. The RNA is first extracted, after which DNA contamination is removed, and short fragments of RNA are made, then reverse transcribed into cDNA. The adaptors (red) are ligated, and fragment size selection is performed. Finally, the cDNAs are sequenced to generate short reads. B) Data analysis. Low-quality reads and artefacts such as contaminant DNA adaptor sequences and PCR duplicates are removed after sequencing. To improve the quality of the sequence, errors (red crosses) are optionally removed. The reads are then assembled into transcripts, and the errors are removed via post-assembly processes (blue crosses). The transcripts are then normalised, and the expression of each transcript is measured by counting the number of reads that align to each transcript, followed by measuring the differential expression of genes. Figure adapted from (Martin and Wang, 2011).



### 5.1.1 RNA library preparation

RNAs are temperature-sensitive molecules and are always under constant risk of being degraded by ubiquitous RNase enzymes. The importance of RNA integrity comes from the fact that it strongly influences gene expression analysis (Becker *et al.*, 2010). The integrity of RNA is not constant among similar experiments; this can be overcome by careful processing and proper handling following RNA extraction (Schroeder *et al.*, 2006). Many conventional applications, including gel OD measurements, Nano-drop OD measurements, and denaturing agarose gel electrophoresis have been used to measure RNA integrity. However, these applications are susceptible to interference from contaminants present in the sample and have shown inadequate levels of sensitivity in being able to detect small and subtle amounts of RNA degradation (Imbeaud *et al.*, 2005).

Today, highly innovative lab-on-chip technologies such as the Bioanalyzer 2100 (Agilent Technologies, USA) and Experion (Bio-Rad Laboratories, USA) have proved to be useful tools for measuring RNA integrity. For example, when using the Bioanalyzer 2100 system, RNA samples are first separated according to their molecular weight using the channels present on the microchip, and then detected fluorescently with the use of lasers. The intensity of fluorescence correlates with the RNA quantity of a given size. Determination of the quality and integrity of RNA is based on the 16S/23S ratio. The result is expressed as a number called the RNA integrity number (RIN), which can be extracted from the shape of the curve obtained from the electropherogram. The RIN number can range from 1 to 10, where 10 represents the most intact RNA, and 1 represents highly degraded RNA (Fleige and Pfaffl, 2006, Jahn *et al.*, 2008).

### 5.1.2 Preparation of cDNA library

Isolation of high-quality and quantity RNA is a key step towards achieving successful RNA-sequencing analysis. Currently, there are many commercially available kits or organic solvents which are used in most procedures. The method should not bias the sampling across the transcriptome (Croucher and Thomson, 2010), and rRNA depletion prior to generating the cDNA library is a commonly applied approach in RNA-sequencing analysis (Petrova *et al.*, 2017).

In traditional RNA-sequencing experiments, random hexamers are used to make cDNA, which is followed by second-strand DNA synthesis. This protocol of cDNA library preparation has led to the loss of valuable information concerning which strand was provided with the original mRNA template. In other words, the conventional method of preparing cDNA libraries for RNA-sequencing results in an equal number of sense and antisense strands. Consequently, the strand-specific signal in the RNA sample is lost. It is worth noting that in the Illumina RNA protocol, the cDNA libraries are constructed only from the first-strand cDNA. Therefore, DNA strand specificity is maintained in the RNA-sequencing data (Levin *et al.*, 2010, Dominic Mills *et al.*, 2013).

### 5.1.3 Sequence library preparation

One of the differences between current RNA-sequencing platforms such as Illumina, Roche 454 and PacBio is the read length (ranging from 35 nucleotides to 400 nucleotides) (Thompson and Milos, 2011). This difference can have a significant influence on the pre-sequencing process steps of the DNA library. In general, these steps include shearing large amounts of DNA into suitable platform-specific size ranges. Next, an end-polishing process occurs, resulting in the production of blunt-ended DNA fragments. Later, specific adapters are ligated to the 3' and 5' end of the fragment. It should be noted that each sequencing platform uses an extra set of unique adapter sequences that are compatible with subsequent steps in the process. An example of various adapters used in different platforms is illustrated in Figure 5.2 (Buermans and Den Dunnen, 2014).

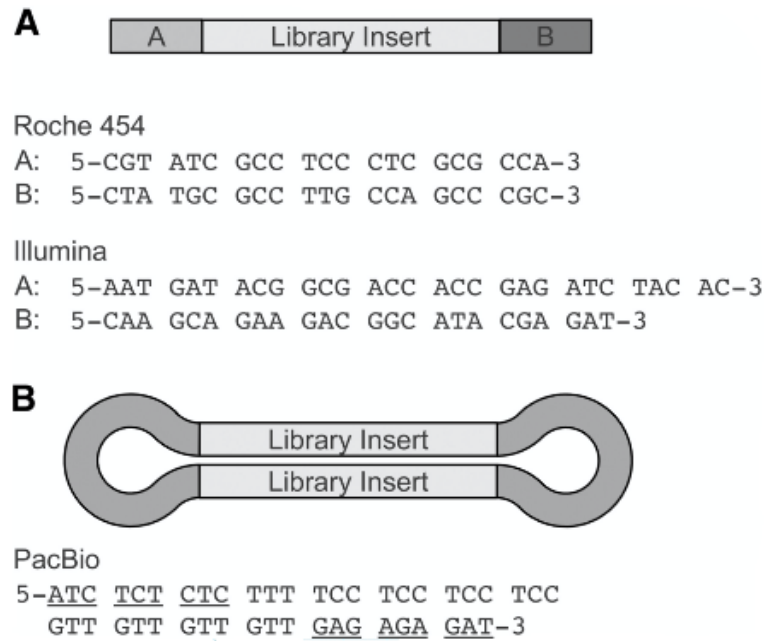


**Figure 5.2. Structure of sequence library molecules for different platforms.** Linear library molecules (Panel A) contain different adapter sequences at the 5' [A] and 3' [B] ends of the library inserts. Circular library molecules (Panel B) contain identical adapter molecules at both ends of the insert.

In the Illumina platform, all sequencing processes and imaging steps occur in multi-lane flow cells. All cDNA molecules are attached to surfaces inside the flow cell lanes and are amplified by PCR (Buermans and Den Dunnen, 2014). The sequence of each molecule can then either be from one end (i.e. single-end reads) or from both ends (i.e. pair-end reads) (Wang *et al.*, 2009).

The term 'depth of sequencing' is commonly used among RNA-sequencing researchers and is defined as the total number of all reads per sample. It is vital when the RNA-sequencing experiment aims to detect and quantify low abundance transcripts (Croucher and Thomson, 2010). Although increasing the depth of sequencing level in RNA-sequencing is desired by many researchers, its high cost can be an obstacle. Hence, an RNA-sequencing experiment designer should be meticulous in finding the appropriate balance between the number of reads per sample (depth of sequencing) and the number of samples needed to be sequenced (breadth of sequencing) (Haas *et al.*, 2012). On this point, the priority of depth of sequencing over breadth of sequencing can be determined, depending on the purpose of the experiment. For instance, in experiments where detecting rare transcripts is critical, the focus should be on the

depth of sequencing. However, if statistical confidence is required, breadth of sequencing can be considered to be more important (Sims *et al.*, 2014). As the study here was the first to be done with mycobacterial species, the transcriptional analysis was focused on both the depth of sequencing (74 bp read length) and the breadth of sequencing (3 biological replicates) for statistical confidence.

### 5.1.4 Base calling and quality score

Once the sequencing platform generates raw data, it is converted to nucleotide sequences via a process named base calling. The raw data generated by the sequencing platform can be expressed in different forms (fluorescence intensity, electrical impulse, etc.) depending on the sequencing platform being used. Hence, base calling is a platform-specific process. However, the overall pipeline across different sequencing platforms is similar (Duncan and Patel, 2017).

In the Illumina platform, for example, sequencing is performed via a process called sequencing by synthesis (SBS), which takes place in a flow cell consisting of eight lanes. Each lane has a lawn of oligonucleotides that have a generic sequence. After adding universal adapters to the sample DNA, the sample will be flooded into the flow cell lanes. Then, the target molecules are immobilised by binding to the oligonucleotide lawn. A bridge amplification process then takes place to generate approximately 1,000 copies of each target molecule which form clusters on the flow cell (figure 5.3). Millions of clusters are generated, each of them representing one target molecule from one sample (Cacho *et al.*, 2015).

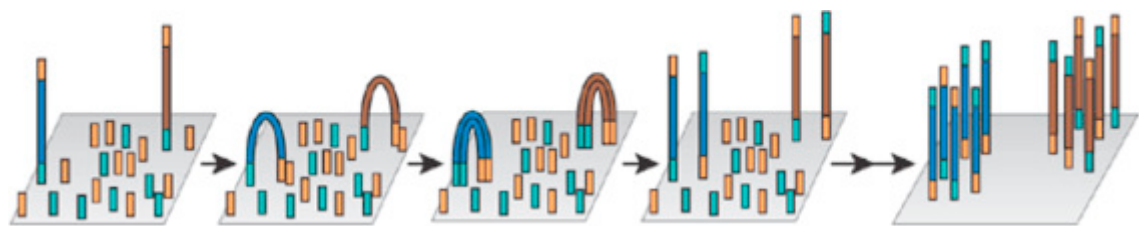
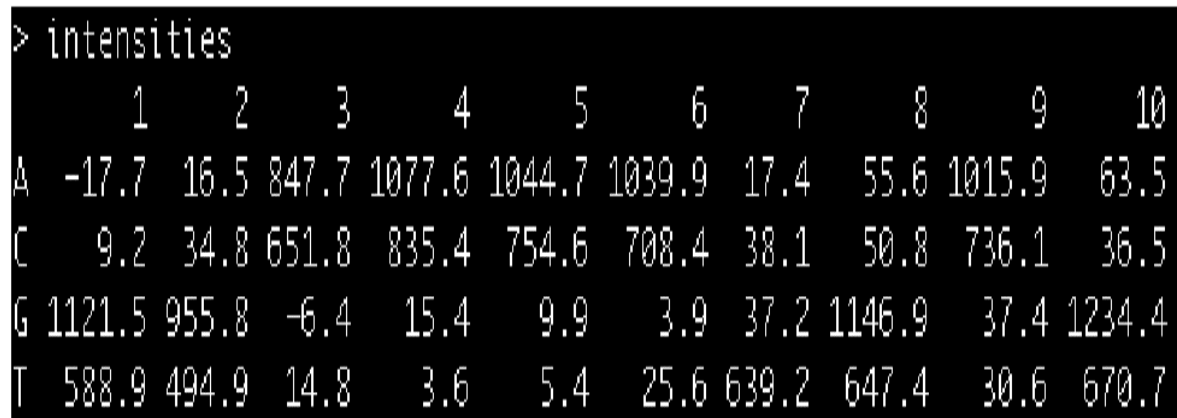


**Figure 5.3. Illumina sequencing.** The Illumina platform immobilises individual product molecules on a flow cell and then uses bridge PCR to form clonally amplified colonies (Duncan and Patel, 2017).

After the generation of clusters, multi-sequencing cycles occur until the complementary strand synthesis is completed. This happens in parallel for each cluster. The bases used in SBS are labelled fluorescently and attached with reversible terminators. These bases are incorporated in each cycle during sequencing. The purpose of the attached terminators is to allow for the sequential incorporation of the bases one at a time. When a single base is incorporated, a laser excites each of the clusters, allowing for the emission of fluorescence which can then be imaged to identify the incorporated base. Finally, the reversible terminator is removed to allow for the following labelled base to be incorporated in the next sequencing cycle (Cacho *et al.*, 2015).

At the end of each sequencing cycle, four images are captured and read through four different filters, one for each of the dyes used for each base. The images are processed to produce values which represent the intensity for the corresponding nucleotide channels A, C, G and T (Cacho *et al.*, 2015). An example of intensity output for the first ten cycles of a single cluster is illustrated in Figure 5.4.



```
> intensities
      1      2      3      4      5      6      7      8      9     10
A -17.7  16.5 847.7 1077.6 1044.7 1039.9  17.4   55.6 1015.9  63.5
C   9.2  34.8 651.8  835.4  754.6  708.4  38.1   50.8  736.1  36.5
G 1121.5 955.8  -6.4   15.4    9.9    3.9  37.2 1146.9   37.4 1234.4
T  588.9 494.9  14.8    3.6    5.4   25.6 639.2  647.4   30.6  670.7
```

**Figure 5.4. An example of intensity values for the first ten cycles of a read.** The rows represent the nucleotide channels, and the columns represent the cycles. The read can be considered to be GGAAAATGA.

The images translated into base calls are represented in FASTQ format, in which each nucleotide is designated with an ASCII- encoded quality number corresponding to a Phred score (Q). The Phred score is used to measure base calling accuracy and can be defined as the probability (P) that the corresponding base call is incorrect by the following equation:

$$P = 10^{-(Q/10)}$$

Where Q represents the quality score ranging from 0 to 41; therefore the error rate ranges from 1 to 0.00008 for each base call (Cock *et al.*, 2009, Del Fabbro *et al.*, 2013).

Most low-quality base calls are generated towards the end of the reads and need to be removed before analysis, as they can lead to increased false-positive variant calls (Ledergerber and Dessimoz, 2011). Therefore, FASTQ files go through extensive analytic algorithms to detect poor Phred score bases and to delete them prior to alignment. This step is performed routinely by a process called 'trimming'. During trimming, low-quality reads and/or bases and sequencing artefacts are removed (Chen *et al.*, 2014).

### 5.1.5 Alignment and annotation of transcripts

Following the filtration of FASTQ files, data analysis is initiated to detect and quantify the transcripts. The data analysis can be divided into three steps. First is the alignment of reads, then the assembly of transcripts, and finally the quantification of transcripts. These steps require extensive bioinformatic processes and software, and approaches developed for this purpose are freely available. It should be noted that even a small RNA-sequencing experiment, with only one sample, can produce a tremendous number of sequencing reads (up to hundreds of gigabytes worth of data) (Trapnell *et al.*, 2012).

Sequence alignment is the process by which all the individual transcripts are mapped to their locations in the genome(s) of interest. Regardless of which sequence platform generated the raw data, any available aligning software can be used (Duncan and Patel, 2017). Transcript assembly is another critical step in data analysis. Because of the short length of sequence reads obtained via RNA-sequencing platforms, reconstructing the full length of transcripts is essential. This process, known as transcriptome assembly, can be done through two strategies, reference-based and *de novo* (Martin and Wang, 2011). In the reference-based strategy; the sequencing reads are aligned to a sequenced reference genome. This approach is favoured when a high-quality sequence genome already exists, as it is fast and highly sensitive. On the other hand, the *de novo* strategy

involves assembling transcripts by combining overlapping reads without a reference genome to reconstruct transcript sequences (Moreton *et al.*, 2016). As the Mtb H37Rv genome sequence is available, the reference-based strategy was used as assembly approach in the current study.

### 5.1.6 Normalisation methods

Measuring the concentration of the original RNAs in an RNA-sequencing analysis is a challenge. The extent to which the transcript's quantification can represent the absolute RNA concentration is a question that can be answered by the normalisation of the quantified reads (Mortazavi *et al.*, 2008). Several approaches have been proposed for the normalisation of quantified reads:

**Total count (TC):** The total number of reads divided by the total number of mapped reads (or library size).

**Upper quartile (UQ):** Similar to TC, but the total number of reads is replaced by the upper quartile of counts, which are different from 0 in the computation (Bullard *et al.*, 2010).

**Median (Med):** Also similar to TC above, but the total number of reads is replaced by the median counts, which are different from 0 in the computation.

**DESeq:** For this normalisation method, the DESeq Bioconductor package is used. It is based on the assumption that for most genes, there is no differential expression. The median ratio of each gene is divided by the geometric mean of the total read counts (Anders and Huber, 2010).

**Trimmed Mean of M values (TMM):** For this normalisation method, the edgeR Bioconductor package is used; it is also based on the assumption that there are no differential expressions for most genes. It is a factor used for the computation of lanes results, where one lane is considered as a reference while the other lanes are test samples. For each test sample, TMM calculates the weighted mean of the log ratio between the reference lane and the test lane (Robinson and Oshlack, 2010).

**Quantile (Q):** This was initially used for microarray data. It is implemented in the Bioconductor package Limma, which matches the distribution of gene counts across lanes (Bolstad *et al.*, 2004).

**Transcript per Million (TPM):** This is a modified version of RPKM used to measure transcript abundance. It can be calculated from the following equation:

$$\langle \text{TPM} \rangle_g = \frac{10^6}{N}$$

N: the total number of transcripts in a sequencing run.

TPM is proportional to RPKM within a sample but provides a higher sensitivity level when applied between samples compared to RPKM (Wagner *et al.*, 2012).

**Reads Per Kilobase per Million mapped reads (RPKM):** This is a measurement of read density that represents the absolute concentration of the transcript in the original sample. It provides a comparison of transcript levels, both within and between sample normalisation, to correct for differences in both gene length and library sizes (Mortazavi *et al.*, 2008). To calculate the RPKM for a particular gene, the following equation is used:

$$\text{RPKM}_g = \frac{r_g \times 10^9}{\text{fl}_g \times R}$$

$r_g$ : the number of reads mapped to a particular gene.

$\text{fl}_g$ : (feature length): the number of nucleotides in a mapped region of a gene.

R: the total number of reads from the sequencing run of that sample (Wagner *et al.*, 2012).

Following the introduction of RPKM by Mortazavi *et al.* in 2008, many different versions have been proposed, including the normalisation approach with the Rockhopper software. This program is widely used for prokaryotic RNA-sequencing analysis. It normalises read counts by first excluding genes with zero expression, then using the upper quartile of the gene expression level (McClure *et al.*, 2013).



### 5.1.7 Detection of differentially expressed (DE) genes

There are many different objectives behind running RNA-sequencing experiments, such as estimating the abundance of transcripts (Li and Dewey, 2011) or detecting of alternative splicing (Griffith *et al.*, 2010) and/or novel transcripts (Robertson *et al.*, 2010). However, in many biological studies, the main goal of RNA-sequencing experiments is to detect DE genes between samples (Oshlack *et al.*, 2010).

The Fisher's exact test statistic model has been implemented for the detection of DE genes in data analysis for RNA-sequencing. Moreover, two statistical models have also been proposed, these being the likelihood ratio and the t-statistics models (both based on generalised linear methods) (Bullard *et al.*, 2010). It should be noted that these models are based on the null hypothesis that the logarithmic fold change between the test sample and control for a gene's expression is exactly precisely zero (Love *et al.*, 2014).

### 5.1.8 Aims and objectives

This chapter introduces and discusses the data obtained from RNA-sequencing analysis. The main aim of this research was to study the transcriptional signatures of *M. bovis* BCG and Mtb cells in aerosols.

The objectives were:

- To determine the impact of the nebulisation process on the transcriptional profile on Mtb cells.
- To determine whether specific genes influence the selectivity of Mtb cells to be successfully aerosolised.
- To determine whether specific genes contribute to the survival of Mtb cells in aerosols.

## 5.2 Methods

### 5.2.1 5M Guanidinium thiocyanate (GTC) solution

GTC is a chaotropic substance which denatures proteins and therefore stabilises nucleic acids (Mason *et al.*, 2003). The original GTC<sub>a</sub> has been used previously to collect sputum/bacterial cultures (4 vols GTC<sub>a</sub> added to 1 vol sample) (Garton *et al.*, 2008). When this solution was applied into biosamplers for aerosol collection it failed, as GTC crashes out of solution. Hence, new modified GTC solutions were optimised named GTC<sub>b</sub> and GTC<sub>c</sub>. GTC<sub>b</sub> contains a lower 2.5M concentration of GTC (which is enough to halt transcription, but low enough not to come out of solution during collection). GTC<sub>b</sub> also contains no tween and this helped to eliminate the frothy mess during collection. GTC<sub>c</sub>, on the other hand, contains Tween 80 and lauryl sarcosine. Aerosols samples were collected in 16 ml GTC<sub>b</sub> then 4 ml GTC<sub>c</sub> was added (1 vol GTC<sub>c</sub> added to 4 vols GTC<sub>b</sub>). Compositions of three GTC solutions are shown in the table below:

**Table 5.1. Compositions of GTC solutions.**

Reagent	GTC <sub>a</sub>	GTC <sub>b</sub>	GTC <sub>c</sub>
GTC	295.4 g	147.7 g	295.4 g
Sodium N-Lauryl sarcosine	2.5 g	-	15 g
1M Trisodium Citrate pH 7.0	12.5 ml	12.5 ml	-
Tween 80	2.5 g	-	15 g
Dithiothreitol *(DTT)	0.5 g	-	-

The compositions were added to 200 ml DW in 500 ml Durham bottles and dissolved overnight via incubation at 37 °C, with shaking at 100 RPM. Next, the solutions were made up to a final volume of 500 ml with DW and stored away from heat and light. On the same day of the experiment, 7 µl/ml β-mercaptoethanol was added to the GTC solutions.

### 5.2.2 Growth condition and test procedure

From the previous chapter's investigation, it was observed that there was no difference in the survival pattern of Mtb H37Rv and *M. bovis* BCG using either the 3-Jet Collison or the Ultrasonic Omron nebuliser. However, the ultrasonic Omron nebuliser generated a higher number of aerosols than the Collison nebuliser over the 5 min of nebulisation. Therefore, the work in this chapter was done using the Ultrasonic Omron nebuliser.

The preparation of the bacterial inoculum was as described in section 4.2.1 above, and the test procedure was as described in section 4.2.4, with some modifications. Standard volume air samples ( $12.5 \text{ L min}^{-1}$ ) were withdrawn from the drum for 1 min using SKC impingers containing 16 ml 2.5 M GTCb. Aerosol samples were removed over a period of 2 hrs at three different time points; early sample (at 0 min post-spray), middle sample (at 30 min post-spray) and late sample (at 120 min post-spray). Once the samples were collected, the final concentration of GTC was amended with 4 ml of GTCc. 1 ml of the original suspension was collected as the pre-nebulisation sample, and the 1 ml of suspension which remained inside the reservoir was collected as the post-nebulisation sample. Both samples were treated with GTC as with the aerosol samples. Triplicate runs were performed for each strain.

The samples were kept at  $-80^\circ\text{C}$  freezer until RNA extraction was carried out.

### 5.2.3 DNase I solution (digestion buffer)

DNase I powder (provided in the Turbo-DNase kit) was dissolved in 550  $\mu\text{l}$  DNase-RNase-Free water. Aliquots of 10  $\mu\text{l}$  were made and stored at  $-20^\circ\text{C}$ . Then, the required 10  $\mu\text{l}$  of DNase I solution was mixed with 70  $\mu\text{l}$  Buffer RDD which was provided in the Turbo-DNase kit

### 5.2.4 RNA extraction

Prior to RNA extraction, the GTC samples were centrifuged at  $3000 \times g$  for 30 min. Then, most of the supernatant was decanted, except for 1 ml which was used to re-suspend the pellet. This 1 ml was then transferred to 2 ml screw-top micro-centrifuge tubes and pelleted at  $16,000 \times g$  for 5 min. Next, the supernatant was removed and replaced with 1 ml Trizol and then placed at  $-80^\circ\text{C}$  awaiting RNA extraction.

RNA extraction was done by using Direct-zol RNA MicroPrep kits (Cat number: R2060, Zymoresearch). The protocol was followed as per the manufacturer's instructions with a few optimisations. Samples were defrosted, and 250 µl of 0.1 mm lysing matrix was carefully added to the cells in Trizol. The cells were then lysed using a reciprocal shaker (FastPrep-24 5G, MP Biomedicals) with a speed setting of 6.5 m/s for 45 sec). Samples were left to cool at RT for 10 min. Next, the samples were centrifuged at 16,000 x g for 5 min, after which the supernatants were transferred to fresh 1.5 ml Eppendorf tubes. Depending on the amount of sample transferred, an equal volume of RNase free 100 % ethanol was added and mixed in thoroughly. 500 µl of the sample was then loaded onto a Zymo-Spin column in a collection tube and centrifuged at 16,000 x g for 1 min. The flow-through was discarded and this was repeated for the remainder of the sample.

Next, 400 µl of Direct-zol RNA Pre-Wash solution was added to each column and centrifuged at 16,000 x g for 1 min. The flow-through was discarded. After this, the columns were loaded with 40 µl of DNA digestion buffer and incubated at RT for 15 min. When the incubation step was complete, 400 µl of Direct-zol RNA Pre-Wash solution was added to each column and centrifuged at 16,000 x g for 1 min. Next, 700 µl of Direct-zol RNA Wash solution was added to each column and centrifuged at 16,000 x g for 2 min. The columns were transferred to fresh 1.5 ml Eppendorf tubes. The RNA bound to the column membrane was eluted by pipetting 50 µl of RNase-free water directly on the column membrane, after which the columns were centrifuged at 16,000 x g for 1 min. Finally, The RNA samples were stored at -80 °C, in preparation for the next step.

### **5.2.5 Turbo Dnase treatment**

Turbo DNase treatment was applied to the samples to remove any residual DNA by using the TURBO DNA-free™ Kit (Ambion, Cat; AM 1907). The protocol was followed as per the manufacturer's instructions with the following modifications: 5 µl Turbo DNase buffer and 1 µl Turbo DNase reagent were added to the extracted RNA sample and mixed gently. Then, the samples were incubated at 37 °C for 30 min, after which 1 µl of Turbo DNase was added. The samples were incubated for a further 30 min at 37 °C. Next, 10 µl inactivation reagent was added and mixed gently for 3 min, and then

centrifuged for 5 min at 16,000 x g. The aqueous phase was transferred to a new Eppendorf tube to prevent any carryover of the inactivation reagent.

### **5.2.6 On-column DNase digestion**

For further refinement of extracted RNA, the samples were treated with on-column DNase I digestion. This step was performed using an RNeasy Mini kit (Qiagen, Cat; 74104). The protocol was followed as per the manufacturer's instructions. Firstly, the sample volume was increased to 100 µl with RNase-free water. Next, 350 µl of buffer RLT and 250 µl 100 % ethanol were added. The total 700 µl sample was then transferred to the RNeasy spin column before being placed in a 2 ml collection tube and centrifuged at 16,000 x g for 15 sec. The flow-through was discarded and 500 µl buffer RPE was added to the RNeasy spin column and centrifuged at 16,000 x g for 15 sec. The flow through was discarded and 500 µl of buffer RPE was added to the RNeasy spin column and centrifuged at 16,000 x g for 2 min. The RNeasy spin column was then placed in a new 2 ml collection tube and centrifuged at 16,000 x g for 1 min. After this, the RNeasy spin column was placed in a new 1.5 ml collection tube and 50 µl RNase-free water was added directly to the spin column membrane and centrifuged at 16,000 x g for 1 min to elute the RNA. Finally, 1 µl of the crude RNA was used for quantification of RNA by Bioanalyzer (section 5.2.7), and the remaining RNA was stored at -80 °C until needed.

### **5.2.7 Measuring RNA integrity number (RIN)**

The integrity and concentration of the extracted RNA were assessed using the Agilent RNA 6000 Nano-kit purchased from Agilent Technologies (Kidlington, UK). The protocol was followed as per the manufacturer's instructions. Firstly, 550 µl of Agilent RNA 6000 Nano gel matrix was loaded into a spin filter column and centrifuged at 4000 RPM for 10 min. Then, 65 µl of the matrix was filtered into 0.5 ml RNase-free microfuge tube. Secondly, 1 µl of RNA 6000 Nano dye concentrate (mixed thoroughly for 10 sec) was added to the 65 µl and mixed thoroughly. The gel-dye mix was then centrifuged for 10 min at 14000 RPM.

Each RNA Nano-chip contains 16 wells. One well was marked black G, two wells were marked blue G, one well as a ladder and 12 wells were assigned for the samples. 9 µl of

the gel-dye mixture was loaded into the black G and blue G wells. 5 µl of the RNA 6000 Nano marker was loaded into the remaining 13 wells. Next, 1 µl of the RNA ladder was loaded into the ladder well, and 1 µl of each RNA sample was loaded into each of the 12 sample wells. Then, the chip was horizontally placed onto a vortex using an adapter and mixed for 60 sec at 3000 RPM. Finally, the chip was carefully placed into the Agilent Bioanalyzer 2100 receptacle. From the list of programs in the Agilent 2100, expert software prokaryotic – Nano RNA was selected to run the chip.

### **5.2.8 NextSeq-500 Illumina workflow**

The RNA samples were sent for RNA-sequencing analysis using the Illumina platform (vertis Biotechnologie - Germany). The BaseSpace software is integrated with the sequencing workflow. This software is the genomics computing environment in Illumina that is used for data analysis, storage, and collaboration. Further information on the platform can be found in the NextSeq 500 System Guide (15046563 I) at <http://support.illumina.com/> (Illumina, 2020).

### **Starting the sequencing run**

RNA samples were firstly reverse transcribed to make a cDNA library. Then, the cDNA strands were fragmented into 75 nt bases. Next, universal and specific adaptors were attached to the fragment ends. A list of the adapters used can be found in the appendices. Prior to performing a sequencing run, the libraries of cDNA with the adaptors were denatured and diluted to 3 pM, after which they were loaded onto reagent cartridges in a flow cell.

### **Cluster generation**

Single DNA molecules were bound to the surface of the flow cell and amplified to make clusters. The amplification ranged from 14 – 28.

## Sequencing

Single-end sequencing was performed, during which clusters were imaged via 2-channel sequencing chemistry and filter combinations that were specific to each fluorescent-labelled chain terminator. The process of imaging was repeated for each cycle of sequencing. The software performed base calling, filtering and quality scoring following image analysis.

## Analysis

As the run progressed, the software automatically transferred base calling files to BaseSpace for secondary analysis. FASTQ files were generated for each sample, containing details of the sequencing, including the quality score. These files were transferred to the University of Leicester for further processing.

### 5.2.9 Trimming low-quality reads

Trimming was performed in collaboration with Dr Richard Haigh from the department of Respiratory Sciences, Leicester University.

The universal and Illumina-specific adapters were removed, along with any low-quality or repeating sequences, using Trimmomatic version 0.32 (Bolger *et al.*, 2014). The quality score was set at Phred > 33, with a minimum acceptable fragment of 25 nt. The output files were generated in FASTA and SAM formats for downstream processing. The command line for trimming was written in Linux-based text. The complete script which was applied for trimming in this study can be found in the appendices. The FASTQ files before and after the quality control steps were visualised via the fastqc 0.11.2 program, using the ALICE High-Performance Computing Facility at the University of Leicester.

### **5.2.10 Alignment and normalisation of reads**

The trimmed reads were aligned and mapped against the H37Rv genome using Rockhopper 2.0.3.

### **Rockhopper processing of reads**

The FASTA files generated after the trimming of reads were loaded on to the Rockhopper software version 2.0.3 for Windows (Wellesley – MA, USA). The files contained three replicates per sample. Reads were mapped using Bowtie2 to align the reads and TPM analysis.

Dynamic programming alignment was applied when the reads did not precisely match the reference genome based on the Smith-Waterman algorithm (Smith and Waterman, 1981), since this algorithm is limited to 15 % mismatches. These were corrected via insertion and deletion scores in the dynamic programming table based on the Phred quality score (Ewing and Green, 1998). The transcript abundance was measured by normalising the expression levels into RPKM.

### **5.2.11 Differential expression of genes**

This step was done using the Rockhopper software 2.0.3. Before calculating the DE, the variance in expression of a gene was estimated by calculating the variance of the gene expression across replicates.

As the variance is affected by the expression level, a highly expressed gene would have higher variance across the replicates. Therefore, the local regression model (Anders and Huber, 2010) was applied to the normalised counts to achieve smooth estimations of the variance. Then, the DE of genes between conditions were determined by performing statistical tests for the null hypothesis. Thus, negative binomial distribution was used as a statistical model in which a two-sided p-value was computed as the probability of observing the expression levels of a gene in two conditions.

To control the false discovery rate due to multiple tests being performed across the set of genes, q-values were set using the Benjamini-Hochberg procedure (Benjamini and



Hochberg, 1995). A gene is designated as being DE if its expression in two different conditions is different at the threshold level of  $q < 0.01$ .

The q-value is an adjusted p-value taking into account the false discovery rate (FDR) in RNA-sequencing experiments. When thousands of variables (gene expression level) are measured, applying q-value becomes necessary. A p-value of 0.05 implies that researchers are willing to accept that 5 % of all tests will be false positive. On the other hand, q-value of 0.05 implies that researchers are willing to accept 5 % of the tests found to be statistically significant by p-value will be false positive (Wang et al., 2010).

## 5.3 Results

While the work in this chapter was initiated more than nine months before submission, low RNA yields and difficulties in preparing growth contemporaneously with Goldberg drum availability meant that RNA-sequencing results of sufficient quality for inclusion here were only obtained three weeks before submission. An initial analysis is presented here.

These RNA studies included aerosol experiments with both *M. bovis* BCG and Mtb H37Rv. The samples went through all the same preparation steps and were sent for RNA-sequencing. However, data analysis showed that 2 replicates of *M. bovis* BCG had low a percentage of alignment reads to genome reference (5.3.3). While there may be value in further analyse of these samples, the higher yield data from the Mtb H37Rv experiments are the main focus in this chapter.

### 5.3.1 Sequencing results

After quality control, the RNA samples were sent for RNA-sequencing. The library pool was sequenced on Illumina NextSeq 500 system using 74 bp read length.

**Table 5.2. Reads information taken after RNA-sequencing for Mtb H37Rv.**

Sample	Adaptor	PCR cycle	Total sequences
Pre-Nb	ACGTCCTG	13	10,315,476
T0	GTCAGTAC	25	12,495,522
T30	ATAGAGAG	18	9,439,734
T120	AGAGGATA	14	10,441,578
Post-Nb	CTCCTTAC	26	11,303,132
Pre-Nb	ACACGCCT	12	7,903,114
T0	CAGGTACT	22	11,454,117
T30	TCACTGAT	22	9,191,956
T120	AAGTACAT	13	8,840,250
Post-Nb	ACTGTAAT	22	10,475,112
Pre-Nb	CCACTTTG	13	7,095,297
T0	ACGATGTG	22	10,943,260
T30	AAGTGTTA	22	10,270,156
T120	ATTGACTG	22	9,401,873
Post-Nb	CTGGGATG	12	6,887,075

The sequencing report shown in Table 5.2 was generated containing details of sequencing including sequence of adaptors, number of cycles and the total number of sequences. The total number of sequences for all samples was 146,457,652 with the average sequence number per sample of 9,763,840. The reads were then assessed for base and sequence quality scores which were detailed in FASTQ files.

### 5.3.2 Alignment of reads

Table 5.3 shows the alignment % of each sample of Mtb H37Rv and *M. bovis* BCG against Mtb H37Rv reference genome and *M. bovis* BCG (strain Pasteur 1173P2 chromosome) reference genome, respectively. This was done in Rockhopper software version 2.0.3 (McClure et al., 2013). Rockhopper uses Bowtie2 as integrated alignment software which has been attested for its superior capacity compared with other alignment tools (Tjaden, 2015). The alignment of Mtb ranged from 52 to 98 % with the exception of sample T0 in the second set, where the alignment was only 18 %. Aerosol samples of *M. bovis* samples show weak alignments % in two sets of experiments (2 %) while pre- and post-samples show 97-98 % alignments to the reference genome. Based on this data, *M. bovis* BCG samples were not taken forward for further analysis.

Sample		Total reads	Aligned reads	% Aligned reads	Sample		Total reads	Aligned reads	% Aligned reads
<b><i>Mycobacterium tuberculosis</i> H37Rv</b>					<b><i>Mycobacterium bovis</i> BCG</b>				
PreNeb		9,961,934	9,767,800	98%	PreNeb		8,562,294	8,367,153	98%
T0		12,347,306	7,249,519	59%	T0		11,681,313	241,740	2%
T30		9,364,888	8,882,259	95%	T30		11,922,549	187,724	2%
T120		9,948,469	9,706,940	98%	T120		12,931,432	232,969	2%
PostNeb		11,110,560	5,763,766	52%	PostNeb		9,397,425	9229348	98%
PreNeb		7,903,114	7,047,832	89%	PreNeb		11,232,232	10,997,513	98%
T0		11,454,117	2,049,231	18%	T0		10,672,156	4,022,270	38%
T30		9,191,956	7,045,829	77%	T30		10,801,800	3,166,775	29%
T120		8,840,250	7,636,424	86%	T120		10,202,093	6,637,216	65%
PostNeb		10,475,112	5,594,317	53%	PostNeb		7,410,503	7,201,918	97%
PreNeb		7,095,297	6,153,010	87%	PreNeb		10,110,268	9,473,540	94%
T0		10,943,260	5,790,660	53%	T0		9,788,461	179,907	2%
T30		10,270,156	6,183,891	60%	T30		9,201,947	159,157	2%
T120		9,401,873	7,217,811	77%	T120		8,440,104	133,126	2%
PostNeb		6,887,075	6,207,874	90%	PostNeb		11,202,220	10,973,540	98%

**Table 5.3. Overview of the Alignments % of Mtb H37Rv and *M. bovis* BCG.** Data from RNA-sequencing were trimmed and aligned against the reference genome using Rockhopper software version 2.0.3 for windows. Mtb H37Rv showed 52-98 % alignments while 2 replicates of *M. bovis* BCG aerosols samples showed weak alignments (2 %). Green represent good alignment, Yellow represents moderate alignment, Orange represents poor alignment.

### 5.3.3 Proportion of ribosomal RNA

The results based on mapped reads to Mtb H37Rv reference genome revealed a proportion of rRNA to total RNA ranged from 57 % to 85 % in overall the samples.

	Pre-Nb	T0	T30	T120	Post-Nb
<b>1<sup>st</sup> experiment</b>	57 %	85 %	84 %	60 %	85 %
<b>2<sup>nd</sup> experiment</b>	60 %	79 %	82 %	58 %	81 %
<b>3<sup>rd</sup> experiment</b>	57 %	76 %	82 %	82 %	60 %
<b>Average</b>	58 %	80 %	83 %	67 %	75 %

**Table 5.4. Proportion of rRNA to total RNA.** The reads were mapped against Mtb H37Rv genome in the Rockhopper software.

### 5.3.5. Genes with no detected expression

Rockhopper does not include zero expression values in its analysis. 13 open reading frames (ORFs) were found to have absolutely no expression values in any condition tested (pre-neb, post-neb, T0, T30 and T120). Subsequently, the genes were organised based on functional categories using the Tuberculist website (Table 5.5).

**Table 5.5. Genes with no expression detected.**

Functional category	Genes with no detected expression
Conserved Hypothetical	7
Insertion seqs and phages	3
Intermediary metabolism and respiration	1
Regulatory proteins	1
Lipid metabolism	1
<b>Total</b>	<b>13</b>

### 5.3.4 Differentially expressed (DE) genes

The main question here was the change of transcriptional pattern of Mtb in adaptation to the nebulisation process, aerosolisation, and survival within aerosols. For this initial analysis of the expression data generated by Rockhopper (section 5.2.6.1), two rules were applied to assess potentially differentially expressed genes: 1) A change of two-fold or more between samples and 2) a q-value equal to or below 0.01. The observed differences between compared samples are summarised in Table 5.6.

	Expression increased > 2-fold	Expression decreased > 2-fold	Total DE genes
Pre vs Post Nebulisation	117	6	123
Post vs T0	32	33	65
T0 vs T30	21	41	62
T30 vs T120	40	23	63
T120 vs T0	20	6	26

**Table 5.6. Number of differentially expressed genes between the different conditions.**

Considering first the effects within the nebulisation reservoir, this comparison gave the largest set of differentially expressed genes. The DE genes in each comparison group were categorised according to their function using the Tuberculist website. The majority of DE genes in the first 4 comparison groups were conserved hypotheticals followed by either cell wall and cell processes, or intermediary metabolism and respiration categories. In the fifth group (T120 vs T0), the majority of DE genes were belonged to the cell wall and cell processes followed by intermediary metabolism and respiration categories then conserved hypotheticals categories. The overall view of DE genes classification in each comparison groups is shown in Figures 5.5 – 5.10. The top 5 significantly increased, and top 5 significantly decreased transcripts for each comparison group are shown in Tables 5.7 – 5.11. The full list of DE genes in each comparison group can be found in the Appendix.

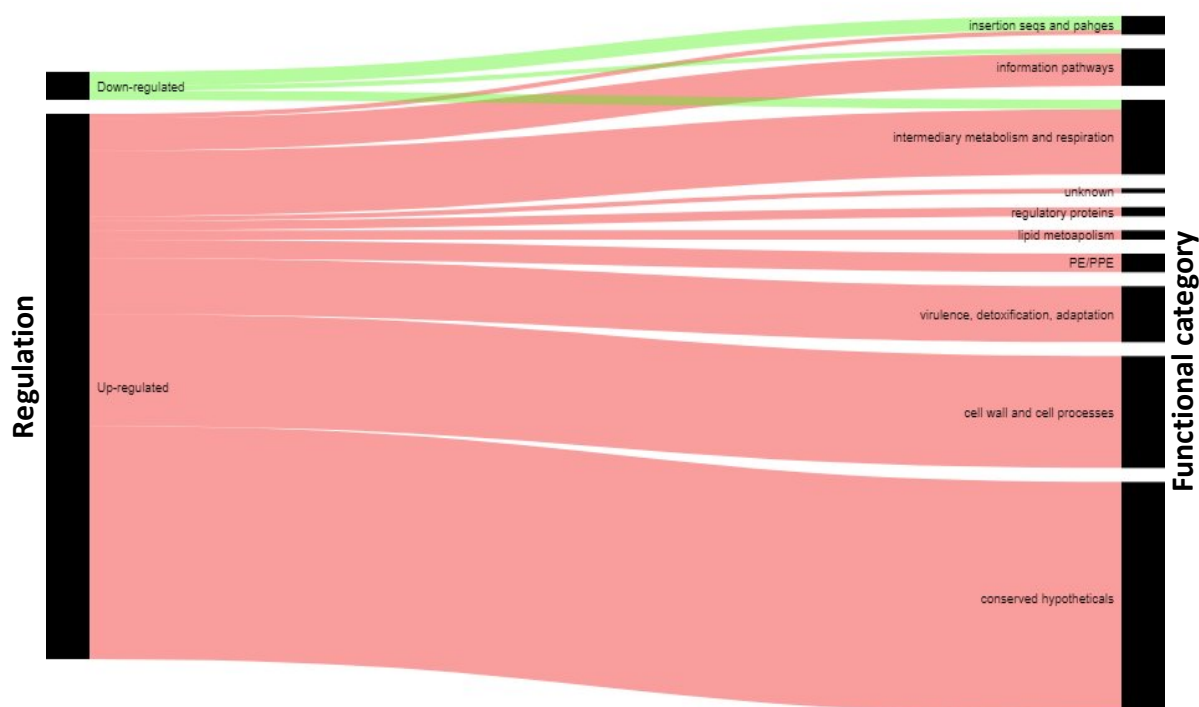


**Figure 5.5.** The parallel set diagram showing DE genes detected at between pre-neb and post-neb samples. DE genes at post-nebulisation relative to pre-nebulisation was created based on  $q$ -value  $< 0.01$ . The genes were classified into up-regulated and down-regulated then grouped into 10 different functional categories via searching the Tuberculist website.

Gene	Annotation	Fold-change
<i>thyX</i>	Thymidylate synthase ThyX	8.33
<i>Rv3831</i>	Hypothetical protein	7.80
<i>Rv2898c</i>	Endonuclease	7.00
<i>Rv0964c</i>	Hypothetical protein	5.14
<i>Rv1271c</i>	Secreted protein	4.77
<i>Rv0829</i>	Transposase	-14.00
<i>Rv2810c</i>	Transposase	-8.08
<i>Rv_1572c</i>	Hypothetical protein	-8.00
<i>Rv2141c</i>	Hypothetical protein	-4.59
<i>echA8</i>	Enoyl-CoA hydratase EchA8	-4.16

**Table 5.7.** . List of the top 5 significant DE genes in a comparison between post-nebulisation and post-nebulisation samples. Red columns represent up-regulated genes, and green columns represent down-regulated genes. The list was created based on  $q$ -value  $< 0.01$ .

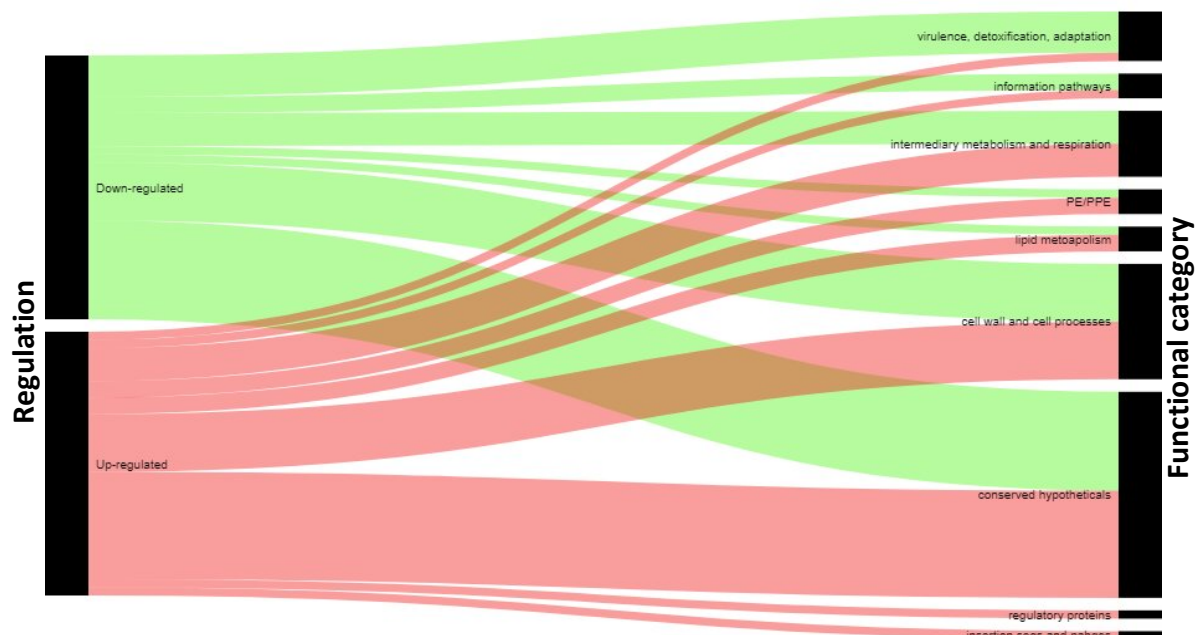


**Figure 5.6. The parallel set diagram showing DE genes detected at between T0 and post-neb samples.** DE genes at T0 relative to post-nebulisation was created based on q-value < 0.01. The genes were classified into up-regulated and down-regulated then grouped into 9 different functional categories via searching the Tuberculist website.

Gene	Annotation	Fold-change
<i>Rv1761c</i>	Hypothetical protein	29.5
<i>lppA</i>	Lipoprotein LppA	25
<i>Rv1157c</i>	Hypothetical protein	22
<i>Rv1227c</i>	Transmembrane protein	22
<i>Rv0043c</i>	HTH-type transcriptional regulator	21
<i>vapB17</i>	Antitoxin VapB17	-44
<i>Rv3748</i>	Hypothetical protein	-37
<i>lppl</i>	Lipoprotein Lppl	-31
<i>nlhH</i>	Carboxylesterase NlhH	-26
<i>Rv2781c</i>	Alanine-rich oxidoreductase	-26

**Table 5.8. List of the top 5 significant DE genes in a comparison between T0 and post-nebulisation samples.** Red columns represent up-regulated genes, and green columns represent down-regulated genes. The list was created based on q-value < 0.01.

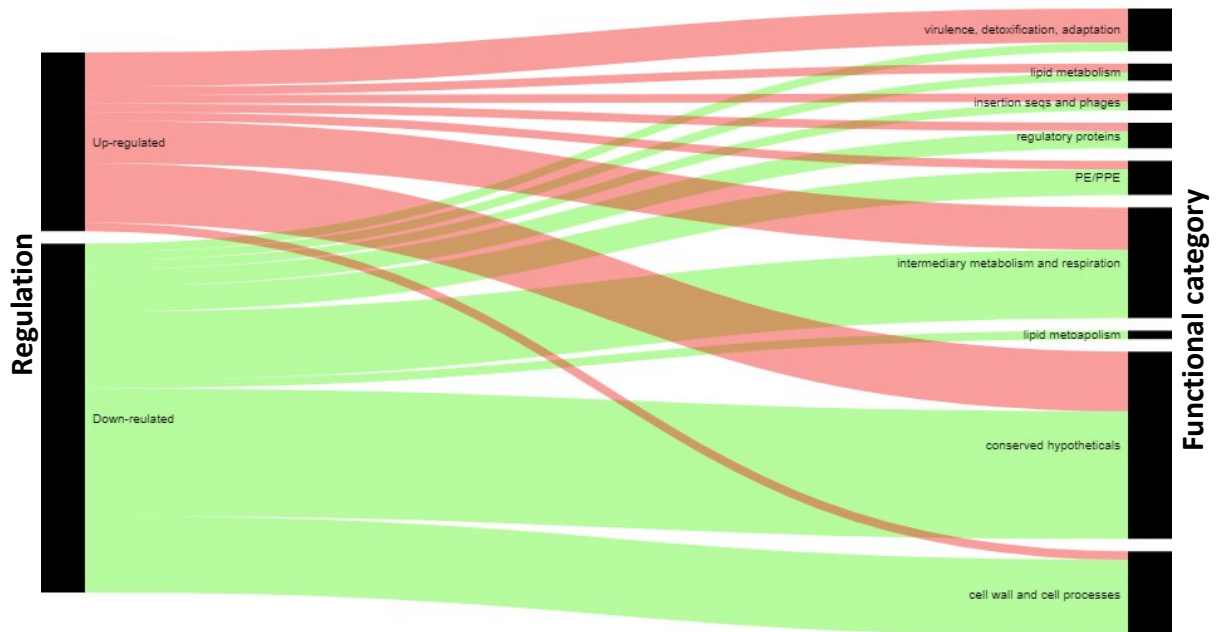


**Figure 5.7. The parallel set diagram showing DE genes detected at between T30 and T0 samples.** DE genes at T30 relative to T0 was created based on q-value < 0.01. The genes were classified into up-regulated and down-regulated then grouped into 9 different functional categories via searching the Tuberculist website.

Gene	Annotation	Fold-change
<i>vapC32</i>	Toxin VapC32	44
<i>lppl</i>	Lipoprotein Lppl	41
<i>PE7</i>	PE family protein PE7	32
<i>Rv3748</i>	Hypothetical protein	28
<i>TB18.6</i>	Hypothetical protein	26
<i>dipZ</i>	Prevent-host-death family protein	-31
<i>Rv0356c</i>	Hypothetical protein	-19
<i>PE33</i>	PE family protein PE33	-15.5
<i>Rv2856A</i>	Hydrogenase nickel incorporation protein HypB	-15
<i>Rv2415c</i>	Hypothetical protein	-12.3

**Table 5.9. List of the top 5 significant DE genes in a comparison between T30 and T0 samples.** Red columns represent up-regulated genes, and green columns represent down-regulated genes. The list was created based on q-value < 0.01.



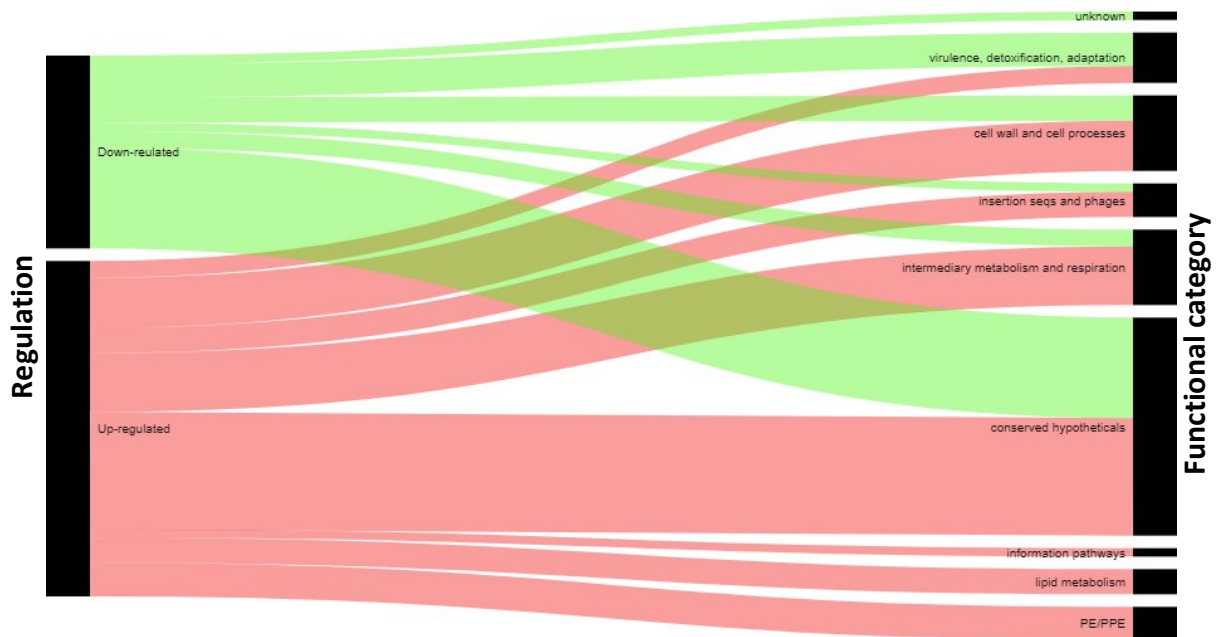


**Figure 5.8.** The parallel set diagram showing DE genes detected at between T120 and T30 samples. DE genes at T120 relative to T30 was created based on q-value < 0.01. The genes were classified into up-regulated and down-regulated then grouped into 9 different functional categories via searching the Tuberculist website.

Gene	Annotation	Fold-change
<i>Rv2810c</i>	Transposase	24
<i>Rv3555c</i>	Hypothetical protein	11
<i>Rv2415c</i>	Competence protein ComEA	9
<i>Rv2732c</i>	Transmembrane protein	7
<i>echA8</i>	Enoyl-CoA hydratase EchA8	6
<i>PPE46</i>	PE family protein PE27A	-7.85
<i>Rv2669</i>	N-acetyltransferase	-5.75
<i>higA</i>	Antitoxin HigA	-5.14
<i>Rv0031</i>	Transposase	-5.00
<i>Rv1137c</i>	Hypothetical protein	-4.60

**Table 5.10.** List of the top 5 significant DE genes in a comparison between T120 and T30 samples. Red columns represent up-regulated genes, and green columns represent down-regulated genes. The list was created based on q-value < 0.01.

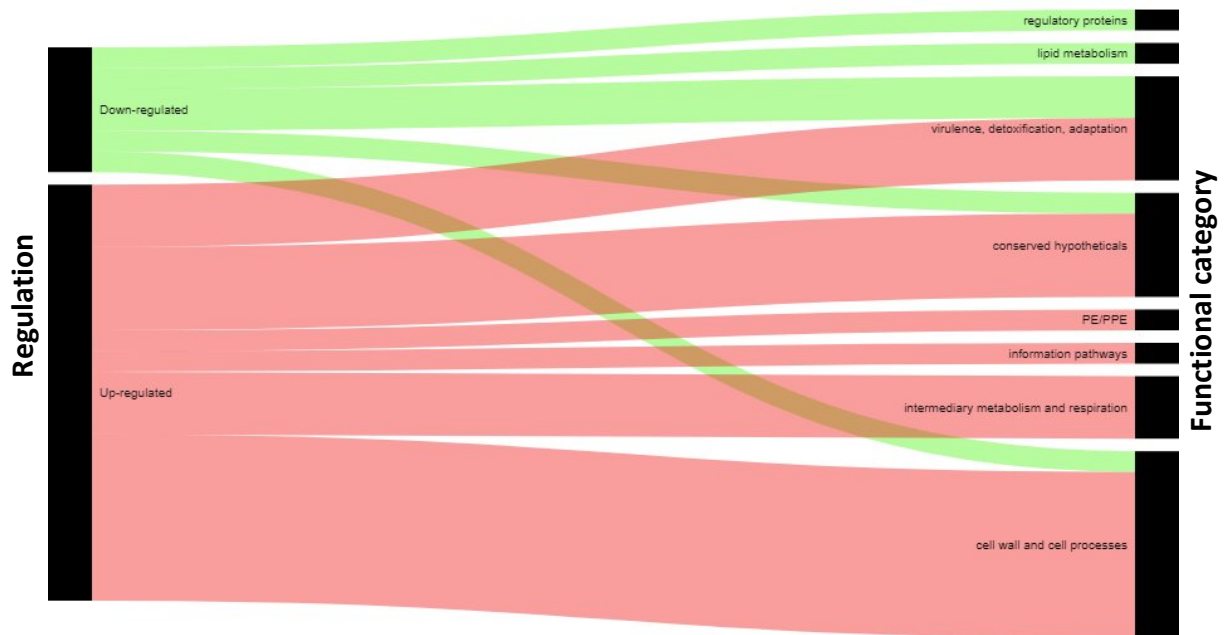


**Figure 5.9. The parallel set diagram showing DE genes detected at between T120 and T0 samples.** DE genes at T120 relative to T0 was created based on q-value < 0.01. The genes were classified into up-regulated and down-regulated then grouped into 9 different functional categories via searching the Tuberculist website.

Gene	Annotation	Fold-change
<i>lpqO</i>	Lipoprotein LpqO	8
<i>Rv1115</i>	Hypothetical protein	7
<i>PE_PGRS34</i>	PE-PGRS family protein PE_PGRS34	6
<i>Rv0612</i>	Hypothetical protein	4
<i>Rv0347</i>	Membrane protein	4
<i>fadD18</i>	Fatty-acid-CoA ligase FadD18	-3.5
<i>relK</i>	Toxin RelK	-3.0
<i>fic</i>	Cell filamentation protein Fic	-2.2
<i>Rv3098B</i>	Toxin	-2.1
<i>Rv0339c</i>	Transcriptional regulator	-2.0

**Table 5.11. List of the top 5 significant DE genes in a comparison between T120 and T0 samples.** Red columns represent up-regulated genes, and green columns represent down-regulated genes. The list was created based on q-value < 0.01.

Careful inspection of the gene categories failed to reveal any clear changes in expression attributable to responses to stimuli such as desiccation, activation of regulons or specific metabolic shifts.

In order to determine whether any changes could be associated with the effects of established transcription factors, DE gene lists were loaded into the transcription factor (TF) overexpression tables developed by Rustad and colleagues (Rustad et al., 2014). These are based on the genes detected to be DE in response to overexpression of all the recognised TFs in Mtb. The tables assign probability values associating specific DE patterns with specific TFs. The DE lists indicated in table 5.6 were assessed in this way, and the results are shown in table 5.12.

Although several TFs are identified with q values below 0.01 the associations found are very modest with generally less than 10 % of large (>50 genes) regulon genes DE.

A) DE genes due to nebulisation process									
Up regulated genes Post/Pre (total 117)					Down regulated genes Post/Pre (total 6)				
TF	Name	No of genes Ind	TF Ind	Ind Sig	TF	Name	No of genes Rep	TF Rep	Rep Sig
Rv0023		25	489	2.94E-03	Rv1176c		1	2	2.98E-03
Rv1033c	trcR	3	13	5.53E-03	Rv2250c		2	61	3.26E-03
Rv0623	vapB30	1	1	2.91E-02	Rv0260c		2	154	1.97E-02
Rv0465c	ramB	1	1	2.91E-02	Rv2374c	hrcA	1	20	2.95E-02
Rv0474		1	1	2.91E-02	Rv1186c		1	21	3.09E-02
Rv1725c		1	1	2.91E-02					
Rv2884		4	41	3.00E-02					
Rv3133c	dosR	6	83	3.25E-02					
Rv1776c		2	12	4.57E-02					
B) DE genes due to aerosolisation									
Up regulated genes T0/Post (total 32)					Down regulated genes T0/Post (total 33)				
Rv2242	mabR	2	29	2.18E-02	Rv0302		1	6	4.82E-02
C) DE genes due to early adaptation stage									
Up regulated genes T30/T0 (total 32)					Down regulated genes T30/T0 (total 41)				
Rv3082c	virS	2	2	2.59E-05	Rv0238		10	345	1.88E-03
Rv3416	whiB3	4	255	4.01E-02	Rv0757	phoP	4	65	4.01E-03
					Rv0377		1	3	3.03E-02
					Rv1152		1	3	3.03E-02
D) DE genes due to late adaptation stage									
Up regulated genes T120/T0 (total 20)					Down regulated genes T120/T0 (total 4)				
Rv0653c		1	2	9.91E-03					
Rv1846c	blai	1	2	9.91E-03					
Rv3852	hns	1	4	1.97E-02					
Rv0602c	tcrA	1	6	2.95E-02					
Rv1657	argR	1	7	3.43E-02					
Rv2760c	vapB42	1	8	3.91E-02					
E) DE genes due to late adaptation / early adaptation stage									
Up regulated genes T120/T30 (total 38)					Down regulated genes T120/T30 (total 23)				
Rv0678		2	21	1.63E-02	Rv0678		2	12	1.99E-03
Rv3197A	whiB7	2	35	4.25E-02	Rv2788	sirR	3	72	7.52E-03
					Rv0576		5	252	1.23E-02
					Rv2703	sigA	2	45	2.66E-02
					Rv3574	kstR	2	61	4.66E-02

**Table 5.12. TF associated with DE genes at five different stages.** A) during nebulisation process, B) due to aerosolisation, C) due to early adaptation stage, D) due to late adaptation stage, E) due to late adaptation stage compared with early adaptation stage. Tables on the left side showed induced genes and tables on the right side shows repressed genes. The highest significant values are marked with dark red and the lowest significance values marked with light red.

### **5.3.5 Transcriptional pattern of DosR regulon**

The expression genes that are regulated by the universal stress regulon in Mtb, DosR were investigated across all the samples. As can be seen from Table 5.13, the majority of these genes were highly expressed in Pre- nebulisation samples compared with other samples. There were 7 genes significantly DE in total, 5 genes were between Pre-and post-nebulisation and 2 genes were between T120 and T0.

## Chapter 5: Transcriptional changes in Mtb H37Rv on aerosol In-vitro Studied by RNA-Seq

gene	Expression						q-value				
	Pre-Nb	T0	T30	T120	Post-Nb		Post/Pre	Post/T0	T30 vs T0	T120 vs T30	T120 vs T0
Rv0079	1471	763	901	1296	1005		8.11E-01	1.00E+00	1.00E+00	7.07E-01	4.70E-01
Rv0080	1171	1032	1215	1214	1089		4.98E-01	1.00E+00	1.00E+00	1.00E+00	1.00E+00
Rv0081	227	272	285	224	280		1.46E-02	1.00E+00	1.00E+00	1.00E+00	1.00E+00
nrdZ	164	101	104	114	130		1.00E+00	1.00E+00	1.00E+00	7.59E-01	1.00E+00
Rv0571c	143	73	87	99	51		2.15E-01	1.00E+00	1.00E+00	1.00E+00	2.06E-21
Rv0572c	45	49	61	35	17		1.00E+00	1.00E+00	1.00E+00	2.86E-01	6.53E-01
pncB2	32	18	15	28	14		1.00E+00	1.00E+00	9.17E-01	4.33E-01	1.00E+00
Rv0574c	105	84	72	86	80		6.79E-01	1.00E+00	1.00E+00	1.00E+00	1.29E-01
Rv1735c	10	11	16	16	32		2.54E-19	1.00E+00	1.00E+00	1.00E+00	9.71E-01
hrp1	556	1340	1883	670	1436		8.81E-05	1.00E+00	1.00E+00	1.24E-01	6.10E-01
RVBD_3129	25	58	60	38	63		1.97E-12	1.00E+00	9.84E-01	5.13E-01	7.30E-01
Rv1733c	707	887	722	644	579		9.67E-01	1.00E+00	9.38E-01	1.00E+00	7.47E-01
Rv1734c	15	5	1	21	3		1.00E+00	1.00E+00	1.00E+00	1.00E+00	1.00E+00
narX	639	333	319	459	295		7.61E-01	1.00E+00	1.00E+00	7.01E-01	1.20E-01
narK2	428	276	310	336	333		1.00E+00	1.00E+00	1.00E+00	7.90E-01	1.00E+00
Rv1738	8419	5301	6296	7528	5309		7.24E-01	1.00E+00	1.00E+00	1.00E+00	1.00E+00
Rv1812c	44	31	44	39	27		5.21E-01	1.00E+00	1.00E+00	1.00E+00	1.00E+00
Rv1813c	715	437	594	538	512		1.00E+00	1.00E+00	1.00E+00	1.00E+00	9.76E-01
Rv1996	724	1059	1055	566	916		3.95E-01	1.00E+00	1.00E+00	6.28E-01	9.45E-01
ctpF	181	168	228	152	181		4.35E-01	1.00E+00	1.00E+00	1.00E+00	1.00E+00
Rv1998c	29	16	11	19	13		1.00E+00	1.00E+00	9.54E-01	1.00E+00	7.30E-01
Rv2003c	82	55	68	55	35		1.00E+00	1.00E+00	1.00E+00	1.00E+00	5.40E-01
Rv2004c	140	88	123	95	113		7.32E-01	1.00E+00	1.00E+00	1.00E+00	1.00E+00
Rv2005c	585	396	556	421	533		5.34E-01	1.00E+00	1.00E+00	1.00E+00	1.50E-01
otsB1	34	21	30	26	37		1.62E-01	9.61E-01	1.00E+00	1.00E+00	1.00E+00
fdxA	1204	1334	2026	1215	1625		2.15E-01	1.00E+00	9.68E-01	7.80E-01	9.57E-01
Rv2028c	275	287	299	251	220		7.91E-01	1.00E+00	1.00E+00	1.00E+00	8.15E-01
pfkB	1102	582	500	737	482		4.24E-01	1.00E+00	9.73E-01	6.39E-01	1.00E+00
Rv2030c	1553	1012	936	1157	1051		9.79E-01	1.00E+00	1.00E+00	1.00E+00	1.00E+00
hspX	1796	4184	5629	2012	3533		1.05E-01	1.00E+00	1.00E+00	4.59E-01	9.58E-01
acg	1414	1073	1262	1088	986		9.01E-01	1.00E+00	1.00E+00	9.92E-01	7.41E-01
Rv0569	691	1541	1429	611	1594		4.01E-04	1.00E+00	1.00E+00	2.31E-01	6.87E-01
TB31.7	22557	4566	4628	14333	6333		1.00E+00	1.00E+00	1.00E+00	1.00E+00	9.72E-01
Rv2624c	303	585	466	293	432		8.39E-02	1.00E+00	9.02E-01	1.00E+00	1.00E+00
Rv2625c	1035	657	576	700	839		7.08E-01	1.00E+00	9.63E-01	8.16E-01	9.55E-01
Rv2627c	1044	1077	1328	851	1037		6.01E-01	1.00E+00	1.00E+00	1.00E+00	1.00E+00
Rv2628	1557	1261	1393	1125	1327		6.41E-01	1.00E+00	1.00E+00	1.00E+00	8.12E-01
Rv2629	489	650	676	439	566		3.59E-01	1.00E+00	1.00E+00	9.70E-01	8.45E-01
Rv2630	214	191	279	193	335		2.88E-03	9.41E-01	1.00E+00	9.60E-01	7.38E-01
Rv2631	90	94	92	86	66		7.03E-01	1.00E+00	1.00E+00	1.00E+00	1.00E+00
Rv3126c	590	281	240	348	198		1.35E-01	1.00E+00	9.88E-01	6.52E-01	5.21E-01
Rv3127	1498	1485	1963	1210	1380		6.75E-01	1.00E+00	1.00E+00	1.00E+00	1.00E+00
tgs1	1830	2317	3000	1711	2191		8.09E-01	1.00E+00	1.00E+00	1.00E+00	1.00E+00
Rv3131	2186	2005	2342	1855	1700		1.00E+00	1.00E+00	1.00E+00	1.00E+00	7.35E-175
devS	583	387	556	488	413		8.18E-01	1.00E+00	9.55E-01	1.00E+00	9.37E-01
devR	916	1005	1138	788	866		5.21E-01	1.00E+00	1.00E+00	1.00E+00	1.00E+00
Rv3134c	1643	951	985	1221	978		1.00E+00	1.00E+00	1.00E+00	8.19E-01	1.00E+00

**Table 5.13. Expression of genes regulated by DosR regulon at different stages with q values.**  
7 genes (highlighted in red colour) were significantly DE.

## 5.4 Discussion

RNA-sequencing was chosen in this study because of its capacity to detect and quantify low abundance transcripts in samples with very low RNA concentration. This is a critical issue as the nature of the experiments here involved the use of aerosols samples. The poor yields of extracted RNA from aerosol samples were observed here. In contrast to bacterial cultures, where a high concentration of cells is present, the extracted RNA yields are very high (ex; pre and post nebulisation samples). The low concentration of cells in aerosol samples ( $10^3$ - $10^4$ ) had contributed to these poor RNA yields. One possible solution is to increase the time of sampling (here it was 1 min) and reduce the number of sampling time points (here it was 6 time points). Another possible solution is to increase the starting inoculum (here it was  $10^8$ ). Although the ultrasonic Omron nebuliser generated higher number of aerosols compared with the 3-jet Collison nebuliser, other aerosol generators can generate higher aerosols than the Ultrasonic Omron, and further investigations are required to test this possibility. The main task in this chapter was to identify differences in the gene expression of Mtb cells at the nebulisation process, during aerosolisation, and during survival in aerosols.

### 5.4.1 Sequencing results

The cDNA pool was sequenced on an Illumina NextSeq 500 system using 74 bp read length. This complies with the recommended range of 30-400 bp (Wang *et al.*, 2009). Although longer reads can reduce the complexity of transcriptome assembly, shorter reads can enhance the number of high-quality reads (Martin and Wang, 2011). The number of PCR amplification cycles varied between samples, while PCR cycles were 12-13 for the reservoir samples, aerosols samples required 22-25 cycles. The difference in the number of cycles was due to the different concentration of RNA between aerosol and the reservoir samples (Table 5.2).

### 5.4.2 Quality control of extracted RNA

The bioanalyser failed to detect the RIN of four samples, while the RIN of the majority of the samples was approximately 1. T0 from the 2<sup>nd</sup> experiment showed RIN of 5, which might indicate contamination with genomic DNA and this explained the low percentage of alignment of reads observed above. Although these numbers were low, the average sequencing reads was 976,384,004 per sample.

### 5.4.3 Alignment of reads

The percentage of alignment reads was varied between Mtb H37Rv and *M. bovis* BCG and between the replicates of each strain. Only one replicate of *M. bovis* BCG showed a satisfactory alignment (29-98 %) while aerosol samples of the other two replicates showed only 2 % (Table 5.3). Thus, the data obtained for *M. bovis* BCG was excluded from the work in this chapter. On the other hand, the three replicates of Mtb H37Rv showed a satisfactory percentage of alignment reads (52-98 %), with the exception of only one sample (T0, 2<sup>nd</sup> experiment, 18 %) and thus was the focus of the work in this chapter.

There are two possible reasons for the weak alignment of 2 replicates of *M. bovis* BCG observed here; contamination of foreign DNA/RNA species or issues with library construction (e.g. high level of adapter dimers). Potential sources of unmapped reads can be investigated manually by inspect a few randomly selected read sequences and to run BLAST (website <https://blast.ncbi.nlm.nih.gov/Blast.cgi>). This will indicate whether the samples have been contaminated by DNA/RNA from other species (e.g. bacteria) or by artefacts of library construction (Ji and Sadreyev, 2018). This investigation was not done here and could be a target for future work.

#### **5.4.4 Genes with no detected expression**

From a total of 4032 genes, only 13 genes were found to have no transcripts in any of the samples. This small proportion reflects a high mapping capacity of Bowtie2 software. Nonetheless, there might be reasons other than mapping capacity for the absence of transcripts in the output.

A gene might have no detectable RNA before RNA-sequencing, either due to low concentration at the time of sample collection or because of rapid degradation during preparation. Another reason could be technical issues in RNA-sequencing. For instance, it is possible that the base calling of some sequences from a particular gene was particularly poor, or generated overall low-quality reads and resulted in their removal after trimming. The majority of the not expressed genes were conserved Hypothetical (7 genes), 3 genes belonged to the insertion sequences and pro-phage category, and 3 genes were split into regulatory protein, lipid metabolism and intermediary metabolism and respiration categories (Table 5.5).

#### **5.4.5 Differentially expressed genes (DE)**

The data analysis of the RNA-sequencing results showed no clear pattern of Mtb transcriptional response at any of the stages tested, namely the nebulisation process, aerosolisation and survival in aerosols. One potentially significant finding was the differentially expressed genes (DE) profile between T0 and post-nebulisation. These samples were taken close to each other in the experiment with little opportunity for transcriptional patterns to change yet 65 DE genes were detected. One explanation for this could be the selection of different cell populations with different transcriptomes remaining in the nebuliser reservoir on the one hand, and entering aerosol on the other.

The total number of significantly up-regulated genes across all stages was 239, while 107 genes were down-regulated genes (Table 5.6). These genes represent 8 % of the total coding genes in the reference genome used (4032). It should be noted that these



genes overlapped between stages reflecting the difficulty of obtaining a clear pattern of the transcriptional profile of Mtb cells.

#### **Pre vs Post-nebulisation (Nebulisation stage)**

A total of 123 genes were differentially expressed during the nebulisation stage (117 genes were up-regulated, and 6 genes were down-regulated). Figure 5.5 shows the functional categories of these genes and Table 5.7 shows the top 5 significantly DE genes. This stage produced the highest number of significantly DE genes compared with aerosolisation and survival stages. This observation was in contrast to a previous report on *E.coli*, where aerosolisation stage produces the highest number of DE genes (Ng et al., 2018). This difference in the observation between the current study and Ng's study could result from the difference in the nebulisers used and the period of nebulisation. In Ng's study, the 6-Jet Collison nebuliser was used, and the nebulisation time was for 3 min, while the Ultrasonic Omron nebuliser and nebulisation time of 5 min were chosen in the current study. Only 4 genes were up-regulated in response to nebulisation phase in Ng's study, and 3 of them were cold shock proteins (Ng et al., 2018). In the current study, *cspA*, encoding the cold sock protein, was up-regulated in response to nebulisation phase. This demonstrates that the fall in temperature of the bacterial solution due to droplet evaporation stimulates a cold-stress respond in the bacteria during nebulisation.

#### **T0 vs post-nebulisation (aerosolisation stage)**

During this stage, 65 DE genes were detected (32 genes were up-regulated and 33 genes were down-regulated). Figure 5.6 shows the functional categories of these genes and Table 5.8 describes the top 5 significantly DE genes. One notable observation among the up-regulated genes are those encoding PE9 and PE33 proteins. These proteins belong to the PE/PPE family which have been reported to increase CSH previously (Singh et al., 2016). Other genes involved in the synthesis of the hydrophobic cell wall were also up-regulated here including *lppA* and *fabG3*. This observation might indicate the importance of CSH on the selectivity of cells for aerosolisation.

### **T30 vs T0, T120 vs T30, T120 vs T0 (survival stage)**

The investigation of transcriptional signature changes during this stage has been divided into three groups; early survival (T30 vs T0), late survival (T120 vs T30) and overall survival (T120 vs T0). The function categories of these genes are illustrated in Figures 5.9, 5.10 and 5.11, respectively. The top 5 significantly DE genes are listed in Tables 5.7, 5.8 and 5.9, respectively. The highest number of DE genes were detected at the late survival stage (40 DE genes). One notable observation among the up-regulated genes through all stages was the presence of genes related to toxin-antitoxin system (TA). TA systems are typically composed of a protein toxin and a more labile antagonistic antitoxin, which can be a protein or non-coding RNA (Yamaguchi et al., 2011). The toxin's function is targeting essential cellular processes such as DNA replication, cell wall synthesis, cell division or translation. This function can be regulated by the presence of antitoxin. The activation of TA systems could facilitate bacterial survival during stress until conditions become more favorable (Gerdes and Maisonneuve, 2012). Mtb has a significantly high number of TA systems in its chromosome when compared with other mycobacteria and it has been proposed that TA systems are critical in the adaptation process during stress conditions (Sala et al., 2014). As survival of Mtb in aerosols is surrounded with many stressors, this observation could indicate the important role of this system during aerosol survival of Mtb.

DosR regulon is a universal stress regulon in Mtb. It has been reported to be associated with heat-shock, hypoxia, and nitric oxide exposure conditions (Park *et al.*, 2003, Voskuil *et al.*, 2003). Moreover, Garton and associates have demonstrated induced DosR regulon in transcriptional signatures of Mtb in sputum samples (Garton *et al.*, 2008). In the current study, 7 significantly DE genes regulated by DosR were detected including *Rv1735c* and *Rv3131*, which encode immunogenic antigens, inducing gamma-interferon responses in whole-blood cultures from Mtb-exposed adults in Uganda, The Gambia, and South Africa, indicating that might be good vaccine candidates (Black et al., 2009). Another gene which is significantly DE is *Rv2626c* (*hrp1*); the protein has been reported to induce strong T- and B-cell responses in a mice challenge experiment

indicating the possibility of this protein to be a good vaccine candidate (Roupie et al., 2007). The other genes including *Rv3129*, *Rv0569*, *Rv2630*, and *Rv0571c* were reported to be induced during hypoxia, low levels of nitric oxide (NO), and carbon monoxide (CO) (Sherman et al., 2001, Voskuil et al., 2003, Shiloh et al., 2008). Among these 7 DE genes, there are 3 genes; *Rv1735c*, *Rv2626c* and *Rv2630* have been reported to be up-regulated significantly in sputum samples compared with *in vitro* and aerobic growth (Garton et al., 2008).

It can be seen from table 5.13 that most of the DosR regulon genes were overexpressed at pre-nebulisation samples indicating that Mtb cells were exposed to stress conditions before being nebulised. Such stress could be due to experimental designs, where cells are first exposed to RT and then harvested by scraping into DW and vortexed vigorously with beads to break up clumps. All of these steps could activate transcriptional signatures that were seen in pre-nebulisation samples. These possibilities could explain the fact that no transcriptional signature pattern was observed at the different stages. It might also explain why there was very little decline in any of the viability assessments over the 120 min experimental period.

It should be noted that these pioneering experiments have revealed the importance of optimising the experimental design in future work to minimise the stressor's exposure to Mtb cells prior to nebulisation. Such an approach can be achieved, for example, by growing the cells inside the reservoir of the sample generator which can be incubated in 37 °C incubator, then nebulised directly into the drum. Another possible optimisation can be achieved by taking control samples after each step in the procedure and subjecting these samples for RNA-sequencing to explore the influence of each step on the transcriptional signatures of the cells.

## 5.5 Conclusions

- Although the RIN number of the majority of samples was low, the average reads per sample was 9,763,840 indicating enough data for further analysis.
- The efficiency of the mapping of whole transcripts to the reference genome of 2 replicates of *M. bovis* was 2 % and hence was not subject to further analysis.
- The efficiency of the mapping of whole transcripts to the reference genome of Mtb H37Rv ranged from 53 to 98 %, and hence was the focus of the analysis work here.
- The proportion of rRNA in the samples ranged from 58 to 83 %.
- The frequency of genes with no detected expression was 13 from a total of 4032 annotated genes.
- There was no clear transcriptional pattern at any of the stages tested.
- Significantly DE genes were at the highest level at the nebulisation stage compared with aerosolisation and survival stages.
- Mtb cells showed stress transcription prior to the nebulisation and hence might influence the overall change of transcriptional signatures in the following stages.

## 6.1 General Discussion

The topic of this research is understanding the physiological states of Mtb relating to transmission. Based upon the hypothesis of Minnikin (2015), that CSH plays a significant role in propensity of cells for aerosolisation (Minnikin *et al.*, 2015), and the preliminary evidence of Barer (Nardell *et al.*, 2016), that specific genes may contribute to the adaptation of Mtb cells during transmission, this study was directed to investigate these hypotheses. To do so, in the early stage of this research factors affecting results from the widely used MATH technique to measure CSH were investigated. Comparisons were then made with the Congo Red and microsphere bead techniques as means to measure CSH at the single-cell level. Next, experiments using different nebulisers were conducted to relate CSH to the propensity of cells for aerosolisation. The middle stage of this research focused on resolving assessing discrepant outcomes of previous survival studies of Mtb in aerosols using Mtb and *M. bovis* BCG. In the final stage, experiments were established toward the transcriptional response changes of Mtb cells to the nebulisation process, aerosolisation, and survival in aerosols.

The main technique to measure CSH used here was MATH. However, studies using this technique have not followed a standardised protocol, which made the comparison of the outcomes of these studies difficult. It should be noted that the work here did not attempt to investigate the fundamental understanding of the microbial adhesion to hydrocarbons or the mechanism of surface hydrophobicity. Rather it was aimed at evaluating the sensitivity of this technique to different operational parameters using *M. smegmatis* and *M. bovis* BCG. The main observation was that *M. bovis* was more hydrophobic than *M. smegmatis* across all experiments, regardless of the modified factor being tested. This finding provided strong confidence in the MATH technique as a reliable method of differentiating mycobacterial CSH. It should be noted that these experiments were done for the first time with mycobacteria in the current study and no previous study investigated the influence of different factors on the CSH measurement of Mycobacterial cells. With regards to the impact of several factors on measuring CSH, the most significant factor was the vortex duration, which affected the CSH dramatically with both strains. Also, the hexadecane-aqueous phase volume ratio and DW as a suspended medium showed significant influence on *M. bovis* BCG CSH values.

Therefore, a digital vortex was purchased. CSH values of *M. bovis* BCG were affected by the stage it is harvested as the values were higher at the stationary phase compared with the exponential phase indicating CSH-related adaptation mechanisms of the cells to the environment. Further investigations are required to assess the impact of different nutrients in the growth medium to identify these mechanisms.

Variations in CSH values in control samples and among replicates were noted in the current study. This could be due to the clumping feature of Mycobacterial cells during the washing step regardless of the buffer used. Other explanations of these variations could have come from the adherence of a proportion of cells to the tube walls rather than at the aqueous/hexadecane interface or from the hexadecane droplets that merged within the aqueous phase affecting the spectrophotometer readings. However, these possibilities were not included in the current investigation and further work including microscopic experiments are required to test these possibilities.

Other projects in the laboratory focused on capturing the aerosolised cells using in-house prepared masks containing optimised in-house filters, and exploring the CSH of these cells required techniques to measure CSH at single cell level. To test this possibility, Congo Red and microsphere beads were included in the current research. Although both techniques showed the ability to determine the CSH at single cell level, they required more optimisation since they were time-consuming. Nonetheless, both methods, including the previously undescribed Congo Red, clearly demonstrated population heterogeneity with respect to CSH. This approach can be taken to the next level in future work by applying microscopic analysis directly on these filters.

To test the hypothesis that CSH influences the propensity of cells for aerosolisation, three nebulisers with different operating mechanisms were used to nebulise *M. bovis* BCG cells. The results of these experiments indicated a reduction in the CSH percentage of cells in the reservoir post-nebulisation compared with the original suspension pre-nebulisation. This provided indirect evidence that more hydrophobic cells were aerosolised in preference to less hydrophobic cells. It is possible that this phenomenon could also be attributed to the effects of the nebulisation mechanisms on the cell surface characteristics leading to a loss of hydrophobic features within the reservoir. Another possible reason for the CHS levels reduction could be the adherence of a

proportion of hydrophobic cells to the nebuliser's reservoir walls. Further investigation into these possible reasons could be through cell envelope lipids analysis pre- and post-nebulisation and via a staining techniques solution (Hori *et al.*, 2008) to detect adherence cells on the reservoir walls.

It is worth noting that in a parallel project in this laboratory, mixed populations of the hydrophilic smooth and the hydrophobic rough variants of *M. abscessus* were nebulised and CFU counts were assessed pre- and post-nebulisation. The results of this experiment showed no difference between the two strains pre- and post-nebulisation, rejecting the above hypothesis. However, the possibility of losing GPLs, representing up to 85 % of the surface-exposed lipids in *M. abscessus* smooth strain (Catherinot *et al.*, 2009) during nebulisation, might contribute to the conversion of the phenotype to rough in the reservoir post nebulisation. Thus, increasing the number of rough phenotype cells and subsequently overestimating of the rough colonies found post-nebulisation. Further investigations into the efficiency of aerosolised hydrophobic cells are required to provide solid evidence to accept or reject the above hypothesis. Such investigations might be achieved by assessing lipid body profile analysis of the cells pre- and post-nebulisation.

Successful transmission of *Mtb* cells relies on several factors, and one of these is the ability of the tubercle bacillus to adapt to survival in aerosols. Investigations into this type of research involves the use of nebulisers. While several kinds of nebulisers are available currently, many studies have used the Collison nebuliser (1, 3 and 6-jet). In the work here, the 3-jet Collison nebuliser and the ultrasonic Omron nebuliser were used. The aim of using two nebulisers was in an attempt to expand the possibility of mimicking the natural production of aerosols from the respiratory system. The PMA stain test showed that the integrity of mycobacterial cells was affected by both nebulisers. However, at least 75 % and 82 % of the cells were PMA-resistant with Collison and Omron nebulisers, respectively. In order to achieve a better representation of the natural transmission mechanisms, other considerations can be taking in account when conducting *in vitro* aerosol studies. For example, the spray fluid in aerosolisation experiments can be modified to achieve a better representation of the natural fluid in the respiratory tract.

The survival of Mtb H37Rv and *M. bovis* BCG in aerosols was studied in this work using both nebulisers. The pattern of survival in aerosols of both strains was similar, where around 50 % of the cells survived after 2 hrs of getting into air. This finding was assessed first by P-CFU then confirmed by MPN and PMA-qPCR. These techniques were used for the first time to detect Mtb cells in aerosols in the current study. Although these techniques detected different numbers of aerosolised Mtb cells, the survival pattern of these cells was similar. It is worth noting that the survival of mycobacterial cells for 4 hrs was tested with a single experiment with *M. bovis* BCG, which showed a survival of above 50 % after 4 hrs. All survival experiments reported here were performed using lawn growth for preparing the inoculum, and the RH inside the Goldberg drum was 85 %. To obtain better insight into the influence of these factors on the survival of cells in aerosols, further experiments at different environmental conditions are required.

Studying the transcriptional signature of Mtb during three different stages, the nebulisation process, aerosolisation process, and survival in aerosols has revealed a total of 339 significantly DE genes (230 up-regulated, 109 down-regulated). Around 40 % of these genes were at the nebulisation stage. The possibility that many genes were induced before starting nebulisation was influenced by the observation of DosR regulon, where the majority of its genes were induced at the pre-nebulisation stage. Transcriptional responses of Mtb cells to the nebulisation process, aerosolisation, and survival in aerosols showed no clear pattern under these conditions. Although the complexity of conducting these experiments is a key challenge, these pioneer experiments provided validity of the system which can be developed in future work.



## 6.2 Conclusions and Future work

- MATH technique was easy, simple and showed reproducible results with mycobacterial strains. Testing more parameters, including microscopic analysis, could be a target in future work. It would be also important to repeat experiments described in this study.
- Relative Congo Red and microsphere beads showed the ability to measure CSH on single cells. The techniques require further optimisation.
- While preliminary indirect evidence relating CSH on the propensity of cells for aerosolisation was obtained here, further direct investigations into the efficiency of CSH by direct means are required including lipid profile analysis to cells pre- and post-nebulisation.
- *M. bovis* BCG and Mtb H37Rv consistently showed > 50 % survival in aerosol for up to 2 hrs. The influence of different environmental conditions on the survival of mycobacterial cells in air could be tested in the future. Other factors can also be investigated including the nature of the spray fluid.
- The Omron ultrasonic nebuliser was compatible with the Collison nebuliser with the advantage of delivering more aerosolised cells than Collison with a similar level of damage as indicated by PMA assay.
- The transcriptional profile of Mtb cells using the Omron ultrasonic nebuliser undergoing the nebulisation process was different from that at aerosolisation and survival in aerosols.
- No obvious transcriptional pattern of Mtb cells under the tested conditions was obtained.

- Genes of DosR regulon were up-regulated at pre-nebulisation samples compared with the post nebulisation and aerosol samples. These expression patterns should be confirmed in the future studies.

# References

- ABDULWHAB, M. 2019. Use of Face-Mask Sampling as a Means of Characterising the Microbiota Exhaled from Human Respiratory Tract in Health and Disease. *Department of Infection, Immunity and Inflammation*, Leicester University.
- AKKERMAN, O. W., VAN DER WERF, T. S., DE BOER, M., DE BEER, J. L., RAHIM, Z., ROSSEN, J. W., VAN SOOLINGEN, D., KERSTJENS, H. A. & VAN DER ZANDEN, A. G. 2013. Comparison of 14 molecular assays for detection of *Mycobacterium tuberculosis* complex in bronchoalveolar lavage fluid. *Journal of Clinical Microbiology*, 51, 3505-3511.
- AL-HUMADI, H. W., AL-SAIGH, R. J. & AL-HUMADI, A. W. 2017. Addressing the challenges of tuberculosis: a brief historical account. *Frontiers In Pharmacology*, 8, 689.
- ALEXANDER, K. A., LAVER, P. N., MICHEL, A. L., WILLIAMS, M., VAN HELDEN, P. D., WARREN, R. M. & VAN PITTIUS, N. C. G. 2010. Novel *Mycobacterium tuberculosis* complex pathogen, *M. mungi*. *Emerging Infectious Diseases*, 16, 1296-1299.
- ALLEGRA, S., LECLERC, L., MASSARD, P. A., GIRARDOT, F., RIFFARD, S. & POURCHEZ, J. 2016. Characterization of aerosols containing *Legionella* generated upon nebulization. *Scientific Reports*, 6, 33998.
- ALLEN, S., BATUNGWANAYO, J., KERLIKOWSKA, K., LIFSON, A. R., WOLF, W., BOGAERTS, J., SWTKIN, G. & HOPEWELL, P. C. 1992. Two-year Incidence of Tuberculosis in Cohorts of HIV-infected and Uninfected Urban Rwandan Women. *Am Rev Respir Dis*, 146, 1439-1444.
- ALLISON, D. B., CUI, X., PAGE, G. P. & SABRIPOUR, M. 2006. Microarray data analysis: from disarray to consolidation and consensus. *Nature Reviews Genetics*, 7, 55-65.
- ALTAF, M., MILLER, C. H., BELLOWES, D. S. & O'TOOLE, R. 2010. Evaluation of the *Mycobacterium smegmatis* and BCG models for the discovery of *Mycobacterium tuberculosis* inhibitors. *Tuberculosis*, 90, 333-337.
- ALWINE, J. C., KEMP, D. J. & STARK, G. R. 1977. Method for detection of specific RNAs in agarose gels by transfer to diazobenzyloxymethyl-paper and hybridization with DNA probes. *Proceedings of the National Academy of Sciences*, 74, 5350-5354.
- AMARAL, P., LEHOCKY, M., BARROS-TIMMONS, A., ROCHA-LEÃO, M., COELHO, M. & COUTINHO, J. 2006. Cell surface characterization of *Yarrowia lipolytica* IMUFRJ 50682. *Yeast*, 23, 867-877.

- AMBALAM, P., KONDEPUDI, K. K., NILSSON, I., WADSTRÖM, T. & LJUNGH, Å. 2012. Bile stimulates cell surface hydrophobicity, Congo red binding and biofilm formation of *Lactobacillus* strains. *FEMS Microbiology Letters*, 333, 10-19.
- ANDERS, S. & HUBER, W. 2010. Differential expression analysis for sequence count data. *Genome Biology*, 11, R106.
- ANDERSON, J. & DARK, F. 1967. Studies on the effects of aerosolization on the rates of efflux of ions from populations of *Escherichia coli* strain B. *Microbiology*, 46, 95-105.
- ARSENIC, R., TREUE, D., LEHMANN, A., HUMMEL, M., DIETEL, M., DENKERT, C. & BUDCZIES, J. 2015. Comparison of targeted next-generation sequencing and Sanger sequencing for the detection of PIK3CA mutations in breast cancer. *BMC Clinical Pathology*, 15, 20.
- BALDI, F., IVOŠEVIĆ, N., MINACCI, A., PEPI, M., FANI, R., SVETLIČIĆ, V. & ŽUTIĆ, V. 1999. Adhesion of *Acinetobacter venetianus* to diesel fuel droplets studied with in situ electrochemical and molecular probes. *Appl. Environ. Microbiol.*, 65, 2041-2048.
- BANGE, F.-C., COLLINS, F. & JACOBS, W. 1999. Survival of mice infected with *Mycobacterium smegmatis* containing large DNA fragments from *Mycobacterium tuberculosis*. *Tubercle and Lung Disease*, 79, 171-180.
- BANULS, A.-L., SANOU, A., VAN ANH, N. T. & GODREUIL, S. 2015. *Mycobacterium tuberculosis*: ecology and evolution of a human bacterium. *Journal of Medical Microbiology*, 64, 1261-1269.
- BARTEK, I., WOOLHISER, L., BAUGHN, A., BASARABA, R., JACOBS, W., LENAERTS, A. & VOSKUIL, M. 2014. *Mycobacterium tuberculosis* Lsr2 is a global transcriptional regulator required for adaptation to changing oxygen levels and virulence. *MBio*, 5, e01106-14.
- BASSER, P., MCMAHON, T. & GRIFFITH, P. 1989. The mechanism of mucus clearance in cough. *Trans ASME*, 111, 288-297.
- BECKER, C., HAMMERLE-FICKINGER, A., RIEDMAIER, I. & PFAFFL, M. 2010. mRNA and microRNA quality control for RT-qPCR analysis. *Methods*, 50, 237-243.
- BELL, A. 2013. Towards understanding lipid body formation in mycobacteria in Tuberculosis. *PhD, University of Leicester*.
- BENJAMINI, Y. & HOCHBERG, Y. 1995. Controlling the false discovery rate: a practical and powerful approach to multiple testing. *Journal of the Royal Statistical Society: series B (Methodological)*, 57, 289-300.

- BERMUDEZ, L. E. & GOODMAN, J. 1996. *Mycobacterium tuberculosis* invades and replicates within type II alveolar cells. *Infection and Immunity*, 64, 1400-1406.
- BERNEY, M., WEILENMANN, H.-U. & EGLI, T. 2006. Flow-cytometric study of vital cellular functions in *Escherichia coli* during solar disinfection (SODIS). *Microbiology*, 152, 1719-1729.
- BEUTH, J. & UHLENBRUCK, G. 1995. Adhesive properties of bacteria. *Principles of cell adhesion*. CRC Press Boca Raton.
- BHATT, A., MOLLE, V., BESRA, G. S., JACOBS JR, W. R. & KREMER, L. 2007. The *Mycobacterium tuberculosis* FAS-II condensing enzymes: their role in mycolic acid biosynthesis, acid-fastness, pathogenesis and in future drug development. *Molecular Microbiology*, 64, 1442-1454.
- BHATT, A. & JACOBS JR, W. R. 2009. Gene essentiality testing in *Mycobacterium smegmatis* using specialized transduction. *Methods Mol Biol*, 465, 325-336.
- BINJOMAH, A. Z. A. 2014. Studies on the phenotypes of *Mycobacterium tuberculosis* in sputum. *Department of Infection, Immunity and Inflammation*. Leicester University.
- BLACK, G. F., THIEL, B. A., OTA, M. O., PARIDA, S. K., ADEGBOLA, R., BOOM, W. H., DOCKRELL, H. M., FRANKEN, K. L., FRIGGEN, A. H. & HILL, P. C. 2009. Immunogenicity of novel DosR regulon-encoded candidate antigens of *Mycobacterium tuberculosis* in three high-burden populations in Africa. *Clin. Vaccine Immunol.*, 16, 1203-1212.
- BOLGER, A. M., LOHSE, M. & USADEL, B. 2014. Trimmomatic: a flexible trimmer for Illumina sequence data. *Bioinformatics*, 30, 2114-2120.
- BOLSTAD, B., COLLIN, F., SIMPSON, K., IRIZARRY, R. & SPEED, T. 2004. Experimental design and low-level analysis of microarray data. *International Review of Neurobiology*, 60, 25-58.
- BORGDORFF, M. & VAN SOOLINGEN, D. 2013. The re-emergence of tuberculosis: what have we learnt from molecular epidemiology? *Clinical Microbiology and Infection*, 19, 889-901.
- BRENNAN, P. J. 2003. Structure, function, and biogenesis of the cell wall of *Mycobacterium tuberculosis*. *Tuberculosis*, 83, 91-97.
- BRENNAN, P. J. & NIKAIIDO, H. 1995. The envelope of mycobacteria. *Annual Review of Biochemistry*, 64, 29-63.
- BROOKS, J. D. & FLINT, S. H. 2008. Biofilms in the food industry: problems and potential solutions. *International Journal of Food Science & Technology*, 43, 2163-2176.

- BROWN-ELLIOTT, B. A., GRIFFITH, D. E. & WALLACE, R. J. 2002. Newly described or emerging human species of nontuberculous mycobacteria. *Infectious Disease Clinics*, 16, 187-220.
- BROWN, A. 1953. The Survival of Airborne Microorganisms II. Experiments With *Escherichia Coli* Near 0° c. *Australian Journal of Biological Sciences*, 6, 470-480.
- BROWN, R. F. 2016. Investigating the evolutionary origins and cell biology of Negativicutes. *University of Warwick*.
- BUERMANS, H. & DEN DUNNEN, J. 2014. Next generation sequencing technology: advances and applications. *Biochimica et Biophysica Acta (BBA)-Molecular Basis of Disease*, 1842, 1932-1941.
- BUJDÁKOVÁ, H., DIDIÁŠOVÁ, M., DRAHOVSKÁ, H. & ČERNÁKOVÁ, L. 2013. Role of cell surface hydrophobicity in *Candida albicans* biofilm. *Open Life Sciences*, 8, 259-262.
- BULLARD, J. H., PURDOM, E., HANSEN, K. D. & DUDOIT, S. 2010. Evaluation of statistical methods for normalization and differential expression in mRNA-Seq experiments. *BMC Bioinformatics*, 11, 94.
- BUNT, C. R., JONES, D. S. & TUCKER, I. G. 1993. The effects of pH, ionic strength and organic phase on the bacterial adhesion to hydrocarbons (BATH) test. *International Journal of Pharmaceutics*, 99, 93-98.
- BUSSCHER, H. 1990. Relative importance of surface free energy as a measure of hydrophobicity in bacterial adhesion to solid surface. *Microbial Cell Surface Hydrophobicity*, 335-359.
- BUSSCHER, H., VAN DE BELT-GRITTER, B. & VAN DER MEI, H. 1995. Implications of microbial adhesion to hydrocarbons for evaluating cell surface hydrophobicity 1. Zeta potentials of hydrocarbon droplets. *Colloids and Surfaces B: Biointerfaces*, 5, 111-116.
- CACHO, A., SMIRNOVA, E., HUZURBAZAR, S. & CUI, X. 2015. A comparison of base-calling algorithms for illumina sequencing technology. *Briefings in Bioinformatics*, 17, 786-795.
- CANCHI, D. R., PASCHEK, D. & GARCÍA, A. E. 2010. Equilibrium study of protein denaturation by urea. *Journal of the American Chemical Society*, 132, 2338-2344.
- CANGELOSI, G. A., PALERMO, C. O., LAURENT, J.-P., HAMLIN, A. M. & BRABANT, W. H. 1999. Colony morphotypes on Congo red agar segregate along species and drug susceptibility lines in the *Mycobacterium avium-intracellulare* complex. *Microbiology*, 145, 1317-1324.

- CARRERA, M., KESAVAN, J., ZANDOMENI, R. & SAGRIPANTI, J.-L. 2005. Method to determine the number of bacterial spores within aerosol particles. *Aerosol Science and Technology*, 39, 960-965.
- CARROLL, M. V., LACK, N., SIM, E., KRARUP, A. & SIM, R. B. 2009. Multiple routes of complement activation by *Mycobacterium bovis* BCG. *Molecular Immunology*, 46, 3367-3378.
- CATHERINOT, E., ROUX, A.-L., MACHERAS, E., HUBERT, D., MATMAR, M., DANNHOFFER, L., CHINET, T., MORAND, P., POYART, C. & HEYM, B. 2009. Acute respiratory failure involving an R variant of *Mycobacterium abscessus*. *Journal of Clinical Microbiology*, 47, 271-274.
- CHEN, C., KHALEEL, S. S., HUANG, H. & WU, C. H. 2014. Software for pre-processing Illumina next-generation sequencing short read sequences. *Source Code for Biology and Medicine*, 9, 8.
- CHEN, J. M., GERMAN, G. J., ALEXANDER, D. C., REN, H., TAN, T. & LIU, J. 2006. Roles of Lsr2 in colony morphology and biofilm formation of *Mycobacterium smegmatis*. *Journal of Bacteriology*, 188, 633-641.
- CHEN, W., GREEN, K. D. & GARNEAU-TSODIKOVA, S. 2012. Cosubstrate tolerance of the aminoglycoside resistance enzyme Eis from *Mycobacterium tuberculosis*. *Antimicrobial Agents and Chemotherapy*, 56, 5831-5838.
- CLARK, S., HALL, Y., KELLY, D., HATCH, G. & WILLIAMS, A. 2011. Survival of *Mycobacterium tuberculosis* during experimental aerosolization and implications for aerosol challenge models. *Journal of Applied Microbiology*, 111, 350-359.
- CLEGG, S. L., SEINFELD, J. H. & BRIMBLECOMBE, P. 2001. Thermodynamic modelling of aqueous aerosols containing electrolytes and dissolved organic compounds. *Journal of Aerosol Science*, 32, 713-738.
- CLEGG, S. L., SEINFELD, J. H. & EDNEY, E. O. 2003. Thermodynamic modelling of aqueous aerosols containing electrolytes and dissolved organic compounds. II. An extended Zdanovskii–Stokes–Robinson approach. *Journal of Aerosol Science*, 34, 667-690.
- CLEMENT, C. G. & TRUONG, L. D. 2014. An evaluation of Congo red fluorescence for the diagnosis of amyloidosis. *Human Pathology*, 45, 1766-1772.
- CLIFTON, I., FLETCHER, L., BEGGS, C., DENTON, M., CONWAY, S. & PECKHAM, D. 2010. An aerobiological model of aerosol survival of different strains of *Pseudomonas aeruginosa* isolated from people with cystic fibrosis. *Journal of Cystic Fibrosis*, 9, 64-68.

- COBELENS, F., VAN LETH, F. & VAN'T HOOG, A. 2014. Design of pragmatic trials of tuberculosis interventions. *The Lancet*, 383, 213-214.
- COCK, P. J., FIELDS, C. J., GOTO, N., HEUER, M. L. & RICE, P. M. 2009. The Sanger FASTQ file format for sequences with quality scores, and the Solexa/Illumina FASTQ variants. *Nucleic Acids Research*, 38, 1767-1771.
- COLE, S. T., BROSCHE, R., PARKHILL, J., GARNIER, T., CHURCHER, C., HARRIS, D., GORDON, S. V., EIGLMEIER, K., GAS, S., BARRY, C. E., 3RD, TEKAIA, F., BADCOCK, K., BASHAM, D., BROWN, D., CHILLINGWORTH, T., CONNOR, R., DAVIES, R., DEVLIN, K., FELTWELL, T., GENTLES, S., HAMLIN, N., HOLROYD, S., HORNSBY, T., JAGELS, K., KROGH, A., MCLEAN, J., MOULE, S., MURPHY, L., OLIVER, K., OSBORNE, J., QUAIL, M. A., RAJANDREAM, M. A., ROGERS, J., RUTTER, S., SEEGER, K., SKELTON, J., SQUARES, R., SQUARES, S., SULSTON, J. E., TAYLOR, K., WHITEHEAD, S. & BARRELL, B. G. 1998. Deciphering the biology of *Mycobacterium tuberculosis* from the complete genome sequence. *Nature*, 393, 537-544.
- CONDITIONS, N. C. C. F. C. & NICE, C. F. C. P. A. 2011. Tuberculosis: clinical diagnosis and management of tuberculosis, and measures for its prevention and control.
- COOK, G. M., BERNEY, M., GEBHARD, S., HEINEMANN, M., COX, R. A., DANILCHANKA, O. & NIEDERWEIS, M. 2009. Physiology of mycobacteria. *Advances in Microbial Physiology*, 55, 81-319.
- COPELAND, N. G. 2018. Computational Analysis of High-replicate RNA-seq Data in *Saccharomyces Cerevisiae*: Searching for New Genomic Features. *University of Dundee*.
- CORBETT, E. L., WATT, C. J., WALKER, N., MAHER, D., WILLIAMS, B. G., RAVIGLIONE, M. C. & DYE, C. 2003. The growing burden of tuberculosis: global trends and interactions with the HIV epidemic. *Archives of Internal Medicine*, 163, 1009-1021.
- CORTES, M. A., NESSAR, R. & SINGH, A. K. 2010. Laboratory maintenance of *Mycobacterium abscessus*. *Current Protocols in Microbiology*, 18, 10D. 1.1-10D. 1.12.
- COUSINS, D. V., BASTIDA, R., CATALDI, A., QOUS, V., REDROBE, S., DOW, S., DUIGNAN, P., MURRAY, A., DUPONT, C. & AHMED, N. 2003. Tuberculosis in seals caused by a novel member of the *Mycobacterium tuberculosis* complex: *Mycobacterium pinnipedii* sp. nov. *International Journal of Systematic and Evolutionary Microbiology*, 53, 1305-1317.
- COX, C. 1969. The cause of loss of viability of airborne *Escherichia coli* K12. *Microbiology*, 57, 77-80.
- COX, C. 1989. Airborne bacteria and viruses. *Science Progress (1933-)*, 469-499.



- COX, C. S. 1987. The aerobiological pathway of microorganisms, Chichester UK, *John Wiley & Sons*.
- CRICK, D. C., MAHAPATRA, S. & BRENNAN, P. J. 2001. Biosynthesis of the arabinogalactan-peptidoglycan complex of *Mycobacterium tuberculosis*. *Glycobiology*, 11, 107R-118R.
- CRICK, F. 1970. Central dogma of molecular biology. *Nature*, 227, 561.
- CROUCHER, N. J. & THOMSON, N. R. 2010. Studying bacterial transcriptomes using RNA-seq. *Current Opinion in Microbiology*, 13, 619-624.
- CULLEN, A. R., CANNON, C. L., MARK, E. J. & COLIN, A. A. 2000. *Mycobacterium abscessus* infection in cystic fibrosis: colonization or infection? *American Journal of Respiratory and Critical Care Medicine*, 161, 641-645.
- DABISCH, P., BOWER, K., DORSEY, B. & WRONKA, L. 2012. Recovery efficiencies for *Burkholderia thailandensis* from various aerosol sampling media. *Frontiers in Cellular and Infection Microbiology*, 2, 78.
- DANIEL, J., MAAMAR, H., DEB, C., SIRAKOVA, T. D. & KOLATTUKUDY, P. E. 2011. *Mycobacterium tuberculosis* uses host triacylglycerol to accumulate lipid droplets and acquires a dormancy-like phenotype in lipid-loaded macrophages. *PLoS Pathog*, 7, e1002093.
- DAWSON, R., ELLIOTT, D., ELLIOTT, W. & JONES, K. 1969. *Data for Biochemical Research*. (2nd Edn), Clarendon Press.
- DE ASSUNÇÃO, T. M., BATISTA JR, E. L., DEVES, C., VILLELA, A. D., PAGNUSSATTI, V. E., DE OLIVEIRA DIAS, A. C., KRITSKI, A., RODRIGUES-JUNIOR, V., BASSO, L. A. & SANTOS, D. S. 2014. Real time PCR quantification of viable *Mycobacterium tuberculosis* from sputum samples treated with propidium monoazide. *Tuberculosis*, 94, 421-427.
- DE JONG, B. C., ANTONIO, M. & GAGNEUX, S. 2010. *Mycobacterium africanum*—review of an important cause of human tuberculosis in West Africa. *PLoS Neglected Tropical Diseases*, 4, e744.
- DE LA RUA-DOMENECH, R. 2006. Human *Mycobacterium bovis* infection in the United Kingdom: incidence, risks, control measures and review of the zoonotic aspects of bovine tuberculosis. *Tuberculosis*, 86, 77-109.
- DEFRA 2014. Ricardo AEA Report for Defra, Department for Environment, Food and Rural Affairs *Air Pollution in the UK 2013*.

- DEL FABBRO, C., SCALABRIN, S., MORGANTE, M. & GIORGI, F. M. 2013. An extensive evaluation of read trimming effects on Illumina NGS data analysis. *PLoS One*, 8, e85024.
- DELOGU, G., SALI, M. & FADDA, G. 2013. The biology of *Mycobacterium tuberculosis* infection. *Mediterranean Journal of Hematology and Infectious Diseases*, 5, e2013070.
- DHARMADHIKARI, A. S., MPHAHLELE, M., STOLTZ, A., VENTER, K., MATHEBULA, R., MASOTLA, T., LUBBE, W., PAGANO, M., FIRST, M. & JENSEN, P. A. 2012. Surgical face masks worn by patients with multidrug-resistant tuberculosis: impact on infectivity of air on a hospital ward. *American Journal of Respiratory and Critical Care Medicine*, 185, 1104-1109.
- DOMINIC MILLS, J., KAWAHARA, Y. & JANITZ, M. 2013. Strand-specific RNA-seq provides greater resolution of transcriptome profiling. *Current Genomics*, 14, 173-181.
- DONLON, B. & COLLERAN, E. 1993. A comparison of different methods to determine the hydrophobicity of acetogenic bacteria. *Journal of Microbiological Methods*, 17, 27-37.
- DOYLE, R. J. 2000. Contribution of the hydrophobic effect to microbial infection. *Microbes and Infection*, 2, 391-400.
- DOYLE, R. J. & ROSENBERG, M. 1990. Microbial cell surface hydrophobicity, *American Society for Microbiology*.
- DOYLE, R. J. & ROSENBERG, M. 1995. [44] Measurement of microbial adhesion to hydrophobic substrata. *Methods in Enzymology*, 253, 542-550.
- DRUETT, H. 1969. A mobile form of the Henderson apparatus. *Epidemiology & Infection*, 67, 437-448.
- DU PLESSIS, D., WARREN, R., RICHARDSON, M., JOUBERT, J. & VAN HELDEN, P. 2001. Demonstration of reinfection and reactivation in HIV-negative autopsied cases of secondary tuberculosis: multilesional genotyping of *Mycobacterium tuberculosis* utilizing IS 6110 and other repetitive element-based DNA fingerprinting. *Tuberculosis*, 81, 211-220.
- DUARY, R. K., RAJPUT, Y. S., BATISH, V. K. & GROVER, S. 2011. Assessing the adhesion of putative indigenous probiotic *Lactobacilli* to human colonic epithelial cells. *The Indian Journal of Medical Research*, 134, 664-671.
- DUBNAU, E., CHAN, J., RAYNAUD, C., MOHAN, V. P., LANÉELLE, M. A., YU, K., QUÉMARD, A., SMITH, I. & DAFFÉ, M. 2000. Oxygenated mycolic acids are necessary for virulence of *Mycobacterium tuberculosis* in mice. *Molecular Microbiology*, 36, 630-637.

- DUNCAN, D. & PATEL, N. 2017. Next-Generation Sequencing in the Clinical Laboratory. *Diagnostic Molecular Pathology, Elsevier*, 25-33.
- DUTT, A. K. 2011. Epidemiology and Host Factors. *Tuberculosis and Nontuberculosis Mycobacterial Infections*, 6.
- DYE, C., BASSILI, A., BIERRENBACH, A., BROEKMANS, J., CHADHA, V., GLAZIOU, P., GOPI, P., HOSSEINI, M., KIM, S. & MANISSERO, D. 2008. Measuring tuberculosis burden, trends, and the impact of control programmes. *The Lancet Infectious Diseases*, 8, 233-243.
- EDWARDS, D., MAN, J., BRAND, P., KATSTRA, J., SOMMERER, STONE, H., NARDELL, E. & SCHEUCH, G. 2004. Inhaling to mitigate exhaled bioaerosols. *Proceedings of the National Academy of Sciences*, 101, 17383-17388.
- EHRT, S. & SCHNAPPINGER, D. 2009. Mycobacterial survival strategies in the phagosome: defence against host stresses. *Cellular Microbiology*, 11, 1170-1178.
- ESTEBAN, J., PÉREZ-TANOIRA, R., PÉREZ-JORGE-PEREMARCH, C. & GÓMEZ-BARRENA, E. 2014. Bacterial adherence to biomaterials used in surgical procedures. *Microbiology for Surgical Infections. Elsevier*, 41-57.
- ESTILLORE, A. D., TRUEBLOOD, J. V. & GRASSIAN, V. H. 2016. Atmospheric chemistry of bioaerosols: heterogeneous and multiphase reactions with atmospheric oxidants and other trace gases. *Chemical Science*, 7, 6604-6616.
- ETIENNE, G., LAVAL, F., VILLENEUVE, C., DINADAYALA, P., ABOUWARDA, A., ZERBIB, D., GALAMBA, A. & DAFTE, M. 2005. The cell envelope structure and properties of *Mycobacterium smegmatis* mc2155: is there a clue for the unique transformability of the strain? *Microbiology*, 151, 2075-2086.
- EWING, B. & GREEN, P. 1998. Base-calling of automated sequencer traces using phred. II. Error probabilities. *Genome Research*, 8, 186-194.
- FALKINHAM, J. O. 2003. Mycobacterial aerosols and respiratory disease. *Emerging Infectious Diseases*, 9, 763-767.
- FENG, J. Q. 2018. A Computational Analysis of Gas Jet Flow Effects on Liquid Aspiration in the Collision Nebulizer.
- FENNELLY, K. P., JONES-LÓPEZ, E. C., AYAKAKA, I., KIM, S., MENYHA, H., KIRENGA, B., MUCHWA, C., JOLOBA, M., DRYDEN-PETERSON, S. & REILLY, N. 2012. Variability of infectious aerosols produced during coughing by patients with pulmonary tuberculosis. *American Journal of Respiratory and Critical Care Medicine*, 186, 450-457.

- FIEGEL, J., CLARKE, R. & EDWARDS, D. A. 2006. Airborne infectious disease and the suppression of pulmonary bioaerosols. *Drug Discovery Today*, 11, 51-57.
- FILIATRAULT, M. J. 2011. Progress in prokaryotic transcriptomics. *Current Opinion in Microbiology*, 14, 579-586.
- FITZWATER, S. P., CAVIEDES, L., GILMAN, R. H., CORONEL, J., LACHIRA, D., SALAZAR, C., CARLOS SARAVIA, J., REDDY, K., FRIEDLAND, J. S. & MOORE, D. A. 2010. Prolonged infectiousness of tuberculosis patients in a directly observed therapy short-course program with standardized therapy. *Clinical Infectious Diseases*, 51, 371-378.
- FLEIGE, S. & PFAFFL, M. W. 2006. RNA integrity and the effect on the real-time qRT-PCR performance. *Molecular Aspects of Medicine*, 27, 126-139.
- FLETCHER, L. A., CHEN, Y., WHITAKER, P., DENTON, M., PECKHAM, D. G. & CLIFTON, I. J. 2016. Survival of *Mycobacterium abscessus* isolated from people with cystic fibrosis in artificially generated aerosols. *European Respiratory Journal*, 48, 1789-1791.
- FLETCHER, M. 1996. Diversity of surfaces and adhesion strategies. *Bacterial Adhesion: Molecular and Ecological Diversity*, 19.
- FLOTO, R. A., OLIVIER, K. N., SAIMAN, L., DALEY, C. L., HERRMANN, J.-L., NICK, J. A., NOONE, P. G., BILTON, D., CORRIS, P. & GIBSON, R. L. 2016. US Cystic Fibrosis Foundation and European Cystic Fibrosis Society consensus recommendations for the management of non-tuberculous mycobacteria in individuals with cystic fibrosis. *Thorax*, 71, i1-i22.
- FLYNN, J. L. & CHAN, J. 2001. Tuberculosis: latency and reactivation. *Infection and Immunity*, 69, 4195-4201.
- FORD, C. B., LIN, P. L., CHASE, M. R., SHAH, R. R., IARTCHOUK, O., GALAGAN, J., MOHAIDEEN, N., IOERGER, T. R., SACCHETTINI, J. C. & LIPSITCH, M. 2011. Use of whole genome sequencing to estimate the mutation rate of *Mycobacterium tuberculosis* during latent infection. *Nature Genetics*, 43, 482.
- FORTUNE, S. M., SOLACHE, A., JAEGER, A., HILL, P. J., BELISLE, J. T., BLOOM, B. R., RUBIN, E. J. & ERNST, J. D. 2004. *Mycobacterium tuberculosis* inhibits macrophage responses to IFN- $\gamma$  through myeloid differentiation factor 88-dependent and-independent mechanisms. *The Journal of Immunology*, 172, 6272-6280.
- FROTA, C. C., HUNT, D. M., BUXTON, R. S., RICKMAN, L., HINDS, J., KREMER, K., VAN SOOLINGEN, D. & COLSTON, M. J. 2004. Genome structure in the vole bacillus, *Mycobacterium microti*, a member of the *Mycobacterium tuberculosis* complex with a low virulence for humans. *Microbiology (Reading, England)*, 150, 1519.

- GACHON, C., MINGAM, A. & CHARRIER, B. 2004. Real-time PCR: what relevance to plant studies? *Journal of Experimental botany*, 55, 1445-1454.
- GAGNEUX, S. 2013. Genetic diversity in *Mycobacterium tuberculosis*. Pathogenesis of *Mycobacterium tuberculosis* and its Interaction with the Host Organism. *Springer*, 374, 1-25.
- GANNON, B., HAYES, C. & ROE, J. 2007. Survival rate of airborne *Mycobacterium bovis*. *Research in Veterinary Science*, 82, 169-172.
- GARNIER, T., EIGLMEIER, K., CAMUS, J.-C., MEDINA, N., MANSOOR, H., PRYOR, M., DUTHOY, S., GRONDIN, S., LACROIX, C. & MONSEMPE, C. 2003. The complete genome sequence of *Mycobacterium bovis*. *Proceedings of the National Academy of Sciences*, 100, 7877-7882.
- GARTON, N. J., WADDELL, S. J., SHERRATT, A. L., LEE, S.-M., SMITH, R. J., SENNER, C., HINDS, J., RAJAKUMAR, K., ADEGBOLA, R. A. & BESRA, G. S. 2008. Cytological and transcript analyses reveal fat and lazy persister-like bacilli in tuberculous sputum. *PLoS Med*, 5, e75.
- GAWAD, J. & BONDE, C. 2018. Current affairs, future perspectives of tuberculosis and antitubercular agents. *Indian Journal of Tuberculosis*, 65, 15-22.
- GEERTSEMA-DOORNBUSCH, G., VAN DER MEI, H. & BUSSCHER, H. 1993. Microbial cell surface hydrophobicity the involvement of electrostatic interactions in microbial adhesion to hydrocarbons (MATH). *Journal of Microbiological Methods*, 18, 61-68.
- GERDES, K. & MAISONNEUVE, E. 2012. Bacterial persistence and toxin-antitoxin loci. *Annual Review of Microbiology*, 66, 103-123.
- GHODBANE, R., RAOULT, D. & DRANCOURT, M. 2014. Dramatic reduction of culture time of *Mycobacterium tuberculosis*. *Sci Rep*, 4, 4236.
- GLICKMAN, M. S., COX, J. S. & JACOBS JR, W. R. 2000. A novel mycolic acid cyclopropane synthetase is required for cording, persistence, and virulence of *Mycobacterium tuberculosis*. *Molecular Cell*, 5, 717-727.
- GLICKMAN, M. S. & JACOBS, W. R. 2001. Microbial pathogenesis of *Mycobacterium tuberculosis*: dawn of a discipline. *Cell*, 104, 477-485.
- GOLDBERG, L., WATKINS, H., BOERKE, E. & CHATIGNY, M. 1958. The Use of a Rotating Drum for the Study of Aerosols over Extended Periods of Time. *American Journal of Hygiene*, 68, 85-93.

- GOSWAMI, P. & SINGH, H. D. 1991. Different modes of hydrocarbon uptake by two *Pseudomonas* species. *Biotechnology and Bioengineering*, 37, 1-11.
- GRAYSTON, J., WANG, S., KUO, C. & CAMPBELL, L. 1989. Current knowledge on *Chlamydia pneumoniae*, strain TWAR, an important cause of pneumonia and other acute respiratory diseases. *European Journal of Clinical Microbiology and Infectious Diseases*, 8, 191-202.
- GREENING, C., VILLAS-BÔAS, S. G., ROBSON, J. R., BERNEY, M. & COOK, G. M. 2014. The growth and survival of *Mycobacterium smegmatis* is enhanced by co-metabolism of atmospheric H<sub>2</sub>. *PLoS One*, 9, e103034.
- GRIFFITH, M., GRIFFITH, O. L., MWENIFUMBO, J., GOYA, R., MORRISSY, A. S., MORIN, R. D., CORBETT, R., TANG, M. J., HOU, Y.-C. & PUGH, T. J. 2010. Alternative expression analysis by RNA sequencing. *Nature Methods*, 7, 843-847.
- GRUFT, H., KATZ, J. & BLANCHARD, D. C. 1975. Postulated source of *Mycobacterium intracellulare* (Battey) infection. *American Journal of Epidemiology*, 102, 311-318.
- GUNNELS, J. J., BATES, J. H. & SWINDOLL, H. 1974. Infectivity of sputum-positive tuberculous patients on chemotherapy. *American Review of Respiratory Disease*, 109, 323-330.
- GUTIERREZ-VAZQUEZ, J. 1956. Studies on the Rate of Growth of Mycobacteria: I. Generation Time of *Mycobacterium Tuberculosis* on Several Solid and Liquid Media and Effects Exerted by Glycerol and Malachite Green. *American Review of Tuberculosis and Pulmonary Diseases*, 74, 50-58.
- GUTIERREZ, M. C., BRISSE, S., BROSCHE, R., FABRE, M., OMAÏS, B., MARMIESSE, M., SUPPLY, P. & VINCENT, V. 2005. Ancient origin and gene mosaicism of the progenitor of *Mycobacterium tuberculosis*. *PLoS Pathogens*, 1, e5.
- HAAS, B. J., CHIN, M., NUSBAUM, C., BIRREN, B. W. & LIVNY, J. 2012. How deep is deep enough for RNA-Seq profiling of bacterial transcriptomes? *BMC Genomics*, 13, 734.
- HACKENDAHL, N. C., MAWBY, D. I., BEMIS, D. A. & BEAZLEY, S. L. 2004. Putative transmission of *Mycobacterium tuberculosis* infection from a human to a dog. *J Am Vet Med Assoc*, 225, 1573-1577, 1548.
- HADDRELL, A. E. & THOMAS, R. J. 2017. Aerobiology: experimental considerations, observations, and future tools. *Appl. Environ. Microbiol.*, 83, e00809-17.
- HAMBLETON, P. 1971. Repair of wall damage in *Escherichia coli* recovered from an aerosol. *Microbiology*, 69, 81-88.

- HAN, T., WREN, M., DUBOIS, K., THERKORN, J. & MAINELIS, G. 2015. Application of ATP-based bioluminescence for bioaerosol quantification: Effect of sampling method. *Journal of Aerosol Science*, 90, 114-123.
- HANCOCK, I. 1991. Microbial cell surface architecture. *Microbial Cell Surface Analysis*, 21-59.
- HANDLEY, B. & WEBSTER, A. 1995. Some factors affecting the airborne survival of bacteria outdoors. *Journal of Applied Bacteriology*, 79, 368-378.
- HAZEN, K., BRAWNER, D., RIESSELMAN, M., JUTILA, M. & CUTLER, J. 1991. Differential adherence of hydrophobic and hydrophilic *Candida albicans* yeast cells to mouse tissues. *Infection and Immunity*, 59, 907-912.
- HAZEN, K. & HAZEN, B. 1987. A polystyrene microsphere assay for detecting surface hydrophobicity variations within *Candida albicans* populations. *Journal of Microbiological Methods*, 6, 289-299.
- HE, S., WURTZEL, O., SINGH, K., FROULA, J. L., YILMAZ, S., TRINGE, S. G., WANG, Z., CHEN, F., LINDQUIST, E. A. & SOREK, R. 2010. Validation of two ribosomal RNA removal methods for microbial metatranscriptomics. *Nature Methods*, 7, 807-812.
- HE, Z. & DE BUCK, J. 2010. Cell wall proteome analysis of *Mycobacterium smegmatis* strain MC2 155. *BMC Microbiology*, 10, 121.
- HEARD, J., JOHNSON, B. B., WELLS, J. D. & ANGOVE, M. J. 2009. Measuring 'hydrophobicity' of filamentous bacteria found in wastewater treatment plants. *Colloids and Surfaces B: Biointerfaces*, 72, 289-294.
- HEATHER, J. M. & CHAIN, B. 2016. The sequence of sequencers: The history of sequencing DNA. *Genomics*, 107, 1-8.
- HEGDE, P., QI, R., ABERNATHY, K., GAY, C., DHARAP, S., GASPARD, R., HUGHES, J., SNESRUD, E., LEE, N. & QUACKENBUSH, J. 2000. A concise guide to cDNA microarray analysis. *Biotechniques*, 29, 548-562.
- HEIDELBERG, J., SHAHAMAT, M., LEVIN, M., RAHMAN, I., STELMA, G., GRIM, C. & COLWELL, R. 1997. Effect of aerosolization on culturability and viability of gram-negative bacteria. *Appl. Environ. Microbiol.*, 63, 3585-3588.
- HERSEN, G., MOULARAT, S., ROBINE, E., GÉHIN, E., CORBET, S., VABRET, A. & FREYMUTH, F. 2008. Impact of Health on Particle Size of Exhaled Respiratory Aerosols: Case-control Study. *CLEAN–Soil, Air, Water*, 36, 572-577.
- HETT, E. C. & RUBIN, E. J. 2008. Bacterial growth and cell division: a mycobacterial perspective. *Microbiol Mol Biol Rev*, 72, 126-156.

- HILDA, J. N., SELVARAJ, A. & DAS, S. D. 2012. *Mycobacterium tuberculosis* H37Rv is more effective compared to vaccine strains in modulating neutrophil functions: an in vitro study. *FEMS Immunology & Medical Microbiology*, 66, 372-381.
- HORI, K., WATANABE, H., ISHII, S. I., TANJI, Y. & UNNO, H. 2008. Monolayer adsorption of a “bald” mutant of the highly adhesive and hydrophobic bacterium *Acinetobacter* sp. strain Tol 5 to a hydrocarbon surface. *Appl. Environ. Microbiol.*, 74, 2511-2517.
- HOUBEN, R. M. & DODD, P. J. 2016. The global burden of latent tuberculosis infection: a re-estimation using mathematical modelling. *PLoS Medicine*, 13, e1002152.
- HOWARD, S. T., RHOADES, E., RECHT, J., PANG, X., ALSUP, A., KOLTER, R., LYONS, C. R. & BYRD, T. F. 2006. Spontaneous reversion of *Mycobacterium abscessus* from a smooth to a rough morphotype is associated with reduced expression of glycopeptidolipid and reacquisition of an invasive phenotype. *Microbiology*, 152, 1581-1590.
- HSU, B.-M. & HUANG, C. 2002. Influence of ionic strength and pH on hydrophobicity and zeta potential of *Giardia* and *Cryptosporidium*. *Colloids and Surfaces A: Physicochemical and Engineering Aspects*, 201, 201-206.
- HUANG, S.-H., KUO, Y.-M., LIN, C.-W., KE, W.-R. & CHEN, C.-C. 2019. Experimental Characterization of Aerosol Suspension in a Rotating Drum. *Aerosol and Air Quality Research*, 19, 688-697.
- HUEBNER, R. 1996. BCG vaccination in the control of tuberculosis. *Tuberculosis*, 215, 263-282.
- Illumina, 2014. Available at <http://support.illumina.com/> (Accessed: 28 May 2020).
- IMBEAUD, S., GRAUDENS, E., BOULANGER, V., BARLET, X., ZABORSKI, P., EVENO, E., MUELLER, O., SCHROEDER, A. & AUFRAY, C. 2005. Towards standardization of RNA quality assessment using user-independent classifiers of microcapillary electrophoresis traces. *Nucleic Acids Research*, 33, e56-e56.
- JAHN, C. E., CHARKOWSKI, A. O. & WILLIS, D. K. 2008. Evaluation of isolation methods and RNA integrity for bacterial RNA quantitation. *Journal of Microbiological Methods*, 75, 318-324.
- JAMUAR, S. S. & TAN, E.-C. 2015. Clinical application of next-generation sequencing for Mendelian diseases. *Human Genomics*, 9, 10.
- JANKUTE, M., NATARAJ, V., LEE, O. Y.-C., WU, H. H., RIDELL, M., GARTON, N. J., BARER, M. R., MINNIKIN, D. E., BHATT, A. & BESRA, G. S. 2017. The role of hydrophobicity in tuberculosis evolution and pathogenicity. *Scientific Reports*, 7, 1315.



- JARLIER, V. & NIKAIDO, H. 1990. Permeability barrier to hydrophilic solutes in *Mycobacterium chelonae*. *Journal of Bacteriology*, 172, 1418-1423.
- JARVIS, B., WILRICH, C. & WILRICH, P. T. 2010. Reconsideration of the derivation of Most Probable Numbers, their standard deviations, confidence bounds and rarity values. *Journal of Applied Microbiology*, 109, 1660-1667.
- JI, F. & SADREYEV, R. I. 2018. RNA-seq: Basic bioinformatics analysis. *Current protocols in Molecular Biology*, 124, e68.
- JOHNSON, D. 1999. The effect of phosphate buffer on aerosol size distribution of nebulized *Bacillus subtilis* and *Pseudomonas fluorescens* bacteria. *Aerosol Science and Technology*, 30, 202-210.
- JOHNSON, G. R. & MORAWSKA, L. 2009. The mechanism of breath aerosol formation. *Journal of Aerosol Medicine and Pulmonary Drug Delivery*, 22, 229-237.
- JONES-LÓPEZ, E. C., NAMUGGA, O., MUMBOWA, F., SSEBIDANDI, M., MBABAZI, O., MOINE, S., MBOOWA, G., FOX, M. P., REILLY, N. & AYAKAKA, I. 2013. Cough aerosols of *Mycobacterium tuberculosis* predict new infection. A household contact study. *American Journal of Respiratory and Critical Care Medicine*, 187, 1007-1015.
- JÖNSSON, B. E., GILLJAM, M., LINDBLAD, A., RIDELL, M., WOLD, A. E. & WELINDER-OLSSON, C. 2007. Molecular epidemiology of *Mycobacterium abscessus*, with focus on cystic fibrosis. *Journal of Clinical Microbiology*, 45, 1497-1504.
- JORDAO, L., BLECK, C. K., MAYORGA, L., GRIFFITHS, G. & ANES, E. 2008. On the killing of mycobacteria by macrophages. *Cellular Microbiology*, 10, 529-548.
- JUOZAITIS, A., WILLEKE, K., GRINSHUPUN, S. A. & DONNELLY, J. 1994. Impaction onto a glass slide or agar versus impingement into a liquid for the collection and recovery of airborne microorganisms. *Appl. Environ. Microbiol.*, 60, 861-870.
- KADAM, T., RUPA, L., BALHAL, D., TOTEWAD, N. & GYANANATH, G. 2009. Determination of the degree of hydrophobicity—A technique to assess bacterial colonization on leaf surface and root region of lotus plant. *Asian J Exp Sci*, 23, 135-39.
- KAPRELYANTS, A. S., GOTTSCHAL, J. C. & KELL, D. B. 1993. Dormancy in non-sporulating bacteria. *FEMS Microbiology Letters*, 104, 271-285.
- KÄSER, M., RUF, M.-T., HAUSER, J., MARSOLIER, L. & PLUSCHKE, G. 2009. Optimized method for preparation of DNA from pathogenic and environmental mycobacteria. *Appl. Environ. Microbiol.*, 75, 414-418.
- KEFLIE, T. S. & AMENI, G. 2014. Microscopic examination and smear negative pulmonary tuberculosis in Ethiopia. *The Pan African Medical Journal*, 19.

- KENT, P. 1985. Antituberculosis chemotherapy and drug susceptibility testing. In: *Public Health Mycobacteriology. A guide for the level III laboratory*, 159-184.
- KESAVAN, J. & SAGRIPANTI, J.-L. 2015. Evaluation criteria for bioaerosol samplers. *Environmental Science: Processes & Impacts*, 17, 638-645.
- KIM, T. H. & KUBICA, G. P. 1972. Long-term preservation and storage of mycobacteria. *Appl. Environ. Microbiol.*, 24, 311-317.
- KIM, Y. J., LEE, S. M., PARK, B. K., KIM, S. S., YI, J., KIM, H. H., LEE, E. Y. & CHANG, C. L. 2014. Evaluation of propidium monoazide real-time PCR for early detection of viable *Mycobacterium tuberculosis* in clinical respiratory specimens. *Annals of Laboratory Medicine*, 34, 203-209.
- KLEINNIJENHUIS, J., OOSTING, M., JOOSTEN, L. A., NETEA, M. G. & VAN CREVEL, R. 2011. Innate immune recognition of *Mycobacterium tuberculosis*. *Clinical and Developmental Immunology*, 2011.
- KOCHKODAN, V., TSARENKO, S., POTAPCHENKO, N., KOSINOVA, V. & GONCHARUK, V. 2008. Adhesion of microorganisms to polymer membranes: a photobactericidal effect of surface treatment with TiO<sub>2</sub>. *Desalination*, 220, 380-385.
- KOECK, J. L., FABRE, M., SIMON, F., DAFFÉ, M., GARNOTEL, E., MATAN, A., GÉRÔME, P., BERNATAS, J. J., BUISSON, Y. & POURCEL, C. 2011. Clinical characteristics of the smooth tubercle bacilli '*Mycobacterium canettii*' infection suggest the existence of an environmental reservoir. *Clinical Microbiology and Infection*, 17, 1013-1019.
- KONOMI, N., LEBWOHL, E., MOWBRAY, K., TATTERSALL, I. & ZHANG, D. 2002. Detection of mycobacterial DNA in Andean mummies. *Journal of Clinical Microbiology*, 40, 4738-4740.
- KUCUKYILDIRIM, S., LONG, H., SUNG, W., MILLER, S. F., DOAK, T. G. & LYNCH, M. 2016. The rate and spectrum of spontaneous mutations in *Mycobacterium smegmatis*, a bacterium naturally devoid of the postreplicative mismatch repair pathway. *G3: Genes, Genomes, Genetics*, 6, 2157-2163.
- KUKURBA, K. R. & MONTGOMERY, S. B. 2015. RNA sequencing and analysis. *Cold Spring Harbor Protocols*, 2015, pdb. top084970.
- LATHER, P., MOHANTY, A., JHA, P. & GARSA, A. K. 2016. Contribution of cell surface hydrophobicity in the resistance of *Staphylococcus aureus* against antimicrobial agents. *Biochemistry Research International*, 2016.
- LAWN, S. D. & ZUMLA, A. I. 2012. Diagnosis of extrapulmonary tuberculosis using the Xpert® MTB/RIF assay. *Expert Review of Anti-infective Therapy*, 10, 631-635.

- LEDERGERBER, C. & DESSIMOZ, C. 2011. Base-calling for next-generation sequencing platforms. *Briefings in Bioinformatics*, 12, 489-497.
- LEE, M.-R., SHENG, W.-H., HUNG, C.-C., YU, C.-J., LEE, L.-N. & HSUEH, P.-R. 2015. *Mycobacterium abscessus* complex infections in humans. *Emerging Infectious Diseases*, 21, 1638.
- LEUNG, A. N. 1999. Pulmonary tuberculosis: the essentials. *Radiology*, 210, 307-322.
- LEVER, M., WILLIAMS, A. & BENNETT, A. 2000. Survival of mycobacterial species in aerosols generated from artificial saliva. *Letters in Applied Microbiology*, 31, 238-241.
- LEVIN, J. Z., YASSOUR, M., ADICONIS, X., NUSBAUM, C., THOMPSON, D. A., FRIEDMAN, N., GNIRKE, A. & REGEV, A. 2010. Comprehensive comparative analysis of strand-specific RNA sequencing methods. *Nature Methods*, 7, 709.
- LI, B. & DEWEY, C. N. 2011. RSEM: accurate transcript quantification from RNA-Seq data with or without a reference genome. *BMC Bioinformatics*, 12, 323.
- LI, C.-S. & LIN, Y.-C. 2001. Storage effects on bacterial concentration: determination of impinger and filter samples. *Science of the Total Environment*, 278, 231-237.
- LICHTENBERG, D., ROSENBERG, M., SHARFMAN, N. & OFEK, I. 1985. A kinetic approach to bacterial adherence to hydrocarbon. *Journal of Microbiological Methods*, 4, 141-146.
- LIM, A. & DICK, T. 2001. Plate-based dormancy culture system for *Mycobacterium smegmatis* and isolation of metronidazole-resistant mutants. *FEMS Microbiology Letters*, 200, 215-219.
- LINDAHL, M., FARIS, A., WADSTRÖM, T. & HJERTEN, S. 1981. A new test based on 'salting out' to measure relative hydrophobicity of bacterial cells. *Biochimica et Biophysica Acta (BBA)-General Subjects*, 677, 471-476.
- LOPEZ-MARIN, L. M. 2012. Nonprotein structures from mycobacteria: emerging actors for tuberculosis control. *Clinical and Developmental Immunology*, 2012.
- LOUDON, R. G., BUMGARNER, L. R., LACY, J. & COFFMAN, G. K. 1969. Aerial Transmission of Mycobacteria 1, 2. *American Review of Respiratory Disease*, 100, 165-171.
- LOUDON, R. G. & ROBERTS, R. M. 1968. Singing and the dissemination of tuberculosis. *American Review of Respiratory Disease*, 98, 297-300.
- LOUDON, R. G. & SPOHN, S. K. 1969. Cough frequency and infectivity in patients with pulmonary tuberculosis. *American Review of Respiratory Disease*, 99, 109-111.

- LOVE, M. I., HUBER, W. & ANDERS, S. 2014. Moderated estimation of fold change and dispersion for RNA-seq data with DESeq2. *Genome Biology*, 15, 550.
- MAINELIS, G. 1999. Collection of airborne microorganisms by electrostatic precipitation. *Aerosol Science and Technology*, 30, 127-144.
- MAHAIRAS, G. G., SABO, P. J., HICKEY, M. J., SINGH, D. C. & STOVER, C. K. 1996. Molecular analysis of genetic differences between *Mycobacterium bovis* BCG and virulent *M. bovis*. *Journal of Bacteriology*, 178, 1274-1282.
- MARRAKCHI, H., LANÉELLE, M.-A. & DAFFÉ, M. 2014. Mycolic acids: structures, biosynthesis, and beyond. *Chemistry & Biology*, 21, 67-85.
- MARTIN, J. A. & WANG, Z. 2011. Next-generation transcriptome assembly. *Nature Reviews Genetics*, 12, 671.
- MASON, P., NEILSON, G., DEMPSEY, C., BARNES, A. & CRUICKSHANK, J. 2003. The hydration structure of guanidinium and thiocyanate ions: implications for protein stability in aqueous solution. *Proceedings of the National Academy of Sciences*, 100, 4557-4561.
- MASTORIDES, S. M., OEHLER, R. L., GREENE, J. N., SINNOTT IV, J. T., KRANIK, M. & SANDIN, R. L. 1999. The detection of airborne *Mycobacterium tuberculosis* using micropore membrane air sampling and polymerase chain reaction. *Chest*, 115, 19-25.
- MATUKA, O., SINGH, T. S., BRYCE, E., YASSI, A., KGASHA, O., ZUNGU, M., KYAW, K., MALOTLE, M., RENTON, K. & O'HARA, L. 2015. Pilot study to detect airborne *Mycobacterium tuberculosis* exposure in a South African public healthcare facility outpatient clinic. *Journal of Hospital Infection*, 89, 192-196.
- MAY, K. 1973. The Collison nebulizer: description, performance and application. *Journal of Aerosol Science*, 4, 235-243.
- MCCLURE, R., BALASUBRAMANIAN, D., SUN, Y., BOBROVSKYY, M., SUMBY, P., GENCO, C. A., VANDERPOOL, C. K. & TJADEN, B. 2013. Computational analysis of bacterial RNA-Seq data. *Nucleic Acids Research*, 41, e140-e140.
- MCKAY, G., OTTERBURN, M. S. & AGA, J. A. 1985. Fuller's earth and fired clay as absorbents for dyestuffs external mass transport processes during adsorption. *Water, Air, and Soil Pollution*, 26, 149-161.
- MCNEIL, M., DAFFE, M. & BRENNAN, P. 1991. Location of the mycolyl ester substituents in the cell walls of mycobacteria. *Journal of Biological Chemistry*, 266, 13217-13223.

- MCNEIL, M., DAFTE, M. & BRENNAN, P. J. 1990. Evidence for the nature of the link between the arabinogalactan and peptidoglycan of mycobacterial cell walls. *Journal of Biological Chemistry*, 265, 18200-18206.
- MICHEL, A. L., MULLER, B. & VAN HELDEN, P. D. 2010. *Mycobacterium bovis* at the animal-human interface: a problem, or not? *Vet Microbiol*, 140, 371-81.
- MILES, A., MISRA, S. & IRWIN, J. 1938. The estimation of the bactericidal power of the blood. *Journal of Hygiene*, 38, 732-749.
- MILLS, A. L. & POWELSON, D. K. 1996. Bacterial interactions with surfaces in soils. *Bacterial Adhesion: Molecular and Ecological Diversity*, 25-57.
- MINNIKIN, D. E., LEE, O., WU, H., NATARAJ, V., DONOGHUE, H. D., RIDELL, M., WATANABE, M., ALDERWICK, L., BHATT, A. & BESRA, G. S. 2015. Pathophysiological implications of cell envelope structure in *Mycobacterium tuberculosis* and related taxa. *Tuberculosis*, 95, 133-139.
- MORETON, J., IZQUIERDO, A. & EMES, R. D. 2016. Assembly, assessment, and availability of de novo generated eukaryotic transcriptomes. *Frontiers in Genetics*, 6, 361.
- MORIARTY, J. & GROTHBERG, J. 1999. Flow-induced instabilities of a mucus-serous bilayer. *Journal of Fluid Mechanics*, 397, 1-22.
- MOROZOVA, O., HIRST, M. & MARRA, M. A. 2009. Applications of new sequencing technologies for transcriptome analysis. *Annual Review of Genomics and Human Genetics*, 10, 135-151.
- MORTAZAVI, A., WILLIAMS, B. A., MCCUE, K., SCHAEFFER, L. & WOLD, B. 2008. Mapping and quantifying mammalian transcriptomes by RNA-Seq. *Nature Methods*, 5, 621.
- MUDD, S. & MUDD, E. B. 1924. The penetration of bacteria through capillary spaces: Iv. A kinetic mechanism in interfaces. *Journal of Experimental Medicine*, 40, 633-645.
- MUKAMOLOVA, G. V., TURAPOV, O., MALKIN, J., WOLTMANN, G. & BARER, M. R. 2010. Resuscitation-promoting factors reveal an occult population of tubercle bacilli in sputum. *American Journal of Respiratory and Critical Care Medicine*, 181, 174-180.
- MUNOZ-ELIAS, E. J. & MCKINNEY, J. D. 2006. Carbon metabolism of intracellular bacteria. *Cell Microbiol*, 8, 10-22.

- NARDELL, E. A., WILLIAMS, C. M., BELL, A. J., MALINGA, L., RAMSHEH, M. Y., BAKIR, A., GARTON, N. J., STOLTZ, A., DEKOCK, E. & WADDELL, S. 2016. TB airborne transmission: first gene expression signatures of captured, uncultured *M. tuberculosis* from human source aerosol. *D107. TUBERCULOSIS INFECTION AND DISEASE: EPIDEMIOLOGY AND DIAGNOSIS*. American Thoracic Society.
- NESBITT, W., DOYLE, R. & TAYLOR, K. 1982. Hydrophobic interactions and the adherence of *Streptococcus sanguis* to hydroxylapatite. *Infection and Immunity*, 38, 637-644.
- NG, T. W., IP, M., CHAO, C. Y., TANG, J. W., LAI, K. P., FU, S. C., LEUNG, W. T. & LAI, K. M. 2018. Differential gene expression in *Escherichia coli* during aerosolization from liquid suspension. *Applied Microbiology and Biotechnology*, 102, 6257-6267.
- NGUYEN, V. 1997. Diagnosis and treatment of disease caused by nontuberculous mycobacteria. This official statement of the American Thoracic Society was approved by the Board of Directors, March 1997. Medical Section of the American Lung Association. *Am J Respir Crit Care Med*, 156, S1-S25.
- NIEMANN, S., RICHTER, E. & RÜSCH-GERDES, S. 2002. Biochemical and genetic evidence for the transfer of *Mycobacterium tuberculosis* subsp. *caprae* Aranaz et al. 1999 to the species *Mycobacterium bovis* Karlson and Lessel 1970 (approved lists 1980) as *Mycobacterium bovis* subsp. *caprae* comb. nov. *International Journal of Systematic and Evolutionary Microbiology*, 52, 433-436.
- NIEMANN, S., KUBICA, T., BANGE, F., ADJEI, O., BROWNE, E., CHINBUAH, M., DIEL, R., GYAPONG, J., HORSTMANN, R. & JOLOBA, M. 2004. The species *Mycobacterium africanum* in the light of new molecular markers. *Journal of Clinical Microbiology*, 42, 3958-3962.
- NIKOVSKAYA, G., GORDIENKO, A. & GLOBAL, L. 1989. Hydrophilic hydrophobic properties of microorganisms under different growth-conditions. *MICROBIOLOGY*, 58, 356-359.
- NOCKER, A. & CAMPER, A. K. 2009. Novel approaches toward preferential detection of viable cells using nucleic acid amplification techniques. *FEMS Microbiology Letters*, 291, 137-142.
- NOCKER, A., CHEUNG, C.-Y. & CAMPER, A. K. 2006. Comparison of propidium monoazide with ethidium monoazide for differentiation of live vs. dead bacteria by selective removal of DNA from dead cells. *Journal of Microbiological Methods*, 67, 310-320.
- OBUEKWE, C. O., AL-JADI, Z. K. & AL-SALEH, E. S. 2007. Sequential hydrophobic partitioning of cells of *Pseudomonas aeruginosa* gives rise to variants of increasing cell-surface hydrophobicity. *FEMS Microbiology Letters*, 270, 214-219.

- OCEPEK, M., PATE, M., ZOLNIR-DOVC, M. & POLJAK, M. 2005. Transmission of *Mycobacterium tuberculosis* from human to cattle. *J Clin Microbiol*, 43, 3555-7.
- OJHA, A. K., BAUGHN, A. D., SAMBANDAN, D., HSU, T., TRIVELLI, X., GUERARDEL, Y., ALAHARI, A., KREMER, L., JACOBS, W. R. & HATFULL, G. F. 2008. Growth of *Mycobacterium tuberculosis* biofilms containing free mycolic acids and harbouring drug-tolerant bacteria. *Molecular Microbiology*, 69, 164-174.
- OSHLACK, A., ROBINSON, M. D. & YOUNG, M. D. 2010. From RNA-seq reads to differential expression results. *Genome Biology*, 11, 220.
- PANDEY, A. K. & SASSETTI, C. M. 2008. Mycobacterial persistence requires the utilization of host cholesterol. *Proc Natl Acad Sci U S A*, 105, 4376-80.
- PANDEY, B. D., POUDEL, A., YODA, T., TAMARU, A., ODA, N., FUKUSHIMA, Y., LEKHAK, B., RISAL, B., ACHARYA, B. & SAPKOTA, B. 2008. Development of an in-house loop-mediated isothermal amplification (LAMP) assay for detection of *Mycobacterium tuberculosis* and evaluation in sputum samples of Nepalese patients. *Journal of Medical Microbiology*, 57, 439-443.
- PARK, H. D., GUINN, K. M., HARRELL, M. I., LIAO, R., VOSKUIL, M. I., TOMPA, M., SCHOOLNIK, G. K. & SHERMAN, D. R. 2003. Rv3133c/dosR is a transcription factor that mediates the hypoxic response of *Mycobacterium tuberculosis*. *Molecular Microbiology*, 48, 833-843.
- PARKER, B. C., FORD, M. A., GRUFT, H. & FALKINHAM III, J. O. 1983. Epidemiology of infection by nontuberculous mycobacteria: IV. Preferential aerosolization of *Mycobacterium intracellulare* from natural waters. *American Review of Respiratory Disease*, 128, 652-656.
- PATTERSON, B. & WOOD, R. 2019. Is cough really necessary for TB transmission? *Tuberculosis (Edinburgh, Scotland)*, 117, 31.
- PEDLEY, S., BARTRAM, J. & ORGANIZATION, W. H. 2004. Pathogenic Mycobacteria in Water: A Guide to Public Health Consequences, Monitoring and Management (*Emerging Issues in Water and Infectious Disease Series*), Unspecified.
- PETROVA, O. E., GARCIA-ALCALDE, F., ZAMPALONI, C. & SAUER, K. 2017. Comparative evaluation of rRNA depletion procedures for the improved analysis of bacterial biofilm and mixed pathogen culture transcriptomes. *Scientific Reports*, 7, 41114.
- PORTEVIN, D., DE SOUSA-D'AURIA, C., HOUSSIN, C., GRIMALDI, C., CHAMI, M., DAFFÉ, M. & GUILHOT, C. 2004. A polyketide synthase catalyzes the last condensation step of mycolic acid biosynthesis in mycobacteria and related organisms. *Proceedings of the National Academy of Sciences*, 101, 314-319.

- POZHITKOV, A. E., TAUTZ, D. & NOBLE, P. A. 2007. Oligonucleotide microarrays: widely applied—poorly understood. *Briefings in Functional Genomics and Proteomics*, 6, 141-148.
- QADRI, F., HOSSAIN, S. A., CIZNÁR, I., HAIDER, K., LJUNGH, A., WADSTROM, T. & SACK, D. A. 1988. Congo red binding and salt aggregation as indicators of virulence in *Shigella* species. *Journal of Clinical Microbiology*, 26, 1343-1348.
- RANA, A. K., SINGH, A., GURCHA, S. S., COX, L. R., BHATT, A. & BESRA, G. S. 2012. Ppm1-encoded polyprenyl monophosphomannose synthase activity is essential for lipoglycan synthesis and survival in mycobacteria. *PLoS One*, 7.
- RANA, A. K. 2014. Investigating novel drug targets and the biosynthetic pathways of lipids in mycobacteria. PhD thesis, *University of Birmingham*.
- RATLEDGE, C. & STANFORD, J. 1982. The biology of the mycobacteria. *Academic of San Deigo*, USA, 53-94
- REID, R. & TESTER, M. 1992. Measurements of Ca<sup>2+</sup> fluxes in intact plant cells. *Philosophical Transactions of the Royal Society of London. Series B: Biological Sciences*, 338, 73-82.
- REPONEN, T., WILLEKE, K., ULEVICIUS, V., GRINSHUPUN, S. A. & DONNELLY, J. 1997. Techniques for dispersion of microorganisms into air. *Aerosol Science and Technology*, 27, 405-421.
- REYRAT, J.-M. & KAHN, D. 2001. *Mycobacterium smegmatis*: an absurd model for tuberculosis? *Trends in Microbiology*, 9, 472-474.
- RIEDER, H. L. 1999. Epidemiologic basis of tuberculosis control. *International Union Against Tuberculosis and Lung Disease (IUATLD)*.
- RIPOLL, F., PASEK, S., SCHENOWITZ, C., DOSSAT, C., BARBE, V., ROTTMAN, M., MACHERAS, E., HEYM, B., HERRMANN, J.-L. & DAFFÉ, M. 2009. Non mycobacterial virulence genes in the genome of the emerging pathogen *Mycobacterium abscessus*. *PloS One*, 4, e5660.
- ROBERTSON, G., SCHEIN, J., CHIU, R., CORBETT, R., FIELD, M., JACKMAN, S. D., MUNGALL, K., LEE, S., OKADA, H. M. & QIAN, J. Q. 2010. De novo assembly and analysis of RNA-seq data. *Nature Methods*, 7, 909.
- ROBINSON, M. D. & OSHLACK, A. 2010. A scaling normalization method for differential expression analysis of RNA-seq data. *Genome Biology*, 11, R25.



- ROSENBERG, E., KAPLAN, N., PINES, O., ROSENBERG, M. & GUTNICK, D. 1983. Capsular polysaccharides interfere with adherence of *Acinetobacter calcoaceticus* to hydrocarbon. *FEMS Microbiology Letters*, 17, 157-160.
- ROSENBERG, M. 1984. Bacterial adherence to hydrocarbons: a useful technique for studying cell surface hydrophobicity. *FEMS Microbiology Letters*, 22, 289-295.
- ROSENBERG, M. 1991. Basic and applied aspects of microbial adhesion at the hydrocarbon: water interface. *Critical Reviews in Microbiology*, 18, 159-173.
- ROSENBERG, M. 2006. Microbial adhesion to hydrocarbons: twenty-five years of doing MATH. *FEMS Microbiology Letters*, 262, 129-134.
- ROSENBERG, M., GUTNICK, D. & ROSENBERG, E. 1980. Adherence of bacteria to hydrocarbons: a simple method for measuring cell-surface hydrophobicity. *FEMS Microbiology Letters*, 9, 29-33.
- ROTHSCHILD, B. M., MARTIN, L. D., LEV, G., BERCOVIER, H., BAR-GAL, G. K., GREENBLATT, C., DONOGHUE, H., SPIGELMAN, M. & BRITTAIN, D. 2001. *Mycobacterium tuberculosis* complex DNA from an extinct bison dated 17,000 years before the present. *Clinical Infectious Diseases*, 33, 305-311.
- ROUPIE, V., ROMANO, M., ZHANG, L., KORF, H., LIN, M. Y., FRANKEN, K. L., OTTENHOFF, T. H., KLEIN, M. R. & HUYGEN, K. 2007. Immunogenicity of eight dormancy regulon-encoded proteins of *Mycobacterium tuberculosis* in DNA-vaccinated and tuberculosis-infected mice. *Infection and Immunity*, 75, 941-949.
- RÜHS, P. A., BÖCKER, L., INGLIS, R. F. & FISCHER, P. 2014. Studying bacterial hydrophobicity and biofilm formation at liquid–liquid interfaces through interfacial rheology and pendant drop tensiometry. *Colloids and Surfaces B: Biointerfaces*, 117, 174-184.
- RULE, A. M., KESAVAN, J., SCHWAB, K. J. & BUCKLEY, T. J. 2007. Application of flow cytometry for the assessment of preservation and recovery efficiency of bioaerosol samplers spiked with *Pantoea agglomerans*. *Environmental Science & Technology*, 41, 2467-2472.
- RUSSELL, D. G. 2007. Who puts the tubercle in tuberculosis? *Nature Reviews Microbiology*, 5, 39-47.
- RUSTAD, T. R., MINCH, K. J., MA, S., WINKLER, J. K., HOBBS, S., HICKEY, M., BRABANT, W., TURKARSLAN, S., PRICE, N. D. & BALIGA, N. S. 2014. Mapping and manipulating the *Mycobacterium tuberculosis* transcriptome using a transcription factor overexpression-derived regulatory network. *Genome Biology*, 15, 502.
- RYAN, K. J. & RAY, C. G. 2004. Medical microbiology. *McGraw Hill*, 4, 370.

- SAINI, G. 2010. Bacterial hydrophobicity: assessment techniques, applications and extension to colloids. PhD thesis, *Oregon state University*, USA
- SAKAMOTO, K. 2012. The pathology of *Mycobacterium tuberculosis* infection. *Vet Pathol*, 49, 423-39.
- SALA, A., BORDES, P. & GENEVAUX, P. 2014. Multiple toxin-antitoxin systems in *Mycobacterium tuberculosis*. *Toxins*, 6, 1002-1020.
- SANDHU, G. K. 2011. Tuberculosis: current situation, challenges and overview of its control programs in India. *Journal of Global Infectious Diseases*, 3, 143.
- SANTARPIA, J. L., PAN, Y.-L., HILL, S. C., BAKER, N., COTTRELL, B., MCKEE, L., RATNESAR-SHUMATE, S. & PINNICK, R. G. 2012. Changes in fluorescence spectra of bioaerosols exposed to ozone in a laboratory reaction chamber to simulate atmospheric aging. *Optics Express*, 20, 29867-29881.
- SARKAR, D. 2012. Mycobacterial glycolipids: pathways to synthesis and role in virulence. PhD thesis, *University of Birmingham*, UK.
- SCHROEDER, A., MUELLER, O., STOCKER, S., SALOWSKY, R., LEIBER, M., GASSMANN, M., LIGHTFOOT, S., MENZEL, W., GRANZOW, M. & RAGG, T. 2006. The RIN: an RNA integrity number for assigning integrity values to RNA measurements. *BMC Molecular Biology*, 7, 3.
- SHERMAN, D. R., VOSKUIL, M., SCHNAPPINGER, D., LIAO, R., HARRELL, M. I. & SCHOOLNIK, G. K. 2001. Regulation of the *Mycobacterium tuberculosis* hypoxic response gene encoding  $\alpha$ -crystallin. *Proceedings of the National Academy of Sciences*, 98, 7534-7539.
- SHERRATT, A. L. 2008. Lipid bodies in mycobacteria. Infection immunity and inflammation. PhD thesis, *Leicester University*, UK.
- SHILOH, M. U., MANZANILLO, P. & COX, J. S. 2008. *Mycobacterium tuberculosis* senses host-derived carbon monoxide during macrophage infection. *Cell Host & Microbe*, 3, 323-330.
- SHINNICK, T. & GOOD, R. 1994. Mycobacterial taxonomy. *European Journal of Clinical Microbiology and Infectious Diseases*, 13, 884-901.
- SHU, Z., WEIGEL, K. M., SOELBERG, S. D., LAKEY, A., CANGELOSI, G. A., LEE, K.-H., CHUNG, J.-H. & GAO, D. 2012. Cryopreservation of *Mycobacterium tuberculosis* complex cells. *Journal of Clinical Microbiology*, 50, 3575-3580.

- SIA, J. K., GEORGIEVA, M. & RENGARAJAN, J. 2015. Innate immune defenses in human tuberculosis: an overview of the interactions between *Mycobacterium tuberculosis* and innate immune cells. *Journal of Immunology Research*, 2015.
- SIMS, D., SUDBERY, I., ILOTT, N. E., HEGER, A. & PONTING, C. P. 2014. Sequencing depth and coverage: key considerations in genomic analyses. *Nature Reviews Genetics*, 15, 121-132.
- SINDE, E. & CARBALLO, J. 2000. Attachment of *Salmonella* spp. and *Listeria monocytogenes* to stainless steel, rubber and polytetrafluorethylene: the influence of free energy and the effect of commercial sanitizers. *Food Microbiology*, 17, 439-447.
- SINGH, P., RAO, R. N., REDDY, J. R. C., PRASAD, R., KOTTURU, S. K., GHOSH, S. & MUKHOPADHYAY, S. 2016. PE11, a PE/PPE family protein of *Mycobacterium tuberculosis* is involved in cell wall remodeling and virulence. *Scientific Reports*, 6, 1-16.
- SMITH, C. J. & OSBORN, A. M. 2009. Advantages and limitations of quantitative PCR (Q-PCR)-based approaches in microbial ecology. *FEMS Microbiology Ecology*, 67, 6-20.
- SMITH, I. 2003. *Mycobacterium tuberculosis* pathogenesis and molecular determinants of virulence. *Clinical Microbiology Reviews*, 16, 463-496.
- SMITH, N. H., GORDON, S. V., DE LA RUA-DOMENECH, R., CLIFTON-HADLEY, R. S. & HEWINSON, R. G. 2006. Bottlenecks and broomsticks: the molecular evolution of *Mycobacterium bovis*. *Nat Rev Microbiol*, 4, 670-81.
- SMITH, T. F. & WATERMAN, M. S. 1981. Identification of common molecular subsequences. *Journal of Molecular Biology*, 147, 195-197.
- SNAPPER, S., MELTON, R., MUSTAFA, S., KIESER, T. & JR, W. J. 1990. Isolation and characterization of efficient plasmid transformation mutants of *Mycobacterium smegmatis*. *Molecular Microbiology*, 4, 1911-1919.
- SOTO, C. Y., CAMA, M., GIBERT, I. & LUQUIN, M. 2000. Application of an easy and reliable method for sulfolipid-I detection in the study of its distribution in *Mycobacterium tuberculosis* strains. *FEMS Microbiology Letters*, 187, 103-107.
- SPAHR, U. & SCHAFROTH, K. 2001. Fate of *Mycobacterium avium* subsp. paratuberculosis in Swiss hard and semihard cheese manufactured from raw milk. *Appl. Environ. Microbiol.*, 67, 4199-4205.
- SRIKANTH, P., SUDHARSANAM, S. & STEINBERG, R. 2008. Bio-aerosols in indoor environment: Composition, health effects and analysis. *Indian Journal of Medical Microbiology*, 26, 302.

- STEPHAN, J., BENDER, J., WOLSCHEENDORF, F., HOFFMANN, C., ROTH, E., MAILÄNDER, C., ENGELHARDT, H. & NIEDERWEIS, M. 2005. The growth rate of *Mycobacterium smegmatis* depends on sufficient porin-mediated influx of nutrients. *Molecular Microbiology*, 58, 714-730.
- STEWART, S. L., GRINSHUPUN, S. A., WILLEKE, K., TERZIEVA, S., ULEVICIUS, V. & DONNELLY, J. 1995. Effect of impact stress on microbial recovery on an agar surface. *Appl. Environ. Microbiol.*, 61, 1232-1239.
- STOKES, R. W., NORRIS-JONES, R., BROOKS, D. E., BEVERIDGE, T. J., DOXSEE, D. & THORSON, L. M. 2004. The glycan-rich outer layer of the cell wall of *Mycobacterium tuberculosis* acts as an antiphagocytic capsule limiting the association of the bacterium with macrophages. *Infection and Immunity*, 72, 5676-5686.
- STONE, R. & JOHNSON, D. 2002. A note on the effect of nebulization time and pressure on the culturability of *Bacillus subtilis* and *Pseudomonas fluorescens*. *Aerosol Science & Technology*, 36, 536-539.
- STREIT, S., MICHALSKI, C. W., ERKAN, M., KLEEFF, J. & FRIESS, H. 2009. Northern blot analysis for detection and quantification of RNA in pancreatic cancer cells and tissues. *Nature Protocols*, 4, 37.
- SULTAN, L., NYKA, W., MILLS, C., O'GRADY, F., WELLS, W. & RILEY, R. 1960. Tuberculosis disseminators: a study of the variability of aerial infectivity of tuberculous patients. *American Review of Respiratory Disease*, 82, 358-369.
- SUPPLY, P., MARCEAU, M., MANGENOT, S., ROCHE, D., ROUANET, C., KHANNA, V., MAJLESSI, L., CRISCUOLO, A., TAP, J. & PAWLIK, A. 2013. Genomic analysis of smooth tubercle bacilli provides insights into ancestry and pathoadaptation of *Mycobacterium tuberculosis*. *Nature Genetics*, 45, 172.
- TEITELBAUM, R., SCHUBERT, W., GUNTHER, L., KRESS, Y., MACALUSO, F., POLLARD, J. W., MCMURRAY, D. N. & BLOOM, B. R. 1999. The M cell as a portal of entry to the lung for the bacterial pathogen *Mycobacterium tuberculosis*. *Immunity*, 10, 641-650.
- TERZIEVA, S., DONNELLY, J., ULEVICIUS, V., GRINSHUPUN, S. A., WILLEKE, K., STELMA, G. N. & BRENNER, K. P. 1996. Comparison of methods for detection and enumeration of airborne microorganisms collected by liquid impingement. *Appl. Environ. Microbiol.*, 62, 2264-2272.
- THOMAS, P., SEKHAR, A. & MUJAWAR, M. 2012. Nonrecovery of varying proportions of viable bacteria during spread plating governed by the extent of spreader usage and proposal for an alternate spotting-spreading approach to maximize the CFU. *Journal of Applied Microbiology*, 113, 339-350.

- THOMAS, R. J., WEBBER, D., HOPKINS, R., FROST, A., LAWS, T., JAYASEKERA, P. N. & ATKINS, T. 2011. The cell membrane as a major site of damage during aerosolization of *Escherichia coli*. *Appl. Environ. Microbiol.*, 77, 920-925.
- THOMPSON, J. F. & MILOS, P. M. 2011. The properties and applications of single-molecule DNA sequencing. *Genome Biology*, 12, 217.
- THOMPSON, K.-A., BENNETT, A. & WALKER, J. 2011. Aerosol survival of *Staphylococcus epidermidis*. *Journal of Hospital Infection*, 78, 216-220.
- TJADEN, B. 2015. De novo assembly of bacterial transcriptomes from RNA-seq data. *Genome Biology*, 16, 1.
- TRAPNELL, C., ROBERTS, A., GOFF, L., PERTEA, G., KIM, D., KELLEY, D. R., PIMENTEL, H., SALZBERG, S. L., RINN, J. L. & PACHTER, L. 2012. Differential gene and transcript expression analysis of RNA-seq experiments with TopHat and Cufflinks. *Nature Protocols*, 7, 562.
- TSENG, C.-C., HSIAO, P.-K., CHANG, K.-C., CHEN, W.-T., YIIN, L.-M. & HSIEH, C.-J. 2014. Optimization of propidium monoazide quantitative PCR for evaluating performances of bioaerosol samplers for sampling airborne *Staphylococcus aureus*. *Aerosol Science and Technology*, 48, 1308-1319.
- TURAPOV, O., O'CONNOR, B. D., SARYBAEVA, A. A., WILLIAMS, C., PATEL, H., KADYROV, A. S., SARYBAEV, A. S., WOLTMANN, G., BARER, M. R. & MUKAMOLOVA, G. V. 2016. Phenotypically adapted *Mycobacterium tuberculosis* populations from sputum are tolerant to first-line drugs. *Antimicrobial Agents and Chemotherapy*, 60, 2476-2483.
- TURGEON, N., TOULOUSE, M.-J., MARTEL, B., MOINEAU, S. & DUCHAINE, C. 2014. Comparison of five bacteriophages as models for viral aerosol studies. *Appl. Environ. Microbiol.*, 80, 4242-4250.
- ULRICHS, T., KOSMIADI, G. A., JÖRG, S., PRADL, L., TITUKHINA, M., MISHENKO, V., GUSHINA, N. & KAUFMANN, S. H. 2005. Differential organization of the local immune response in patients with active cavitary tuberculosis or with nonprogressive tuberculoma. *The Journal of Infectious Diseases*, 192, 89-97.
- UNAMBA, C. I., NAG, A. & SHARMA, R. K. 2015. Next generation sequencing technologies: the doorway to the unexplored genomics of non-model plants. *Frontiers in Plant Science*, 6, 1074.
- USLAN, D. Z., KOWALSKI, T. J., WENGENACK, N. L., VIRK, A. & WILSON, J. W. 2006. Skin and soft tissue infections due to rapidly growing mycobacteria: comparison of clinical features, treatment, and susceptibility. *Archives of Dermatology*, 142, 1287-1292.

- VAN DER MEI, H., ROSENBERG, M. & BUSSCHER, H. 1991. Assessment of microbial cell surface hydrophobicity. *Microbial Cell Surface Analysis*, 6, 263-287.
- VAN PELT, A., WEERKAMP, A., UYEN, M. H., BUSSCHER, H. J., DE JONG, H. P. & ARENDS, J. 1985. Adhesion of *Streptococcus sanguis* CH3 to polymers with different surface free energies. *Appl. Environ. Microbiol.*, 49, 1270-1275.
- VAN SOOLINGEN, D., BORGDORFF, M. W., DE HAAS, P. E., SEBEK, M. M., VEEN, J., DESSENS, M., KREMER, K. & VAN EMBDEN, J. D. 1999. Molecular epidemiology of tuberculosis in the Netherlands: a nationwide study from 1993 through 1997. *The Journal of Infectious Diseases*, 180, 726-736.
- VANGUILDER, H. D., VRANA, K. E. & FREEMAN, W. M. 2008. Twenty-five years of quantitative PCR for gene expression analysis. *Biotechniques*, 44, 619-626.
- VANHAECKE, E. & PIJCK, J. 1988. Bioluminescence assay for measuring the number of bacteria adhering to the hydrocarbon phase in the BATH test. *Appl. Environ. Microbiol.*, 54, 1436-1439.
- VARELA RAMIREX, C. 2014. Metabolism and transport of complex metabolites of mycobacteria. PhD thesis, *University of Birmingham*.
- VERRALL, A. J., G. NETEA, M., ALISJAHBANA, B., HILL, P. C. & VAN CREVEL, R. 2014. Early clearance of *Mycobacterium tuberculosis*: a new frontier in prevention. *Immunology*, 141, 506-513.
- VERREAUULT, D., MOINEAU, S. & DUCHAINE, C. 2008. Methods for sampling of airborne viruses. *Microbiol. Mol. Biol. Rev.*, 72, 413-444.
- VERSCHOOR, J. A., BAIRD, M. S. & GROOTEN, J. 2012. Towards understanding the functional diversity of cell wall mycolic acids of *Mycobacterium tuberculosis*. *Progress in Lipid Research*, 51, 325-339.
- VILJOEN, A., GUTIÉRREZ, A. V., DUPONT, C., GHIGO, E. & KREMER, L. 2018. A simple and rapid gene disruption strategy in *Mycobacterium abscessus*: on the design and application of glycopeptidolipid mutants. *Frontiers in Cellular and Infection Microbiology*, 8, 69.
- VOSKUIL, M. I., SCHNAPPINGER, D., VISCONTI, K. C., HARRELL, M. I., DOLGANOV, G. M., SHERMAN, D. R. & SCHOOLNIK, G. K. 2003. Inhibition of respiration by nitric oxide induces a *Mycobacterium tuberculosis* dormancy program. *The Journal of Experimental Medicine*, 198, 705-713.
- WAGNER, E. M. 2013. Monitoring gene expression: quantitative real-time rt-PCR. *Lipoproteins and Cardiovascular Disease*. 1027, 19-45.

- WAGNER, G. P., KIN, K. & LYNCH, V. J. 2012. Measurement of mRNA abundance using RNA-seq data: RPKM measure is inconsistent among samples. *Theory in Biosciences*, 131, 281-285.
- WALKER, S. L., HILL, J. E., REDMAN, J. A. & ELIMELECH, M. 2005. Influence of growth phase on adhesion kinetics of *Escherichia coli* D21g. *Appl. Environ. Microbiol.*, 71, 3093-3099.
- WALKER, T. M., IP, C. L., HARRELL, R. H., EVANS, J. T., KAPATAI, G., DEDICOAT, M. J., EYRE, D. W., WILSON, D. J., HAWKEY, P. M. & CROOK, D. W. 2013. Whole-genome sequencing to delineate *Mycobacterium tuberculosis* outbreaks: a retrospective observational study. *The Lancet Infectious Diseases*, 13, 137-146.
- WAMPANDE, E. M., MUPERE, E., JAGANATH, D., NSEREKO, M., MAYANJA, H. K., EISENACH, K., BOOM, W. H., GAGNEUX, S., JOLOBA, M. L. & UNIT, T. R. 2015. Distribution and transmission of *Mycobacterium tuberculosis* complex lineages among children in peri-urban Kampala, Uganda. *BMC Pediatrics*, 15, 140.
- WAN, G.-H., LU, S.-C. & TSAI, Y.-H. 2004. Polymerase chain reaction used for the detection of airborne *Mycobacterium tuberculosis* in health care settings. *American Journal of Infection Control*, 32, 17-22.
- WANG, L., FENG, Z., WANG, X., WANG, X. & ZHANG, X. 2010. DEGseq: an R package for identifying differentially expressed genes from RNA-seq data. *Bioinformatics*, 26, 136-138.
- WANG, Z., GERSTEIN, M. & SNYDER, M. 2009. RNA-Seq: a revolutionary tool for transcriptomics. *Nature Reviews Genetics*, 10, 57.
- WATANABE, S., ZIMMERMANN, M., GOODWIN, M. B., SAUER, U., BARRY 3RD, C. E. & BOSHOF, H. I. 2011. Fumarate reductase activity maintains an energized membrane in anaerobic *Mycobacterium tuberculosis*. *PLoS Pathogens*, 7, e1002287.
- WEBB, S. 1969. The effects of oxygen on the possible repair of dehydration damage by *Escherichia coli*. *Microbiology*, 58, 317-326.
- WELLS, W. 1934. On air-borne infection: Study II. Droplets and droplet nuclei. *American journal of Epidemiology*, 20, 611-618.
- WENDT, S. L., GEORGE, K. L., PARKER, B. C., GRUFT, H. & FALKINHAM III, J. O. 1980. Epidemiology of infection by nontuberculous mycobacteria: III. Isolation of potentially pathogenic mycobacteria from aerosols. *American Review of Respiratory Disease*, 122, 259-263.
- WESTERGREN, G. & OLSSON, J. 1983. Hydrophobicity and adherence of oral *streptococci* after repeated subculture in vitro. *Infection and Immunity*, 40, 432-435.

- WHO 2018. Rapid communication: key changes to treatment of multidrug-and rifampicin-resistant tuberculosis (MDR/RR-TB). *World Health Organization*.
- WILLIAMS, C. M., ABDULWHAB, M., BIRRING, S. S., DE KOCK, E., GARTON, N. J., STOLTZ, A., HALDAR, P. & BARER, M. R. 2018. Twenty-four hour face mask sampling in pulmonary tuberculosis reveals three distinct patterns of bacterial aerosol production dissociated from conventional markers of transmission risk. *bioRxiv*, 426825.
- WILLIAMS, C. M., CHEAH, E. S., MALKIN, J., PATEL, H., OTU, J., MLAGA, K., SUTHERLAND, J. S., ANTONIO, M., PERERA, N. & WOLTMANN, G. 2014. Face mask sampling for the detection of *Mycobacterium tuberculosis* in expelled aerosols. *PloS One*, 9, e104921.
- WILLIAMS, K. J., BRYANT, W. A., JENKINS, V. A., BARTON, G. R., WITNEY, A. A., PINNEY, J. W. & ROBERTSON, B. D. 2013. Deciphering the response of *Mycobacterium smegmatis* to nitrogen stress using bipartite active modules. *BMC Genomics*, 14, 436.
- WONG, M. L. & MEDRANO, J. F. 2005. Real-time PCR for mRNA quantitation. *Biotechniques*, 39, 75-85.
- WOOD, R., MORROW, C., BARRY III, C. E., BRYDEN, W. A., CALL, C. J., HICKEY, A. J., RODES, C. E., SCRIBA, T. J., BLACKBURN, J. & ISSAROW, C. 2016. Real-time investigation of tuberculosis transmission: developing the respiratory aerosol sampling chamber (RASC). *PloS One*, 11.
- WRANGSTADH, M., CONWAY, P. L. & KJELLEBERG, S. 1986. The production and release of an extracellular polysaccharide during starvation of a marine *Pseudomonas* sp. and the effect thereof on adhesion. *Archives of Microbiology*, 145, 220-227.
- WURIE, F. B., LAWN, S. D., BOOTH, H., SONNENBERG, P. & HAYWARD, A. C. 2016. Bioaerosol production by patients with tuberculosis during normal tidal breathing: implications for transmission risk. *Thorax*, 71, 549-554.
- XU, Z., WEI, K., WU, Y., SHEN, F., CHEN, Q., LI, M. & YAO, M. 2013. Enhancing bioaerosol sampling by Andersen impactors using mineral-oil-spread agar plate. *PloS One*, 8, e56896.
- YAKUPOVA, E. I., BOBYLEVA, L. G., VIKHLYANTSEV, I. M. & BOBYLEV, A. G. 2019. Congo Red and amyloids: history and relationship. *Bioscience Reports*, 39, BSR20181415.
- YAMAGUCHI, Y., PARK, J.-H. & INOUE, M. 2011. Toxin-antitoxin systems in bacteria and archaea. *Annual Review of Genetics*, 45, 61-79.



- YANG, C., LUO, T., SUN, G., QIAO, K., SUN, G., DERIEMER, K., MEI, J. & GAO, Q. 2012. *Mycobacterium tuberculosis* Beijing strains favor transmission but not drug resistance in China. *Clinical Infectious Diseases*, 55, 1179-1187.
- YATES, T. A., KHAN, P. Y., KNIGHT, G. M., TAYLOR, J. G., MCHUGH, T. D., LIPMAN, M., WHITE, R. G., COHEN, T., COBELENS, F. G. & WOOD, R. 2016. The transmission of *Mycobacterium tuberculosis* in high burden settings. *The Lancet Infectious Diseases*, 16, 227-238.
- YOUNG, R. A., BLOOM, B. R., GROSSKINSKY, C. M., IVANYI, J., THOMAS, D. & DAVIS, R. W. 1985. Dissection of *Mycobacterium tuberculosis* antigens using recombinant DNA. *Proceedings of the National Academy of Sciences*, 82, 2583-2587.
- YPMA, R. J., ALTES, H. K., VAN SOOLINGEN, D., WALLINGA, J. & VAN BALLEGOOIJEN, W. M. 2013. A sign of superspreading in tuberculosis: highly skewed distribution of genotypic cluster sizes. *Epidemiology*, 395-400.
- ZHEN, H., HAN, T., FENNELL, D. E. & MAINELIS, G. 2014. A systematic comparison of four bioaerosol generators: Affect on culturability and cell membrane integrity when aerosolizing *Escherichia coli* bacteria. *Journal of Aerosol Science*, 70, 67-79.
- ZINK, A., SOLA, C., REISCHL, U., GRABNER, W., RASTOGI, N., WOLF, H. & NERLICH, A. 2004. Molecular identification and characterization of *Mycobacterium tuberculosis* complex in ancient Egyptian mummies. *International Journal of Osteoarchaeology*, 14, 404-413.
- ZITA, A. & HERMANSSON, M. 1997. Determination of bacterial cell surface hydrophobicity of single cells in cultures and in wastewater in situ. *FEMS Microbiology Letters*, 152, 299-306.
- ZOUEKI, C. W., TUFENKJI, N. & GHOSHAL, S. 2010. A modified microbial adhesion to hydrocarbons assay to account for the presence of hydrocarbon droplets. *Journal of Colloid and Interface Science*, 344, 492-496.
- ZWERLING, A., COJOCARIU, M., MCINTOSH, F., PIETRANGELO, F., BEHR, M. A., SCHWARTZMAN, K., BENEDETTI, A., DENDUKURI, N., MENZIES, D. & PAI, M. 2012. TB screening in Canadian health care workers using interferon-gamma release assays. *PLoS One*, 7, e43014.

## Appendix

Up- regulated genes at Pre vs Post- nebuliation stage			
Gene	Designation	Annotation	Fold-change
<i>thyX</i>	RVBD_2754c	thymidylate synthase ThyX	8.33
<i>Rv3831</i>	RVBD_3831	hypothetical protein	7.80
<i>Rv2898c</i>	RVBD_2898c	endonuclease	7.00
<i>Rv0964c</i>	RVBD_0964c	hypothetical protein	5.14
<i>Rv1271c</i>	RVBD_1271c	secreted protein	4.77
<i>Rv2806</i>	RVBD_2806	membrane protein	4.69
<i>RVBD_0741</i>	RVBD_0741	transposase	4.17
<i>vapC48</i>	RVBD_3697c	toxin VapC48	4.00
<i>Rv0310c</i>	RVBD_0310c	hypothetical protein	3.71
<i>Rv2683</i>	RVBD_2683	hypothetical protein	3.65
<i>higA</i>	RVBD_1956	antitoxin HigA	3.57
<i>Rv0986</i>	RVBD_0986	adhesion component transport ABC transporter ATP-binding protein	3.57
<i>Rv2492</i>	RVBD_2492	hypothetical protein	3.57
<i>mmpS2</i>	RVBD_0506	membrane protein MmpS2	3.46
<i>vapC25</i>	RVBD_0277c	toxin VapC25	3.37
<i>Rv0330c</i>	RVBD_0330c	hypothetical protein	3.33
<i>fic</i>	RVBD_3641c	cell filamentation protein Fic	3.32
<i>Rv0028</i>	RVBD_0028	hypothetical protein	3.26
<i>PE34</i>	RVBD_3746c	PE family protein PE34	3.25
<i>Rv1671</i>	RVBD_1671	membrane protein	3.25
<i>Rv2336</i>	RVBD_2336	hypothetical protein	3.25

<i>Rv1735c</i>	RVBD_1735c	membrane protein	3.20
<i>Rv3486</i>	RVBD_3486	hypothetical protein	3.07
<i>RVBD_3216</i>	RVBD_3216	hypothetical protein	3.03
<i>Rv0078A</i>	RVBD_0078A	hypothetical protein	3.01
<i>Rv2308</i>	RVBD_2308	hypothetical protein	3.00
<i>cspA</i>	RVBD_3648c	cold shock protein A CspA	2.98
<i>Rv1428c</i>	RVBD_1428c	hypothetical protein	2.86
<i>Rv3198A</i>	RVBD_3198A	glutaredoxin-like protein	2.84
<i>Rv2040c</i>	RVBD_2040c	sugar-transport ABC transporter permease	2.83
<i>Rv3749c</i>	RVBD_3749c	antitoxin	2.82
<i>kdtB</i>	RVBD_2964B	hypothetical protein	2.76
<i>Rv1231c</i>	RVBD_1231c	membrane protein	2.75
<i>Rv3047c</i>	RVBD_3047c	hypothetical protein	2.71
<i>Rv1012</i>	RVBD_1012	hypothetical protein	2.71
<i>Rv0401</i>	RVBD_0401	transmembrane protein	2.70
<i>infA</i>	RVBD_3462c	translation initiation factor IF-1 InfA	2.69
<i>esxW</i>	RVBD_3620c	ESAT-6 like protein EsxW	2.68
<i>TB9.4</i>	RVBD_3208A	hypothetical protein	2.66
<i>Rv2809</i>	RVBD_2809	hypothetical protein	2.64
<i>Rv1025</i>	RVBD_1025	hypothetical protein	2.60
<i>Rv3528c</i>	RVBD_3528c	hypothetical protein	2.58
<i>aac</i>	RVBD_0262c	aminoglycoside 2'-N-acetyltransferase Aac	2.58
<i>hrp1</i>	RVBD_2626c	hypoxic response protein 1 Hrp1	2.58
<i>ptpA</i>	RVBD_2234	phosphotyrosine protein phosphatase PtpA	2.57
<i>Rv0123</i>	RVBD_0123	hypothetical protein	2.55
<i>Rv0691A</i>	RVBD_0691A	mycofactocin protein	2.54
<i>RVBD_3129</i>	RVBD_3129	hypothetical protein	2.52
<i>rpfD</i>	RVBD_2389c	esuscitation-promoting factor RpfD	2.50

<i>Rv1961</i>	RVBD_1961	hypothetical protein	2.50
<i>Rv2297</i>	RVBD_2297	hypothetical protein	2.50
<i>Rv3840</i>	RVBD_3840	transcriptional regulator	2.47
<i>esxD</i>	RVBD_3891c	ESAT-6 like protein EsxD	2.46
<i>vapC17</i>	RVBD_2527	toxin VapC17	2.41
<i>Rv2993c</i>	RVBD_2993c	2-hydroxyhepta-2,4-diene-1,7-dioate isomerase	2.39
<i>esxK</i>	RVBD_1197	ESAT-6 like protein EsxK	2.38
<i>def</i>	RVBD_0429c	polypeptide deformylase Def	2.38
<i>lpqX</i>	RVBD_1228	lipoprotein LpqX	2.37
<i>Rv1171</i>	RVBD_1171	hypothetical protein	2.36
<i>pip</i>	RVBD_0840c	proline iminopeptidase Pip	2.36
<i>Rv3742c</i>	RVBD_3742c	oxidoreductase	2.35
<i>esxP</i>	RVBD_2347c	ESAT-6 like protein EsxP	2.34
<i>dnaA</i>	RVBD_0001	chromosomal replication initiator protein DnaA	2.34
<i>PPE58</i>	RVBD_3426	PPE family protein PPE58	2.34
<i>vapC30</i>	RVBD_0624	toxin VapC30	2.34
<i>PPE1</i>	RVBD_0096	PPE family protein PPE1	2.33
<i>Rv0948c</i>	RVBD_0948c	chorismate mutase	2.32
<i>Rv0569</i>	RVBD_0569	hypothetical protein	2.30
<i>Rv2312</i>	RVBD_2312	hypothetical protein	2.30
<i>RVBD_1792</i>	RVBD_1792	ESAT-6-like protein EsxK	2.29
<i>Rv2146c</i>	RVBD_2146c	YggT family protein	2.29
<i>Rv0325</i>	RVBD_0325	hypothetical protein	2.28
<i>Rv1290A</i>	RVBD_1290A	hypothetical protein	2.28
<i>Rv2600</i>	RVBD_2600	transmembrane protein	2.28
<i>Rv2781c</i>	RVBD_2781c	oxidoreductase	2.27
<i>Rv1377c</i>	RVBD_1377c	transferase	2.26
<i>Rv2288</i>	RVBD_2288	hypothetical protein	2.25

<i>Rv0061c</i>	RVBD_0061c	hypothetical protein	2.22
<i>Rv2516c</i>	RVBD_2516c	hypothetical protein	2.21
<i>Rv0810c</i>	RVBD_0810c	hypothetical protein	2.21
<i>Rv0919</i>	RVBD_0919	N-acetyltransferase	2.21
<i>Rv3632</i>	RVBD_3632	membrane protein	2.21
<i>TB7.3</i>	RVBD_3221c	biotinylated protein	2.20
<i>lprI</i>	RVBD_1541c	lipoprotein LprI	2.20
<i>echA4</i>	RVBD_0673	enoyl-CoA hydratase EchA4	2.20
<i>Rv2271</i>	RVBD_2271	hypothetical protein	2.20
<i>Rv3788</i>	RVBD_3788	hypothetical protein	2.20
<i>lipX</i>	RVBD_1169c	PE family protein lipase LipX	2.19
<i>Rv3402c</i>	RVBD_3402c	hypothetical protein	2.19
<i>Rv2901c</i>	RVBD_2901c	hypothetical protein	2.18
<i>Rv3424c</i>	RVBD_3424c	hypothetical protein	2.16
<i>Rv3851</i>	RVBD_3851	membrane protein	2.16
<i>infC</i>	RVBD_1641	initiation factor if-3 InfC	2.15
<i>mku</i>	RVBD_0937c	DNA end-binding protein Mku	2.14
<i>Rv1766</i>	RVBD_1766	hypothetical protein	2.13
<i>RVBD_3749Ac</i>	RVBD_3749Ac	toxin	2.13
<i>dnaN</i>	RVBD_0002	DNA polymerase III DnaN	2.13
<i>vapC39</i>	RVBD_2530c	toxin VapC39	2.12
<i>icd2</i>	RVBD_0066c	isocitrate dehydrogenase Icd2	2.10
<i>Rv1500</i>	RVBD_1500	glycosyltransferase	2.10
<i>Rv3922c</i>	RVBD_3922c	hemolysin	2.09
<i>rpsJ</i>	RVBD_0700	30S ribosomal protein S10 RpsJ	2.09
<i>Rv2633c</i>	RVBD_2633c	hypothetical protein	2.08
<i>Rv0913c</i>	RVBD_0913c	carotenoid cleavage dioxygenase	2.07
<i>Rv3226c</i>	RVBD_3224B	hypothetical protein	2.07

<i>Rv1144</i>	RVBD_1144	3-hydroxyacyl-CoA dehydrogenase/3-hydroxy-2-methylbutyryl-CoA dehydrogenase	2.07
<i>higB</i>	RVBD_1955	toxin	2.05
<i>TB16.3</i>	RVBD_2185c	hypothetical protein	2.04
<i>moeW</i>	RVBD_2338c	molybdopterin biosynthesis protein MoeW	2.03
<i>Rv2876</i>	RVBD_2876	transmembrane protein	2.03
<i>Rv1489A</i>	RVBD_1489A	methylmalonyl-CoA mutase	2.02
<i>lppX</i>	RVBD_2945c	lipoprotein LPpx	2.019
<i>bcpB</i>	RVBD_1608c	peroxidoxin BcpB	2.00
<i>espC</i>	RVBD_3615c	ESX-1 secretion-associated protein EspC	2.00
<i>icl1</i>	RVBD_0467	isocitrate lyase Icl	2.00
<i>nuoK</i>	RVBD_3155	NADH dehydrogenase subunit K NuoK	2.00
<i>thiG</i>	RVBD_0417	thiamine biosynthesis protein ThiG	2.00

#### Down- regulated genes at Pre vs Post- nebulation stage

Gene	Designation	Annotation	Fold-change
<i>RVBD_0829</i>	RVBD_0829	transposase	-14.00
<i>RVBD_2810c</i>	RVBD_2810c	transposase	-8.08
<i>RVBD_1572c</i>	RVBD_1572c	hypothetical protein	-8.00
<i>Rv2141c</i>	RVBD_2141c	hypothetical protein	-4.59
<i>echA8</i>	RVBD_1070c	enoyl-CoA hydratase EchA8	-4.16
<i>Rv0139</i>	RVBD_0139	oxidoreductase	-4.02

Up- regulated genes at T0 vs Post-nebulisation stage			
Gene	Designation	Annotation	Fold-change
<i>Rv1761c</i>	RVBD_1761c	hypothetical protein	29.50
<i>lppA</i>	RVBD_2543	lipoprotein LppA	25.00
<i>Rv1157c</i>	RVBD_1157c	hypothetical protein	22.00
<i>Rv1227c</i>	RVBD_1227c	transmembrane protein	22.00
<i>Rv0043c</i>	RVBD_0043c	HTH-type transcriptional regulator	21.00
<i>spoU</i>	RVBD_3366	tRNA/rRNA methylase SpoU	20.00
<i>Rv0356c</i>	RVBD_0356c	hypothetical protein	19.00
<i>PE9</i>	RVBD_1087A	PE family protein PE9	17.00
<i>Rv1515c</i>	RVBD_1515c	hypothetical protein	17.00
<i>mmr</i>	RVBD_3065	multidrug resistance protein Mmr	13.25
<i>Rv3525c</i>	RVBD_3525c	siderophore-binding protein	13.00
<i>RVBD_1137c</i>	RVBD_1137c	hypothetical protein	13.00
<i>Rv3209</i>	RVBD_3209	threonine and proline-rich protein	12.00
<i>Rv2661c</i>	RVBD_2661c	hypothetical protein	11.50
<i>Rv3123</i>	RVBD_3123	hypothetical protein	11.50
<i>Rv3196A</i>	RVBD_3196A	hypothetical protein	11.38
<i>acpA</i>	RVBD_0033	acyl carrier protein AcpA	10.00
<i>pta</i>	RVBD_0408	phosphate acetyltransferase	9.50
<i>Rv1203c</i>	RVBD_1203c	hypothetical protein	8.50
<i>Rv1686c</i>	RVBD_1686c	ABC transporter permease	8.50
<i>Rv2822c</i>	RVBD_2822c	CRISPR type III-associated protein Csm2	8.50
<i>lipW</i>	RVBD_0217c	esterase LipW	8.00
<i>Rv2165c</i>	RVBD_2165c	rRNA small subunit methyltransferase H	7.86

<i>PE33</i>	RVBD_3650	PE family protein PE33	7.75
<i>bioD</i>	RVBD_1570	ATP-dependent dethiobiotin synthetase BioD	7.50
<i>Rv2787</i>	RVBD_2787	alanine-rich protein	7.50
<i>Rv2719c</i>	RVBD_2719c	membrane protein	7.20
<i>Rv1744c</i>	RVBD_1744c	membrane protein	7.00
<i>Rv0546c</i>	RVBD_0546c	hypothetical protein	6.75
<i>vapC26</i>	RVBD_0582	ribonuclease VapC26	6.33
<i>Rv3827c</i>	RVBD_3827c	transposase	6.13
<i>fabG3</i>	RVBD_2002	20-beta-hydroxysteroid dehydrogenase	5.90

Down- regulated genes at T0 vs Post-nebulisation stage			
Gene	Designation	Annotation	Fold-change
<i>Rv0470A</i>	RVBD_0470A	mycolic acid synthase PcaA	-55.00
<i>vapB17</i>	RVBD_2526	antitoxin VapB17	-44.00
<i>Rv3748</i>	RVBD_3748	hypothetical protein	-37.00
<i>lppl</i>	RVBD_2046	lipoprotein Lppl	-31.00
<i>nlhH</i>	RVBD_1399c	lipase LipH	-26.00
<i>Rv3851</i>	RVBD_3851	membrane protein	-26.00
<i>mog</i>	RVBD_0865	molybdopterin biosynthesis protein Mog	-22.00
<i>Rv2781c</i>	RVBD_2781c	oxidoreductase	-22.00
<i>Rv3831</i>	RVBD_3831	hypothetical protein	-19.50
<i>PE34</i>	RVBD_3746c	PE family protein PE34	-17.33
<i>RVBD_1136</i>	RVBD_1136	enoyl-CoA hydratase	-17.00
<i>RVBD_3771c</i>	RVBD_3771c	hypothetical protein	-16.66
<i>Rv1231c</i>	RVBD_1231c	membrane protein	-16.50



<i>era</i>	RVBD_2364c	GTP-binding protein Era	-14.00
<i>vapB12</i>	RVBD_1721c	antitoxin VapB12	-14.00
<i>Rv0401</i>	RVBD_0401	transmembrane protein	-13.50
<i>Rv0044c</i>	RVBD_0044c	oxidoreductase	-13.00
<i>Rv0807</i>	RVBD_0807	hypothetical protein	-10.40
<i>Rv0979c</i>	RVBD_0979c	hypothetical protein	-10.25
<i>vapC39</i>	RVBD_2530c	toxin VapC39	-8.50
<i>Rv2772c</i>	RVBD_2772c	transmembrane protein	-8.20
<i>Rv1290A</i>	RVBD_1290A	hypothetical protein	-8.00
<i>Rv0879c</i>	RVBD_0879c	transmembrane protein	-7.88
<i>Rv1025</i>	RVBD_1025	hypothetical protein	-7.50
<i>mazE9</i>	RVBD_2801A	antitoxin MazE9	-7.46
<i>Rv1351</i>	RVBD_1351	hypothetical protein	-7.42
<i>Rv0964c</i>	RVBD_0964c	hypothetical protein	-7.20
<i>0008c</i>	RVBD_0008c	membrane protein	-7.00
<i>sigM</i>	RVBD_3911	sigma-70 family RNA polymerase sigma factor SigM	-7.00
<i>RVBD_3216</i>	RVBD_3216	hypothetical protein	-6.58
<i>mutT4</i>	RVBD_3908	mutator protein MutT4	-6.37
<i>mazF8</i>	RVBD_2274c	toxin MazF8	-6.28
<i>cut4</i>	RVBD_3452	cutinase Cut4	-5.90

Up- regulated genes at T30 vs T0 stage			
Gene	Designation	Annotation	Fold-change
<i>vapC32</i>	RVBD_1114	toxin VapC32	44.00
<i>lppi</i>	RVBD_2046	lipoprotein Lppi	41.00
<i>PE7</i>	RVBD_0916c	PE family protein PE7	32.00
<i>Rv3748</i>	RVBD_3748	hypothetical protein	28.00
<i>TB18.6</i>	RVBD_2140c	hypothetical protein	26.00
<i>nlhH</i>	RVBD_1399c	lipase LipH	21.00
<i>vapB12</i>	RVBD_1721c	antitoxin VapB12	17.00
<i>era</i>	RVBD_2364c	GTP-binding protein Era	15.00
<i>mog</i>	RVBD_0865	molybdopterin biosynthesis protein Mog	14.00
<i>Rv3742c</i>	RVBD_3742c	oxidoreductase	11.00
<i>Rv3741c</i>	RVBD_3741c	oxidoreductase	9.00
<i>Rv1351</i>	RVBD_1351	hypothetical protein	8.00
<i>Rv2647</i>	RVBD_2647	hypothetical protein	8.00
<i>mazE9</i>	RVBD_2801A	antitoxin MazE9	7.00
<i>Rv1692</i>	RVBD_1692	HAD hydrolase, family IIA	7.00
<i>cmtR</i>	RVBD_1994c	ArsR family transcriptional regulator CmtR	7.00
<i>pks9</i>	RVBD_1664	polyketide synthase Pks9	7.00
<i>Rv2135c</i>	RVBD_2135c	hypothetical protein	7.00
<i>Rv0979c</i>	RVBD_0979c	hypothetical protein	7.00
<i>Rv0807</i>	RVBD_0807	hypothetical protein	6.00
<i>vapC39</i>	RVBD_2530c	toxin VapC39	6.00

Down- regulated genes at T30 vs T0 stage			
Gene	Designation	Annotation	Fold-change
			0
<i>PE8</i>	RVBD_1040c	PE family protein PE8	expression at T30
			0
<i>PE9</i>	RVBD_1087A	short-chain Z-isoprenyl diphosphate synthase	expression at T30
			0
<i>acpA</i>	RVBD_0033	acyl carrier protein AcpA	expression at T30
			0
<i>RVBD_1089</i>	RVBD_1089	PE family protein PE10	expression at T30
<i>dipZ</i>	RVBD_2873A	prevent-host-death family protein	-31.00
<i>Rv0356c</i>	RVBD_0356c	hypothetical protein	-19.00
<i>PE33</i>	RVBD_3650	PE family protein PE33	-15.50
<i>RVBD_2856A</i>	RVBD_2856A	hydrogenase nickel incorporation protein HypB	-15.00
<i>Rv2415c</i>	RVBD_2415c	competence protein ComEA	-12.33
<i>Rv1761c</i>	RVBD_1761c	exported protein	-11.80
<i>Rv1049</i>	RVBD_1049	transcriptional repressor	-9.00
<i>Rv3525c</i>	RVBD_3525c	siderophore-binding protein	-8.66
<i>frdC</i>	RVBD_1554	fumarate reductase FrdC	-8.00
<i>Rv3829c</i>	RVBD_3829c	dehydrogenase	-8.00
<i>Rv2805</i>	RVBD_2805	hypothetical protein	-7.66
<i>Rv2600</i>	RVBD_2600	transmembrane protein	-7.50
<i>uspB</i>	RVBD_2317	sugar-transport ABC transporter integral membrane protein UspB	-7.50

<i>Rv0539</i>	RVBD_0539	glycosyltransferase	-7.40
<i>RVBD_1667c</i>	RVBD_1667c	ABC macrolide transporter ATP-binding protein	-7.33
<i>Rv0161</i>	RVBD_0161	oxidoreductase	-6.66
<i>RVBD_2810c</i>	RVBD_2810c	transposase	-6.62
<i>whiB7</i>	RVBD_3197A	transcriptional regulator WhiB-like WhiB7	-6.37
<i>lppA</i>	RVBD_2543	lipoprotein LppA	-6.25
<i>Rv1949c</i>	RVBD_1949c	hypothetical protein	-6.20
<i>Rv2102</i>	RVBD_2102	hypothetical protein	-6.00
<i>Rv3123</i>	RVBD_3123	hypothetical protein	-5.75
<i>Rv1455</i>	RVBD_1455	hypothetical protein	-5.66
<i>Rv1686c</i>	RVBD_1686c	ABC transporter efflux protein DrrB	-5.66
<i>lprE</i>	RVBD_1252c	lipoprotein LprE	-5.50
<i>Rv2732c</i>	RVBD_2732c	transmembrane protein	-5.45
<i>Rv1671</i>	RVBD_1671	membrane protein	-5.00
<i>Rv1995</i>	RVBD_1995	hypothetical protein	-5.00
<i>vapB21</i>	RVBD_2758c	antitoxin VapB21	-4.84
<i>cdd</i>	RVBD_3315c	cytidine deaminase Cdd	-4.75
<i>Rv1770</i>	RVBD_1770	hypothetical protein	-4.57
<i>fabG3</i>	RVBD_2002	3-alpha-(or 20-beta)-hydroxysteroid dehydrogenase FabG3	-4.21
<i>fdxB</i>	RVBD_3554	oxidoreductase FdxB	-4.00
<i>Rv2228c</i>	RVBD_2228c	multifunctional RNASE H/alpha-ribazole phosphatase/acid phosphatase	-3.90
<i>Rv2731</i>	RVBD_2731	alanine and arginine rich protein	-3.23
<i>Rv2165c</i>	RVBD_2165c	ribosomal RNA small subunit methyltransferase H	-3.23
<i>Rv0690c</i>	RVBD_0690c	hypothetical protein	-2.89

Up- regulated genes at T120 vs T30 stage			
Gene	Designation	Annotation	Fold-change
<i>RVBD_2810c</i>	RVBD_2810c	transposase	24.00
<i>Rv3555c</i>	RVBD_3555c	hypothetical protein	11.00
<i>Rv2415c</i>	RVBD_2415c	competence protein ComEA	9.00
<i>Rv2732c</i>	RVBD_2732c	transmembrane protein	7.00
<i>echA8</i>	RVBD_1070c	enoyl-CoA hydratase EchA8	6.00
<i>vapB42</i>	RVBD_2760c	antitoxin VapB42	6.00
<i>Rv2141c</i>	RVBD_2141c	hypothetical protein	5.00
<i>Rv0992c</i>	RVBD_0992c	5-formyltetrahydrofolate cyclo-ligase	5.00
<i>Rv0499</i>	RVBD_0499	hypothetical protein	5.00
<i>RVBD_1036c</i>	RVBD_1036c	transposase	5.00
<i>PPE31</i>	RVBD_1807	PPE family protein PPE31	5.00
<i>Rv0966c</i>	RVBD_0966c	hypothetical protein	5.00
<i>vapB26</i>	RVBD_0581	antitoxin VapB26	5.00
<i>Rv1770</i>	RVBD_1770	hypothetical protein	5.00
<i>adh</i>	RVBD_1530	alcohol dehydrogenase Adh	5.00
<i>Rv2774c</i>	RVBD_2774c	hypothetical protein	4.00
<i>leuB</i>	RVBD_2995c	3-isopropylmalate dehydrogenase LeuB	4.00
<i>0008c</i>	RVBD_0008c	membrane protein	4.00
<i>Rv0531</i>	RVBD_0531	membrane protein	4.00
<i>Rv1647</i>	RVBD_1647	adenylate cyclase	4.00
<i>Rv0139</i>	RVBD_0139	oxidoreductase	4.00
<i>Rv2896c</i>	RVBD_2896c	DNA protecting protein DprA	4.00
<i>Rv2085</i>	RVBD_2085	transposase	4.00

<i>Rv0874c</i>	RVBD_0874c	hypothetical protein	4.00
<i>PE_PGRS21</i>	RVBD_1087	PE-PGRS family protein PE_PGRS21	4.00
<i>Rv2522c</i>	RVBD_2522c	hypothetical protein	4.00
<i>murE</i>	RVBD_2158c	UDP-N-acetylmuramoylalanyl-D-glutamate-2,6-diaminopimelate ligase MurE	4.00
<i>dedA</i>	RVBD_2637	transmembrane protein	4.00
<i>Rv2307c</i>	RVBD_2307c	hypothetical protein	4.00
<i>Rv1290c</i>	RVBD_1290c	hypothetical protein	3.00
<i>gcvT</i>	RVBD_2211c	aminomethyltransferase GcvT	3.00
<i>pheA</i>	RVBD_3838c	prephenate dehydratase PheA	3.00
<i>PE_PGRS22</i>	RVBD_1091	PE-PGRS family protein PE_PGRS22	3.00
<i>Rv3480c</i>	RVBD_3480c	diacylglycerol acyltransferase	3.00
<i>papA4</i>	RVBD_1528c	polyketide synthase associated protein PapA4	3.00
<i>Rv3092c</i>	RVBD_3092c	integral membrane protein	3.00
<i>mbtL</i>	RVBD_1344	acyl carrier protein MbtL	3.00
<i>PE_PGRS35</i>	RVBD_1983	PE-PGRS family protein PE_PGRS35	3.00
<i>Rv1627c</i>	RVBD_1627c	nonspecific lipid-transfer protein	3.00
<i>thrB</i>	RVBD_1296	homoserine kinase ThrB	3.00

Down- regulated genes at T120 vs T30 stage			
Gene	Designation	Annotation	Fold-change
<i>PPE46</i>	RVBD_3018Bc	PE family protein PE27A	-7.85
<i>Rv2669</i>	RVBD_2669	N-acetyltransferase	-5.75
<i>higA</i>	RVBD_1956	antitoxin HigA	-5.14
<i>RVBD_0031</i>	RVBD_0031	transposase	-5.00
<i>RVBD_1137c</i>	RVBD_1137c	hypothetical protein	-4.60

<i>RVBD_3599c</i>	RVBD_3599c	hypothetical protein	-4.21
<i>Rv1505c</i>	RVBD_1505c	sialic acid O-acetyltransferase NeuD	-4.00
<i>Rv3033</i>	RVBD_3033	hypothetical protein	-3.60
<i>Rv1045</i>	RVBD_1045	hypothetical protein	-3.45
<i>Rv3122</i>	RVBD_3122	hypothetical protein	-3.44
<i>vapC38</i>	RVBD_2494	toxin VapC38	-3.38
<i>Rv0193c</i>	RVBD_0193c	hypothetical protein	-3.28
<i>kdtB</i>	RVBD_2964B	hypothetical protein	-3.27
<i>Rv3773c</i>	RVBD_3773c	hypothetical protein	-3.26
<i>Rv3705A</i>	RVBD_3705A	proline rich protein	-3.23
<i>Rv3566A</i>	RVBD_3566A	hypothetical protein	-3.21
<i>fic</i>	RVBD_3641c	cell filamentation protein Fic	-3.17
<i>glnA3</i>	RVBD_1878	glutamine synthetase GlnA3	-3.14
<i>mazE6</i>	RVBD_1991A	antitoxin MazE6	-3.11
<i>Rv1957</i>	RVBD_1957	hypothetical protein	-3.00
<i>nat</i>	RVBD_3566c	arylamine N-acetyltransferase Nat	-2.88
<i>mmpS2</i>	RVBD_0506	membrane protein MmpS2	-2.83
<i>Rv3836</i>	RVBD_3836	hypothetical protein	-2.68

Up- regulated genes at T120 vs T0 stage			
Gene	Designation	Annotation	Fold-change
<i>lpqO</i>	RVBD_0604	lipoprotein LpqO	8.00
<i>Rv1115</i>	RVBD_1115	exported protein	7.00
<i>PE_PGRS34</i>	RVBD_1840c	PE-PGRS family protein PE_PGRS34	6.00
<i>Rv0612</i>	RVBD_0612	hypothetical protein	4.00
<i>Rv0347</i>	RVBD_0347	membrane protein	4.00
<i>otsB2</i>	RVBD_3372	trehalose-6-phosphate phosphatase OtsB2	4.00
<i>Rv3421c</i>	RVBD_3421c	universal bacterial protein YeaZ	4.00
<i>Rv0541c</i>	RVBD_0541c	integral membrane protein	3.00
<i>vapC42</i>	RVBD_2759c	toxin VapC42	3.00
<i>Rv0460</i>	RVBD_0460	hydrophobic protein	3.00
<i>Rv1865c</i>	RVBD_1865c	oxidoreductase	3.00
<i>argJ</i>	RVBD_1653	glutamate N-acetyltransferase ArgJ	3.00
<i>Rv1075c</i>	RVBD_1075c	exported protein	2.00
<i>Rv0420c</i>	RVBD_0420c	transmembrane protein	2.00
<i>Rv1360</i>	RVBD_1360	oxidoreductase	2.00
<i>Rv3094c</i>	RVBD_3094c	hypothetical protein	2.00
<i>recC</i>	RVBD_0631c	exonuclease V gamma chain RecC	2.00
<i>Rv0194</i>	RVBD_0194	transmembrane multidrug efflux pump	2.00
<i>Rv1478</i>	RVBD_1478	invasion-associated protein	2.00
<i>Rv3728</i>	RVBD_3728	drug:H+ antiporter-2 (14 Spanner) (DHA2) family drug resistance MFS transporter	2.00



Down- regulated genes at T120 vs T0 stage			
Gene	Designation	Annotation	Fold-change
<i>fadD18</i>	RVBD_3513c	fatty-acid-CoA ligase FadD18	-3.50
<i>Rv1157c</i>	RVBD_1157c	alanine and proline rich protein	-3.14
<i>relK</i>	RVBD_3358	toxin RelK	-3.00
<i>RVBD_3098B</i>	RVBD_3098B	toxin	-2.14
<i>Rv2669</i>	RVBD_2669	N-acetyltransferase	-2.12
<i>Rv0339c</i>	RVBD_0339c	transcriptional regulator	-2.00